ЖУРНАЛ
ПРИКЛАДНОЙ ХИМИИ

Volume 32, No. 10

October, 1959

JOURNAL OF
APPLIED CHEMISTRY
OF THE USSR

(ZHURNAL PRIKLADNOI KHIMII)

IN ENGLISH TRANSLATION

CONSULTANTS BUREAU, INC.

UNDER THE DIRECTION OF THE AMERICAN CERAMIC SOCIETY...

a major source of scientific communication —

GLASS AND CERAMICS

TRANSLATED FROM RUSSIAN

This Soviet monthly, published for glass and ceramics researchers, technologists and production workers, provides Western scientists with reports on the latest technical advances from the laboratories and plants of the USSR.

Translation of GLASS AND CERAMICS, prompted by the recognition given to Soviet work in the field, permits *you* to take advantage of their intensified research program. Using these accurate translations by a staff of bilingual scientists can eliminate costly duplication of research. Scientists in this country can learn the *specifics* about how their Soviet counterparts upgrade products and improve processes; design unique, improved equipment; break production records and reduce costs.

GLASS AND CERAMICS will be published in the most effective manner possible to bridge the 3-year gap since this journal was last available in complete translation.

1957 issues will be published in 3 separate volumes, each of which will contain 4 issues. Nos. 1–4 March; Nos., 5–8—April; Nos. 9–12—June. The remaining 1958 and 1959 issues will be brought out in four-issue volumes on a bimonthly basis until the backlog has been diminished.

Subscription price: $80.00 per year.

Detailed tables of contents will be sent upon request.

You will also be interested in . . .

THE STRUCTURE OF GLASS

Proceedings of a Conference Held in Leningrad on the Structure of Glass

"*. . .The Glass Division of the American Ceramic Society and the National Science Foundation are to be congratulated for making this inspiring collection available . . .*"
—JOURNAL OF CHEMICAL EDUCATION

"*The book should be of great interest to scientific and technical personnel interested in glass technology, ceramics, the states of matter, and any work involving the vitreous state. They should all have the experience of reading this book . . . there exists in the scientific literature of the USSR, a whole new reference field that should be as easily available to Western scientists and vice-versa.*"
—CHEMISTRY IN CANADA

"*. . . a stimulating experience. . .*"
—TRANS., BRITISH CERAMIC SOCIETY

"*. . . lively discussions which show the diversity of opinions on every experimental report.*"
—THE GLASS INDUSTRY

"*. . . the volume is excellent . . . The translation was well worth while . . .*" —R. W. Douglas, NATURE

"*. . . an excellent volume . . .*"
SOUTH AFRICAN JOURNAL OF SCIENCE

Cloth | 296 pages | profusely illustrated | $20.00

Order on approval from

CONSULTANTS BUREAU ENTERPRISES, INC.

227 West 17th Street • New York 11, N. Y.

Volume 32, No. 10

October, 1959

JOURNAL OF
APPLIED CHEMISTRY
OF THE USSR

(ZHURNAL PRIKLADNOI KHIMII)

A publication of the Academy of Sciences of the USSR

IN ENGLISH TRANSLATION

Year and issue of first translation:
Vol. 23, No. 1 January 1950

	U. S. and Canada	*Foreign*
Annual subscription	*$60.00*	*$65.00*
Annual subscription for libraries of nonprofit academic institutions	*20.00*	*25.00*
Single issue	*7.50*	*7.50*

Copyright 1960
CONSULTANTS BUREAU ENTERPRISES, INC.
227 West 17th Street, New York, N. Y.

Editorial Board
(ZHURNAL PRIKLADNOI KHIMII)

P. P. Budnikov, S. I. Vol'fkovich, A. F. Dobryanskii,
O. E. Zvyagintsev, N. I. Nikitin (Editor in Chief),
G. V. Pigulevskii, M. E. Pozin, L. K. Simonova
(Secretary), V. V. Skorchelletti, N. P. Fedot'ev

Note: The sale of photostatic copies of any portion of this copyright translation is expressly prohibited by the copyright owners.

Printed in the United States of America

JOURNAL OF APPLIED CHEMISTRY OF THE USSR

Volume 32, Number 10 October, 1959

CONTENTS

	PAGE	RUSS. PAGE
VIII Mendeleev Conference on General and Applied Chemistry	2181	2129
Titanium-Containing Forsterite Refractories. P. P. Budnikov and B. N. Bogomolov	2192	2139
Chemical Selection of Scheelite and Calcite in Ores with Regeneration of the Reagents . A. S. Chernyak	2201	2148
State of Copper Sulfide in Iron-Containing Silicate Melts. S. E. Vaisburd and V. L. Kheifets	2206	2153
Reaction of Aluminum with Cryolite-Alumina Melts. V. P. Mashovets and R. V. Svoboda	2210	2157
Mechanism of the Decomposition of Apatite by Phosphoric Acid. M. E. Pozin, B. A. Kopylev and D. F. Zhil'tsova	2217	2164
Investigation of the Thermochemical Decomposition of Calcium Sulfate and its Interaction with Carbon. A. M. Ginstling and A. D. Volkov	2223	2171
Interaction Between Iron Sulfides and Ferrous Sulfate. N. Sh. Safiullin	2230	2178
Production of High-Grade Calcium and Barium Peroxides. S. Z. Makarov and N. K. Grisgor'eva	2237	2184
Interaction of Barium and Calcium Carbonates with Sulfur Dioxide in the Presence of a Reducing Agent. V. V. Pechkovskii	2241	2189
Influence of γ-Radiation on the Physiocochemical Properties of Some Cation Exchangers. A. M. Semushin and I. A. Kuzin	2245	2193
Investigation of the Steam-Distillation Process . E. K. Siirde and P. G. Romankov	2249	2197
A Study of the Rate of CO_2 Absorption by Monoethanolamine Solution in a Horizontal Mechanical Absorber. S. N. Ganz, S. B. Leibovich, N. A. Malyshevich and M. A. Lokshin	2259	2207
Enrichment Coefficient of a Single Rectification Sieve Plate. A. A. Noskov, G. V. Burova and P. Fel'desh	2263	2211
Heat Transfer from a Fluidized Catalyst Bed to the Heat-Exchange Surface . V. B. Sarkits, D. G. Traber and I. P. Mukhlenov	2271	2218

CONTENTS (continued)

	PAGE	RUSS. PAGE
Application of the Thermal Diffusion Method in the Purification of Dyes. B. M. Bogoslovskii, B. M. Yavorskii and A. D. Virnik	2278	2225
Plastic Film Light-Filters Absorbing Long-Wave and Near Infrared Regions of the Spectrum . E. A. Veller and B. A. Porai-Koshits	2282	2230
Technology of the Electrochemical Deposition of Cobalt—Tungsten Alloy and its Properties. N. P. Fedot'ev, P. M. Vyacheslavov, E.G. Kruglova and G.P. Andreeva .	2287	2235
Some Physiocochemical and Technological Properties of Electrolytes for Electrochemical Polishing of Steel. G. P. Maitak and G. S. Tret'yakova	2294	2242
Fired Air-Depolarization Electrodes. N. I. Galkina, G. M. Popova, D. L. Kondrashov and R. Kh. Burshtein	2299	2247
Permeability of Certain Organic Polymer Films to Atmospheric Moisture . A. A. Berlin and K. P. Lesina	2304	2252
The Catalyst Concentration During Synthesis of Vinyl Acetate over a Heterogeneous Catalyst . E. N. Rostovskii and I. A. Arbuzova	2310	2258
The Aging of Cable Rubber. R. I. Dubrovnik	2314	2261
The Deionization of Acid Protein Hydrolyzates with Anion-Exchanging Resins. A. B. Davankov, A. N. Oratynskaya, V. M. Laufer and A. G. Lipinskii	2321	2269
Investigation of the Catalytic Conversion of Methanol Formaldehyde in a Fluidized Catalyst Bed. M. V. Polyakov, V. V. Shalya and Z. Z. Vysotskii	2327	2275
Polyamide Powder Sorbents for Determination of Tannides. P. Ya. Frenkel' and A. N. Mikhailov	2334	2283
High-Pressure Destructive Hydrogenation of Tuimazin Petroleum. Ya. P. Katsobashvili and N. P. Volynskii	2341	2290
Emulsion Copolymerization of Hexafluorobutadiene with Diene Compounds . A. L. Klebanskii and O. A. Timofeev	2344	2294
The Behavior of Sulfur During the Chlorination of Coal. B. I. Losev, N. S. Vorob'eva, V. K. Ninin and E. A. Zimakova	2350	2300
Isomerization of Tetrahydronaphthalene. V. V. Tishchenko and Yu. I. Perin	2354	2304
Contribution to the Question of the Characteristics of Benzene in the Chemical Industry. M. Illyukevich	2359	2308
Oxalate Method for the Determination of Alkaloids in Ephedra . M. I. Goryaev, S. A. Moshkevich, R. N. Sazonova and I. M. Shabanov	2364	2313

CONTENTS (continued)

	PAGE	RUSS. PAGE
Preparation of Ethers of Alkylene Chlorohydrins. N. P. Smetankina and V. S. Étlis	2372	2320
Production of Individual Alcohols from Sperm Whale Oil. P. S. Ugryumov	2376	2324
Synthesis of 3,3'-Dinitrobenzidine and the Analytical Reagents Arsenazo II, Toron II, and Phenazo. V. I. Kuznetsov and S. B. Zavvin	2381	2329
Direct Synthesis of Methylchlorosilanes in a Fluidized Bed. K. A. Andrianov, S. A. Golubtsov, I. V. Trofimova and N. P. Lobusevich	2385	2332
Brief Communications		
Diffusion of Water Vapor and the Flow of Air in Porous Glass. D. P. Dobychin	2389	2336
Activated Carbon from Sulfite-Cellulose Liquors. B. N. Dashkevich and M. N. Karpinskii	2393	2339
Investigation of the Chemical Nature of Cracked Petroleum Residuums. E. I. Kazakov and V. P. Kuznetsova	2397	2342
Dehydration of n-Amyl Alcohol on Aluminum Oxide. I. S. Lishanskii, A. A. Korotkov, G. A. Andreeva and A. G. Zak	2400	2344
Interaction of Adipic and Sebacic Acids with Urea and Acetylurea. M. S. Dudkin	2403	2347
Catalytic Hydrogenation of Quinoline. A. N. Kost, L. D. Pertsov, L. G. Yudin and S. F. Kalinkin	2406	2349
Solution of Quartz in Feldspar Melts. V. Z. Petrova, A. I. Avgustinik, P. F. Konovalov and E. P. Konovalova	2409	2351
Investigation of the Effect of Antimony on the Nature of Lead Passivation in Sulfuric Acid Solutions. É. S. Vaisberg, E. V. Krivolapova and B. N. Kabanov	2413	2354
Determination of the True Specific Gravity of Cellulose. V. I. Sharkov and V. P. Levanova	2417	2357
Paramagnetic Resonance in Coals. V. I. Losev and É. A. Bylyna	2419	2359
1-(4'-Sulfophenyl)-3-Methyl-5-Pyrazolone From Acetoacetamide. P. A. Levin	2422	2361
Conversion of Etherates (Oxonium Compounds of Sulfuric Acid with β-Chloro Ethers) into a Crystalline State. A. K. Seleznev	2425	2363
Cohydrolysis of Dimethyldichlorosilane with (1-Cyano-1-Methylethoxy)-Methyldichlorosilane. I. K. Stavitskii and S. N. Borisov	2428	2366
Preparation of Pure Linalyl Chloride. G. V. Pigulevskii, V. G. Kostenko, and L. F. Andreeva.	2430	2367
Book Review		
Yu. S. Musabekov. Synthetic Chemistry at a New Stage. Yaroslavl' Book Press, 1958 Reviewed by I. G. Filatov	2433	2371
Erratum	2436	

VIII MENDELEEV CONFERENCE ON GENERAL AND APPLIED CHEMISTRY

The VIII Mendeleev Conference took place in Moscow from March 16 to 23 and served as a review of the development of theoretical and applied chemistry in our country. This conference differed from previous ones in that the subject matter was more varied and important and the number of reports and participants was very great. Not only chemists of all the special fields but also scientists whose fields were related to chemistry, such as physics, biology and agriculture, participated. There were 2230 official delegates but on some days there were audiences of 10-11 thousand persons.

About 200 foreign chemists came to the conference and many of them participated actively in its work. Foreign scientists presented more than 50 reports.

The VIII Mendeleev Conference met soon after the XXI Congress of the Communist Party of the Soviet Union which had approved the seven-year plan on the further development of the national economy and therefore the work of many participants in the Mendeleev Conference was directed towards realizing the directives of the XXI Congress of the CPSU.

Much attention was paid to problems connected with the preparation of synthetic materials, the synthesis of organic substances from natural gases and oil, processing of new forms of mineral raw material, production of mineral fertilizers and chemical means of plant protection, construction of chemical equipment, automation and many other problems of chemical science and techniques.

At the conference the work of Soviet physicochemists on the study of the structure of substances, kinetics and catalysis of chemical reactions, the chemistry of complex compounds and radioactive materials, sorption and surface phenomena, and corrosion were examined.

The work of the conference was divided into 17 sections: inorganic chemistry and technology, organic chemistry and technology, analytical chemistry, physical chemistry, colloid chemistry, polymer chemistry and technology, chemistry of natural compounds and biochemistry, agricultural chemistry, fertilizers and insecto-fungicides, chemistry and chemical technology of fuels, chemistry and technology of food products, silicate chemistry and technology, radiochemistry and isotope chemistry, theoretical and applied electrochemistry, chemistry of metals, and alloys, the economics, planning and organization of chemical plants, the basic processes and equipment of chemical technology, and the history of chemistry and chemical technology. In addition, there were meetings of a symposium on higher chemical and technological education and of the commission on chemical nomenclature.

There were 11 reports read at the plenary meetings and about 1500 at meetings of the sections.

In a short review it is impossible to give even a superficial description of the very varied work of the VIII Mendeleev Conference. We will mention here only those reports which would interest most readers of the Journal of Applied Chemistry.

At the plenary meetings the foremost scientists of our country gave reports on the latest achievements in different fields of chemistry.

A. N. Nesmeyanov read a report on the theme "D. I. Mendeleev's periodic system and organic chemistry" in which he introduced the listerners to a series of general rules characterizing heteroorganic compounds.

For a long time hydrocarbon (alkyl, aryl and other) derivatives of the elements which have a chemical bond between the carbon and the element atoms have occupied a central position in the great variety of their structure. D. I. Mendeleev devoted much attention to them in his main articles on establishing the periodic law.

The alkyl groups are more or less stably bound to the element only through the sp valence levels. Here the presence of unused d or f valence electrons considerably weakens the stability of the alkyl derivatives obtained and makes them atypical and involatile, such as tetramethylplatinum, or makes their existence impossible (an explanation proposed by the author of the report for one of the laws described by D. I. Mendeleev).

All the possible structures of carbon compounds of all the elements form the immense domain of the new, rapidly growing organic chemistry of all the elements of the periodic system in the place of the old organic chemistry of organogen elements.

Heteroorganic chemistry is joining this new organic chemistry and reuniting the branches of chemistry that were separated one hundred and fifty years ago, namely, organic and inorganic.

V. I. Spitsin described the present state of Mendeleev's periodic law, stages in its development, and the ever-increasing field in which it is applicable, including the extension of the theory of atomic structure and the discovery of new radioactive elements.

V. S. Fedorov discussed problems in scientific and technical progress in the chemical industry. V. A. Kargin spoke of basic problems in polymer chemistry.

N. N. Semenov gave a report on the theme "Basic problems in chemical kinetics". He described the most important results of recent investigations on chemical reaction rates which are of great importance in not only the theoretical study of reaction mechanisms but also chemical technology.

In a report on the basic problems of radiochemistry, A. P. Vinogradov described trends in the application of radioactive isotopes and nuclear radiation to the synthesis and polymerization of organic compounds as well as applications in medicine and other fields.

V. A. Énge1'gardt read a report devoted to the main problems of biochemistry and showed that the latest investigations may provide the chemical basis of a series of important vital processes and thus be of help in the medical fight against some serious illnesses.

The chemical problems in agriculture in the USSR were described in the report presented by A. V. Sokolov. From the volume of mineral fertilizer production projected in the seven-year plan (35 million tons in 1965) one can expect a great increase in some farm crops. The use of new chemical agents in agriculture (insectofungicides, herbicides, defoliants) will greatly promote an increase in the crop yield.

Ya. K. Syrkin reported the present state of the problem of valence. The accumulation of new experimental material requires a further expansion and development in the study of the nature of valence. This development is primarily connected with new data on the fuller use of unshared valence electrons, unsaturated electron pairs and empty orbits, which results in the formation of bridge compounds, dimers, trimers, and other compounds. Tri-, tetra- and multicentered orbits are acquiring greater significance when an electron pair moves within the field of three, four, and more centers. As a result compounds are formed in which, for example, a CH_3 group or a hydrogen atom is bound simultaneously to several adjacent atoms.

These new types of bonds play an important role in catalysis. Lately new compounds have been synthesized whose structure may be comprehended only in the light of the theory of molecular orbits. This generalizing theory covers all types of bonds from ionic to covalent ones in very different classes of compounds, while the double centered bonds are included as an important but exceptional case. This theory is being developed successfully and helps to predict the properties of a series of organic cyclic molecules with conjugated bonds. The theory explains the nature of bonds in complex compounds better than was possible previously.

The chemical aspects of the application of atomic energy were examined in the report by A. P. Aleksandrov, in which he reviewed modern methods of using atomic energy in chemical techniques.

V. B. Nikolaev presented a report on the basic problems of chemical apparatus and equipment construction and he explained in the report a series of new principles and types of high-capacity equipment for chemical plants.

More than 100 reports were given at the meetings of the section on inorganic chemistry and technology and these included various branches of chemistry. The communications dealing with the study of peroxide compounds attracted much attention.

I. A. Kazarnovskii (Moscow) gave a report on the mechanism of the formation of peroxides and their oxidizing action. The mechanism of oxidation of barium oxide to barium peroxide was investigated with the aid of labeled oxygen, the spontaneous decomposition of the solid perhydrate $K_2O_2 \cdot 2H_2O_2$ was investigated by a magnetic method, and finally the reaction of potassium ozonide with heavy water was studied. It was shown that the actual oxidizing agents in all three classes of peroxides are free hydroxyl radicals. The great differences in the degree of this action is mainly due to different concentrations of hydroxy radicals, which in the case of ozonides is greater by several orders than in Fenton's reagent.

S. Z. Makarov (Moscow) studied the perhydrate forms of peroxides of Group I and II metals. The results obtained confirmed that the peroxide perhydrates of elements of the secondary subgroups (also lithium and magnesium) were hydroperoxide forms. It was also established that the peroxide perhydrates of Group I metals were capable of forming the corresponding super peroxides on dehydration.

I. I. Vol'nov (Moscow) worked out conditions for the reproducible preparation of calcium, strontium and barium peroxides from peroxide diperoxyhydrates.

T. V. Rode, G. K. Grishenkova and A. V. Zachatskaya (Moscow) studied the reaction of sodium peroxide and superperoxide with sodium carbonate and hydroxide. Physicochemical analysis methods (thermographic, thermal-gas-volumetric, x-ray and chemical methods) were used for the study.

I. N. Lepeshkov (Moscow) described in his report new investigations of the N. S. Kurnakov school in the field of physicochemical analysis of natural salts and water-salt equilibria.

Considerable attention has been paid recently to the physicochemical characteristics of the new salt depositis in the southern Ural, Krasnoyarsk, White Russian and other regions of the country. The study of the hydrochemical conditions of the greatest salt basin in the world, Kara-Bogaz-Gol, was continued. New data were obtained on the lithium, boron, and other technically important contents of natural brine and salts and a series of water-salt systems, including sodium, potassium, magnesium, calcium, lithium, and rubidium salts, were studied at different temperatures.

In addition to laboratory work, field investigations, including large-scale experiments, were carried out in the basins. Plans have been projected for further investigations in this field.

S. I. Vol'fkovich, N. N. Postnikov, L. A. Ionass, V. V. Illarionov and R. E. Remen (Moscow) have worked out a new thermal process of intensive defluorination of unenriched Khibin apatite-nepheline ores and phosphorites of Kara-Tau with steam at the melting point. This yields fertilizers which contain phosphate that is assimilable by plants, while fluorine gases are eliminated. The phosphorites of Kara-Tau, which contain magnesium, are processed successfully by this method without any additions. The process takes place in a cyclone-type, high-capacity furnace. The product is a concentrated fertilizer and feed for livestock.

A series of reports was presented in the section on the chemistry of complex compounds.

I. I. Chernyaev, L. A. Nazarova and V. S. Orlova (Moscow) succeeded in isolating sulfates, nitrates and carbonates of platinum iodopentamine by replacing the hydroxy group in platinum trans-iodohydroxytetraamine with ammonia. The facts they observed in this work are readily explained by the extensive trans-effect of iodine.

A. A. Grinberg (Leningrad) gave new data on the kinetics of complex-formation and on the stability of complex compounds. The study of the kinetics of isotope exchange in complex compounds of platinum, palladium and iridium as well as data on the kinetics of substitution reactions in platinum complex compounds and instability constants of the corresponding compounds indicated that generally, the chemical behavior of complex compounds was determined not only by thermodynamic characteristics but also by the rate at which equilibrium was established. In a number of cases the more thermodynamically stable complexes underwent exchange and substitution reactions much more rapidly.

A large number of reports were devoted to complex compounds connected with the chemical study of rare elements.

O. E. Zvyagintsev, A. Kurbanov and S. M. Starostin (Moscow) investigated ruthenium nitroso compounds; S. I. Ginzburg, N. K. Pshenitsyn and L. G. Sal'skaya (Moscow) studied the nature of colored iridium compounds formed in sulfuric, phosphoric and perchloric acids; E. V. Shenderetskaya and I. I. Chernyaev (Moscow) studied

monovalent rhodium formates; É. P. Deichman (Moscow) studied the composition and properties of indium oxalates and indium compounds with alkali metal oxalates; M. D. Lyutaya and I. V. Tananaev (Moscow) investigated the formation, composition, and properties of mixed hexanitronickeloates of rare earth elements; Z. A. Sheka and E. E. Kriss studied the extraction of lanthanum, neodymium, yttrium and ytterbium nitrates from nitric acid solutions with CCl_4 solutions of tributyl phosphate and dibutyl phosphate, as well as the complex formation reactions occurring in these systems.

About 30 reports were presented at the meetings of the section on agricultural chemistry, fertilizers, and insectofungicides. One of the meetings was opened by the oldest organic chemist, the head of the Russian school of organophosphorus chemists, A. E. Arbuzov. B. A. Arbuzov (Kazan) reported the results of work carried out by the Kazan Chemical Institute of the Academy of Sciences of the USSR in the search for new means of combatting plant pests. The most interesting compound was found to be the mixed diethyl dimethyl ester of dithiopyrophosphoric acid. A number of acyl derivatives of Dipterex were synthesized and their insecticidal and toxic properties studied. Acylation of Dipterex with organic acids reduced its toxicity to warm-blooded animals and produced very [illegible] reduction in the insecticide action.

S. I. Vol'fkovich (Moscow) described the research that he and a group of coworkers at Moscow State University carried out to find new types of highly concentrated complex fertilizers which would not contain any useless components. The introduction of small amounts of salts into potassium, ammonium and magnesium phosphates made it possible to prepare by heating polymeric fertilizers with varying solubilities and, consequently, with different rates of assimilation by plants.

The reaction of carbamide with paraformaldehyde, urotropine, phosphates, and other substances gave polymeric, long-acting fertilizers that were not washed into the depth of the soil by rain and irrigation water.

M. Kh. Chailakhyan (Moscow) gave a report on the new growth stimulants, gibberellins. Gibberellins accelerate plant growth, stop the dormant stage of tree buds as well as root and bulb plants, and induce and accelerate flowering, fruit bearing, and seed germination. These substances are now being widely investigated in the Soviet Union and other countries in order to find economic methods of applying them to agricultural crops under production conditions.

O. K. Kedrov-Zakhman (Moscow) et al. studied the effect of molybdenum on various agricultural plants on turf-podzol and peat-bog soils of the non-black earth belt of the USSR. Their experiments indicate that the use of molybdenum fertilizers should be introduced into the agriculture of the non-black earth belt of the Soviet Union in the near future.

N. N. Mel'nikov (Moscow) presented a report on the synthesis and study of a large group of new organophosphorus insecticides and made a series of interesting observations on the mechanism of the action of organophosphorus insecticides on insects. He also reported the results of work on a new method of preparing dithiophosphoric and dithiopyrophosphoric esters. These compounds are interesting for a study of their use as insecticides, herbicides, and defoliants.

F. V. Turchin's report (Moscow) presented a new concept on the mechanism of the biological fixation of atmospheric nitrogen which occurs in the root nodules of bean plants and is of tremendous importance in the nitrogen cycle in agriculture.

By extensive use of isotopic tracers, F. V. Turchin et al. were able to show that the enzyme synthesis of nitrogenous compounds from atmospheric nitrogen occurs on the inner surface of specific nodule tissue of bean plant roots and that the first product of this synthesis is ammonia, which is then used in the plants for the formation of amino acids and protein.

More than sixty reports were presented at the meetings of the section on silicate chemistry and technology. Of these we should note the report presented by I. S. Lileev et al. (Leningrad) on the investigation of alkali metal gallosilicates and their formation conditions and similarity to aluminosilicates. The following aspects of the role of gallium in silicate chemistry were studied: 1) synthesis of alkali gallosilicates by sintering the oxides $Na_2O-Ga_2O_3-SiO_2$, 2) preparation of glassy alkali gallosilicates and study of their properties, and 3) synthesis of sodium hydrogallosilicates from aqueous solutions of sodium gallate.

A. M. Ginstling and A. D. Volkov (Leningrad) carried out an interesting theoretical and experimental investigation of the thermochemical decomposition of calcium sulfate in crystalline mixtures and obtained extensive experimental data characterizing reactions in the systems $CaSO_4+SiO_2$, $CaSO_4+C$; $CaSO_4+C+SiO_2$, etc.

G. V. Kukolev and K. A. Mikhailova (Kharkov) studied the effect of surface-active additives on the contraction of refractories during pressing and the properties of fired samples; they established that the elastic (reverse) after-effect had a considerable influence on the growth of porosity of samples. Aliphatic acids containing 7-9 carbon atoms per molecule and sulfite-alcohol spent wash were used as surface-active agents.

P. P. Budnikov and V. G. Savel'ev (Moscow) investigated barium monoaluminate as a binder for refractory concretes. $BaO \cdot Al_2O_3$ was synthesized from $BaCO_3$ and Al_2O_3. Chamotte and chromomagnesite were used as fillers for the concrete. Refractory concretes with barium aluminate binder had less additional contraction and a smaller change in weight by volume when heated than concrete based on calcium cements.

N. I. Voronin, N. I. Krasotkina and V. A. Smirnova (Leningrad) confirmed the possibility of preparing high quality carborundum articles based on nitride binder by firing a coke charge in ordinary reverberatory furnaces.

E. V. Matsynin and S. D. Okorokov (Leningrad) investigated the binding properties of the glassy phase of Portland cement clinker. The four, five and six component melts synthesized were investigated petrographically and x-radiographically and their relative crushability, resistance to sulfates, hydration rate, and binding properties under different storage conditions determined.

L. N. Rashkovich and Yu. M. Butt (Kraskovo) gave a report on the mechanism of the formation of a binder by autoclave treatment of lime-sand articles. Of the three possible mechanisms for the reaction of the components during hardening of the samples, the hypothesis that the reaction proceeded in solution was confirmed experimentally. The new formations crystallized from solution as they were less soluble than the starting components. V. A. Tikhonov and L. G. Shpynova (L'vov) gave data on the changes in phase composition of hydration products from aluminate components of Portland cement and this data was obtained from the results of thermal analysis, microscopic, electron microscopic and chemical investigations as well as physico-mechanical tests.

V. V. Vargin and G. O. Karapetyan (Leningrad) investigated the absorption spectra, luminescence, and photochemical properties of cerium glasses, which have considerable stability to ionizing irradiation. The cerium was introduced in various concentrations into silicate, borate, borosilicate and phosphorus glasses of simple composition. The changes in the cerium were determined from the absorption and luminescence spectra as well as the thermoluminescence of the glasses investigated. As a result of the investigations it was established that tri- and tetravalent cerium were present simultaneously in the glasses and that the luminescence activator in the glasses was trivalent cerium.

A. I. Avgustinik (Leningrad) spoke on the problem of a finely dispersed crystalline phase forming from a glassy one. The theoretical rules he found, according to which the concentration-structural and energetic preparedness of groups with the most regular structure plays the main role, were confirmed by the work of E. A. Porai-Koshits (Leningrad) on glass structure.

Voluminous experimental material obtained by normal x-ray and other methods indicates that the structures of a series of complex glasses is chemically heterogeneous.

We will mention a few of the eighty reports presented at the meetings of the section on theoretical and applied electrochemistry. N. V. Nikolaeva-Fedorovich, O. A. Petrii and A. N. Frumkin (Moscow) carried out an interesting investigation of the polarographic behavior of halogen complexes of platinum. M. A. Loshkarev, I. P. Chernobaev and B. I. Tomilov (Dnepropetrovsk) investigated the effect of intermediate reagents on the rate of electrochemical processes. The effect of intermediate reagents on the course of electrochemical reactions was studied in an attempt to overcome one of the essential disadvantages of electrode processes, namely, the limitation of their rate by the slowness of the diffusion process or the high degree of irreversibility of the discharge. The use of intermediate reagents readily overcomes the retardation of the electrode process caused by kinetic hindrances. In this case the intermediate reagent acts as a catalyst in the electrode process and decreases the degree of its irreversibility. The general theory of the process and the main kinetic equations are presented in connection with the solution of a number of interesting technological problems in hydroelectrometallurgy and the electrosynthesis of organic compounds.

K. M. Kartashova and A. M. Sukhotin (Leningrad) worked out a dynamic method for measuring the capacity of electrodes and applied it to the determination of electrocapillary zero potentials. They established that by this method it is possible to investigate the effect of oxygen and other surface-active substances adsorbed at different potentials on the electrocapillary zero potential of chromium steel and some other metals.

D. P. Semchenko and K. G. Il'in (Novocherkassk) investigated the electrochemical formation of higher oxygen compounds of chlorine. Comparison of the experimental material obtained by electrolysis of chloride solutions and by studying the anode polarization of smooth platinum in the same solutions indicated that electrosynthesis of the perchlorates of alkali and alkali earth metals is the result of simultaneous primary discharge of Cl^- and OH^- ions and subsequent secondary chemical and electrochemical reactions.

D. N. Gritsan and D. S. Shun (Kharkov) studied the effect of synthetic detergents and wetting agents on the electrodeposition of metals. It was established that the use of these substances as additives opened new possibilities for controlling electrodeposition and improving the properties of the electrolytic metal deposits.

N. T. Kudryavtsev, G. N. Smolenskaya, V. M. Karataev and R. G. Golovchanskaya (Moscow) worked out conditions for electrolytic coating of titanium and titanium plating which is of great value in machine and instrument construction.

M. F. Lantratov and A. F. Alabyshev (Leningrad) proposed a new fusible electrolyte for preparing metallic sodium. They investigated the basic properties of the ternary electrolyte $NaCl-CaCl_2-BaCl_2$ and carried out prolonged electrolysis experiments on a 3000 ampere electrolyzer. The use of this electrolyte gave good technological characteristics.

The section on basic processes and equipment of chemical technology was organized for the first time at a Mendeleev conference and naturally attracted much attention from our own and foreign scientists. Over four days 75 reports were presented at the section meetings and these fall mainly within the following categories: 1) general problems and hydrodynamic processes, 2) heat processes, and 3) problems of mass transfer.

The report of the chairman of the section, A. N. Planovskii (Moscow) determined the direction of the work by describing the state and ways of developing the study of processes and equipment of chemical technology.

A report on problems of the theory of similarity, which produced much discussion, was both interesting and important in principle. In speaking of the essence and methods of the theory of similarity, A. A. Gukhman (Moscow) presented contemporary views on this method of quantitative investigation that is based on the concept that characteristic variables describe every problem and the problems should be examined in the light of these variables. In substantiating the general forms of application of such variables an important aspect of the theory of similarity was stressed, namely, its contribution to the analysis of a process that is simultaneously of a general and a relative character.

P. G. Romanov (Leningrad) used interesting examples to show the possibility of using the theory of similarity in investigations on chemical technological processes. Experience in the application of the theory of similarity in processing experimental data describing hydrodynamic, thermal, diffusion, and chemical processes has shown that there are many points of view on the system of similarity criteria. By introducing new criteria whose physical meaning is not completely clear, many authors have used similarity incorrectly.

O. M. Todes et al. (Leningrad) presented an analysis of experimental data obtained in investigating the hydrodynamics of a fluidized bed. The approximate universal relation they derived which relates the criteria Re, Ar and the separation of the bed ϵ, is true both for a fluidized bed (from start of fluidization to elimination of particles from the apparatus) and for restricted precipitation of the suspension. In analyzing the equations obtained by studying the hydrodynamics of a fluidized bed, I. P. Mukhlenov (Leningrad) pointed out that there is no complete quantitative analogy for the processes occurring in a fluidized bed in the systems gas – liquid and gas – solid.

S. Ya. Gzovskii (Moscow) investigated the process of mixing and obtained analytical relations for determining the energy consumed in overcoming the internal friction forces of a liquid in a circulating current and formulas for determining the forces acting on the paddles, the point at which the forces are applied, the moment of rotation, and the power expended by the mixers. I. S. Pavlyshenko (Leningrad) introduced the concept of a "determining number of revolutions" and by using it he obtained a relationship between the physicochemical

properties of the disperse phase and the dispersion medium and the geometric dimensions of the apparatus and mixer, on the one hand, and the number of revolutions of the mixer necessary for a practically uniform distribution of phases in the volume mixed, on the other.

The conclusions drawn by P. A. Semenov (Moscow) in studying experimentally the force of interaction of a gas and a liquid at the boundary separating them are of importance in principle for further development of theoretical concepts on the mechanism of gas and liquid mass exchange. A. M. Lastovtsev (Moscow) made some interesting generalizations in studying the size distribution of drops in a liquid spray.

The results of work carried out by M. L. Varlmaov et al. (Odessa) on acoustic coagulation of aerosols formed in chemical plants are promising for industrial use in fine purification of gases.

V. A. Zhuzhikov described theoretical analysis methods, experiments, and processing of experimental data that would be applicable to the study of filtration processes at any position of the filter (with restricted precipitation of solid suspension particles under the effect of gravity). In his report E. M. Gol'din (Leningrad) gave the results of investigating theoretically the movement of matter in the rotor of a vibrational conical centrifuge in relation to various construction and technological parameters. S. Kaminskii (Moscow) demonstrated designs of vibrocentrifuges that would be of interest for industrial application.

There was much valuable material in the reports on problems of heat exchange. Of these we should note the reports given by V. G. Ainshtein, V. Ya. Kruglikov, N. I. Gel'perin and I. B. Rapoport (Moscow) on the heat exchange between a fluidized bed and the surface of a single tube with longitudinal and transverse flow. P. I. Nikolaev and A. N. Planovskii (Moscow) determined experimentally the local heat transfer coefficients from the surface of a horizontal tube to a pseudo fluidized bed of quartz sand. The relations obtained by N. K. Elukhin, M. E. Ivanov and I. P. Vishnev in investigating heat exchange in the condensation and boiling of O_2, N_2 and Ar, provide a basis for designing condensers (evaporators of air separating equipment) and other apparatuses. A. B. Bassel' and A. S. Sakhiev developed the design of a jacketed tubular apparatus with spiral ribs inside the tubes. Investigation of heat exchange during condensation of vapor-gas mixtures in such condensers showed that with spiral ribs the heat transfer coefficient was approximately a factor of 2 greater than that with a smooth tube. I. V. Mazyukevich (Leningrad) gave a report on experimental investigations of heat exchange in the condensation of NH_3 vapor from mixtures with various inert substances.

In characterizing the effect of active component concentration, partial pressure differences, and surface forms on the rate of mass exchange, L. D. Berman (Moscow) gave interesting experimental data which made it possible to refine the existing ideas on the mechanism of mass exchange.

T. K. Sherwood's (USA) report on a new theory of mass transfer which he developed with Ryan for processes accompanied by a chemical reaction, induced a lively discussion. A. V. Lykov spoke in favor of applying Onsager's theory to an investigation of heat and mass exchange processes.

V. V. Kafarov (Moscow) proposed general equations for mass transfer including the factor of the surface's dynamic state for various hydrodynamic conditions.

Yu. V. Poplavskii (Moscow) gave new experimental data on the effect of withdrawal in plate-type apparatuses. A. M. Rozen et al (Moscow) studied hydraulics and mass transfer on screen "pocket" plates of large diameter.

L. S. Aksel'rod (Moscow) and A. A. Noskov (Leningrad) devoted their reports to problems of investigating the hydraulics and efficiency of screen rectification plates.

V. A. Malyusov, N. N. Umnik and N. M. Zhavoronkov (Moscow) investigated multi-stage molecular distillation.

The data given by L. L. Dobroserdov (Leningrad) on the separation of azeotropic mixtures by salt rectification are of practical interest.

In studying the kinetics of molecular transfer in gases, A. G. Usmanov (Kazan') obtained general kinetics equations for all molecular processes, formulated the relations for transfer of the amounts of movement, heat, and mass and on this basis generalized the experimental data on viscosity, heat conductivity and diffusion of many gases and water vapor. S. S. Trainin, M. É. Aérov and N. I. Nikitina (Moscow) described the application of a method of electrohydrodynamic analogy (EGDA) to the investigation of chemical apparatuses. N. I.

Gel'perin (Moscow) investigated extraction from solutions in countercurrent injector columns. A series of reports on the operation of pulsed extraction columns were presented by S. M. Karpacheva, A. M. Rozen and others. Interesting data were obtained by S. Z. Kagan and M. É. Aérov (Moscow) in their study of extractors with mechanical stirring of phases.

M. Yu. Lur'e (Moscow) praised new methods of drying in his report on present problems of drying techniques in the chemical industry.

More than 200 reports were given at the four subsections of the organic chemistry section. The reports were of a very varied nature: some were devoted to elucidating various reaction mechanisms and others to problems of improving known processes, synthesizing new compounds needed by the national economy, and finding more effective catalysts.

A series of reports by A. P. Nesmeyanov et al. (Moscow) were devoted to the development of the new chemistry of ferrocene.

E. A. Karpeiskaya, A. A. Tovstopyatov and A. A. Balandin (Moscow) showed that rhenium was an extremely effective catalyst for a number of organic reactions: dehydrogenation of alcohols, cyclohexane hydrocarbons and cumene to α-methylstyrene.

Yu. G. Mamedaliev (Baku) proposed a new technological process for chlorination of hydrocarbons (methane, ethane, propane, and butane) in a fluidized catalyst bed. I. P. Tsukervanik (Tashkent) worked out a new method of condensation with elimination of hydrogen halide and using powdered metals (Cu, Mo, W, Cr, Ti, Co, Zr) instead of aluminum chloride as catalyst.

In a number of works new catalysts were proposed to replace mercury catalysts in the hydration of acetylene.

A series of reports examined different oxidation processes of solid paraffins, monobasic carboxylic acids to dibasic acids and ethylene to ethylene oxide.

Many reports were devoted to the chemistry of organophosphorus compounds, vinylation of organic substances, destructive nitration of olefine, syntheses based on CO and H_2 and other problems related to organic chemistry and technology.

At meetins of the section of polymer chemistry and technology more than 80 reports were given on the results of work on the preparation of new polymeric materials, the study of their behavior during use and changing the properties of polymers in the desired direction.

Soviet scientists have developed new types of polymers: radioactive plastics which may be used as medicines and as pulse sources, rubbers reinforced with synthetic resins, ion-exchange resins, heat-stable organosilicon polymers containing aluminum, etc.

V. A. Kargin, V. A. Kabanov and I. Yu. Marchenko (Moscow) prepared isotactic polystyrene by polymerizing styrene on a Ziegler catalyst. It was shown by x-ray and density measurements that the polymer obtained may be in a crystalline and in an amorphous state.

The thermomechanical curve for amorphous isotactic polystyrene has a maximum in the temperature range 100-150° which shifts with a change in the rate of temperature increase.

S. N. Ushakov (Leningrad) used new effective "cross-linking agents" – diallylacetals of various aldehydes, methylenebicrotonamide and methylolcrotonamide diester (prepared for the first time). The use of these compounds for copolymerization with methacrylic and vinyl esters made it possible to prepare solid, infusible, and insoluble copolymers by block polymerization.

Three-dimensional cross-linking of vinyl acetate and vinyl alcohol copolymers with crotonamide and methylolcrotonamide is of practical value in the preparation of new types of synthetic fibers with high mechanical strength, special materials for electrovacuum techniques, and insoluble modifications of polyvinyl alcohol for the preparation of benzene and water stable articles.

A. A. Vansheidt and N. N. Kuznetsova (Leningrad) gave a report on the polycondensation of phenoxyacetic acid with formaldehyde and the synthesis of weakly acidic ion-exchange resins based on them. Investigations showed that phenoxyacetic acid reacted with formaldehyde in the presence of strong mineral acids and that under

mild conditions the reaction gave fusible resins that were soluble in aqueous alkali while more drastic conditions and with excess formaldehyde it gave insoluble trimeric polymers which contained chlorine and phenolic hydroxyls together with carbonyls.

In comparison with the resin KF_4, these cationites have an exchange capacity that is half as great but show a very high selectivity in relation to streptomycin and other large organic ions.

V. P. Zubov (Moscow) studied the polymerization of styrene in the presence of some halides. The components were mixed by simultaneous evaporation in vacuum onto a surface cooled with liquid nitrogen. Polymerization occurred when the "colloidal ice" melted on the growing salt crystals.

It was shown that under these conditions the solid surface of such salts as $TiCl_3$ and $BeCl_2$ did not have a stereospecific effect on the polymerization.

There was stereospecific polymerization only when these salts were combined with metal alkyls.

I. P. Losev and L. A. Datskevich (Moscow) synthesized and investigated polyurethan esters. These compounds were the reaction products of diisocyanates and high molecular polyesters prepared from dicarboxylic acids and glycols.

For the synthesis of the polyesters the authors used carbon dioxide and succinic adipic and sebacic acids and the following glycols: ethylene, 1,3-butylene, 1,4-butylene, diethylene and triethylene. The most valuable polyesters for the synthesis of polyurethan esters were those whose molecular weight was up to 2,000. 1,6-Hexamethylene diisocyanate, toluylene diisocyanate etc. were used to obtain elastic materials.

Films with a series of technically valuable properties were prepared from the polyurethan esters. These films were completely insoluble in all organic solvents.

V. V. Korshak, S. L. Sosin and M. V. Chistyakova (Moscow) showed the possibility of using the reaction of free radicals with unsaturated compounds to prepare linear polymers and investigated the conditions and characteristics of this reaction.

K. A. Andrianov (Moscow) described a new class of high polymer materials, polyorganoaluminosiloxanes, whose molecular chains are built of silicon, oxygen, and aluminum atoms. Polyorganoaluminosiloxanes were synthesized from trichlorophenylsilane and from trichloroethylsilane and aluminum chloride. The properties of the polymers obtained were studied and conclusions drawn on the structure of polymer chains.

Z. N. Tarasova, M. Ya. Kaplunov, P. A. Klauzen, B. A. Dogadkin and V. L. Karpov (Moscow) investigated the kinetics of radiation vulcanization of some synthetic and natural rubbers and the physicochemical and mechanical properties of the vulcanizates prepared by radiation in an atomic reactor and from a Co^{60} source with an integral dose of 10^7-10^8 roentgens.

In comparison with the best sulfur vulcanizates containing the same amount of filler, the radiation vulcanizates showed an increased resistance to ageing (by a factor of 4 to 5 at 130°), had lower residual deformations, low hysteresis and high endurance under multiple deformations, and wear resistance. The tensile strength of the radiation vulcanizates was less than that of the best sulfur vulcanizates.

In their report, Z. A. Rogovina and V. A. Derevitskaya (Moscow) gave basic data on the methods of synthesizing new derivatives of cellulose and polyuronic acids, and carboxymethylcelluloses, and investigating the properties of these compounds, on a method of synthesizing new derivatives of polyuronic acids (alginic acid) and carboxyl-containing cellulose ethers (carboxymethylcelluloses).

N. A. Glukhov (Leningrad) synthesized a series of polymeric metalloorganic chelate compounds based on metallic derivatives of acetylacetone and tetraketones of various structures. Acetylacetonates of Zn, Mg, Cu, Ni, Co, Re, and other metals were used as the metal compounds. The polymers synthesized had a high flame resistance.

About seventy reports were presented and discussed at the section on chemistry and chemical technology of fuels. There were two subsections: oil chemistry and coal chemistry. The reports in these sections dealt with crucial problems in the chemistry and technology of fuel gases, oil, coal, and oil shale.

In a detailed report V. P. Sukhanov (Moscow) discussed problems in the preparation of high quality fuels and oils, as well as problems of preparing from oil the starting materials for synthesis of polymers and production of rubber and artificial fibers.

N. M. Kravets (Moscow) gave a report on rational methods of using solid fuel.

In his report on future developments in the production and use of fuel gases, N. V. Lavrov (Moscow) showed what the possibilities were in processing the gases as a chemical raw material for industrial organic synthesis, in particular for the production of acetylene, ethylene and other valuable products.

We should note the interesting investigations carried out in the Oil Institute of the Academy of Sciences of the AzSSR by L. M. Kosheleva, S. D. Mekhtiev, B. F. Pishnamezzade, Sh. É. Éibatova and F. A. Gashimova (Baku) on the separation of cyclohexane and its closest homologs from Baku oil ligroin (top grade Surakhany oil).

A. S. Fomina, L. Ya. Pobul' and Z. A. Degtereva (Tallin) studied the chemical nature of kerogen from Baltic kukersite oil shale. The results obtained were the basis of a new chemical method for processing kukersite shale to dibasic saturated acids which are one of the basic components for the synthesis of a wide range of chemical products.

A. A. Kruglikov's report (Nizhniy Tagil) on the separation and use of dihydric phenols from semi-coking and hydrogenation of Cheremkhovo coals is promising.

The preparation of epoxide resins by condensation of dihydric phenols with epichlorohydrin in an alkaline medium is particularly interesting. The epoxy resins thus obtained are no worse than the resins obtained from difficultly available diphenylolpropane.

New methods of hydrogen production from solid fuels were reported by V. V. Lebedev (Khimki). The new methods of hydrogen production were characterized by compact apparatus and high productivity; they could be used in chemical plants and in the oil and fat industry.

V. Ya. Kruglikova, I. B. Rappoport, A. V. Volynskii and V. V. Muzovskii (Moscow) worked out theoretically and experimentally a highly productive synthesis of hydrocarbons from Co and H_2 on an iron catalyst in a fluidized and stationary bed (on pilot equipment). The report also showed the possibility of prolonged stable operation of the catalyst under highly productive conditions.

A. D. Petrov, E. P. Kaplan, O. M. Nefedov and M. A. Chel'tsova (Moscow) investigated the properties of individual C_{18}–C_{40} polycyclic hydrocarbons of different structural types. S. R. Sergienko, E. V. Lebedev and A. A. Mikhnovskaya (Moscow) obtained new data on the structure of high molecular oil hydrocarbons. V. I. Isagulyants and V. N. Tishkova (Moscow) presented a scientific basis for the synthesis of alkyl- and arylphenol additives to mineral oils and motor fuels. Van Risselberg (Belgium) presented interesting data on the oxidizability of oils.

N. I. Shuikin, N. G. Bekauri and G. N. Maslyanskii (Moscow) devoted their reports to catalytic isomerization of paraffins which resulted in refinement of motor fuel and gave valuable starting materials for the synthesis of rubber and other polymers.

Yu. L. Khmel'nitskii, K. I. Zimina, A. A. Polyakova and V. M. Nikitina (Moscow) gave interesting data on the radiolysis of different types of hydrocarbons. They had developed a mass spectrometric method for determining the structural group composition of ligroins. The method was based on the relation of the mass spectrum to molecular structure.

M. A. Geiman and A. D. Larin (Moscow) synthesized a series of anionic surface-active substances from oil and from oil, lignite, shale, and peat distillates.

Many members of the conference took part in discussing the reports presented. Some of the problems provoked interesting and lively discussion.

At the final meetings of the sections resolutions designating the subjects for further investigation in the given chemical field were passed. In many cases organization problems were also discussed. Thus, for example, the section on processes and apparatus recommended the formation within the system of the Academy of Sciences of the USSR of an institute of the processes and apparatus of chemical technology and an all-union society of

engineers on this subject. The section on agricultural chemistry proposed that the agricultural chemistry laboratories be improved and that an institute of agricultural chemistry be established within the system of the Academy of Sciences of the USSR.

In the next seven years Soviet scientists will be faced with many varied and promising problems. Better coordination between work carried out in scientific institutes and industry must be established in order to solve these problems successfully. The conference pointed out the necessity of increasing the role of factory laboratories and expanding the work carried out jointly by these laboratories, scientific research institutes, and university departments.

At the closing session all the Soviet chemists who had assembled at the VIII Mendeleev Conference appealed to all the chemists of the Soviet Union to carry out new investigations and achievements for the further development of chemical science and industry.

L. K. Simonova and M. I. Kurochkina

TITANIUM-CONTAINING FORSTERITE REFRACTORIES

P. P. Budnikov and B. N. Bogomolov

The historical resolutions of the 21st conference of the Communist Party of the Soviet Union called for a further increase in the output of refractories, an improvement in their quality, and an increase in the number of types. Thus, for example, over a period of seven years the output of forsterite refractories must be increased by a factor of 4-5 in comparison with 1958. This type of refractory may be used not only in nonferrous metallurgy, but also in the cement industry in the sintering zone of rotating furnaces.

Together with such indisputably valuable properties of forsterite refractories as high refractoriness, high deformation temperature under load, low thermal conductivity, a tendency to form strong, dense coatings, a high resistance to cement clinker, and the abundance and availability of the raw materials, this form of refractory also has some shortcomings, the elimination of which would make it possible to obtain really high quality fettling. The most vulnerable part of forsterite refractories is the free periclase contained in them and as our experiments showed, under the action of cement clinker this is saturated by components of the latter and recrystallizes, producing a considerable weakening of the refractory structure [1].

The purpose of our investigations was to prepare forsterite refractories with a minimal periclase content, retaining their valuable qualities with a simultaneous improvement in their thermal properties.

It is known [2-9] that with a fall in the magnesium oxide content of a forsterite refractory there is an increase in porosity and a fall in strength. To compensate for these losses, we added small amounts of technical titanium dioxide to the dunite mixture.

We prepared five stock mixtures with from 0 to 20% of "MK" grade magnesium oxide added to dunite and sixteen mixtures with from 0.5 to 4% of technical TiO_2 added. A total of 21 mixtures with the following compositions were prepared:

Mixture No.	Dunite (%)	MK grade magnesium oxide (%)
0	100	—
1	95	5
2	90	10
2a	85	15
3	80	20

Based on mixture No. 0		Based on mixture No. 1	
Mixture No.	TiO_2 added (%)	Mixture No.	TiO_2 added (%)
4	0.5	8	0.5
5	1	9	1
6	2	10	2
7	4	11	4

Based on mixture No. 2		Based on mixture No. 2	
Mixture No.	TiO_2 added (%)	Mixture No.	TiO_2 added (%)
12	0.5	16	0.5
13	1	17	1
14	2	18	2
15	4	19	4

TABLE 1

Properties of Forsterite Refractories

Mixture No.	Properties of refractories										
	compression strength	porosity (in %)		weight by volume (in g/cc)	specific gravity (in g/cc)	deformation temp. under load of 2 kg/cm² (in °C)		additional shrinkage at 1650° for 2 hours (in %)	heat resist.: 1300° – H_2O (in heat cycles)		refractoriness (in °C)
		apparent	true			initial	breaking		beginning of destruction	20% loss in weight	
0	88	28.8	29.7	2.32	3.30	1560	1660	0	2	3	1760
1	85	27.7	28.2	2.36	3.29	1600	1680	—3.0	2	9	> 1800
2	96	27.6	27.9	2.38	3.30	1630	1680	—1.7	2	8	> 1800
2a	125	27.3	28.3	2.40	3.35	1680	1700	—0.3	2	7	> 1800
3	180	27.1	27.3	2.42	3.33	1670	1700	—0.4	2	5	> 1800
4	107	27.9	29.3	2.36	3.31	1560	1660	—0.2	2	8	1760
5	176	27.2	28.4	2.38	3.31	1620	1660	0	2	8	> 1800
6	162	25.8	25.6	2.40	3.35	1630	1690	0	2	11	> 1800
7	116	28.2	28.1	2.42	3.37	1580	1640	—0.5	2	8	1780
8	158	27.2	27.5	2.40	3.31				3	8	> 1800
9	168	27.5	28.3	2.37	3.31	1630	1690	—0.3	3	7	> 1800
10	146	28.2	28.6	2.34	3.28				3	8	> 1800
11	102	27.2	28.3	2.38	3.32				3	6	> 1800
12	109	28.0	28.5	2.37	3.30				1	8	> 1800
13	144	26.4	27.5	2.42	3.34				2	7	> 1800
14	192	23.4	26.5	2.44	3.32	1660	1690	—0.2	1	9	> 1800
15	176	24.0	25.9	2.46	3.32				1	10	> 1800
16	199	25.6	27.2	2.43	3.34				2	8	> 1800
17	239	26.4	27.2	2.43	3.34				3	7	> 1800
18	233	26.8	27.2	2.43	3.34	1680	1720	—0.2	4	7	> 1800
19	202	26.4	27.2	2.44	3.34				4	7	> 1800

The granular composition of the mixtures, corresponding to the composition adopted for a forsterite refractory, is presented below.

Sieve opening (in mm).	3	2	1	0.8	0.5	0.2	0.09	0.06 > 0.06
Residual fraction on sieve in %)	1-3	15-20	15-25	3-4	3-5	6-7	5-15	7-15 20-30

The dry components were mixed in a laboratory ball mill with a small load of balls.

The stock mixtures, moistened with sulfite-alcohol spent wash (sasw) with a density of 1.24 g/cc (1% on the dry concentrate), were pressed on an industrial hydraulic press. From each of the mixtures we prepared 10 samples with the dimensions 230 × 115 × 65 mm. The raw bricks were dried in tunnel drying kilns at 125° and then fired in a gas chamber furnace under the conditions adopted in a plant. The maximum firing temperature was 1650°. The results of tests on the refractories obtained are given in Table 1 and Figs. 1 and 2.

The investigations showed that a decrease in the free periclase content of forsterite refractories raised their heat resistance, but at the same time considerably reduced their compression strength. The addition of titanium dioxide to dunite with a low magnesium oxide content raised the strength and heat resistance of forsterite refractories without appreciable sintering of the material. The properties of forsterite refractories without MgO added, but with TiO_2 introduced, were similar to those of normal forsterite products.

A study of the microstructure of refractories with various magnesium oxide contents showed that forsterite concretions were formed in all cases; refractories from dunite without the addition of MgO had a more friable structure. It should be noted that in all the samples the forsterite concretion was somewhat less well developed than in refractories of industrial batches, and this is explained by insufficient hand working of the raw material mass before pressing.

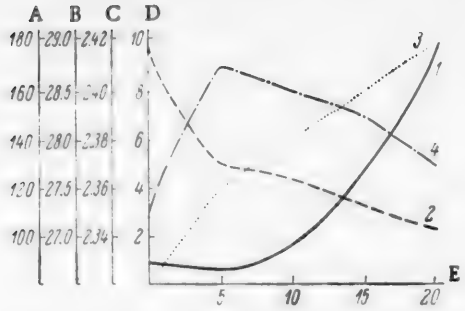

Fig. 1. Properties of forsterite refractories with various MgO contents. A) Strength (kg/cm^2), B) porosity (%), C) weight by volume (g/cc), D) heat resistance (heat cycles), E) MgO content (%). 1) Strength, 2) porosity, 3) weight by volume, 4) heat resistance.

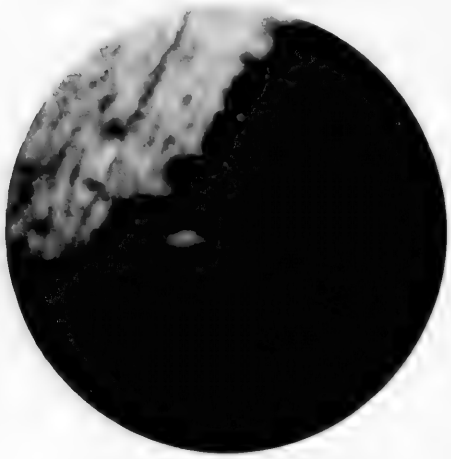

Fig. 3. Titanate dendrites in a titanium-containing forsterite refractory. Magnification 525; light transmitted parallel.

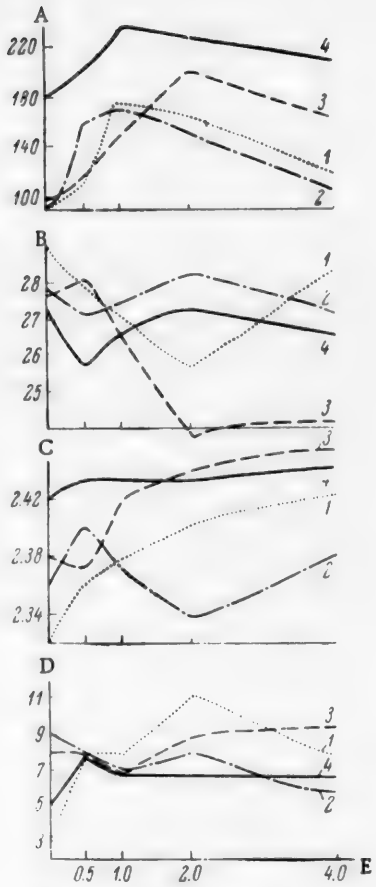

Fig. 2. Properties of titanium-containing forsterite refractories. A) Strength (kg/cm^2), B) porosity (%), C) weight by volume (g/cc), D) heat resistance (heat cycles), E) TiO_2 content (%). Roasted magnesite content (in %): 1) 0, 2) 5, 3) 10, 4) 20.

When 5% of magnesium oxide was added to the dunite, magnesioferrite appeared in the forsterite refractory and a glass was formed. With 10% of MgO the amount of magnesioferrite increased and there was a simultaneous increase in the content of iron oxides, mainly in the form of hematite. Free periclase was not detected in this case but transparent, orange-yellow, needle-like crystals (with a weak green pleochroism) were clearly formed, though we were unable to determine the crystallo-optical indices of these new growths. These new growths contained MgO.

Objects made from dunite with 15 and 20% of magnesium oxide added did not differ from normal industrial forsterite refractories. In samples containing 0.5% of TiO_2 we detected traces of magnesium titanates in the form of fine, black-brown, cubic grains and fine, shapeless, red, isotropic grains. Samples with 1 and 2% of TiO_2 showed the characteristic formation of magnesium titanates as branching red intergrowths, i.e., dendrites (Fig. 3). They lay between separate sections of concretion and in the coarsest pores, as if reinforcing the forsterite concretion.

Under the isotropic dendrites lay a bluish anisotropic substance in the form of needle-like crystals, probably titanates formed by interaction of TiO_2 with the surface of the forsterite concretion. When 4% of TiO_2 was added,

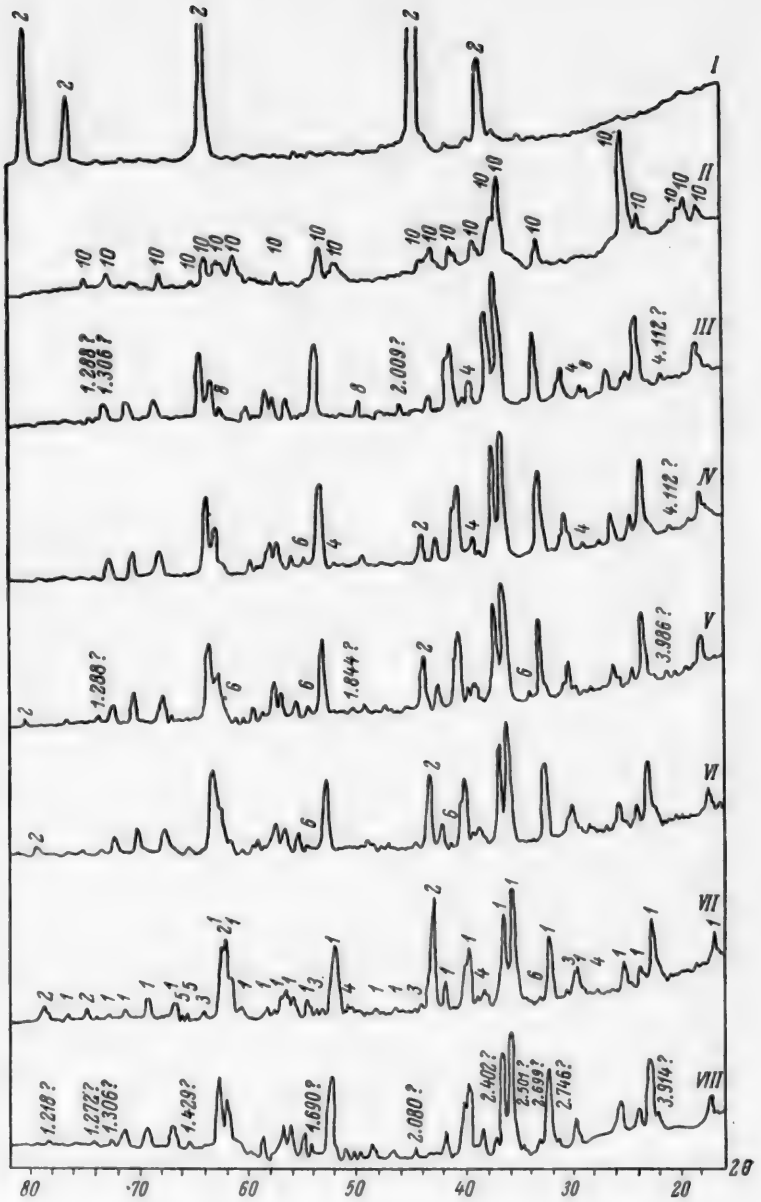

Fig. 4. Phase composition of raw components and fired refractories. I) Roasted magnesite, II) unfired dunite, III, IV, V, VI, and VII) refractories with various MgO contents, namely 0, 5, 10, 15 and 20%, respectively, VIII) titanium-containing dunite refractory with a 2% TiO_2 content.

a large number of dendrites were formed with a simultaneous increase in the magnetite content, though hardly any magnesioferrite was formed. The formation of relatively coarse crystals of magnetite (up to 45 μ) weakened the structure, as was also indicated by the high fracturing observed in the forsterite concretion.

A study of the microstructure of the forsterite refractories we obtained showed that the most stable systems were dunite refractories containing a small amount of MgO (5%) with 1 or 2% of TiO_2. Samples containing 20% of MgO and 1-2% of TiO_2 had a stable structure but, as was noted, the presence of free periclase is undesirable under working conditions in the cement industry [1].

Fig. 5. Action of Portland cement clinker on samples of refractories containing various amounts of MgO.

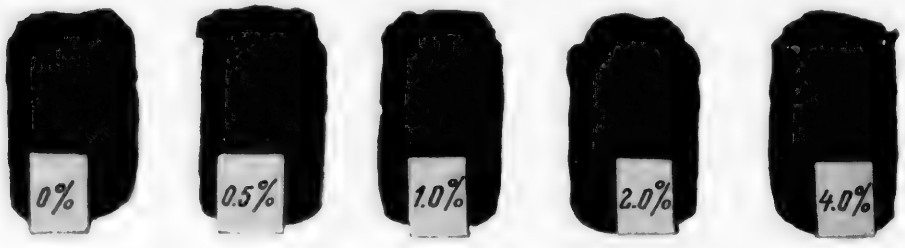

Fig. 6. Action of Portland cement clinker on samples of dunite refractories containing various amounts of TiO_2.

TABLE 2

Granular Composition of Raw Material Mixtures

Granular composition (in mm)	Residue on sieve (in %)					
	3	2	1	0.5	0.5	—
1	—	15	20	10	55	100
2	—	5	15	20	60	100
3	—	—	10	25	65	100
4	—	—	—	30	70	100
Control	5	15	20	5	55	100

The phase composition of the forsterite refractories was studied by means of x-ray structural analysis on a URS-50I apparatus (CuKα, Zn filter). The x-ray pictures obtained are presented in Fig. 4.

Together with x-ray pictures of forsterite refractories containing various amounts of periclase,(0.5, 10, 15 and 20% of roasted magnesite powder was introduced into the dunite mixture; curves III–VII), we give x-ray pictures of "MK" grade magnesite powder (curve I), raw dunite (curve II), and a titanium-containing (2% TiO_2) forsterite refractory (curve VIII).

The x-ray picture of magnesite powder showed five main lines of periclase and very weak lines of forsterite and clinoenstatite. Dunite was represented by main characteristic lines and also by serpentine and fayalite. The forsterite lines were shown quite clearly by all refractories from those based on dunite without

TABLE 3

Firing Conditions for Forsterite Refractories

Furnace No.	Trolley No.	Temperature on burners (in °C)								Firing time, (hours)	
		4	6	8	10	12	14	16	18	total	cycle
1	96	1450—1460	—	1500—1500	—	1570—1570	—	1560—1570	—	12.55	1.26

TABLE 4

Properties of Forsterite Refractories from Mixtures of Various Granular Compositions

Mixtures	Granular composition number of mixture	Weight by volume of raw material (in g/cc)	Firing shrinkage (in %)		Compression strength (kg/cm^2)	Apparent porosity (in %)	Weight by volume of refractory (g/cc)	Water absorption (in %)
			on height	on diameter				
I								
Dunite 93%, magnesite 7% (roasted),	1	2.627	1.24	1.48	150	28.5	2.35	12.0
	2	2.610	1.10	1.32	148	29.1	2.35	12.4
	3	2.592	1.68	1.57	150	28.6	2.36	12.2
	4	2.601	1.84	1.33	202	28.2	2.38	11.8
II								
Dunite 93%, magnesite 7% (roasted), 1% (of 100%) TiO_2	1	2.640	1.35	1.64	200	27.2	2.30	11.4
	2	2.618	1.36	1.95	212	28.0	2.39	11.7
	3	2.628	1.65	1.34	257	27.6	2.40	11.5
	4	2.605	2.28	2.18	288	27.9	2.41	11.6
III								
Dunite 100%, 1% (of 100%) TiO_2	1	2.618	1.67	1.77	162.5	28.3	2.38	11.8
	2	2.623	1.36	1.48	178	28.6	2.39	12.0
	3	2.618	1.30	1.51	203	29.4	2.37	12.4
	4	2.576	3.30	1.92	286	27.5	2.41	11.4
Control: dunite 75%, magnesite 25% (roasted)	Factory	2.695	1.43	1.22	233	25.8	2.47	10.5

TABLE 5

Composition of Raw Material Mixtures and Their Granular Composition

Composition	Residue on sieve (in %)								Total
	3	2	1	0.5	0.2	0.09	0.06	0.06	
Calculated . . .	—	—	10	25	10	15	15	25	100
Obtained							Below 0.09 mm		
A	—	2.2	12.6	19.0	16.0	19.7	30.4		100
B	—	3.2	15.5	16.2	10.4	20.1	Below 0.09 mm 34.5		100

TABLE 6

Firing Conditions for Forsterite Refractories

Furnace No.	Trolley No.	Temperature (in °C) burners 4	6	8	10	12	14	16	18	Firing time (in hours) total	cycle
1	322	1460—1480	—	1540—1540	—	1580—1580	—	1580—1580	—	12.05	1.4

TABLE 7

Properties of Forsterite Refractories

Group and composition	Weight by volume of raw material (g/cc)	Firing shrinkage (in %): on length	on width	on thickness	Compression strength (kg/cm²)	Water absorption (in %)	Apparent porosity (in %)	Weight by volume (g/cc)	Deformation under a load of 2 kg/cm² (in °C): initial	breaking	Heat resistance: water heat cycles: beginning of destruction	20% loss in weight	Refractoriness (in °C)
A — 100% dunite, 1% TiO_2	2.54	2.36	2.41	2.61	230	9.1	23.2	2.50	1650	Above 1650	2	13	> 1750
B — 93% dunite, 7% roasted magnesite, 1% TiO_2	2.57	1.51	1.05	1.62	252	11.5	27.3	2.40	1560	1620	6	7	> 1750
C — 75% dunite, 25% roasted magnesite (factory mixture)	2.61	1.02	0.68	1.04	228	9.9	25.5	2.52	1600	165(	2	10	> 1750

additives up to refractories containing from 5 to 20% of roasted magnesite. The intensity of the forsterite lines was somewhat lower only for refractories based on dunite without additives. With an increase in the MgO content, the intensity of the periclase lines of the refractory increased. When 5% of magnesite was introduced, periclase lines were absent, indicating that the MgO was used in the formation of forsterite and partially in the formation of magnesioferrite. Fayalite and hematite lines were absent. When 10% of MgO was introduced there were lines of free periclase, magnesioferrite, and hematite, and a few very weak lines, whose nature we were unable to determine. At 15 and 20% of MgO, the x-ray pictures of the forsterite refractories were the same as those of industrial forsterite refractories; the intensity of the periclase lines was weaker for 15% of MgO than for 20%.

From the point of view of phase composition, the addition of MgO to the dunite mixture had no essential effect on the structure of the forsterite refractory.

Investigation of the x-ray pictures of titanium-containing forsterite refractories (98% dunite + 2% TiO_2) showed (curve VIII) that when titanium dioxide was introduced into the mixture, magnesium titanates and also hematite were formed; the periclase content fell. When 4% of TiO_2 was added to the mixture, magnetite lines appeared and there was some intensification of the weak magnesium titanate lines. There were no free TiO_2 lines.

The action of Portland cement clinker on the forsterite refractories we prepared was tested by the contact treatment method. The reagent we used was clinker from the "Gigant" cement plant containing (in %):

C_3S 52.3, C_2S 21.2, C_3A 11.3, C_4Ar 11.6, MgO 3.4, $CaSO_4$ 0.67. The results of the tests are shown in Figs. 5 and 6. Figure 5 shows the action of clinker on forsterite refractories with various roasted magnesite contents, but with no TiO_2 introduced. For dunite refractories without MgO added and with 5% of MgO added, the interaction with the clinker was very slight. The cement clinker interacted more strongly with refractories containing 20% of MgO. During the interaction of clinker with the refractory, in the upper part of the latter appeared dark, consolidated zones, inside which magnetite, monticellite, and pyroxenes were formed. Coarse grains of periclase were dispersed during the process.

Figure 6 shows the action of cement clinker on forsterite refractories containing various amounts of TiO_2.

A study of the microstructure showed that when TiO_2 was absent from the refractories, magnetite and pyroxenes were formed by interaction with cement clinker. When TiO_2 was present in the refractory, monticellite and anisotropic, needle-like magnesium titanates were formed.

Thus, the investigation showed that the addition of 1-2% of TiO_2 to a dunite mixture promoted better formation of forsterite concretion and an increase in the density and strength of the refractory material. A reduction in the amount of roasted magnesite in the forsterite refractory raised the heat resistance and resistance to the action of cement clinker.

To raise the quality of forsterite refractories we also studied the effect of the granular composition of the mixture. We took four proportions: I) 93% dunite and 7% roasted magnesite, II) 93% dunite, 7% roasted magnesite and 1% (of 100%) technical TiO_2, and III) 100% dunite and 1% (of 100%) TiO_2. As a control, we took mixture IV, consisting of 75% dunite and 25% roasted magnesite, corresponding in granular composition to the normal factory mix of the Panteleimonov plant (Table 2).

The roasted magnesite and titanium dioxide were finely powdered. The mass after mixing was moistened with sasw (with a density of 1.243 g/cc) on laboratory rollers.

The samples were pressed at 850 kg/cm^2 on a PG-100 press. From each mixture we prepared 7 cylinders with D = 70 mm and h = 60 mm. The dried samples were fired in a factory tunnel furnace No. 1. The firing conditions are given in Table 3.

The results of testing the fired refractories are given in Table 4.

Testing the refractories obtained showed that in all cases the elimination of coarse fractions of dunite from the granular composition raised the compression strength of the objects. The porosity remained almost constant. Forsterite refractories with a low MgO content without titanium dioxide added were found to be too weak at the granular compositions chosen. The addition of a small amount (up to 1%) of titanium dioxide to dunite with a low MgO content made it possible to obtain forsterite refractories whose properties surpassed the technical requirements for normal forsterite refractories.

On the basis of the results obtained, we prepared small batches of industrial refractories from three mixtures: A) 100% dunite + 1% TiO_2, B) 93% dunite + 7% roasted magnesite + 1% TiO_2 and C) 75% dunite + 25% roasted magnesite. The composition of mixture C (control) was the normal one used in a plant. The compositions of the raw material mixtures and their granular compositions are given in Table 5.

The masses were moistened with sasw with a density of 1.225 g/cc, mixed on rollers and pressed on an eight-mold revolving press.

From each mixture we prepared 12 bricks with the dimensions 200 × 120 × 70/62 mm. The dried bricks were fired in a factory tunnel furnace No. 1. The firing conditions are given in Table 6.

The forsterite refractories made were tested. The results of the tests (Table 7) showed that the forsterite refractories (based on dunite containing TiO_2 and also a small amount of MgO) had a sufficient density and compression strength.

Forsterite refractories with 1% of TiO_2 added to the dunite were of particular interest. These refractories had a high density, satisfactory strength and heat resistance, and a high deformation temperature under a load of 2 kg/cm^2.

SUMMARY

1. Forsterite refractories made with a low periclase (5-7%) and titanium dioxide (1-2%) contents have a high density, heat resistance, and resistance to the action of Portland cement clinker.

2. In a forsterite refractory based on dunite with up to 2% TiO_2 added, monticellite and magnesium and magnesium titanates were formed, forsterite concretion was improved, and magnetite was absent. The refractories show promise for use as linings of rotating cement furnaces.

3. When more than 10% MgO was introduced into the dunite mixture, the forsterite refractory contained free periclase, the magnesioferrite content increased and, in addition to monticellite, there appeared hematite and magnetite and also new growths whose nature was not established (detected by the appearance of weak lines during x-ray phase analysis). The resistance of such a forsterite refractory to the action of Portland cement clinker was reduced.

A. I. Uzberg, B. A. Fainerman and N. S. Mitrokhina assisted in the preparation and testing of the forsterite refractories.

LITERATURE CITED

[1] P. P. Budnikov and B. N. Bogomolov, Ogneupory 4 (1959).

[2] A. S. Berezhnoi, Coll. Trans. Inst. Refractories (Kharkhov) [in Russian], 2 (1958).

[3] D. A. Kissin, Ogneupory, 11 (1939).

[4] A. S. Frenkel', Stal', 2 (1950).

[5] V. I. Sinyanskii, L. E. Solomon, and A. P. Khetya, Ogneupory, 5 (1957).

[6] S. V. Glebov, Trans. Inst. Refractories (Leningrad) [in Russian], 18, 66 (1939).

[7] P. P. Budnikov and V. I. Endovitskii, Doklady Akad. Nauk USSR 4, 35 (1940).

[8] Ya. V. Klyucharov, Trudy Giprotsementa 13, (1950).

[9] D. S. Belyankin, B. V. Ivanov, and V. V. Lapin, Petrography of Technical Rocks, [in Russian] (Promstroiizdat, Moscow, 1952) 200.

Received April 22, 1959

CHEMICAL SELECTION OF SCHEELITE AND CALCITE IN ORES WITH REGENERATION OF THE REAGENTS*

A. S. Chernyak

Irkutsk State Scientific Research Institute of Rare Metals

In a previous communication [1] we formulated certain general problems in the chemical selection of minerals and demonstrated an approach to their solution on the example of low grade carbonate-phosphate ores. The results thus obtained stimulated new investigations on chemical selection with regeneration of the reagents applied to combinations of minerals whose separation is of interest to the rare metal industry. Below we give the results of investigations on the separation of the pair of minerals "scheelite-calcite."

The mechanical separation of scheelite ($CaWO_4$) from calcite ($CaCO_3$) is a very difficult problem in the enrichment of skarn scheelite ores, the most important source of tungsten. Despite the great possibilities of the flotation method of enrichment, it does not achieve complete separation of these minerals. The reasons for this are, on the one hand, their fine interpenetration and the impossibility of a mechanical separation of attachments with practically acceptable grinding of the ores and, on the other hand, sedimentation of the minerals during pulverization of the crude concentrates before separatory flotation.

Figure 1 shows examples of the close association of scheelite and calcite in crude concentrates from one of the factories operating. In these concentrates, which contained 5-6% of WO_3, a quarter of the scheelite was in attachments with calcite. Scheelite inclusions in the carbonate (Fig. 1,a) had dimensions of 10-30 μ. The scheelite grains (Fig. 1,b) contained calcium carbonate inclusions with a size of from 75 × 100 to 10 × 20 μ. At the same time, selective concentrates of this factory, containing 56% of WO_3, consisted mainly of a mass of free grains of scheelite and calcite from 25 × 25 to 0.8 × 0.8 μ in size. The calcite content of these concentrates was above 20-25% but subsequent mechanical separation of the minerals in this case was difficult and accompanied by considerable losses of scheelite with the carbonate product. According to data from exploratory work of V. V. Shubina (Irgiredmet), in another of our factories the losses of scheelite with carbonate products reach 30-50%, relative to the amount processed.

Thus the flotation selection process has a low efficiency and is uneconomical in a number of cases. Moreover, the high carbonate content of the scheelite concentrates complicates their subsequent processing, causing a high consumption of reagents both in sintering with sodium carbonate and silica sand and also when the acid method is used.

In the tungsten industry chemical enrichment of carbonate – scheelite products is sometimes used and this consists of solution of the carbonates in hydrochloric acid [2]. The acid consumption reaches 300-600 kg per ton of enriched concentrates. Not to mention a series of technical disadvantages associated with the use of hydrochloric acid, we should note that the acid consumed in solution of the carbonates cannot be regenerated by any acceptable method. In addition, acid decomposition of the carbonates is usually accompanied by 5-10% losses of tungsten.

* Communication II on the chemical selection (with regeneration of the reagents) of practically important combinations of minerals difficult to separate by mechanical treatment of the ores.

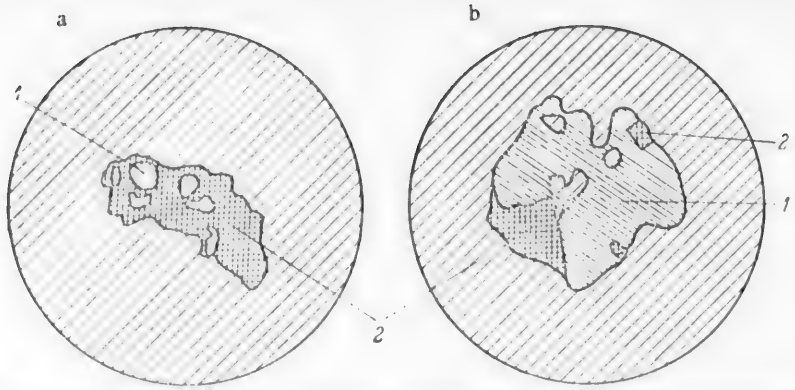

Fig. 1. Attachments of scheelite and calcite in crude factory concentrate. a) Fine inclusions of scheelite in calcite, b) inclusions of calcite in scheelite. 1) Scheelite, 2) calcite. Drawings from polished microsections. Magnification 130.

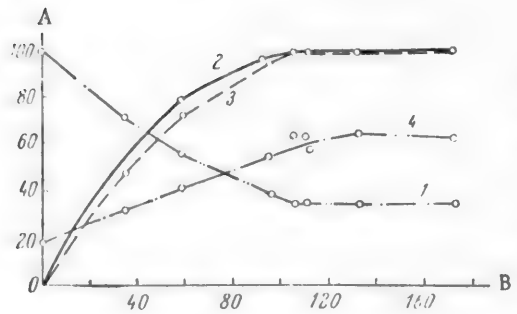

Fig. 2. Selective leaching of calcite from a synthetic mixture of scheelite and calcite. A) Amount (in %), B) H_2SO_3 charge [in % of theoretical required to convert $CaCO_3$ to $Ca(HSO_3)_2$] 1) Solid residue, 2) $CaCO_3$, 3) calcium carbonate in solution, 4) WO_3 in solid residue.

In the light of what has been said, there is considerable interest in chemical methods of separating calcite from scheelite with regeneration of the reagents, based on selective solution of the calcite to leave the scheelite in the original mineral form.

We studied two such methods in which sulfurous acid and ammonium chloride were used.

Selection in sulfurous acid (aqueous solutions of sulfur dioxide) was based on the different stabilities of calcite and scheelite in solutions of this acid. Carbonates of alkaline earth elements, including calcite, are rapidly and completely decomposed by solutions of sulfurous acid at room temperature and acid concentrations from 5 to 100 g/liter. Solution is complete in 20-60 minutes.

We have examined the chemistry of the solution of calcite and the regeneration of sulfurous acid previously [1]. After the solution of calcium bisulfite has been separated from the insoluble scheelite, half of the SO_2 used is readily recovered from it (by heating or blowing through the solution) as quite concentrated gas. Calcium sulfite, $CaSO_3 \cdot 2H_2O$, is simultaneously precipitated quantitatively from the solution and the second half of the acid used is regenerated from this.

Let us examine actual experimental data on the separation of scheelite and calcite with sulfurous acid and regeneration of the acid.

The effect of the concentration of the sulfurous acid solution on the completeness of solution of calcite with a grain size of 0.2 mm, and a sulfurous acid charge of 110% of theoretical over a period of 20 minutes is given below.

Concentration of starting solution with respect to H_2SO_3 (g/liter)	5.6	11.0	21.0	36.0	47.0
Calcium carbonate extracted into solution (in %)	99.15	99.12	98.89	99.02	99.03

The data presented show that even with low H_2SO_3 concentrations (from 5.6 to 47.0 g/liter) the calcium carbonate dissolved practically completely in the sulfurous acid solution. The acid charge need not exceed 105-110% of the theoretical amount required to decompose the calcite and form calcium bisulfite. This is graphically confirmed by data given in Fig. 2. With a smaller charge of acid, part of the calcium remained in the solid residue as sulfite (Fig. 2, curves 2 and 3).

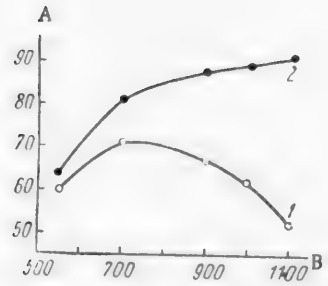

Fig. 3. Reduction of calcium sulfite with charcoal for regeneration of sulfur. A) Degree of reduction of sulfur (in %), B) temperature (in °C). Reduction: 1) to S^{2-}, 2) total to S^0 (sublimate) and S^{2-}.

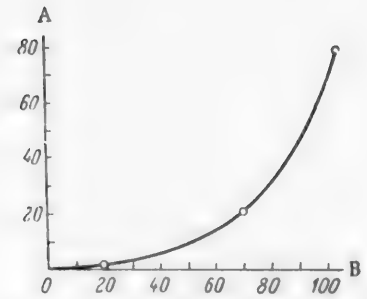

Fig. 4. Relation between degree of solution of calcite and the solution temperature. A) Degree of solution of calcium carbonate (in %), B) temperature (in °C). Duration of experiments, 4 hours, calcite grain size, 0.2 mm.

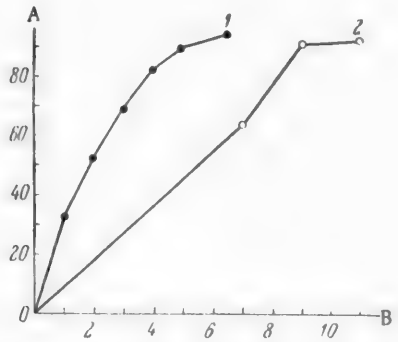

Fig. 5. Duration of leaching of calcite from carbonate-scheelite factory products with ammonium chloride solutions. A) Degree of solution of calcium carbonate (in %), B) duration of leaching (in hours). 1 and 2) The products of two factories.

As experiments showed, scheelite does not interact with sulfurous acid and due to this there are no tungsten losses when the carbonates are dissolved. The stability of scheelite in solutions with an H_2SO_3 concentration of 70-100 g/liter makes it possible to dissolve carbonates in quite dense pulps.

Leaching of calcite at H_2SO_3 concentrations of from 5 to 95 g/liter from synthetic mixtures of scheelite and calcite, containing 18.9% of WO_3 and 36.95% calcium carbonate (66% calcite), made it possible to obtain scheelite concentrates containing 62.1-62.4% of WO_3 with a 2/3 reduction in weight of the starting mixture. The residual calcium carbonate content of the concentrate was 0.95-1.05%. The degree of solution of the calcite was 99%. The solution was carried out at 20° for 20 minutes; the H_2SO_3 charge was 110% of the theoretical consumption for the calcite.

Sulfurous acid (45 g/liter of H_2SO_3) treatment of factory carbonate-scheelite intermediate flotation product, containing 19.56% of WO_3 and 39.76% of calcium carbonate, yielded a conditioned scheelite concentrate with a 75.9% content of WO_3 and only 0.76% of calcium carbonate with a 3/4 reduction in the weight of material. The treatment was without heating, leaching lasted for 2 hours, and the charge of H_2SO_3 was 110% of the theoretical for the calcite.

The filtrates after leaching of calcite from the synthetic mixture of minerals and from the flotation product were checked for tungsten content by qualitative chemical and semiquantitative spectral analyses. Dry residue from the solution was analyzed by the spectral method. No tungsten was detected in the solution by any of the methods.

According to spectral analysis data, dry residues from the solutions contained, apart from calcium and magnesium, only tenths of a percent of manganese, and traces of iron and tin, which confirmed the selective nature of the solution of the carbonate in sulfurous acid.

The regeneration cycle of the solvent was carried out on a laboratory scale. Of the possible methods of regenerating SO_2 bound in normal calcium sulfite, according to data from an investigation, one of considerable interest is the firing of calcium sulfite with charcoal at 700° and this leads to 80% of the sulfur as S^0 and S^{2-}

(Fig. 3). The reduced product may be treated with steam with subsequent burning of the hydrogen sulfide and elementary sulfur to SO_2 by the scheme which is well known in industry.

Thus, complete regeneration of the reagent used is possible. It should be noted that with regeneration of only half of the amount of SO_2 consumed, the method in which this solvent is used is more economical than the solution of carbonates in hydrochloric acid used at the present time.

Selection of scheelite and calcite by ammonium chloride solutions. Examples are known where this reagent is used for the solution of carbonates in the chemical enrichment of uranium ores [3] and for high enrichment of phosphate concentrates [4].

A characteristic of the method is the simplicity of the scheme for regeneration of the reagent. Solution of carbonates (on the example of calcite) proceeds according to reaction (1), going from left to right when the pulp is heated:

$$CaCO_3 + 2NH_4Cl \rightleftarrows \underset{\text{(solution)}}{CaCl_2} + 2NH_3\uparrow + CO_2\uparrow + H_2O. \qquad (1)$$

After separation of the calcium chloride solution from the undissolved residue, ammonia and CO_2 liberated when the carbonate dissolved is passed through this solution. Reaction (1) then proceeds from right to left. After separation from the calcium carbonate precipitate, the regenerated ammonium chloride solution is again used for processing fresh portions of ore.

An investigation showed that this method could be used successfully for separating scheelite and calcite. Under quite aggressive conditions of calcite decomposition by ammonium chloride solutions (an NH_4Cl concentration in the solution of up to 20% and a temperature of 103-104°) scheelite was completely unchanged and all the tungsten remained in the insoluble residue.

The results of experiments with ammonium chloride were very close to those obtained when sulfurous acid was used. For example, leaching calcite from the synthetic mixture with the composition given above yielded a scheelite concentrate with a WO_3 content of 62.2-62.7% and a residual calcium carbonate content of not more than 0.9%. The weight of the ore was thus reduced by a factor of approximately three (32-34% yield of residue).

As analyses of the filtrates showed, the NH_4Cl consumption was approximately the stoichiometric amount required for the calcite. Dry residue from the filtrate was analyzed for tungsten by qualitative chemical and semiquantitative spectral methods. No tungsten was detected in the filtrates. Calcite was dissolved successfully when the grain size of the starting material was 0.074 mm and 0.21 mm.

Leaching of calcite from factory carbonate-scheelite flotation product yielded a concentrate with a WO_3 content of 76.1% when the original content was 19.6% WO_3. The weight of the ore was reduced by 3/4. The calcium carbonate content of the concentrate obtained was 1.04%. No tungsten was lost into the filtrate. It is characteristic that the calcium-containing solution (filtrate) contained little impurity. Spectral analysis showed that dry residue from the solution contained only hundredths of a percent of strontium and magnesium apart from calcium.

We should draw attention to the dependence of the rate of solution of calcite in ammonium chloride on the solution temperature (Fig. 4) and to the kinetics of solution of this mineral at the optimal temperature (Fig. 5). Judging by the curve in Fig. 4, the rate of solution of calcite increases considerably with a rise in the temperature at which the process is carried out. It is therefore recommended that leaching is done at the boiling point (103 104°) of a 20% solution of NH_4Cl. The process usually lasts for 5 — 9 hours. It can be assumed that leaching calcite with ammonium chloride solutions at a higher temperature (under pressure but with removal of the NH_3 and CO_2 liberated from the working space of the autoclave) would make it possible to shorten the calcite leaching time.

In conclusion, the author considers it his duty to thank O. T. Grebennikova for assistance in studying the composition of carbonate — scheelite concentrates and N. L. Kalayanova for participating in the experiments.

SUMMARY

1. Two methods were proposed and studied for the complete chemical selection of scheelite and calcite with regeneration of the reagents used, namely, sulfurous acid and ammonium chloride. The results of the selection were checked on crude factory concentrates.

2. In comparison with solution of calcite with hydrochloric acid, which is used in the tungsten industry, the methods developed are undoubtedly advantageous due to the possibility of regenerating the reagents.

3. The two methods may be of interest in systematic chemical analysis of ores and evidently they may also be used for separating scheelite from magnesium carbonates.

LITERATURE CITED

[1] A. S. Chernyak, Zhur. Priklad. Khim. 30, 7, 844 (1957).*

[2] Mining Congr. J. 39, 1 (1953).

[3] I. Ya. Bashilov, Introduction to the Technology of Rare Elements [in Russian] (State Chem. Tech. Press, 1932).

[4] L. M. Chernyi, Trans. Conference on the Theory and Practice of Flotation Enrichment, [in Russian] (Acad.Sci. USSR Press, 1952).

Received October 30, 1958

* Original Russian pagination. See C. B. translation.

STATE OF COPPER SULFIDE IN IRON-CONTAINING SILICATE MELTS

S. E. Vaisburd and V. L. Kheifets

Planning and Scientific Research Institute of Gipronickel'

Silicate melts containing metal sulfides in a dissolved state are of definite interest as an example of systems capable of forming homogeneous solutions of a nonelectrolyte with semiconductor properties (sulfide) in a liquid with the characteristics of an electrolyte (silicate). The problem of the behavior and state of sulfides in such melts is also of substantial practical interest as solution losses of certain metals with slags and also desulfurization processes are determined to a large extent by sulfides dissolved in slags. In the present work we studied iron-containing silicates with iron and copper sulfides added.

EXPERIMENTAL

The method adopted in the work for measuring the decomposition voltage of liquid slags on platinum electrodes and the methods of processing the experimental data were described in detail previously [1]. The choice of a solution of Cu_2S in a silicate melt as a subject for investigation was determined by the fact that copper is present in liquid slags only as the lower sulfide and not in the oxidized form [2, 3]. This should be regarded as referring only to slags in contact with a sulfide melt; in the absence of the sulfides it is possible to obtain a silicate melt containing cuprous copper [4].

The addition of copper sulfide to a silicate melt leads to the simultaneous appearance of two new elements, copper and sulfur, in the slags studied previously [1]. It was therefore necessary to determine the effect of the presence of sulfur in the slag on the results of the measurements. For this purpose we tested silicate melts with additions of FeS since for slags containing iron silicates, one new element, sulfur, appears in this case. Iron sulfide was chosen, as the bulk of the sulfur in slags is determined by the presence of FeS in them [2]. The amount of iron sulfide added to the silicates corresponded to the sulfur content of normal slag for nickel production, i.e., from 0.1 to 0.5 weight %.

In the work we used silicate melts of the system $CaO-FeO-SiO_2$, but the melts also contained a small amount of MgO (as a result of solution of crucible material) and Fe_2O_3. We also tested polycomponent silicate melts, corresponding in composition to industrial slag from shaft smelting of copper-nickel sulfide ores. Copper was introduced into this slag as the sulfide in an amount corresponding to the normal average content of it in such slags (of the order of 0.1 weight %). As this gave slags with considerably less sulfur than is normally contained in industrial slags, the rest of the sulfur was added in the form of iron sulfide.

The experiments were carried out in magnesia crucibles in an atmosphere of purified nitrogen at 1250 ± 5°. After measurement of the decomposition voltage E, the slags were chilled in a stream of nitrogen. A sample of the cooled slag was carefully withdrawn under a binocular magnifier MBS-2. The chosen sample, which was a silicate part without sulfide or metallic inclusions, was completely analyzed chemically. The analysis data were used for calculating the ionic composition of the slag and the decomposition voltages E^0, allowing for the ferric iron content of the slag [1].

The results of the experiments are given in the table.

The concentrations of ferrous and ferric iron in the slag are given in ionic fractions $N_{Fe^{2+}}$ and $N_{Fe^{3+}}$; the basicity of the slag is expressed by the value $\frac{\Sigma MeO}{2SiO_2}$ and in accordance with this the slags were divided into three

Effect of Sulfur and Copper in Slags on the Decomposition Voltage

Contact in slag (weight %)		Additive	$\frac{\Sigma MeO}{2SiO_2}$	$N_{Fe^{2+}}$	$\log N_{Fe^{2+}}$	$N_{Fe^{3+}}$	E (in mv)	$E^{0'}$ (in mv)
S	Cu							
0.11	—	FeS	0.54	0.235	—0.629	0.019	307	369
0.14	—		0.62	0.263	—0.580	0.019	298	360
0.17	—		0.90	0.353	—0.452	0.040	141	105
0.18	—		0.90	0.380	—0.420	0.034	135	120
0.17	—		1.15	0.298	—0.526	0.030	74	74
0.19	—		1.36	0.374	—0.427	0.031	28	25
0.19	—		1.35	0.377	—0.424	0.032	26	20
0.49	—		1.33	0.372	—0.430	0.034	25	12
0.080	0.33	Cu_2S	0.63	0.258	—0.588	0.024	317	349
0.083	0.41		0.64	0.321	—0.493	0.013	200	310
0.09	0.41		1.36	0.368	—0.434	0.034	20	14
0.29 *	0.10	FeS + Cu_2S	0.63	0.342	—0.466	0.022	187	230
Polycomponent slag without sulfides**			0.72	0.344	—0.463	0.029	213	219
—	0.37	Cu_2O	1.32	0.349	—0.457	0.040	27	—9
—	0.37		0.60	0.283	—0.548	0.030	203	205

*Composition of slag (according to analysis data, weight %): FeO 41.56, Fe_2O_3 2.86, CaO 4.76, MgO 8.91, Al_2O_3 4.00, SiO_2 37.50, Cu 0.10, S 0.29.

**Composition of slag (according to analysis data, weight %): FeO 42.10, Fe_2O_3 3.82, CaO 5.24, MgO 8.44, Al_2O_3 4.83, SiO_2 35.70.

types: basic ones when $\frac{\Sigma MeO}{2SiO_2} > 1$; close to orthosilicates when $\frac{\Sigma MeO}{2SiO_2} \approx 1$; and acidic ones when $\frac{\Sigma MeO}{2SiO_2} > 1$. The experimental values values of the decomposition voltage E given are the averages of 5-6 measurements (absolute error of the order of 10 mv).

DISCUSSION OF RESULTS

The results of measurement of the decomposition voltage of slags containing sulfur are given in the figure together with data obtained previously [1] for slags without sulfides. The straight line shows the nature of the change in the decomposition voltage $E^{0'}$ of orthosilicates (i.e., when $\frac{\Sigma MeO}{2SiO_2} = 1$) with a change in the ferric iron content of the melt, with the assumption that the activity coefficient of iron $\gamma_{Fe^{2+}} = 1$.

The results of determining $E^{0'}$ in slags not containing sulfides lie on the diagram in three groups of points, reflecting the behavior of the three types of slags. Points corresponding to slags close to orthosilicates ($\frac{\Sigma MeO}{2SiO_2} =$ $= 0.9-1.0$) lie close to the line; points corresponding to basic slags, which are characterized by positive deviations, lie below it; points corresponding to acidic slags, for which negative deviations are observed, lie above it. The dotted lines drawn through these points only provisionally illustrate the nature of the change in $E^{0'}$ with a change in $N_{Fe^{2+}}$ in basic and acidic slags as, strictly speaking, they should correspond not simply to type of slag, but to a definite basicity value, i.e., a value of the activity coefficient $\gamma_{Fe^{2+}}$ which is constant for a given group of slags.

As can be seen from the figure, points corresponding to slags with sulfides dissolved in them lie in accordance with basicity and the iron content of the slag in the same way as points characterizing slags without sulfides. Number 11 on the figure marks a point corresponding to a polycomponent industrial slag; the point with the number 12 corresponds to a slag of the same composition (with respect to content of slag-forming oxides), but without sulfides. The position of the points shows that the presence of sulfides in the slag does not affect (within the limits of error) the results of the measurements.

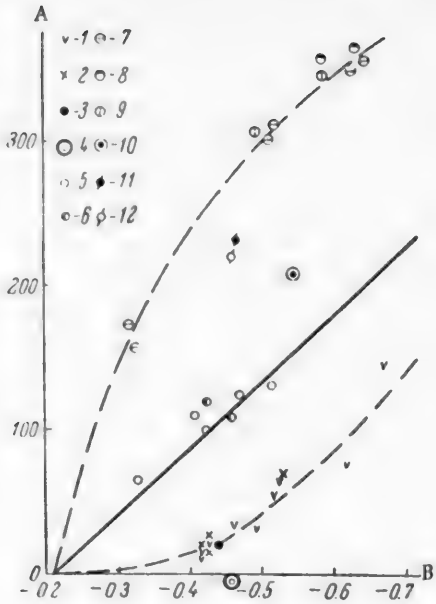

Relation of decomposition voltage to slag composition at 1250°. A) Decomposition voltage $E^{0'}$ (in mv), B) value of lg $N_{Fe^{2+}}$. 1) Basic slags according to data in [1], 2) the same with FeS, 3) the same with Cu_2S, 4) the same with Cu_2O, 5) slags close to orthosilicates according to data in [1], 6) the same with FeS, 7) acidic slags according to data in [1], 8) the same with FeS, 9) the same with Cu_2S, 10) the same with Cu_2O, 11) polycomponent slag of the industrial type and 12) the same without sulfur and copper.

An examination of the data obtained shows that at the concentrations of copper and sulfur tested their simultaneous presence in the slag did not affect the value of the decomposition voltage and neither did it affect the activity of the iron. Thus, when thermodynamic values are being applied to industrial slags, it is sufficient to know the composition of the latter with respect to slag-forming components (oxides), neglecting the presence of sulfides in them.

The table and the figure also give results of measuring the decomposition voltage in acidic and basic slags containing cuprous oxides in the same molar concentrations as in experiments with copper sulfide. As can be seen from the figure, in this case the presence of copper in the slags led to a sharp decrease in the decomposition voltage: the corresponding points lie considerably lower than for slags of the same basicity and with the same iron concentration, but not containing copper in the form of the lower oxide.

Thus, cuprous oxide in the slags leads to a change in the decomposition voltage while the simultaneous presence of copper and sulfur has no effect on this value. As experiments with the addition of iron sulfide showed, the presence of sulfur in the slag does not change the value of $E^{0'}$ and, consequently, does not affect the anode potential. This was to be expected due to the extremely low polarization of the anode and the high iron content of the slag; in the first instance the iron is oxidized on the anode. This change in the decomposition voltage on introduction of cuprous oxide into the slag is due to the fact that the liberation of metal (alloy) on the cathode begins at a more positive cathode potential (in comparison with the same slag without copper) due to the appearance of Cu^+ ions in the slag as a result of dissociation. A similar picture is observed in slags containing nickelous oxide. However, the introduction of copper into the slag in the form of the sulfide does not produce a change in the value of $E^{0'}$, i.e., does not lead to a displacement of the liberation potential of the metal (alloy) on the cathode. This result leads to the conclusion that copper as the sulfide is not present in the slag in the form of the free ion, but forms a stable grouping with the sulfur, similar to an undissociated molecule. This conclusion does not contradict known facts on the characteristics of the solubility of sulfides in iron [5] and manganese slags [6] and on the nature of sulfides themselves, which are undissociated in the liquid state [7, 8].

SUMMARY

1. Comparison of the decomposition voltages of slags containing cuprous oxide, iron sulfide and copper leads to the conclusion that copper sulfide dissolved in an iron-containing slag is present in an undissociated state.

2. The presence of dissolved sulfides of iron and copper in iron-containing slags in amounts corresponding to the concentrations of sulfur and copper in industrial slags has no effect on the thermodynamic activity of iron in the slag.

LITERATURE CITED

[1] S. E. Vaisburd and V. L. Kheifets, Trudy Inst. Gipronikel'-1, 74 (1958).

[2] V. L. Kheifets, T. F. Remen', and N. K. Dmitrieva, Trudy Inst. Gipronikel' 1, 98 (1958).

[3] R. W. Ruddle, Physical Chemistry of the Pyrometallurgy of Copper, [Russian translation](Foreign Lit. Press, 1955).

[4] A. S. Berezhnoi, L. I. Karyakin, and K. E. Dudavskii, Doklady Akad. Nauk SSSR 83, 399 (1952).

[5] Ya. I. Ol'shanskii, Doklady Akad. Nauk SSSR 71, 701 (1950).

[6] J. Bockris, G. Kitchener, S. Ignatowicz, and J. W. Tomlinson, Faraday Soc. 48, 75 (1952).

[7] W. Savelsberg, Z. Elektroch. 46, 379 (1940).

[8] O. A. Esin and I. T. Sryvalin, Zhur. Fiz. Khim. 25, 1503 (1951).

Received September 30, 1958

REACTION OF ALUMINUM WITH CRYOLITE-ALUMINA MELTS

V. P. Mashovets and R. V. Svoboda

Thermodynamic Calculations

The reason for the incomplete current yield of aluminum in the electrolysis of cryolite-alumina melts may be side processes of cathode discharge:

$$\text{incomplete discharge of aluminum } Al^{3+} + 2e \rightarrow Al^{+}, \quad \text{(I)}$$
$$\text{discharge of sodium } Na^{+} + e \rightarrow Na, \quad \text{(II)}$$
$$\text{incomplete discharge of sodium } 2Na^{+} + e \rightarrow Na_2^{+}. \quad \text{(III)}$$

Each of these reactions may also proceed in the absence of external current due to interaction of aluminum with the melt:

$$Al^{3+} + 2Al \rightarrow 3Al^{+} \quad \text{(I')}$$
$$3Na^{+} + Al \rightarrow 3Na + Al^{3+}, \quad \text{(II')}$$
$$6Na^{+} + Al \rightarrow 3Na_2^{+} + Al^{3+}. \quad \text{(III')}$$

These chemical reactions may be regarded as electrochemical ones, consisting of oxidation (anode) and reduction (cathode) processes. For example, reaction (I') may be represented in the form:

$$2Al \rightarrow 2Al^{+} + 2e \text{ (anode process)}, \quad \text{(1a)}$$
$$Al^{3+} + 2e \rightarrow Al^{+} \text{ (cathode process)}. \quad \text{(1c)}$$

Each oxidation process may be coupled with any reduction process. For example, the anode process (1a) may be coupled with the cathode process (2c): $Na^{+} + e \rightarrow Na$, i.e., oxidation of the aluminum to the subfluoride is accompanied by reduction of sodium to the metal.

We calculated [1] the changes in the isobaric potential ΔZ_{1300} and the equilibrium constants of all possible reactions of aluminum with "neutral" cryolite, Na_3AlF_6, and also with "alkaline" and "acid" melts, i.e., containing excess sodium fluoride or aluminum fluoride. The thermodynamic data required for calculating the characteristics of reactions involving sodium subfluoride, Na_2F, are not available. Table 1 gives the characteristics of all the reactions, calculated for comparison for 1 equivalent, i.e., for the exchange of one electron.

As can be seen, all the reactions with cryolite proceed with a considerable increase in the isobaric potential and consequently these reactions cannot proceed spontaneously. With excess sodium fluoride or aluminum fluoride some reactions have $K_e > 10^{-2}$; the most probable of these are reactions No. 6 and 11. Reaction No. 9 even proceeds with a decrease in isobaric potential and consequently must occur spontaneously. However, the formation of aluminum subfluoride with excess sodium fluoride by reaction No. 8, which must precede reaction No. 9, is energetically unfavorable. The sum of reactions No. 8 and 9 is exactly expressed by reaction No. 6. Though reactions No. 6 and 11 are characterized by an increase in the isobaric potential both reactions may proceed to the right as the vapor pressure of the products obtained at 1300° K is considerable.

TABLE 1

Change in Isobaric Potentials and Equilibrium Constants of the Reactions between Aluminum and Components of the Melt

Reaction No.	Reaction	ΔZ_{1300} (in kcal)	e
1	$^1/_3Na_3AlF_6 + {}^1/_3Al \rightleftarrows {}^2/_3AlF_3 + Na$	22.6	$1.6 \cdot 10^{-4}$
2	$^1/_2Na_3AlF_6 + Al \rightleftarrows {}^3/_2NaF + {}^3/_2AlF$	21.4	$2.5 \cdot 10^{-4}$
3	$^1/_5Na_3AlF_6 + Al \rightleftarrows {}^6/_5AlF + {}^3/_5Na$	22.2	$1.9 \cdot 10^{-4}$
4	$^1/_3Na_3AlF_6 + Al \rightleftarrows {}^1/_3AlF_3 + AlF + Na$	28.9	$1.3 \cdot 10^{-5}$
5	$^1/_3Na_3AlF_6 + {}^1/_2AlF \rightleftarrows {}^5/_6AlF_3 + Na$	19.4	$5.5 \cdot 10^{-4}$
6	$2NaF + {}^1/_3Al \rightleftarrows {}^1/_3Na_3AlF_6 + Na$	6.8	$7.3 \cdot 10^{-2}$
7	$NaF + {}^1/_3Al \rightleftarrows {}^1/_3AlF_3 + Na$	14.7	$3.4 \cdot 10^{-3}$
8	$NaF + Al \rightleftarrows AlF + Na$	21.0	$2.7 \cdot 10^{-4}$
9	$^5/_2NaF + {}^1/_2AlF \rightleftarrows {}^1/_2Na_3AlF_6 + Na$	−0.3	1.1
10	$NaF + {}^1/_2AlF \rightleftarrows {}^1/_2AlF_3 + Na$	11.5	$1.2 \cdot 10^{-2}$
11	$^1/_2AlF_3 + Al \rightleftarrows {}^3/_2AlF$	9.6	$2.5 \cdot 10^{-2}$

TABLE 2

Fusion of Al Under Electrolytes in a Sintered Corundum Crucible

	Mole fraction of NaF, cryolite ratio		
	0.8, 4	0.857, 6	1.0, ∞
Duration of experiment (in hours)	4	4	2
Aluminum losses (in g)	0.180	0.468	1.104
Al content of sublimate (in g)	0.121	0.172	0.309
The same (in % of Al loss)	67.3	36.6	28.0
Na content of sublimate (in g)	0.002	0.041	0.890

EXPERIMENTAL

An experimental study of the interaction of aluminum with the electrolyte is possible by several methods:

1. From the loss of metal during its prolonged fusion under the electrolyte in relation to melt composition, temperature, time, etc. Such investigations have been undertaken by many authors; the main difficulties are allowing for the metal loss due to carbide formation (in a graphite crucible) and oxidation. However, the metal losses characterize only the over-all process and give no information on its mechanism.

2. From the change in composition of the electrolyte; the main difficulties are allowing for changes in composition due to side processes, selective absorption by the graphite crucible and evaporation of the melt itself and the reaction products.

3. From the composition of the sublimate as the reaction products are volatile. The main difficulties are protecting the reaction products from oxidation, trapping them completely, and separating them from volatile melt components.

Investigation in a Sintered Corundum Apparatus.

The use of sintered corundum crucibles instead of graphite ones eliminates difficulties due to carbide formation, but makes it necessary to work with an electrolyte saturated with alumina. This makes it extremely difficult to analyze the salt phase so that an investigation of the changes in its composition has to be abandoned.

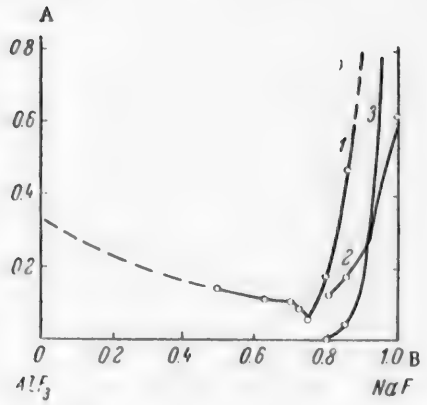

Fig. 1. Results of fusing aluminum under electrolytes in a sintered corundum apparatus. A) Amount of substance (in g). B) NaF content of electrolyte (mole fractions). 1) Aluminum losses; content in sublimates, 2) aluminum, 3) sodium.

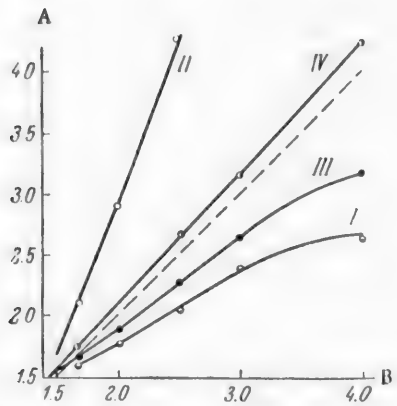

Fig. 2. Change in composition of electrolytes on fusion with aluminum in graphite crucibles. A) Final composition (mole NaF/mole AlF_3), B) initial composition (mole NaF/mole AlF_3). Melt: I) remaining in crucible, II) absorbed by graphite, III) final one, allowing for absorption, IV) evaporating in the absence of aluminum.

The only characteristics that can be investigated are the metal losses and the composition of the sublimates.

The experiments were carried out in a horizontal tubular furnace into which was placed a sintered corundum tube, closed at one end and lined on the inside with copper foil. The sintered corundum tube was tightly connected to an iron tube whose end projected from the furnace and was cooled with a coil to serve as a condenser. Into the hot zone was placed a sintered corundum crucible with a sample of metal (4.5 g) and electrolyte (30 g). Argon was passed into this zone. The emergent gas, carrying the sublimate, encountered screens of perforated copper foil in the zone of 950-1000°. The aluminum subfluoride decomposed here to form a copper – aluminum alloy. The other sublimates condensed in cooler zones.

The temperature of the experiments was 1020° and the duration 4 hours. The loss in weight of the metal was determined by weighting the aluminum button. Determination of the aluminum content of the copper gave the amount of aluminum subfluoride that had sublimed. The condensate was analyzed for NaF, AlF_3 and sodium (as alkali) that had either evaporated in the free form or was formed by decomposition of Na_2F. The sublimates were also subjected to x-ray analysis.

As Fig. 1 shows, the aluminum losses depended on the ratio of the fluorides in the melt and there was a clear minimum corresponding to stoichiometric cryolite (the starting compositions of the salts are given and the final compositions were not determined in these experiments).

Sodium was not detected as alkali in sublimates obtained from "acidic" melts and stoichiometric cryolite ($NaF : AlF_3 \leq 3$). Reduction of sodium evidently did not occur under these conditions. In sublimates from "alkaline" melts ($NaF : AlF_3 \geq 4$) the amount of free sodium was greater the greater the excess of sodium fluoride. Some results are given in Fig. 1 and Table 2.

The data in Table 2 do not make it possible to calculate quantitatively the extent of the separate reactions but can be used for qualitative assessments. The presence of free sodium in the sublimates indicated that reaction No. 6 occurred. The presence of free aluminum (detected in alloys with copper) indicated that reaction No. 6 proceeded through reactions No. 8 and 9, when part of the subfluoride AlF, formed by reaction No. 8, was able to evaporate without undergoing reaction No. 9 and decomposed in the vapor phase by reaction No. 11 going to the left. The amounts of materials did not balance and we are inclined to explain this by the absorption of Na vapor by sintered corundum. Sintered corundum is very strongly corroded in the presence of sodium, probably with the formation of the aluminate and lower oxides or oxyfluorides. As has been stated, the residue of the melt in the crucible could not be analyzed. However, crystallo-optical and x-ray structural methods showed that melts from experiments with pure NaF contained cryolite after the reaction, indicating that reaction No. 6 or 9 occurred.

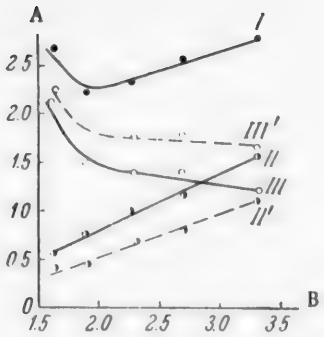

Fig. 3. Aluminum losses in relation to electrolyte composition during fusion in graphite crucibles. A) Aluminum loss (in g), B) melt composition (mole NaF/mole AlF_3). I) Total losses; aluminum consumption, II) in reduction of Na, II') in reduction of NaF to Na_2F, III) in formation of AlF (if NaF is reduced to Na), III') in formation of AlF (if Na_2F is formed).

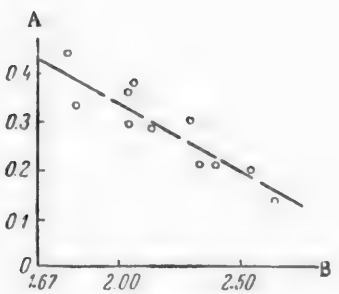

Fig. 4. Amount of aluminum dissolved in 100 g of electrolyte. A) Aluminum content (in %), B) melt composition (mole NaF/mole AlF_3).

The ratio of NaF : AlF_3 in the condensate was always less than in the original melt, i.e., the vapor was enriched in aluminum fluoride. For example, even from "alkaline" melts with a cryolite ratio of 6.0 and 4.0 we obtained "acidic" condensates with a ratio of NaF : AlF_3 of 2.24 and 1.95, respectively. It is interesting that x-ray analysis of these sublimates established that together with cryolite and chiolite* they contained free sodium fluoride. Sodium was evidently reduced by aluminum not only to the metal, but also to the subfluoride, which decomposed on cooling to give free NaF in very "acidic" condensates.

The reduction of sodium from "alkaline" melts was also confirmed by means of radioactive tracers.** For this purpose, into a vertical furnace was placed an iron tube with a welded bottom; on the bottom was placed a sintered corundum crucible with a sample of salts containing the isotope Na^{24} as sodium carbonate. The experimental temperature was 1050°. A counter tube was placed against the upper part of the furnace.

The count rate was taken before and after the introduction of aluminum. It was found that when aluminum was introduced the radiation intensity increased, indicating that the reduction of sodium occurred only in melts containing excess NaF above the cryolite ratio.

When aluminum was heated in "acidic" melts, free sodium was never detected in the condensates. Aluminum was detected in large amounts, the greater the excess of aluminum fluoride in the melt. Thus, reaction No. 11 occurred in "acidic" melts with the formation of the subfluoride AlF, which then decomposed to form an aluminum alloy with the copper screens.

However, here also it was impossible to establish the quantitative relation between the aluminum in the sublimates and the aluminum losses from the original sample. The sublimate always contained a slight excess of aluminum, probably due to deposition of aluminum fluoride on the copper screens which could not be removed completely mechanically.

X-ray analysis of sublimates from "acidic" electrolytes showed that they contained cryolite and chiolite; if the cryolite ratio of the original melt was 1.67 and less, then the condensate also contained free AlF_3 and, in addition, a new phase which was identified as a new compound $NaAlF_4$ that was previously unknown [2].

Investigation in the Presence of Graphite

The interaction of aluminum with the electrolyte in the presence of graphite was complicated by side processes and led to different results.

Samples of aluminum were kept under a layer of electrolyte of given composition in an argon atmosphere; the weight of metal was 15 g and that of salts, 70 g; the temperature was 1060° and in special experiments it was changed to 1150°; the duration of experiments was 3 hours and in individual experiments, from 1 to 5 hours.

*M. S. Beletskii and Yu. G. Saksonov assisted with the x-ray investigations.

**T. A. Potapova assisted with these experiments.

The aluminum and salt phase losses were established by weighing and the change in composition of the melt was determined by hot titration. The aluminum (free or as subfluoride) content of the solidified melt was determined gas-volumetrically.* Allowance was made for the salts penetrating into the graphite by burning the carbon and analyzing the residue for sodium, aluminum and fluorine. The whole of the sodium was considered as NaF and the rest of the fluorine was bound as AlF_3; the excess aluminum was considered either as oxide or bound as carbide and subtracted from the total losses as the formation of Al_2O_3 or Al_4C_3 was not connected with the reactions investigated. This method of calculation is to a certain extent arbitrary, but a more strict calculation is practically impossible.

The loss in weight and change in composition of the melt due to evaporation were established by separate experiments in platinum crucibles. The data obtained made it possible to introduce corrections for selective absorption by graphite and evaporation and establish the change in the electrolyte composition caused only by its interaction with the metal.

In Fig. 2 the broken line corresponds to the composition of the final melt remaining unchanged relative to the initial one; line I corresponds to the directly observed composition of the final melt remaining in the crucible; II represents the composition of the melt absorbed by the graphite; III represents the composition of the final melt if it did not soak into the graphite and finally, IV gives the composition of the final melt if the change had occurred only as a result of evaporation in the absence of metal. Thus, the difference between curves III and IV characterizes the change in composition caused by interaction of the melt with the metal.

The metallic aluminum losses (allowing for the side loss in carbide formation) relative to the electrolyte composition pass through a minimum at approximately $NaF : AlF_3 = 1.9$ as can be seen from curve I in Fig. 3. Here the average composition during the whole of the experiment instead of the initial composition of the melt is plotted on the abscissa.

A knowledge of the over-all aluminum losses and the change in composition of the electrolyte makes it possible to calculate separately the part of the metal consumed in the reduction of AlF_3 to AlF and the part consumed in the reduction of NaF to Na or Na_2F.

The results of the calculations are given in Fig. 3 where curve II shows the aluminum consumed in reduction of sodium to the metal and III gives that consumed in reduction of AlF_3 to AlF. As can be seen, the reduction of sodium also occurred in the very "acidic" region though it also decreased as the NaF content of the melt fell. The formation of aluminum subfluoride proceeded more rapidly the greater the excess of AlF_3 in the melt, especially in the very "acidic" region ($NaF : AlF_3 < 2$). For stiochiometric cryolite the roles of the two reactions were approximately equivalent.

If it is considered that sodium fluoride was reduced only to the subfluoride Na_2F, then the role of this reaction was decreased and the role of AlF formation correspondingly increased as is shown in Fig. 3 by the broken curves II' and III'. With this assumption, the dominating reaction in all the electrolyte compositions investigated was the reduction of AlF_3 to AlF and the effect of the two reactions on the aluminum loss became identical only in very "alkaline" melts ($NaF : AlF_3 > 4$).

The temperature dependence of the aluminum loss was studied over the range 880-1150°. These investigations were carried out in chiolite as, firstly, the use of chiolite made it possible to extend the temperature range into considerably lower temperature and, secondly, the composition of this electrolyte changed little during the experiment (Fig. 2) and this also decreased the calculation errors. It was established that the effect of temperature was very slight. The aluminum losses in a 3 hour experiment increased from 2.02 at 880° to 3.06 g at 1150°. After calculating these losses for the two reactions, we found that the rate of NaF reduction to Na increased by 0.13% per degree and the rate of AlF_3 reduction to AlF increased by 0.53% per degree. Such small temperature coefficients indicate that the limiting stages of the reactions were diffusion processes.

Preliminary data were obtained on the effect of aluminum oxide. The addition of even up to 12 weight % of Al_2O_3 to stiochiometric cryolite apparently had no essential effect on the aluminum losses. The introduction of even 6 weight % of Al_2O_3 into "acidic" electrolytes reduced the aluminum losses by a factor of almost 2. It can be assumed that the presence of aluminum oxide had hardly any effect on the reduction of sodium fluoride, but sharply depressed the reduction of aluminum fluoride to the subfluoride.

*The determinations were carried out by E. L. Zakharov.

The resultsof gas-volumetric determination of free aluminum as a product of subfluoride decomposition in the solidified electrolytes are given in Fig. 4. The composition of the melts corresponds to the moment of solidification of the melt. The aluminum content fell with an increase in th ratio $NaF : AlF_3$ and the general arrangement of the points indicates that the aluminum subfluoride content fell to zero in "alkaline" melts. This is also understandable as in the presence of excess sodium fluoride, aluminum subfluoride that does not evaporate must react vigorously by reaction No. 9. The absolute values we found were higher than those determined previously by other investigators. This may be ascribed to the inert atmosphere we used. The values obtained cannot be regarded as the "solubility" of the subfluoride as saturation was not reached due to its evaporation.

DISCUSSION OF RESULTS

The interaction of aluminum with the molten electrolyte proceeds in essentially different ways in the presence and absence of carbon. In the absence of carbon and in "acidic" and even "neutral" regions, i.e., when $NaF : AlF_3 \leq 3$, aluminum interacts only with aluminum fluoride, reducing it to subfluoride the more rapidly the greater the excess of AlF_3. This reaction also extends into the "alkaline" region. Interaction with sodium fluoride to form subfluoride and metal occurs only in the "alkaline" region and proceeds the more rapidly the greater the NaF excess. However, even in pure sodium fluoride metallic aluminum is oxidized not only to fluoride, bound as cryolite, but partially to subfluoride, which evaporates due to the vigorous nature of the reaction and is unable to react with sodium fluoride. The total aluminum loss in pure sodium fluoride is considerably greater than in pure aluminum fluoride; a minimum loss is clearly observed at stoichiometric cryolite where the reduction of aluminum fluoride is considerably weakened and the reduction of sodium fluoride does not yet occur.

In the presence of carbon the minimum aluminum loss is considerably displaced into the "acidic" region, approximately to electrolytes with the ratio $Na : AlF_3 = 1.9$. This is explained by the fact that although the rate of aluminum fluoride reduction, as in the absence of graphite, increases on going into the "acidic" region, the reduction of sodium extends even into very "acidic" electrolytes, approximately to the ratio $NaF : AlF_3 = 1$. The reduction of AlF_3 to subfluoride remains dominant in "acidic" electrolytes, but even in stoichiometric cryolite the oxidation of aluminum occurs to an equal extent at the expense of AlF_3 and NaF if we consider that the latter is reduced to metallic sodium. If it is assumed that NaF is reduced to Na_2F, then sodium fluoride acquires a dominating role as the oxidant only at $NaF : AlF_3 > 4$.

Thus, the specific effect of carbon is its stimulation of the interaction of aluminum with sodium fluoride even in very "acidic" electrolytes. This effect of carbon may be explained by the formation of compounds of the type NaC_x. At the contact of aluminum with the graphite, there arises the short-circuited galvanic cell $Al/Na^+/C$ in which the graphite plays the part of the positive and the aluminum the negative electrode. As the cell is short-circuited the graphite is polarized to the potential of the aluminum. This potential is insufficient for the discharge of Na^+ ions on the aluminum electrode from "acidic" electrolytes; this follows from the fact that in the absence of graphite the sodium is not reduced by aluminum in "acidic" electrolytes. However, when this potential is applied to graphite (from its contact with the aluminum), the discharge of sodium ions on the graphite electrode becomes possible:

$$Na^+ + xC + e \rightarrow NaC_x.$$

The potential of this process is displaced in a positive direction due to the free energy of bonding of the sodium with the carbon.

This is confirmed by the commonly known fact that graphite or carbon cathodes which are not covered with aluminum are corroded during electrolysis. If potassium ions are introduced into the electrolyte then the corrosion of the carbon is increased as the energy of interaction of potassium with carbon is considerably greater than sodium. A practical result is the fact that in baths with a carbon lining it is advantageous to use "acidic" electrolytes to reduce the aluminum loss. However, this involves a number of complications, namely, high volatility of the electrolyte, a reduced electroconductivity, and a fall in the solubility of alumina. Therefore the use of excessively "acidic" electrolytes is hardly convenient or profitable. If it is possible to realize a bath with a noncarbon lining, then it is best to use stoichiometric cryolite in it.

SUMMARY

1. Thermodynamic calculations on a number of possible reactions showed that the interaction of aluminum with stoichiometric cryolite is very improbable. There may be marked reduction of excess sodium fluoride in "alkaline" melts to give sodium and reduction of excess aluminum fluoride in "acidic" melts to give aluminum subfluoride.

2. Experimental investigation of the reactions in sintered corundum apparatus confirmed the fact that reduction of sodium fluoride occurs only in the "alkaline" region. The reduction of aluminum fluoride to the subfluoride proceeds both in "acidic" and "alkaline" regions, but the rate of this reaction falls with an increase in the molecular ratio of $NaF : AlF_3$. The minimum aluminum loss is observed in stoichiometric cryolite.

3. Investigation in a graphite apparatus showed that the presence of graphite stimulates reduction of sodium, which also occurs in "acidic" melts under these conditions. The minimum aluminum loss in the presence of graphite is observed at a ratio of $NaF : AlF_3 = 1.9$. The effect of graphite is explained by the fact that it binds the sodium evolved.

LITERATURE CITED

[1] R. V. Svoboda and V. P. Mashovets, Trudy VAMI 39, 307 (1957).

[2] V. P. Mashovets, M. S. Beletskii, Yu. G. Saksonov, and R. V. Svoboda, Doklady Akad. Nauk SSSR 113, 1290 (1957). *

Received November 26, 1958

* Original Russian pagination. See C. B. translation.

MECHANISM OF THE DECOMPOSITION OF APATITE BY PHOSPHORIC ACID

M. E. Pozin, B. A. Kopylev, and D. F. Zhil'tsova

Leningrad Lensoviet Technological Institute

The production of double superphosphate, like that of simple superphosphate, has an essential shortcoming, namely the low rate of the process at the product curing stage. To achieve a high degree of decomposition it is necessary to store the product for a long period. When all the optimal conditions are maintained as regards concentration, acid norms, and temperature, the degree of decomposition of apatite by phosphoric acid in the chamber product equals approximately 55%, but after 15 days storage it is about 80-85% [1]. Previous investigations have been directed at studying the optimal conditions and shortening the curing period of double superphosphate [1, 2]. However, neither increasing the acid norms nor changing the temperature led to appreciable shortening of the second stage of the process, i.e., curing of the product.

The decomposition of phosphates in the production of double superphosphate begins in pure phosphoric acid and ends in saturated solutions of the system $CaO-P_2O_5-H_2O$. The composition of the liquid phase changes continuously during the whole course of the reaction. Thus, not only the magnitude of the driving forces, but also other factors determining the rate of the process may change during the decomposition process.

Previous investigations in this field have pertained either to decomposition of phosphate in a large excess of pure phosphoric acid when the possibility of saturation of the solution with salts and crystallization of the latter is excluded [3] or to solution in saturated solutions of the system $CaO-P_2O_5-H_2O$ with a large excess of the liquid phase [4, 5]. These investigations, which made it possible to draw a number of valuable conclusions, were carried out under conditions which differed considerably from the industrial ones. Therefore it seemed interesting to study the decomposition of apatite under the conditions used practically, i.e., with industrial ratios of acid and phosphate, and the present investigation is devoted to this.

EXPERIMENTAL

To solve the problem of determining the rate of double superphosphate formation under production conditions, we carried out experiments at the solid : liquid ratios used practically. In this case there was a considerable change in the acid concentration, degree of supersaturation of the solution by monocalcium phosphate, etc., during the process. In addition to the solid : liquid ratio, the concentration and temperature of the starting acid are of great importance in the interaction of apatite with phosphoric acid. In this connection experiments were carried out with various acid concentrations at different temperatures and different norms, i.e., amounts of acid. The effect of these factors on the stages of reagent mixing and chamber curing of the product (i.e., in the period 2-3 hours after the beginning of mixing) was studied.

The decomposition rate was determined graphically from the "degree of decomposition – time" curve. Data on the change in the degree of decomposition of apatite by phosphoric acid were published previously [6].

Effect of Acid Concentration on Decomposition Rate. The acid concentration very strongly affected the initial decomposition rate. Thus, acid containing 45.6% P_2O_5 in the stoichiometric amount decomposed apatite at a rate of 0.640 g/min in the 5th minute at 20° while acid containing 53.6% of P_2O_5 decomposed apatite twice as rapidly. Figure 1 gives a 5-minute isochronal curve of the rates (curve III). The initial rates increased with an increase in the acid concentration from 21.0 to 53.6% of P_2O_5. A further increase in the acid concen-

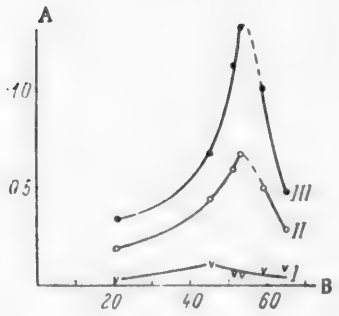

Fig. 1. Isothermal–isochronal relations of the decomposition rate of apatite to the phosphoric acid concentration at 20° and with the stoichiometric amount. A) Decomposition rate (in g/min), B) acid concentration (in % P_2O_5). Time (in min): I) 120, II) 30, III) 5.

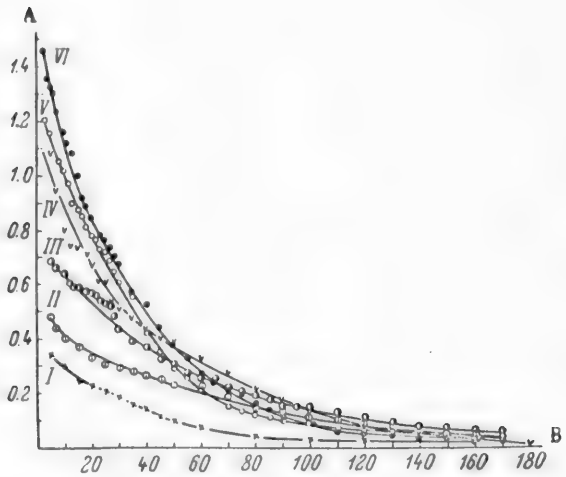

Fig. 2. Change in apatite decomposition rate with time. A) Decomposition rate (in g/min), B) time (in min). Acid concentration (in % P_2O_5): I) 21.0, II) 64.77, III) 45.6, IV) 59.0, V) 51.5, VI) 53.6.

tration led to a fall in the decomposition rate. Thus there is an optimal acid concentration at which the decomposition rate in the initial stage is highest. This may be explained by the fact that with an increase in acid concentration up to 53.6% of P_2O_5, the hydrogen ion concentration increases despite a fall in the degree of dissociation of the acid. A further increase in the acid concentration, which involves a sharp fall in the degree of its dissociation, leads to a decrease in the decomposition rate.

However the acid concentration only affected the initial decomposition rate. As Figs. 1 and 2 show, approximately 60 minutes after the beginning of the experiment the rates for all acids with the exception of 21% P_2O_5 became approximately identical. Thus, as the reaction proceeded the acid concentration hardly affected the decomposition rate.

Effect of Temperature on Decomposition Rate. Like the acid concentration, temperature only affected the initial decomposition rate. Thus, in the 5th minute the decomposition of an apatite concentrate by acid containing 53.6% of P_2O_5 at 20° and with the stoichiometric amount of acid was about 1.3 g/min and at 40°, about 3.7 g/min (Fig. 3), while for 51.5% acid the rates were ~1.14 and 2.4 g/min, respectively (Fig. 4). At temperatures of 40-70° the curves of decomposition rate were much steeper than at 20°.

Despite the fact that the initial rates at elevated temperatures were considerably greater, they decreased considerably more rapidly and even 15-20 minutes after the beginning of decomposition they became less than those at 20°. Only after 60-90 minutes did the decomposition rates become approximately equal and as the decomposition proceeded the temperature had no noticeable effect on the decomposition rate. In general an increase in temperature from 40 to 70° hardly affected the decomposition rate. All the values of the rates for these temperatures lay on one curve.

Effect of Hydrogen Ion Concentration in the System. It is known that partial replacement of phosphoric acid by its salt strongly reduces the rate of phosphate decomposition [3]. In accordance with this, the concentration of hydrogen ions for such systems was calculated from the formula for buffer solutions:

$$C_{H^+} = K_s \cdot \frac{C_a}{C_s \cdot \alpha}.$$

Since we were only interested in the nature of the relation between rate and hydrogen ion concentration and not in their absolute values, it was assumed that $\alpha = 1$ in the calculations. When allowance was made for the actual values of α, the curves of the relation between the rate and the hydrogen ion concentration were displaced into the region of higher values of C_{H^+}. The higher the solution concentration, the greater was the displacement of the curves. However, the nature of the curves did not change. The amount of monocalcium phos-

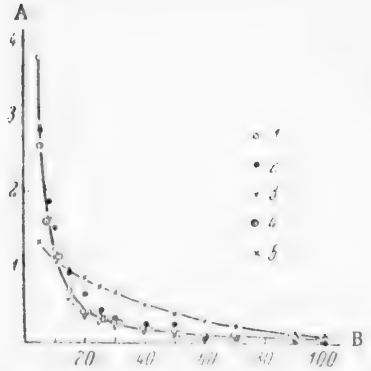

Fig. 3. Rate of apatite decomposition by acid containing 53.6% P_2O_5 at various temperatures. A) Decomposition rate (in g/min), B) time (in min). Temperature (in °C): 1) 40, 2) 50, 3) 60, 4) 70, 5) 20.

phate (C_s) in the liquid phase was determined graphically [3, 7] from the equilibrium diagram of the system $CaO-P_2O_5-H_2O$.

As Fig. 5 shows, the relation between the decomposition rate of apatite concentrate by phosphoric acid (at 20° and with the stoichiometric amount of acid) and the hydrogen ion concentration was curved during the whole of the experiment, though it changed somewhat with time. At the beginning of decomposition, for acids with concentrations of from 45.6 to 59.0% P_2O_5 a decrease in hydrogen ion concentration produced a slow fall in the rate. On the other hand, towards the end of the experiments a small change in C_{H^+} produced a sharp fall in rate.

If the degree of dissociation of the salt is considered in calculating the hydrogen ion concentration, the curves are apparently arranged in a different order. The degree of dissociation of the salt depends on the dilution of the solution. The more concentrated the solution, the smaller is the value of α. Therefore, if α is considered in the calculations, curve III will apparently lie to the right of II and then V, VI, IV and I. However, the mutual disposition of curves IV and V does not change as α for them may be approximately the same or slightly less for IV than for V, i.e., curve IV will always be to the right of V. The arrangement of curves IV and V alone shows that at the same hydrogen ion concentration in the solution the decomposition rates are different. Curve II must lie to the left of all the other curves, i.e., in the region of the lowest hydrogen ion concentrations.

The data presented show that during chamber curing of the product the rate of apatite decomposition by phosphoric acid is not directly proportional to the concentration of hydrogen ions in the system.

Mechanism of the Interaction of Apatite With Phosphoric Acid. From all that has been said above we can apparently draw the conclusion that the decomposition of apatite by phosphoric acid may be divided into two stages. The first, which is a very short stage, has a high temperature coefficient; when the temperature is raised from 20 to 40°, for 51.5% acid the rate in the 3rd minute increases by a factor of 1.73 and for 53.6% acid in the 5th minute, by a factor of 1.68, but as the process proceeds the temperature coefficient decreases and assumes values characteristic of diffusion processes; the first stage is also characterized by high decomposition rates and the acid concentration has an effect on the decomposition rate.

Thus the first stage has all the characteristics of purely chemical reactions whose rate is determined by both temperature and concentrations of the reacting components. In the second stage both acid concentration and temperature have little effect on the decomposition rate and the reaction proceeds as a diffusion process. In the first, very brief moment the decomposition of apatite in the production of double superphosphate proceeds in phosphoric acid that is not saturated with monocalcium phosphate. As the reaction proceeds the liquid phase is saturated with salts. This occurs the more rapidly the higher the concentration of the initial phosphoric acid. Thus, when acid with a concentration of P_2O_5 of 54% is used at 75° and with the stoichiometric amount of acid, the liquid phase is saturated with monocalcium phosphate at approximately 6% decomposition of apatite (K). For acid with 40% P_2O_5 at 75° saturation is reached at $K \simeq 20\%$ and for 20% acid, at $K \simeq 30\%$. With further decomposition the reaction products must crystallize. The presence of a fall in concentration between the boundary layer and the over-all mass of the solution and vigorous stirring possibly would somewhat facilitate the removal of reaction products from the boundary layer. This did not occur in the experiments. It can therefore be assumed that salts will crystallize in the boundary layer to form a film on the apatite grains, hindering the approach of hydrogen ions to the apatite surface.

The fact that the decomposition of apatite in the production of double superphosphate proceeds in two stages indicates that it would be incorrect to describe it by the law characterizing either of these stages.

Chepelevetskii [3] established that in the decomposition of apatite by 20% (with respect to P_2O_5) phosphoric acid at solid: liquid = 1 : 20, the rate of solution was directly proportional to the hydrogen ion concentra-

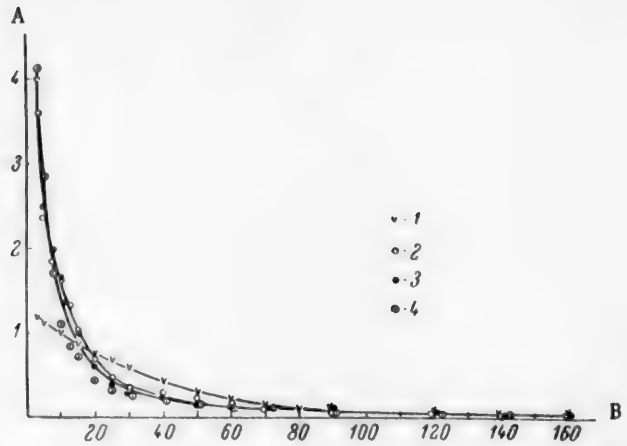

Fig. 4. Rate of apatite decomposition by acid containing 51.5% P_2O_5 at various temperatures. A) Decomposition rate (in g/min), B) time (in min). Temperature (in °C): 1) 20, 2) 40, 3) 50, 4) 60.

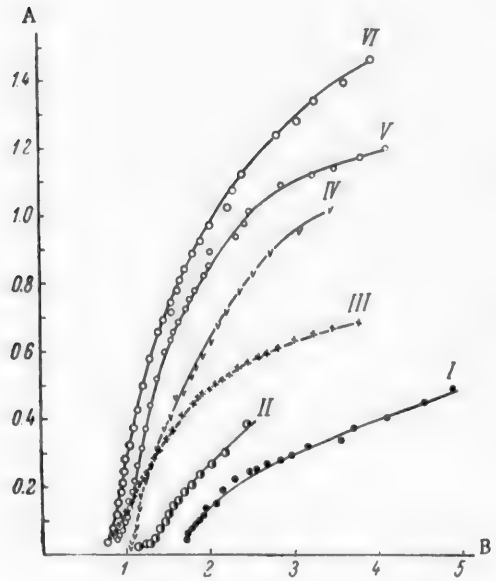

Fig. 5. Relation between the decomposition rate of apatite by phosphoric acid and the hydrogen ion concentration. A) Decomposition rate (in g/min), B) hydrogen ion concentration (in g-ion/liter $\cdot 10^{-2}$). Original acid concentration (in % P_2O_5): I) 64.77, II) 21.0, III) 45.6, IV) 59.0, V) 51.1, VI) 53.6.

tion and had a high temperature coefficient. In these experiments there was no possibility of the formation of solutions saturated with monocalcium phosphate or of an appreciable change in viscosity. In our experiments this relation between the rate and the hydrogen ion concentration was true only in the first stage for which we obtained 1-3 points at 20° since this stage and the beginning of the change into the second was complete in 5-10 minutes. At temperatures above 40° we were unable to record this stage at all as it was complete before withdrawal of the first sample.

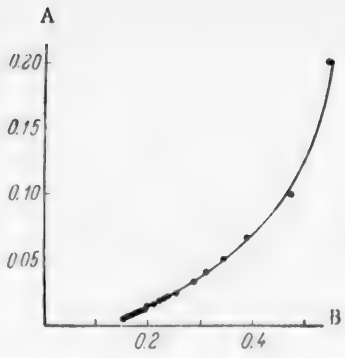

Fig. 6. Relation between $\frac{1}{y}$ and $\frac{1}{\tau}$. A) Value of $\frac{1}{\tau}$, B) value of $\frac{1}{y} \cdot 10^{-1}$ (y is the degree of decomposition of apatite by 59.0% P_2O_5 in % and τ is time in minutes).

A certain gap in time between the beginning of salt crystallization, determined graphically, and the change to the second stage of decomposition apparently may be explained both by supersaturation of the solution by monocalcium phosphate and also by the fact that the film first formed may not show an appreciable resistance to the diffusion of hydrogen ions.

The applicability of the rule established by Chepelevetskii to the first stage in our experiments is confirmed both by the dependence of the initial rate on acid concentration and the existence of an optimal concentration at which the maximum hydrogen ion concentration is apparently observed and by the high temperature coefficient at the beginning of decomposition.

Thus, the first stage of decomposition obeys all the main rules established by Chepelevetskii for the solution of apatite in phosphoric acid which is not saturated with monocalcium phosphate.

When the solution becomes saturated with monocalcium phosphate a film of salts forms on the apatite grains and as this grows it shows an ever increasing resistance to the diffusion of hydrogen ions.

The higher the acid concentration, the faster the system reaches the region of saturated solutions, the earlier film formation begins and the faster the process changes to the second stage when the predominating factor affecting the rate is the resistance of the monocalcium phosphate film. This also explains the fact that at the same hydrogen ion concentrations the acid with a P_2O_5 content of 59.0% decomposes apatite at a lower rate than 53.6% acid. Apatite is decomposed even more slowly by 64.77% acid because by the time that $C_{H^+} \simeq 3$-4 g-ion/liter has been reached there is apparently quite a dense crust on the apatite grains.

Though the bulk of apatite decomposition in double superphosphate production occurs in saturated solutions of the $CaO-P_2O_5-H_2O$ system, we cannot describe the whole process by rules characterizing this stage. The degree of decomposition of apatite in artificially prepared saturated solutions is less than in the actual process [6]. This is probably explained by the tendency of the system towards supersaturation, which leads to an increase in the duration of the first stage, and also the absence of a sharp boundary between the first and second stages.

It is known [8] that when a process is retarded only by the resistance of the film formed, the rate of the process changes by an equation which gives a straight line plot of $\frac{1}{y}$ against $\frac{1}{\tau}$ where y is the amount of substance reacted up to the moment of time τ.

As Fig. 6 shows, the solution process as a whole is described by a much more complex relationship. However, if we exclude the first points referring to the first 15-20 minutes of decomposition, then the process is well described by this relation.

The fact that the interaction of apatite with phosphoric acid is a two-stage process makes it possible to explain the comparatively slight effect of the amount of acid and temperature over the range 40-80° on the degree of phosphate decomposition. With an increase in the amount of acid the duration of the first stage increases as crystallization of the salt begins at a higher degree of decomposition. However, it is only possible to attain a high degree of decomposition by increasing the amount of acid to such an excess that crystallization of monocalcium phosphate is completely excluded or the latter only crystallizes in an amount which cannot affect the decomposition rate. This is well confirmed by experiments [3] in which at solid : liquid = 1 : 20 the degree of apatite decomposition by acid with a 20% P_2O_5 concentration reached ~90% after 2.5 hours.

Judging by the fact that over the temperature range 40-80° the decomposition rates in the second stage are the same, a rise in temperature over these limits does not appreciably affect the rate of diffusion of reagents through the film. Consequently a higher degree of decomposition at an elevated temperature may only be achieved as a result of an increase in the solubility of monocalcium phosphate. The solubility of monocalcium

phosphate is very low when the liquid phase contains 53-54% of P_2O_5. The degree of decomposition corresponding to saturation is about 1.5% at 25° and about 6% at 75°. This explains the insignificant effect of temperature on the degree of apatite decomposition by phosphoric acid. The more noticeable effect of temperature from 20 to 40° on the degree of apatite decomposition is apparently connected with the definite nature of the temperature dependence of the diffusion rate.

Thus, on the basis of the results obtained we can consider that the rate of apatite decomposition by phosphoric acid for so-called "thickening" pulps is determined by the acid concentration and temperature in the first stage and by the rate of diffusion of hydrogen ions through the solid film of reaction products in the second stage. For "nonthickening" pulps, i.e.,for dilute acids, the decomposition rate is determined by the hydrogen ion concentration.

SUMMARY

1. The decomposition of apatite by phosphoric acid for "thickening" pulps proceeds by two stages. In the first, very brief stage the decomposition rate depends both on the concentration and amount of acid and on temperature over the range 40-80°. In the second stage the decomposition rate depends little on these factors.

2. The second stage of the decomposition is solution,complicated by the formation of a difficultly penetrable film of reaction products. The rate of the process in the second stage is determined by the rate of diffusion of reagents through the solid film of monocalcium phosphate.

LITERATURE CITED

[1] E. B. Brutskus and D. L. Tsyrlin, Khim. Prom. 7, 394 (1956).

[2] S. K. Voskresenskii, Trudy NIUIF 153 (1940).

[3] M. L. Chepelevetskii et al., Trudy NIUIF 137 (1937).

[4] K. S. Krasnov, Zhur. Priklad. Khim. 26, 11, 1114 (1953).*

[5] K. S. Krasnov,Zhur. Priklad. Khim. 28, 12, 1275 (1955).*

[6] M. E. Pozin, B. A. Kopylev, and D. F. Zhil'tsova, Zhur. Priklad. Khim. 32, 3, 509 (1959).*

[7] M. L. Chepelevetskii and E. B. Brutskus, Superphosphate, Physicochemical Bases of Production, [in Russian] (State Chem. Press, 1958).

[8] Protective Films on Salts, Coll. Edited by A.V. Nikolaeva, [in Russian](Acad. Sci. USSR Press, 1944).

Received June 2, 1959

* Original Russian pagination. See C. B. translation.

INVESTIGATION OF THE THERMOCHEMICAL DECOMPOSITION OF CALCIUM SULFATE AND ITS INTERACTION WITH CARBON

A. M. Ginstling and A. D. Volkov

The industrial importance of various processes in the chemical treatment of calcium sulfate, the natural reserves of which are practically inexhaustible in our country [1], are well known. Some of the most interesting of these processes are high-temperature reactions in crystalline mixtures containing $CaSO_4$ which are accompanied by the formation of sulfur dioxide and some calcium compound. An important position among these reactions is occupied by interactions in the system calcium sulfate + carbon. Many investigations have been devoted to their study [2 – 6]. The aim of some of these investigations was the preparation of calcium sulfide.[2, 4, 5] and of others, the preparation of sulfur dioxide [6]. We will consider some of these investigations briefly.

In much of his work Budnikov [4, 6] studied the interaction of gaseous reducing agents with calcium sulfate and also its reduction by solid carbon in a suspended state. Terashkevich and Evetskii [5] made a detailed investigation of the reduction of calcium sulfate by carbon. In this and other work on the given process, information has been obtained on its course and yield of final products relative to the composition of the starting mixtures, temperature, and some other conditions; some important rules were established, a knowledge of which is essential for industrial realization of the process.

Nonetheless, despite their basic importance, the thermodynamic and kinetic aspects of the process have hardly been studied. The present work is devoted to them.

In the decomposition of calcium sulfate in the system $CaSO_4 + C$, together with reduction of the sulfate and formation of sulfur dioxide, there are also side reactions giving elementary sulfur and other products. These side reactions naturally affect the rate of formation and yield of the main products. Therefore a knowledge of not only the main but also the side reactions under various conditions is necessary for a definite selection of the optimal conditions for the corresponding industrial processes.

Unfortunately, the conclusions of different investigators on the various problems relating to the processes examined are, to a considerable extent, contradictory. The process most disputed is the formation of elementary sulfur.

Shensk and Jordan [7] consider that sulfur is formed as a result of three reactions:

$$CaSO_4 + 3CaS = 4CaO + 2S_2,$$
$$CaS + 2SO_2 = CaSO_4 + S_2,$$
$$2CaS + SO_2 = 2CaO + 1.5S_2.$$

In the opinion of Zawadzki [8], sulfur is formed by the reaction

$$CaS + 2SO_2 = CaSO_4 + S_2.$$

Weychert and Leyko [9] think that sulfur is liberated as a result of two reactions:

$$CaS + 2SO_2 = CaSO_4 + S_2,$$
$$2CaS + SO_2 = 2CaO + 1.5S_2$$

TABLE 1

Change in the Isobaric-Isothermal Potential for Some Reactions in the System $CaSO_4$ + C at Various Temperatures (in cal/mole)

Reaction	$\Delta Z'_{700°}$	$\Delta Z°_{800°}$	$\Delta Z'_{850°}$	$\Delta Z'_{900°}$	$\Delta Z'_{950°}$	$\Delta Z°_{1000°}$	$\Delta Z°_{1050°}$	$\Delta Z°_{1100°}$
	cal/mole							
1	—45308	—52921	—56985	—61021	—65029	—69009	— 72961	— 76833
2	—45291	—61957	—70236	—78475	—86670	—94830	—102943	—111015
3	—44522	—44385	—44230	—44032	—43913	—43795	— 43614	— 43403
4	68054	49907	40974	32087	23325	14633	6056	— 2424
5	— 8766	—23843	—31321	—38757	—46136	—53480	— 60765	— 68005
6	—50074	—58200	—71207	—78209	—85191	—92153	— 99088	—105999
7	—41313	—40355	—39894	—39466	—39066	—38686	— 38333	— 38007

TABLE 2

Decomposition of Natural Calcium Sulfate at Various Temperatures

SO_2 determined (% of theoretical)	$CaSO_4$ decomp time (min and sec)			
	950°	1000°	1050°	1100°
4.37 *	33.0	15.50	6.35	4.35
8.74	59.30	24.45	10.45	6.20
13.11	80.55	32.15	13.45	7.55
17.48	100.20	41.00	16.40	9.30
21.85	119.50	48.30	19.35	10.55
34.96	175.30	—	27.35	14.10
48.07	256.00	92.20	35.15	18.30
61.18	—	113.40	43.50	22.05
69.92	—	130.00	50.35	24.45
78.66	—	149.30	58.10	28.00
91.77	—	194.20	79.20	48.30
94.28	—	290.20	145.00	78.00
94.68	—	318.00	—	—

* For brevity, only part of the data is presented.

These hypotheses may be compared by means of thermodynamic analysis. Certain experimental data which do not agree with the known [8] description of the process mechanism also compel attention.

Thus, on studying the production of SO_2 from anhydrite in a pilot plant tubular furnace and analyzing samples taken from various sections of it, Weychert and Leyko [9] observed that considerable amounts of calcium sulfide were formed in the reaction mixture at 900-1200°. The sulfide disappeared completely in the sintering zone (above 1200°), even under the conditions when the amount of CaS at the beginning of this zone exceeded the amount needed for complete stoichiometric reaction with the remaining sulfate. At the same time, a considerable amount of calcium oxide appeared. The authors explained this by an acceleration of the interaction of sulfide with sulfate. However, this explanation ignores the problem of how the excess calcium sulfide is consumed.

Also there is no single opinion on the main reactions in the reduction of calcium sulfate by carbon. Gofman and Mostovich [2] consider that at 800° the reaction proceeds according to the equation

$$CaSO_4 + 2C = CaS + 2CO_2,$$

and at temperatures above 800°, according to the equation

$$CaSO_4 + 4C = CaS + 4CO.$$

From investigations of the same process, Terashkevich and Evetskii [5] came to the conclusion that at 900-1100° the reaction proceeds with the evolution of CO_2 and not carbon monoxide. In this connection it is natural to compare the probabilities of the different reactions in the system examined by means of thermodynamic calculations. It is all the more profitable to do this as thermodynamic characteristics of the system $CaSO_4 + C$ are extremely sparse: the values of the equilibrium constants at 700-1000° have been calculated by the approximate equation of Nernst only for the reaction $CaSO_4 + 4CO \rightleftharpoons CaS + 4CO_2$ [5].

By using the method of Temkin and Shvartsman [10], in the present article the authors calculated the changes in the isobaric-isothermal potential ΔZ^0_T over the temperature range 700-1100° for seven reactions of the system $CaSO_4 + C$:

$$CaSO_4 + 2C = CaS + 2CO_2, \quad (1)$$
$$CaSO_4 + 4C = CaS + 4CO, \quad (2)$$
$$CaSO_4 + 4CO = CaS + 4CO_2, \quad (3)$$
$$CaS + 3CaSO_4 = 4CaO + 4SO_2, \quad (4)$$
$$3CaS + CaSO_4 = 4CaO + 2S_2, \quad (5)$$
$$2CaS + SO_2 = 2CaO + 1.5S_2, \quad (6)$$
$$CaS + 2SO_2 = CaSO_4 + S_2. \quad (7)$$

The thermodynamic data required for the calculations were taken from the literature [11-14].

By analyzing the results of the calculations presented in Table 1 and Fig. 1 (the numbers of the curves in which correspond to the numbers of the reactions in the text) we may draw some conclusions on the probabilities of individual reactions under different conditions. At temperatures above 800° the reduction of calcium sulfate by carbon must evidently proceed by reaction (2) with the formation of carbon monoxide. This agrees with the data of Gofman and Mostovich [2].

On comparing the reactions forming sulfur, (5)-(7), we see that reaction (6) is most probable; however, reactions (6) and (7) require sulfur dioxide and with the absence or an insufficiency of SO_2 reaction (5) is possible.

In particular, from this it follows that in an industrial furnace in the temperature zone 800-1000°, where the reaction mixture contains a considerable amount of calcium sulfide, reactions (5) and (6) may occur, depending on the presence of SO_2. At higher temperatures the equilibrium of reaction (4) is displaced towards the formation of sulfur dioxide, which facilitates the formation of sulfur by reaction (6).

Thus, there may be all three reactions for the formation of elementary sulfur in an industrial furnace, depending on the temperature and the composition of the solid and gas phases in its separate zones. The data of Weychert and Leyko [9] presented above may be explained in the following way on the basis of the values of ΔZ^0_T obtained. The consumption of sulfide in an amount greater than that required for stoichiometric interaction with sulfate is caused by the occurrence of reactions forming sulfur and calcium oxide [at relatively low temperatures, (5) and at higher temperatures (6)]. This simultaneously explains a second fact, namely, the formation of a large amount of calcium oxide during the time of high calcium sulfide consumption. As regards the main reaction for sulfur dioxide formation, (4), it can be seen that its occurrence is promoted by a high temperature (above 1000°) and the presence of quite a large amount of $CaSO_4$ in the reaction mixture in comparison with calcium sulfide.

It is understood that the calculations and arguments presented only characterize the thermodynamic probability of the individual reactions of the system considered under various conditions and do not consider the effect on these reactions of such factors as a change in the aggregate state of the separate phases, the crystal structure and surface contact area of the reagents and the rate of their diffusion and also do not characterize the rate of the above reactions with time. To elucidate the effect of certain factors on the rate of interaction of calcium sulfate with carbon, a detailed investigation of the kinetics of this reaction was undertaken.

Previous work in this field was for somewhat different purposes. The results of experiments on the kinetics of both the reduction of $CaSO_4$ to CaS and the decomposition of calcium sulfate mixed with carbon to CaO and sulfur dioxide characterize the change in composition of appropriate reaction mixtures over large time intervals.

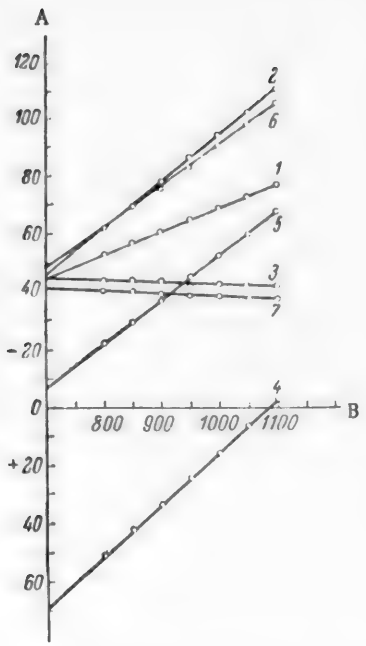

Fig. 1. Change in the isobaric-isothermal potentials of the main reactions in the system $CaSO_4$ + C at various temperatures. A) Change in isobaric-isothermal potentials ΔZ_T^0 (kcal/mole), B) temperature t (in °C).

Thus, Losev and Nikitin [3] determined the degree of decomposition of calcium sulfate in a mixture of $2CaSO_4$ + C at temperatures of 800-1100° after 1, 2, 3 hours, etc. In experiments on the reduction of calcium sulfate by solid carbon in a suspended state, Budnikov and Krech [4] established that an increase in the duration of the process led to a decrease in the calcium sulfide as a result of its interaction with sulfate. In studying the reaction in a mixture of $CaSO_4$ + 4C at temperatures of 800, 900, 1000 and 1100°, Terashkevich and Evetskii [5] determined the change in composition of the reaction mixture 20, 40, and 60 minutes after the beginning of the experiment.

The absence of more detailed data on the kinetics of the interaction of calcium sulfate with carbon may be explained by the experimental difficulties.

In the present work we proposed to study the kinetics of this reaction through data on the composition of the solid and gaseous reaction products. The experiments were performed in the apparatus illustrated in Fig. 2. The starting materials used were calcium sulfate obtained by firing analytical grade gypsum and natural gypsum (from the Zvoz deposit in the Arkhangel'sk region), containing 0.2% of R_2O_3 and traces of MgO, at 800° for 4 hours and sugar charcoal as a powder with a grain size in the range of 0.06 to 0.086 mm. Mixtures were prepared with a ratio of 0.6 mole of carbon to 1 mole of calcium sulfate, which is close to the ratio used in industrial charges [15]. For the experiments we used 1 g samples of mixture in a stream of dry, oxygen- and carbon dioxide-free nitrogen with a flow rate of 30 ml/min. The temperature deviations of the electronic potentiometer did not exceed ±5°. The degree of decomposition of the calcium sulfate was determined from the amount of SO_2, which was determined iodometrically and semicontinuously [16, 17] in apparatus 15 (Fig. 2). The solid residue was analyzed for calcium oxide content by neutralization, calcium sulfide iodometrically, and calcium sulfate by a gravimetric method. The plan of the apparatus and the design of the SO_2 absorption equipment made it possible to obtain more than 50 points for each experiment characterizing the kinetics of the process.

To determine the effect of temperature on the kinetics of sulfur dioxide formation in the decomposition of anhydrite (obtained from pure and natural gypsum), experiments were carried out at 950, 1000, 1050, and 1100°. The results, which are presented in Fig. 3 and Table 2, characterize the substantial effect of temperature on the rate of the process.*

Thus, "pure" samples yielded 20% of the theoretically possible amount of SO_2 in 155 minutes at 950°, in 60 minutes at 1000°, in 23 minutes at 1050° and in 11 minutes at 1100°. As a result of the action of a very small amount of impurities the decomposition of calcium sulfate obtained from natural gypsum differed somewhat from the decomposition of "pure" samples. The decomposition of natural samples was more rapid at 950 and 1000°. However, with a further rise in temperature the decomposition rates of natural and "pure" samples were very close to each other.

To study the kinetics of the change in composition of the solid phases, we carried out experiments for different times from 5 to 340 minutes. The results obtained are presented in Figs. 4 and 5 and Table 3.

On examining the data presented it is readily seen that temperature has a different effect on the reduction of calcium sulfate to the sulfide and the interaction of sulfide with sulfate. The amount of calcium sulfide in the reaction mixture passes through a maximum as the process proceeds and the position and absolute value of this maximum vary for different temperatures. At 1000° the sulfide content of the mixture reaches a maximum

*For brevity, only part of the data is presented.

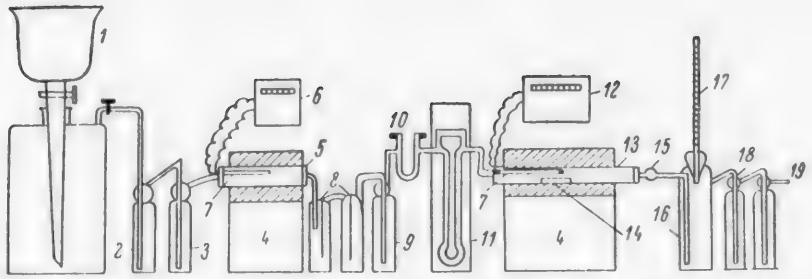

Fig. 2. Plan of apparatus. 1) Gasometer with N_2, 2) bottle with pyrogallol, 3) bottle with 30% KOH solution, 4) tubular resistance furnace, 5) quartz tube with copper turnings, 6) electronic control ÉRM-47, 7) chromel-alumel thermocouple, 8) bottles with $CaCl_2$, 9) bottle with H_2SO_4, 10) tube with P_2O_5, 11) rheometer, 12) automatic electronic potentiometer ÉPV-01, 13) quartz tube, 14) boat, 15) tube with glass wool, 16) apparatus for SO_2 absorption, 17) burette with 0.1 N I_2, 18) bottle with 0.1 N I_2, 19) bottle with 0.1 N $Na_2S_2O_3$.

TABLE 3

Time Dependence of the Composition of the Solid Decomposition Product of Natural Calcium Sulfate at 1050°

Time (in min)	Composition of solid product* (in %)			
	$CaSO_4$	CaS	CaO	total
5	76.11	16.92	6.77	99.80
15	60.11	19.27	20.38	99.76
30	41.60	11.15	47.18	99.93
60	16.83	1.68	81.33	99.84
90	5.04	0.60	94.32	99.96
145	1.27	0.06	98.55	99.88

*Calculated on $CaSO_4$.

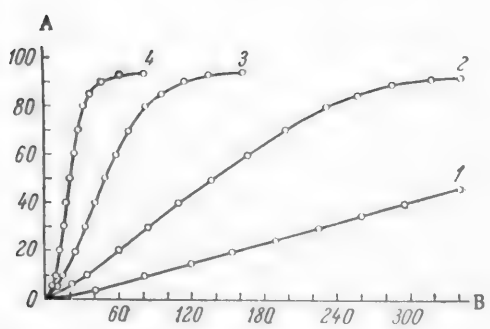

Fig. 3. Kinetics of SO_2 liberation in the decomposition of $CaSO_4$ (analytical grade). A) SO_2 content (in % of initial sulfur), B) time (in min). Temperature (in °C): 1) 950, 2) 1000, 3) 1050, 4) 1100.

in the first minutes of the experiment and at 1050°, after approximately 5 (for analytical grade material) to 15 minutes (for natural material) from the beginning of the experiment. The small amount of sulfur dioxide formed and the high consumption of sulfate at the beginning of the experiment indicate rapid reduction of sulfate to sulfide in this period. This agrees well with the data from thermodynamic calculations presented above. As is known, the formation of sulfur dioxide occurs according to reaction (4) by the interaction of 1 mole of sulfide with three moles of sulfate. It seemed interesting to calculate the amount of sulfate required for interaction with the maximum amount of sulfide by this reaction. The calculation showed that both at 1000° and at 1050° the maximum amount of sulfide was insufficient

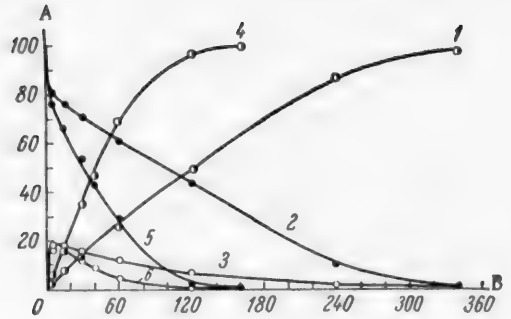

Fig. 4. Kinetics of the change in composition of the solid product in the decomposition of $CaSO_4$ (analytical grade). A) Composition calculated on $CaSO_4$ (in %), B) time (in min). At 1000°: 1) CaO, 2) $CaSO_4$, 3) CaS; at 1050°: 4) CaO, 5) $CaSO_4$, 6) CaS.

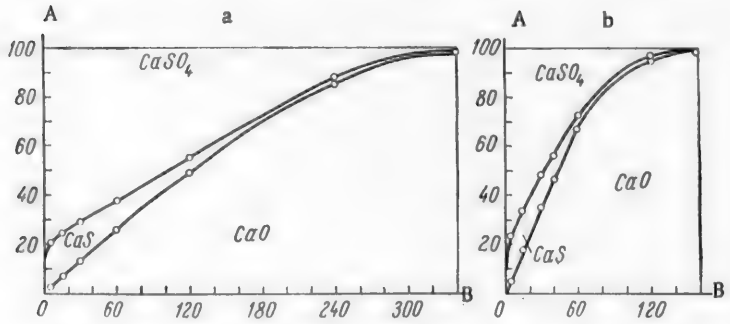

Fig. 5. Balance diagrams of the change in composition of the solid product in the decomposition of $CaSO_4$ (analytical grade). A) Composition calculated on $CaSO_4$ (in %), B) time (in min.). a) At 1000°, b) at 1050°.

for reaction with the remaining sulfate according to equation (4) and the reduction of sulfate continued (there was a very small amount of $CaSO_4$ in the final product).

To determine the course of the reduction process after the maximum had been reached it was necessary to have data on the formation of carbon dioxide and monoxide during the experiment. The results of experiments indicated that several reactions occurred simultaneously in the $CaSO_4$ + C system on heating.

Thermodynamic analysis of the system and experimental investigation of the kinetics of its thermochemical conversions indicate that high temperatures favor the formation of SO_2 as a result of the process. Therefore, bearing in mind the fact that is is impossible to have too great a reduction in temperature from thermodynamic considerations, it is nonetheless profitable to study the possibility of accelerating this process at comparatively low temperatures by the introduction of so-called mineralizers into the starting mixture.

SUMMARY

By an experimental investigation of the kinetics of sulfur dioxide formation and the change in composition of the solid phases during the interaction of calcium sulfate with carbon it was established that temperature has a different effect on the separate reactions of this process.

LITERATURE CITED

[1] Gypsum, [in Russian] Trudy Nauch. Inst. po Udobreniyam, NTO VSNKh, Moscow, 36, 1 (1927).

[2] N. R. Gofman and V. Ya. Mostovich, Coll. Works of V. Ya. Mostovich, I, United Sci. Tech. Press, NKTP, Moscow–Leningrad 167 (1936).

[3] K. I. Losev and A. N. Nikitin, Zhur. Priklad. Khim. 3-4, 169 (1929).

[4] P. P. Budnikov and É. I. Krech, Zhur. Priklad. Khim. 9, 1929 (1936).

[5] V. R. Terashkevich and G. N. Evetskii, Zhur. Priklad. Khim. 9, 2155 (1936).

[6] P. P. Budnikov, Gypsum, Its Investigation and Application [in Russian] (Construction and Architecture State Press, Moscow–Leningrad, 1943) p. 85.

[7] R. Schensk and K. Jordan, Z. anorg. allg. Ch. 178, 4, 389 (1929).

[8] J. Zawadzki, Przeglad Chem. 5, 11-12, 240 (1947).

[9] S. Weychert and J. Leyko, Przemysl Chem. 12 (35), 5, 258, (1956).

[10] M. I. Temkin and L. A. Shvàrtsman, Uspekhi Khim. 17, 259 (1948).

[11] É. V. Britske, A. F. Kapustinskii, B. K. Veselovskii, L. M. Shamovskii, L. G. Chentsova and B. I. Anvaer, Thermal Constants of Inorganic Substances [in Russian] (Acad. Sci. USSR Press, Moscow, 1949).

[12] R. Venner, Thermochemical Calculations [Russian translation] (Foreign Lit. Press, Moscow, 1950).

[13] V. A. Kireev, Course in Physical Chemistry [in Russian] (Moscow, 1955).

[14] F. D. Rossini, D. D. Wagman, W. H. Evans, S. Levine, and I. Ioffe, Selected Values of Chemical Thermodynamic Properties, Nat. Bur. Stand. Circ. 500 (1952).

[15] J. Leyko, Przemysl Chem. 12 (35), 5, 251 (1956).

[16] I. S. Lileev and O. G. Evteeva, Trudy Khim.-Met. Inst., Zap.-Sib. Filial Akad. Nauk SSSR 3, 27 (1949).

[17] S. Yu. Fainberg, Analysis of Ores of Nonferrous Metals [in Russian] (Metallurgy Press, Moscow, 1953) p. 451.

Received December 8, 1958

INTERACTION BETWEEN IRON SULFIDES AND FERROUS SULFATE

N. Sh. Safiullin

At the present time metallurgical plants use hundreds of thousands of tons of sulfuric acid each year in the pickling of metals. The solutions thus formed, which contain 20-25% of $FeSO_4$ and 2-5% of free H_2SO_4 are a waste product of the process and in most cases are dumped into the sewer system after neutralization.

The use of pickling solutions for the preparation of products required for the national economy is therefore a real problem.

In a number of countries pickling solutions are used for the preparation of sulfur dioxide for subsequent conversion to sulfuric acid. The dried iron sulfate is mixed with 5-10% of charcoal and fired [1, 2]. Iron sulfate may also be converted into sulfur dioxide by firing with pyrites or carbonaceous pyrites.

In this connection it seemed interesting to study the interaction of ferrous sulfate with FeS_2 and FeS. Pozin and Ginstling [3] have reported that pyrites has an accelerating action on the thermal decomposition of ferrous sulfate. However, the nature and kinetics of the reaction between these compounds have not been studied sufficiently.

To determine the reaction between iron sulfide and sulfate, we heated mixtures of FeS and $FeSO_4$ in various molar ratios. The changes in the isobaric potentials of the probable reactions were also calculated for temperatures of 900, 1000, and 1100° K.

The experiments were carried out in a tubular electrical furnace by firing mixtures at 800° C in a nitrogen atmosphere.

The apparatus used for this purpose is illustrated in Fig. 1.

A sample of a mixture of FeS and $FeSO_4$ of definite composition was placed in a porcelain boat and introduced into the furnace at the required temperature.

The sulfur dioxide liberated as a result of the reaction was absorbed in 3% hydrogen peroxide solution and determined by titration with 0.1 N alkali solution. The temperature in the furnace was determined with a chromel-alumel thermocouple.

The reaction was considered complete when the evolution of sulfur dioxide ceased. The nature of the reaction occurring in each case was determined from the composition of the gas and the solid residue.

For the experiments we used technical ferrous sulfide containing 68% of FeS and 30% of Fe_3O_4 and ferrous sulfate monohydrate containing 99% of $FeSO_4 \cdot H_2O$.

The experimental results showed that at any ratio of $FeSO_4$/ FeS not exceeding 5, interaction between these compounds proceeded according to the equation

$$FeS + 5FeSO_4 = 2Fe_3O_4 + 6SO_2, \quad (1)$$

and with excess $FeSO_4$ the following reaction began:

$$FeS + 7FeSO_4 = 4Fe_2O_3 + 8SO_2. \quad (2)$$

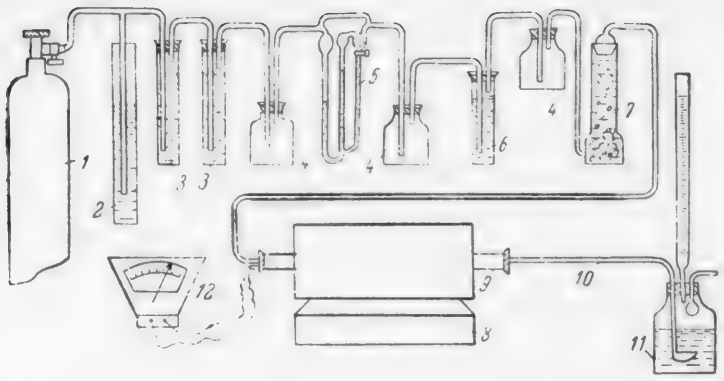

Fig. 1. Plan of apparatus. 1) Nitrogen tank, 2) monostat, 3) absorption cyclinders with an alkaline solution of pyrogallol, 4) buffer bottles, 5) rheometer, 6) vessel with concentrated sulfuric acid, 7) column with soda lime, 8) tubular electric furnace, 9) porcelain tube, 10) glass tube for discharge of gas to absorber vessel, 11) absorber vessel with 3% solution of hydrogen peroxide, 12) galvanometer with chromel-alumel thermocouple.

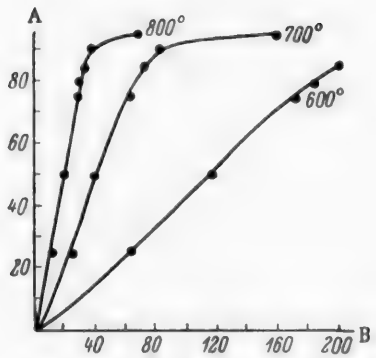

Fig. 2. Desulfurization of a mixture of FeS + 5 $FeSO_4$. A) Degree of desulfurization (in %), B) time (in sec).

Data on the change in the isobaric potentials and the equilibrium constants of these reactions are given below.

	900° K	1000° K	1100° K
ΔZ_1^0	— 83700	—112100	—138900
ΔZ_2^0	—110800	—148300	—183800
K_1	$2.52 \cdot 10^{20}$	$3.16 \cdot 10^{24}$	$6.3 \cdot 10^{27}$
K_2	1.10^{27}	$2.52 \cdot 10^{32}$	$4.0 \cdot 10^{36}$

The change in the isobaric potentials was calculated from data on the change in enthalpy (ΔH_{298}) and isobaric potentials (ΔZ_{298}^0) on formation of the compounds participating in the reactions from the elements under standard conditions and also from the values of their heat capacities [4-9].

As there is no data in the literature on the value of $c_p = f(T)$ for $FeSO_4$, it was arbitrarily assumed that $\Delta H_T = \Delta H_{298}$. The equilibrium constants of the reactions were determined from the equation

$$\log K = -\frac{\Delta Z^0}{4.573T}.$$

To study the kinetics of reaction (1) we prepared ferrous sulfide by thermal decomposition of pyrites at 800° C in a nitrogen atmosphere. The product obtained contained 73.25% of FeS and 5.64% of FeS_2.

The reaction rate was determined from the amount of SO_2 liberated from 0.32 g of mixture over a given time interval. Experiments were carried out at 600, 700, and 800° C. The amount of nitrogen fed into the furnace was kept at 800 ml/min.

The average values of the data obtained are given in Fig. 2.

Figure 3 shows the temperature dependence of the rate constant of the reaction in the coordinates of log K against $\frac{1}{T}$.

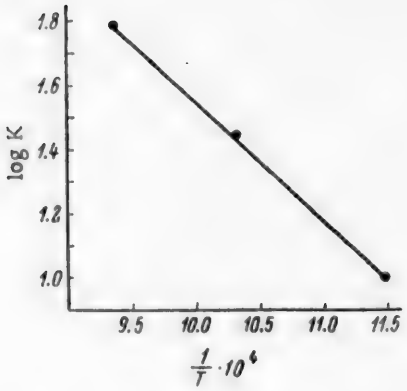

Fig. 3. Relation between log K and $\frac{1}{T}$.

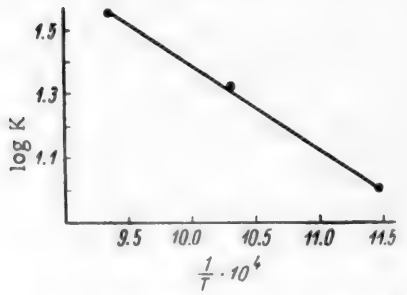

Fig. 5. Relation between log K and $\frac{1}{T}$.

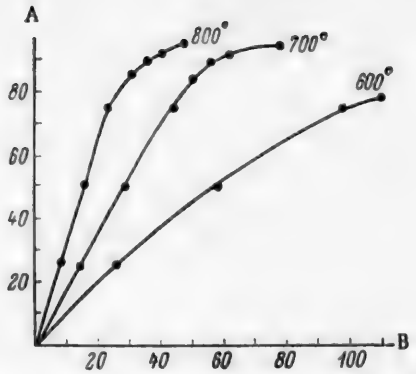

Fig. 4. Desulfurization of FeS_2 + 8$FeSO_4$. A) Degree of desulfurization of mixture (in %) B) time (in sec.).

The nature of the curve obtained, a straight line, shows that the rate of the reaction between FeS and $FeSO_4$ obeys the equation

$$K = K_0 e^{-\frac{E}{RT}},$$

where E is the apparent activation energy.

The average value of the apparent activation energy E between the temperatures 600 and 800°C for our case was about 17700 cal.

The following series of experiments was carried out to study the rate of interaction between pyrites and $FeSO_4$. For the experiments we used iron pyrites with a sulfide sulfur content of 42.4% and 0.45% of sulfate sulfur.

The mixture was prepared on the assumption that the over-all reaction was

$$FeS_2 + 8\,FeSO_4 = 3Fe_2O_4 + 10\,SO_2, \qquad (3)$$

i.e., in analogy with the interaction between FeS and $FeSO_4$ with the formation of Fe_3O_4 and SO_2.

The change in the isobaric potential and the equilibrium constants of this reaction are given below.

	900° K	1000° K	1100° K
ΔZ_3^0	—130680	—179260	—225440
K_3	$6.3 \cdot 10^{31}$	$1.59 \cdot 10^{39}$	$6.3 \cdot 10^{44}$

The order of the values obtained for K_e shows that reaction (3) must proceed practically to completion at 900-1100° K.

The results of the experiments are shown in Fig. 4.

The relation between the rate constant and the temperature is shown in Fig. 5.

The nature of the curve obtained shows that the temperature dependence of the rate constant of the interaction of $FeSO_4$ with FeS_2 is also expressed by the equation

$$K = K_0 \cdot e^{-\frac{E}{RT}}$$

TABLE 1

Comparative Data on the Rates of Desulfurization of $FeSO_4 \cdot H_2O$ and Mixtures of It with Pyrites

Degree of desulfurization (in %)	Decomposition time $FeSO_4$ (in sec) at the temperatures (in °C)		Desulfurization time of the mixture $FeS_2 + 8FeSO_4$ (in sec) at the temperatures (in °C).	
	700°	800°	700°	800°
25	45	27	15	9
50	85	46	28	16
75	175	84	44	24
80	205	98	–	–
85	370	159	51	31
90	–	260	56	36
95	–	–	78	47

TABLE 2

Interaction of Basic Iron Sulfate $Fe_2O(SO_4)_2$ with Pyrites

Degree of desulfurization (in %)	Desulfurization time (in sec.) at the temperature (in °C)	
	700°	800°
25	17	10
50	25	18
75	37	27
85	43	32
90	50	36
95	80	46

The apparent activation energy E was found to be approximately equal to 12700 cal.

The data presented above show that over the temperature range 600-800°C reaction (1) proceeds much more rapidly than reaction (3) and the effect of temperature in accelerating the reaction is stronger in the second case than in the first. The latter gives grounds for assuming that the rates of the two reactions must be comparable at a higher temperature.

Further experiments showed that the addition of inert materials (for example, SiO_2) to a mixture of pyrites and $FeSO_4$ had no noticeable effect on the rate of interaction between them.

TABLE 3

Data on the Desulfurization of a Mixture of FeS_2 + 8$FeSO_4$ at 700°C in an SO_2 Atmosphere

Time from beginning of experiment (in sec).	Sulfur content of solid residue (in %)		
30	12.6	13.1	12.9
50	7.5	8.2	8.0
90	Not detected		Not detected

Table 1 gives comparative data on the rate of desulfurization of a mixture of FeS_2 + 8$FeSO_4$ and the decomposition of $FeSO_4$ in a nitrogen atmosphere at 700 and 800°C (with the same sulfur content in the samples).

Table 1 shows that the addition of pyrites considerably accelerated the desulfurization of $FeSO_4$.

Considering that under practical conditions (with dehydration and firing) ferrous sulfate is readily oxidized to the basic sulfate, we carried out experiments to study the rate of interaction of the basic sulfate with pyrites. The basic sulfate was prepared by oxidation of ferrous sulfate in air at 250°C. The mixture of basic iron sulfate and pyrites was also prepared on the assumption that the reaction formed Fe_3O_4 and SO_2.

The data obtained are given in Table 2.

A comparison of the values obtained with data in Fig. 4 shows that the reactions of pyrites with the two sulfates proceed at almost the same rate. Consequently possible changes of one sulfate into the other during the firing process will not have any effect on the reaction between them and pyrites.

With excess pyrites in the mixture, the following reaction is also possible:

$$FeS_2 + 3FeSO_4 = FeS + Fe_3O_4 + 4SO_2, \quad (4)$$

and this may be explained by the following.

At 600-800°C there is rapid decomposition of pyrites with the formation of ferrous sulfate and sulfur [10, 11]:

$$FeS_2 \rightarrow FeS + S.$$

Thermodynamic calculations show that with sulfur present in the mixture ferrous sulfate must react with it in the first instance:

$$S + 3FeSO_4 = Fe_3O_4 + 4SO_2, \quad (5)$$

and in the absence of excess $FeSO_4$ the ferrous sulfide must remain in the solid residue.

For an experimental check of reaction (4) a mixture of pyrites and ferrous sulfate was prepared with a molar ratio of $FeS_2 : FeSO_4 = 1 : 3$ and fired in a nitrogen atmosphere at 800°C.

Data on the sulfur balance after the firing of a mixture of FeS_2 + 3$FeSO_4$ in a nitrogen atmosphere at 800°C are given below.

Sulfur liberated as SO_2 (in %)	Sulfur remaining in solid residue as FeS (in %)
78.94	19.50
79.01	19.30
79.52	19.70
Average 79.15	19.50

According to stoichiometry, reaction (4) should liberate 80% of the sulfur as SO_2 and 20% should remain in the solid residue as FeS. As can be seen, the experimental values agree well with these values.

Goinosh [12] demonstrated thermodynamically and experimentally the possibility of the interaction of pyrites with ferrous sulfate by the reaction

$$2FeS_2 + FeSO_4 = 3FeS + 2SO_2. \quad (6)$$

Our experiments also confirmed this.

Data on the sulfur balance after the firing of a mixture of $2FeS_2 + FeSO_4$ in a nitrogen atmosphere at 800° are given below.

Sulfur liberated from the mixture as SO_2 (in %)	Sulfur remaining in solid residue as FeS (in %)
38.75	59.74
39.00	59.55
38.41	59.67
38.88	59.77
Average 38.76	59.68

According to reaction (6) 40% of the sulfur should theoretically be liberated as SO_2 and 60% remain as FeS.

Considering that at the present time there is a great demand for concentrated SO_2, we carried out a series of experiments to determine the possibility of using the reaction between pyrites and ferrous sulfate to prepare 100% sulfur dioxide. For this purpose a mixture (10 g sample) of pyrites and ferrous sulfate ($FeS + 8FeSO_4$) in a molar ratio of 1 : 8 was fired in the absence of air at 700°C. The gas liberated was analyzed for the SO_2 and SO_3 content.

Average data obtained during the experiments are given below.

Analysis No.	SO_2 content of gas (in %)	SO_3 content of gas (in %)
1	57.8	0.04
2	73.2	
3	94.6	
4	100.0	
5	100.0	
6	100.0	

Table 3 gives data on the rate of desulfurization of a mixture of FeS_2 + $8FeSO_4$ in an SO_2 atmosphere at 700°C. The degree of desulfurization of the mixture was determined from the sulfur content of the solid residue after firing for a definite time.

As the data presented show, 100% SO_2 may be obtained by oxidation of pyrites with ferrous sulfate and the oxidation process proceeds at a high rate.

The low SO_2 content obtained in the first analyses may be explained by the displacement of nitrogen from the tube; nitrogen was used to remove air from the latter. The average SO_3 content of the gas did not exceed 0.04%.

SUMMARY

1. By thermodynamic calculations and experimental work on the interaction of $FeSO_4$ with FeS and FeS_2 it was established that the interaction of ferrous sulfate with FeS and FeS_2 proceeds quite rapidly.

2. The rate of desulfurization of a mixture of FeS_2 + $8FeSO_4$ is more than 5 times greater than the rate of decomposition of pure $FeSO_4$.

3. Interaction of pyrites with both $FeSO_4$ and with $Fe_2O(SO_4)_2$ proceeds at almost the same rate.

4. Interaction of sulfate with pyrites proceeds at a high rate both in an SO_2 atmosphere and in the absence of air, showing that this reaction may be used for the preparation of 100% sulfur dioxide.

The data obtained are also of interest from the point of view of the theory of firing pyrites as in the firing of the latter one of the intermediate compounds is ferrous sulfate which is in contact with FeS and FeS_2.

LITERATURE CITED

[1] P. Pak'e, Khim. i Khim. Tekh. 2, 57 (1956).

[2] K. Malin, Technology of Sulfuric Acid and Sulfur [in Russian] (State Chem. Press, 1941) p. 60.

[3] M. E. Pozin and A. M. Ginstling, Zhur. Priklad. Khim. 28, 12, 1945 (1950); Zhur. Priklad. Khim. 24, 2, 134 (1951).*

[4] R. Venner, Thermochemical Calculations [Russian translation] (Foreign Lit. Press, 1950) p. 58.

[5] Short Handbook of Physicochemical Values [in Russian] (State Chem. Press, 1955) pp. 8 and 33.

[6] Short Handbook for Chemists [in Russian] (State Chem. Press, 1955) p. 89.

[7] O. Kubachewski and E. Evans, Thermochemistry in Metallurgy [Russian translation] (Foreign Lit. Press, 1954) p. 262.

[8] M. Kh. Karapet'yants, Chemical Thermodynamics [in Russian] (State Chem. Press, 1949) pp. 63 and 512.

[9] K. K. Kelley, Contributions to the Data on Theoretical Metallurgy, Bull. 476 (1949).

[10] K. M. Malin and F. N. Kel'man, Zhur. Priklad. Khim. 8, 229 (1948).

[11] V. S. Udintsova and G. P. Chufarov, Zhur. Priklad. Khim. 14, 1 (1941).

[12] Papir a celulosa 11, 2, 41-44 (1956).

Received August 4, 1958

* Original Russian pagination. See C. B. translation.

PRODUCTION OF HIGH-GRADE CALCIUM AND BARIUM PEROXIDES

S. Z. Makarov and N. K. Grigor'eva

Institute of General and Inorganic Chemistry, Academy of Sciences USSR

As is known, peroxide compounds are mainly used in the formulation of regenerating agents, bleaching, polymerization, and the synthesis of new chemical compounds.

With the exception of peroxides of alkali metals and barium, which are formed by direct oxidation of the metals or their oxides with oxygen, most peroxide compounds are obtained by indirect methods such as treatment of oxides, hydroxides, and salts with hydrogen peroxide.

However, the scientific basis of methods of preparing peroxide compounds required for organizing their production is inadequate.

A study of ternary systems of metal hydroxides with hydrogen peroxide carried out in recent years [1-5] has made it possible to determine the conditions for synthesizing a number of peroxides, including calcium and barium peroxides, and to develop the most profitable methods of preparing high-grade peroxides under industrial conditions.

Synthesis of Calcium Peroxide

The calcium peroxide normally used in industry contains not more than 60-80% of CaO_2. The patents of Jobert [6] do not indicate the quality of the products obtained. High-grade calcium peroxide was obtained under special laboratory conditions by some investigators [7] to establish the physicochemical constants, but the preparation method used has no practical value.

The methods of preparing calcium peroxide existing up to the present time consist essentially of preparation of calcium peroxide hydrates and then dehydration of the latter to anhydrous CaO_2. These methods of preparing calcium peroxide hydrates may be divided into the following groups: 1) methods based on the direct interaction of hydrogen peroxide with calcium hydroxide, used as milk of lime or in the dry form, 2) methods based on exchange decomposition of calcium hydroxide by sodium peroxide in hydrochloric acid ($Ca(OH)_2 - Na_2O_2 - HCl$) 3) methods consisting of treating specially prepared mixtures of sodium peroxide and lime with water or steam (Jobert) and 4) a conversion method based on the interaction of solutions of calcium salts with hydrogen peroxide in an ammonia medium [8].

The preparation of calcium peroxide by methods where calcium hydroxide and sodium peroxide are used as starting materials cannot be considered completely successful and convenient. Commercial calcium hydroxide always contains traces of carbonate which must be removed by firing at 900-1000°. However, in the interaction of calcium hydroxide with both hydrogen peroxide and sodium peroxide it is necessary to use special, hermetically sealed apparatus to prevent the admission of atmospheric carbon dioxide and the formation of carbonates. Sodium peroxide itself as a starting material contains NaOH and Na_2CO_3 as impurities. All this considerably complicates the preparation of high-grade calcium peroxide.

The ammonia method of preparing calcium peroxide from calcium salts under industrial conditions is of particular interest. This method is quite convenient and practicable as it may be carried out in normal apparatus without special precautions. The starting materials used are such accessible and pure substances as calcium salts, hydrogen peroxide, and ammonia.

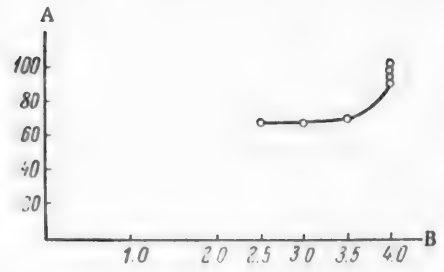

Fig. 1. Effect of $CaCl_2 : H_2O_2$ ratio on the $CaO_2 \cdot 8H_2O$ yield. A) Yield (in %), B) H_2O_2 in number of times the stoichiometric amount.

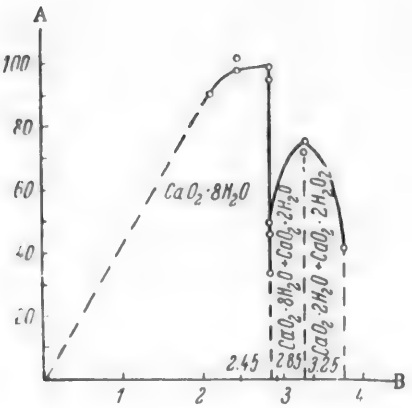

Fig. 2. Effect of H_2O_2 concentration on the formation of calcium peroxide hydrates at +2–+4°C. A) Yield (in %), B) H_2O_2 concentration in solution (in %).

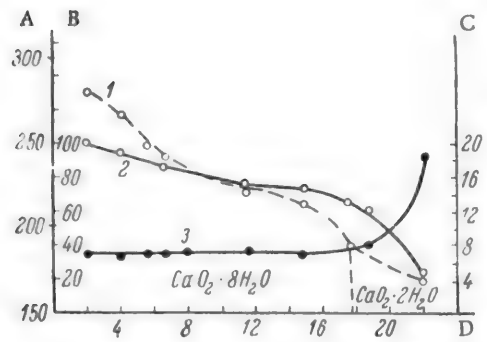

Fig. 3. Effect of reaction mixture temperature on the formation of calcium peroxide hydrates. A) Active O_2 content, 1 (in g %), B) yield, 2 (in %), C) active O_2 content, 3 (in %), D) temperature (in °C).

A study of the solubility of the ternary system $Ca(OH)_2 - H_2O - H_2O_2$ [1-3] in the range -21 to +10° made it possible to establish the presence of hydrates and perhydrates of calcium peroxide, but not of anhydrous calcium peroxide, and also to define the regions of existence of peroxide phases in relation to temperature and hydrogen peroxide concentration in the solution. Under certain conditions pure calcium peroxide octahydrate may be isolated in the form of well-formed crystals, which are converted into pure calcium peroxide under appropriate dehydration conditions.

Preparation of Calcium Peroxide Octahydrate. The formation of calcium peroxide octahydrate from calcium salts by the action of hydrogen peroxide in an ammonia medium proceeds in two stages: calcium hydroxide is first formed and this is then converted into the peroxide by interaction with hydrogen peroxide. The procedure proposed by Riesenfeld and Nottenbohm [8], starting from calcium chloride, gives too low a yield of $CaO_2 \cdot 8H_2O$, which reaches 43% at a low temperature and is only 18% at room temperature. The direct dehydration of $CaO_2 \cdot 8H_2O$ to anhydrous calcium peroxide gives a product containing not more than 17-18% of active oxygen and is unsuitable for the preparation of high-grade peroxide.

The following factors affect the formation of calcium peroxide octahydrate and its yield on calcium: 1) the ratio of $CaCl_2$ and H_2O_2, 2) the H_2O_2 concentration in the reaction mixture, and 3) the temperature at which the $CaO_2 \cdot 8H_2O$ is formed.

In the interaction of metal hydroxides or salts with hydrogen peroxide, peroxide formation only goes to completion when there is a considerable excess of hydrogen peroxide present. Our experiments, results of which are shown graphically in Fig. 1, showed that the yield only reached 92-100% when a 4-fold excess of hydrogen peroxide over the stoichiometric amount was used. A slight decrease in the excess of hydrogen peroxide appreciably reduced the $CaO_2 \cdot 8H_2O$ yield. The H_2O_2 concentration in the reaction mixture had a considerable effect on the formation of $CaO_2 \cdot 8H_2O$. When a hydrogen peroxide concentration in the range from 2.10% to 3.75% was used, the results shown graphically in Fig. 2 were obtained. The most favorable hydrogen peroxide concentration was 2.5% and with this the $CaO_2 \cdot 8H_2O$ yield reached a maximum value of about 100%. A slight increase in the H_2O_2 concentration caused the formation of a mixture of calcium peroxide hydrates, $CaO_2 \cdot 8H_2O$ and $CaO_2 \cdot 2H_2O$. It might have been considered that the formation of a mixture of calcium peroxide hydrates would be advantageous for the preparation of anhydrous CaO_2 since less dehydration would be required subsequently. However, this does not simplify the process but complicates it, as the mixtures obtained have an extremely fine crystal structure and are difficult to filter and

wash. A further increase in the hydrogen peroxide concentration could lead to the formation of calcium peroxide diperhydrate, which is an unstable compound, capable of rapid decomposition with the evolution of heat.

In the formation of pure calcium peroxide octahydrate, temperature plays no less important a role than the H_2O_2 concentration. The temperature affects both the composition of the calcium peroxide compounds obtained and the percentage yield. The results of experiments showing the effect of temperature are given graphically in Fig. 3. A full yield of product can only be obtained at temperatures of the order of +2−+4°. With a rise in temperature the yield falls noticeably and is reduced to 74% at 11.5°. Then there is an even greater fall in yield and at 18° the formation of calcium peroxide dihydrate, $CaO_2 \cdot 2H_2O$, together with $CaO_2 \cdot 8H_2O$ begins.

$CaO_2 \cdot 8H_2O$ is not formed at all at 22° and $CaO_2 \cdot 2H_2O$ separates together with calcium peroxide diperhydrate, $CaO_2 \cdot 2H_2O_2$.

Thus the optimal conditions for the preparation of calcium peroxide octahydrate are: 1) a total concentration of hydrogen peroxide in the solution equal to approximately 2.5%, 2) a ratio of $CaCl_2$ to H_2O_2 of 1:4, 3) a temperature of from 0 to +4°, and 4) an ammonia concentration of approximately 2%.

The process should be carried out by pouring a 20% solution of calcium chloride into a cooled mixture of water, hydrogen peroxide, and ammonia.

Dehydration of Calcium Peroxide Octahydrate. The dehydration of peroxide hydrates is usually complicated by partial decomposition of the main product, which is greater the greater the water of crystallization content of the hydrate. Dehydration of $CaO_2 \cdot 8H_2O$ by direct drying always leads to considerable decomposition of calcium peroxide and lowers its quality. When calcium peroxide dihydrate is dehydrated such phenomena are not observed and calcium peroxide with a high active oxygen content is obtained. Thus, it is more profitable to dehydrate $CaO_2 \cdot 8H_2O$ in two stages: first dehydration of $CaO_2 \cdot 8H_2O$ to $CaO_2 \cdot 2H_2O$ by heating in water to a temperature slightly above that at which six molecules of water of crystallization are eliminated and the compound is converted into calcium peroxide dihydrate and then dehydration of $CaO_2 \cdot 2H_2O$ to CaO_2 by vacuum drying.

Thus, the basic scheme for the preparation of calcium peroxide from calcium chloride, hydrogen peroxide, and ammonia, developed from laboratory experiments, may be represented in the following way: 1) preparation of calcium peroxide octahydrate, 2) conversion of $CaO_2 \cdot 8H_2O$ to calcium peroxide dihydrate, and 3) vacuum drying of $CaO_2 \cdot 2H_2O$ to anhydrous calcium peroxide.

The calcium peroxide obtained contained 20.5-21.0% of active oxygen which corresponds to 93-94% of calcium peroxide. The method was tested in the "Red Chemist" plant of the Ministry of Chemical Industry and adopted for production.

Synthesis of Barium Peroxide

The method of preparing barium peroxide by its direct synthesis from barium oxide and oxygen at high temperature has now lost its value. A study of the solubility of the ternary system $Ba(OH)_2-H_2O_2-H_2O$ over the range -10−+50° [4, 5] confirmed the fact that BaO_2 is not formed in aqueous solutions by direct interaction of barium hydroxide or barium salts with hydrogen peroxide. Only barium peroxide hydrates and perhydrates are formed under these conditions and these may be used for the preparation of barium peroxide.

Existing methods for the preparation of barium peroxide hydrates and perhydrates usually differ in the starting materials, hydrogen peroxide concentration, temperature, and other factors, and are of a preparative nature.

A systematic study of the solubility isotherm in the range -10−+50° showed that the only barium peroxide hydrate, $BaO_2 \cdot 8H_2O$, has a very limited region of existence. From this it is evident that it is unprofitable to prepare barium peroxide through the octahydrate. On the other hand, barium peroxide diperhydrate, $BaO_2 \cdot 2H_2O_2$, has a wide region of existence both with respect to temperature and hydrogen peroxide concentration in the solution. This compound may be prepared both from barium hydroxide by the action of hydrogen peroxide and from barium salts by the action of hydrogen peroxide in an ammonia medium. However, the preparation of $BaO_2 \cdot 2H_2O_2$ from barium hydroxide requires undesirable additional operations connected with freeing commercial barium hydroxide octahydrate from carbonate and iron and with hermetically sealed apparatus. The preparation of $BaO_2 \cdot 2H_2O_2$ from barium salts under industrial conditions is more convenient but requires refinement of reagent ratios and process conditions as both the product yield and the quality depend on these.

Many laboratory experiments, confirmed by large-scale experiments on the synthesis of barium peroxide diperhydrate, $BaO_2 \cdot 2H_2O_2$, from barium chloride and hydrogen peroxide in an ammonia medium, showed that the product obtained both at 0° and at room temperature contained a large amount of $Ba(OH)_2$ and low yields (about 60%) were produced. An increase in the hydrogen peroxide concentration had little effect on the quality and yield of the barium peroxide diperhydrate.

During the formation of barium peroxide diperhydrate there is, apparently, either some decomposition and hence the rise in solubility and formation of $Ba(OH)_2$ or incomplete oxidation of the starting material.

By developing and refining the method of preparing $BaO_2 \cdot 2H_2O_2$ from barium nitrate, hydrogen peroxide, and ammonia, we found conditions for forming $BaO_2 \cdot 2H_2O_2$ which made it possible to obtain a product with the highest active oxygen content in the greatest yield. The main factor affecting the formation of $BaO_2 \cdot 2H_2O_2$ is the quantitative ratio of barium salt to hydrogen peroxide. However, the dilution, i.e., the over-all concentration of hydrogen peroxide in the reaction mixture is also of considerable importance. It was established that the best yield of product (80-85%) with an active oxygen content of 18.5-19.0% was obtained with an over-all hydrogen peroxide concentration in the solution of 3.5-4.0% and at a $Ba : 2H_2O_2$ ratio of 1 : 2.25 or 1 : 2.5. $BaO_2 \cdot 2H_2O_2$ is formed successfully at room temperature and may be dried at 110-115° and atmospheric pressure. The product obtained contained 92-95% of BaO_2 and the yield was 80-85% on barium.

The method of preparing barium peroxide was tested under industrial conditions in the "Red Chemist" plant in Leningrad and adopted for production. The barium peroxide previously produced by the factory contained 84-88% of BaO_2.

SUMMARY

1. Calcium and barium peroxides may be synthesized through the calcium and barium hydrates and perhydrates as the anhydrous peroxides of these elements are not formed by direct interaction of calcium and barium hydroxides and salts with hydrogen peroxide.

2. While calcium peroxide is successfully prepared through calcium peroxide octahydrate at low temperature, barium peroxide is best synthesized through barium peroxide diperhydrate at room temperature.

3. The calcium and barium peroxides obtained are quite satisfactory industrially both in quality and in yield.

LITERATURE CITED

[1] S. Z. Makarov and N. K. Grigor'eva, Izvest. Akad. Nauk SSSR, Otdel. Khim. Nauk 3, 385 (1954).*

[2] S. Z. Makarov and N. K. Grigor'eva, Izvest. Akad. Nauk SSSR, Otdel. Khim. Nauk 4, 598 (1954).*

[3] S. Z. Makarov and N. K. Grigor'eva, Izvest. Akad. Nauk SSSR, Otdel. Khim. Nauk 11, 1289 (1958).*

[4] S. Z. Makarov and N. K. Grigor'eva, Izvest. Akad. Nauk SSSR, Otdel. Khim. Nauk 1, 9 (1959). *

[5] S. Z. Makarov and N. K. Grigor'eva, Izvest. Akad. Nauk SSSR, Otdel. Khim. Nauk 7, 1163 (1959). *

[6] DRP 132706, 21 IV 1902; 7416, 30 IX 1902; 7415, 30 IX 1902; 128716, 21 VI 1902.

[7] V. Kotov and S. I. Raikhshtein, Zhur. Fiz. Khim. 15, 1057 (1941).

[8] E. H. Riesenfeld and W. Nottebohm, Z. anorg. Chem. 85, 405 (1914).

Received December 17, 1958

* Original Russian pagination. See C. B. translation.

INTERACTION OF BARIUM AND CALCIUM CARBONATES WITH SULFUR DIOXIDE IN THE PRESENCE OF A REDUCING AGENT

V. V. Pechkovskii

Perm State University

A study of the interaction of barium and calcium carbonates with sulfur dioxide in the presence of a reducing agent makes it possible to draw conclusions on some physicochemical properties of the sulfur-containing compounds thus formed. Together with this, the elucidation of the rules of formation of sulfur-containing compounds of calcium and barium is of interest in understanding a number of processes occurring in ferrous and nonferrous metallurgy and also the technologies of inorganic substances [1-3]. The literature contains a comparatively small amount of experimental work on the problem considered [4-8].

The purpose of the work was the elucidation of the formation conditions of sulfur-containing compounds of calcium and barium by interaction of carbonates of these metals with sulfur dioxide in a reducing atmosphere. A study was made of the relation of the degree and completeness of formation of sulfites, sulfates, and sulfides of calcium and barium to temperature, content, and nature of the carbon-containing material and SO_2 concentration in the gas phase.

The experimental method was similar to that used previously [9]. Calcium and barium carbonates (analytical grade) and also calcium oxide were used. We worked with dry, pure mixtures of sulfur dioxide and nitrogen. The duration of the experiments was 15 minutes, the sample of barium and calcium carbonates weighed 0.4 g and the SO_2 concentration in the gas phase was kept at 10% in all but specially mentioned cases. The carbon-containing materials used were coke and wood charcoal containing the following, respectively (in %): ash 12.8 and 1.8, sulfur 0.6 and 0.4 and volatile materials 0.7 and 9.4. The solid products from firing were analyzed for sulfide, sulfite, and sulfate sulfur.

Tables 1-4 give the main results of the experiments.

The interaction of metal oxides with sulfur dioxide in a reducing atmosphere is a complex process. Analysis of the experimental material obtained made it possible to give the following scheme for the formation of calcium and barium sulfites, sulfides and sulfates in this process:

$$MeCO_3 \rightleftarrows MeO + CO_2, \quad (1)$$

$$MeO + SO_2 \rightleftarrows MeSO_3, \quad (2)$$

$$4MeSO_3 + 2SO_2 = 4MeSO_4 + S_2, \quad (3)$$

$$SO_2 + C \rightleftarrows 1/2\,S_2 + CO_2, \quad (4)$$

$$CO_2 + C \rightleftarrows 2CO, \quad (5)$$

$$2MeO + S_2 + C = 2MeS + CO_2, \quad (6)$$

$$MeS + 2SO_2 = MeSO_4 + S_2. \quad (7)$$

The data in Tables 1-3 indicate that in the interaction of sulfur dioxide with calcium carbonate in a reducing atmosphere calcium sulfide is formed even at 700°. The degree of formation of calcium sulfide increases with an increase in temperature since the rate of reactions (1), (4) and (6) increases with a rise in temperature. Together with calcium sulfide, the solid products from firing contained calcium sulfite and sulfate and the degree of formation of these fell with a rise in temperature. The latter is due to the fact that with a rise in temperature

TABLE 1

Interaction of Sulfur Dioxide with Calcium Carbonate in the Presence of Carbon. Relation of Degree of Formation of Sulfur-Containing Products to Temperature and Carbon Content of Starting Mixture

Temperature (in °C)	Degree of conversion of calcium carbonate (in %) at the following carbon contents of the mixture (in %)								
	CaS			$CaSO_3$			$CaSO_4$		
	20.0	33.0	43.0	20.0	33.0	43.0	20.0	33.0	43.0
700	0.6	2.2	3.1	4.3	2.5	0.8	9.2	6.8	4.5
800	12.8	18.6	27.3	1.0	0.5	0.3	9.6	5.2	3.0
900	42.4	55.7	70.0	0.3	0.2	0.3	9.9	2.3	0.8
1000	57.1	73.2	78.5	0.3	0.2	0.3	10.0	0.0	0.0

TABLE 2

Interaction of Sulfur Dioxide with Calcium Oxide and Carbonate in the Presence of Carbon. Temperature Dependence of the Degree of Formation of Sulfur-Containing Products. Carbon Content of Initial Mixture 43.0%

Reaction products	Degree of conversion of calcium carbonate and oxide (in %) at the following temperatures (in °C)							
	650		750		850		950	
	CaO	$CaCO_3$	CaO	$CaCO_3$	CaO	$CaCO_3$	CaO	$CaCO_3$
CaS	0.8	0.8	21.0	13.2	51.2	51.0	66.5	77.8
$CaSO_3$	2.7	1.0	1.0	0.5	0.3	0.3	0.5	0.2
$CaSO_4$	8.0	2.0	5.2	3.7	3.0	2.5	0.0	0.0

TABLE 3

Interaction of Barium Carbonate with Sulfur Dioxide in the Presence of Carbon. Temperature Dependence of the Degree of Formation of Sulfur-Containing Products. Carbon Content of Initial Mixture 43.0%

Reaction products	Degree of conversion of barium carbonate (in %) at the following temperatures (in °C)								
	600	650	700	750	800	850	900	950	1000
BaS	0.0	0.0	0.0	15.5	38.8	64.0	74.4	80.0	84.2
$BaSO_3$	19.7	34.4	27.2	15.8	7.6	1.8	1.2	0.8	0.5
$BaSO_4$	22.4	35.7	35.0	40.3	33.2	13.5	6.2	4.7	1.8

the equilibrium of reaction (2) is displaced to the left and that of reaction (4), to the right. With a sufficient carbon content in the charge and at a temperature above 900° calcium sulfide is the main solid sulfur-containing product of the interaction of SO_2 with calcium carbonate (Table 1).

Replacement of calcium carbonate by calcium oxide does not essentially affect the course of the interaction studied (Table 2). However, we should emphasize that in the temperature range 650-750° the degree of formation of calcium sulfide, sulfite, and sulfate is higher when calcium oxide is used than when calcium carbo-

TABLE 4

Interaction of Barium Carbonate with Sulfur Dioxide in the Presence of Carbon. Relation Between the Degree of Formation of Sulfur-containing Products and the SO_2 Concentration in the Gas Phase. Carbon Content of Initial Mixture 33.0%.

Reaction products	Degree of conversion of barium carbonate (in %) at the following SO_2 concentrations in the gas (in %)							
	700°		800°		900°		1000°	
	10.0	20.0	10.0	20.0	10.0	20.0	10.0	20.0
BaS	0.0	0.0	33.8	19.4	71.4	58.5	68.5	55.0
$BaSO_3$	28.6	23.0	5.7	3.2	2.2	2.0	0.5	1.2
$BaSO_4$	51.7	70.4	44.0	64.0	13.6	32.3	2.6	9.3

nate is used. This is explained by the fact that at comparatively low temperatures reaction (1) limits the rate of formation of sulfur-containing compounds of calcium. As follows from the data in Table 2, in the temperature region above 750° the decomposition of calcium carbonate does not limit the rate of formation of sulfur-containing compounds of calcium by interaction of calcium carbonate with sulfur dioxide in a reducing atmosphere.

In general characteristics, the nature of the rules of formation of sulfur-containing compounds of barium is similar to that for calcium. The degree of formation of barium sulfide during the interaction of barium carbonate with sulfur dioxide in a reducing atmosphere increases with a rise in temperature and the temperature dependence of the degree of formation of barium sulfite and sulfate is expressed by a curve with a maximum (Table 3). With a sufficient carbon content in the charge and at a temperature above 1000° the main solid sulfur-containing product of the interaction of sulfur dioxide with barium carbonate is barium sulfide. Analysis of the results presented in Tables 1-3 shows, nonetheless, that there are some peculiarities in the reaction of barium carbonate with sulfur dioxide in a reducing atmosphere. The degree of formation of sulfur-containing compounds of barium under otherwise equal conditions is higher than the degree of formation of sulfur-containing compounds of calcium (Tables 1 and 3). The higher degree of formation of barium sulfite and sulfate is particularly noticeable. Not only are more of these compounds formed, but also the maxima of barium sulfite and sulfate formation are displaced into a higher temperature zone in comparison with formation of the corresponding calcium compounds. All this is explained by the fact that barium sulfide, sulfite, and sulfate have a higher thermal stability than calcium sulfide, sulfite, and sulfate, respectively [4, 5].

Data on the effect of the carbon content of the charge on the formation of sulfur-containing products during the interaction of barium and calcium carbonates with sulfur dioxide are given in Tables 1, 3, and 4. It is clearly seen that when the carbon content of the charge is reduced the degree of sulfide formation under otherwise equal conditions falls and the degree of sulfate formation increases. This is due to the fact that with a deficiency of carbon in the mixture, the rates of reactions (3) and (7) increase and the rates of reactions (4) and (6) decrease.

The properties of the carbon-containing material also have a substantial effect on the rate of sulfide formation. Thus, in the interaction of calcium carbonate with sulfur dioxide in the presence of coke and wood charcoal the degree of calcium sulfide formation was found to be 2.8 and 27.3% at 800°, 22.6 and 70.0% at 900°, and 68.5 and 78.5%, respectively, at 1000°. Consequently at a temperature of up to 900° coke is an inactive carbon-containing material. At temperatures above 1000° the reactivity of coke with respect to the interaction of calcium and barium carbonates with sulfur dioxide approaches that of wood charcoal.

It was then established that an increase in the sulfur dioxide concentration in the gas phase increases the over-all degree of formation of sulfur-containing compounds of calcium and barium. This is connected with an increase in the rate of reactions (2)-(4), (6), and (7) with an increase in the sulfur dioxide concentration in the gas phase. It was found that when the SO_2 concentration in the gas phase was increased from 10.0 to 20% there was an increase in both the degree of calcium sulfide formation and the degree of calcium sulfate formation. A somewhat different picture was observed in the interaction of barium carbonate with sulfur dioxide in the presence of carbon. With an increase in the SO_2 concentration in the gas phase from 10.0 to 20.0% the over-all content

of sulfur-containing barium compounds in the firing products increased but only as a result of a substantial increase in the barium sulfate content. As regards barium sulfide, the content of it even decreased somewhat when the SO_2 concentration in the gas phase was increased from 10.0 to 20.0%.

The rules found indicate that under definite conditions barium sulfite and sulfide may be oxidized rapidly by sulfur dioxide according to reactions (3) and (7). As a result of this, simultaneously with an increase in the sulfur dioxide content of the gas phase it is necessary to increase the carbon content of the charge to increase the barium sulfide yield.

LITERATURE CITED

[1] M. A. Pavlov, Metallurgy of Cast Iron, II [in Russian](Metallurgy Press, 1949).

[2] V. I. Smirnov, Metallurgy of Copper and Nickel [in Russian] (Metallurgy Press, 1950).

[3] M. E. Pozin, Technology of Mineral Salts [in Russian](State Chem. Press, 1949).

[4] A. M. Samarin and I. S. Kulikov, Zhur. Neorg. Khim. 1, 7, 1566 (1956).

[5] S. D. Shargorodskii and Ya. I. Fialkov, Ukrain. Khim. Zhur. 15, 104 (1949).

[6] V. I. Lukashin, Izvest. Akad. Nauk SSSR, Otdel. Tekh. Nauk 1, 131 (1949).

[7] V. E. Vasil'ev, Izvest. Kievsk. Politekh. Inst. 14, 196 (1954).

[8] E. I. Danilova and G. S. Frents, Izvest Akad. Nauk, SSSR, Otdel. Tekh. Nauk 11, 25 (1955).

[9] V. V. Pechkovskii, Zhur. Priklad. Khim. 30, 825 (1957).*

Received December 10, 1958

* Original Russian pagination. See C. B. translation.

INFLUENCE OF γ-RADIATION ON THE PHYSICOCHEMICAL PROPERTIES OF SOME CATION EXCHANGERS

A. M. Semushin and I. A. Kuzin

Lensovet Technological Institute, Leningrad

The possibility of using ion-exchange resins to concentrate and separate both artificial and natural radioactive elements has been shown by many investigators [1-3]. Here it was established that ion-exchange resins are sensitive to the radiation-chemical action of β- and γ-radiations, which leads to a change in their physicochemical properties.

As is known from the literature, the irradiation of both anionites and cationites in either the dry or the swollen state leads to substantial changes in both their exchange capacity and degree of swelling [4-8]. These changes for the separate types of resin are so great that they should be taken into consideration in the sorption of radioactive compounds.

In this paper we give the data obtained in studying the radiation-chemical stability of cationites in the hydrogen form after their irradiation in water with the γ-quanta of Co^{60}.

EXPERIMENTAL

For the irradiation of resins KU-2, KU-1, SBS-1, KFU, KMT and KB-4P-2 we used an active source of 1400 g-equiv of radium with a dose output of 78-200 roentgens per second. The maximum integral dose was 1.38×10^8 roentgens. The absorbed energy was calculated on the basis of 1 cc of water. The presence of resin in the water phase was not taken into consideration, since the density of the investigated cationites in the swollen state is close to the density of water, for which the scattered energy value, corresponding to 1 roentgen, is equal to 93-95 ergs.

All of the residues used in the study were first freed of impurities by washing with acid, alkali, and distilled water.

For irradiation we took known weights of the cationites in the hydrogen form, which were contained in glass test tubes filled with water. The physicochemical properties of the irradiated resins were examined after the resins had been separated from solution and washed thoroughly with water to remove decomposition products. The total amount of acid that had gone into solution was determined by titration of both the solution and the wash waters.

Since a criterion for estimating the radiation-chemical stability of ion-exchange resins does not exist at the present time, then to compare different types of resins a simultaneous consideration of several ionite properties must be made. In our opinion, the most important properties are the exchange capacity of the resin at different pH values, the degree of swelling, and the loss in weight. In this paper the indicated characteristics were determined using conventional methods. In studying the influence of radiation on the exchange capacity of a resin it is necessary to consider the total decrease in the ion-exchange capacity of the original resin sample, due mainly to two causes: dissolution of the cationite and destruction of the functional groups.

The data, characterizing the influence of radiation on the exchange capacity of resins, are given in Table 1 and plotted in Fig. 1.

The experimental results indicate that the studied cationites, containing a sulfo group in the benzene ring, are more stable toward γ-radiation than the carboxylic resins KMT and KB-4P-2, synthesized from methacrylic

TABLE 1

Action of γ-Rays on Carboxylic Resins

Dose		Static exchange capacity (mg-equiv/g)			Swelling in water (in ml/g)			Swelling in 0.1 N NaOH (in ml/g)		
roentgens	ev/cc	KB-4P-2	KMT	KFU	KB-4P-2	KMT	KFU	KB-4P-2	KMT	KFU
0	0	10.22	9.98	5.69	2.46	2.96	2.89	5.5	4.6	5.25
$6.7 \cdot 10^7$	$3.94 \cdot 10^{21}$	8.25	9.34	5.47	2.59	3.00	2.97	8.5	5.9	5.28

TABLE 2

Action of γ-Rays on Different Cationites

Dose		Weight loss (in %)				Density of cationites in hydrated state (in g/cc)			
roentgens	ev/cc	KU-2-2	KU-2-8	KB-4P-2	KU-1	KU-2-8	KB-4P-2	KU-1	SBS
0	0	0	0	0	0	1.190	1.219	1.204	1.191
$0.53 \cdot 10^8$	$3.1 \cdot 10^{21}$	2.5	1.4	1.6	1.1	1.180	1.203	1.218	1.189
$0.7 \cdot 10^8$	$4.1 \cdot 10^{21}$	—	3.7	3.5	1.4	1.173	1.195	1.207	1.183
$0.97 \cdot 10^8$	$5.6 \cdot 10^{21}$	—	4.3	4.0	1.3	1.165	1.201	1.200	1.180
$1.38 \cdot 10^8$	$8.0 \cdot 10^{21}$	—	7.0	8.0	1.0	1.154	1.205	1.200	1.180

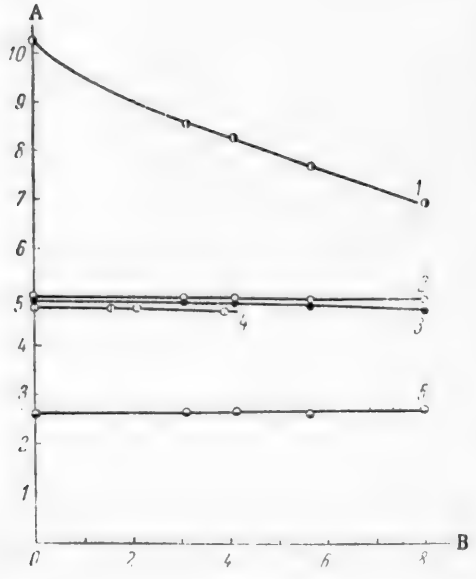

Fig. 1. Change in capacity of cationites as a function of the dose. A) Capacity of cationites (in mg-equiv/g), B) dose (in ev/cc × 10^{21}). 1) KB-4P-2, 2) KU-1, 3) KU-2-8, 4) KU-2-24, 5) SBS-1.

acid. For example, at a dose of 6.7×10^7 roentgens the sulfocationites KU-1, KU-2 and SBS-1 hardly change their capacity because of destruction of functional groups, whereas the carboxylic resins KFU, KMT and KB-4P-2 show a capacity reduction of 4, 7 and 19%, respectively. The relatively small loss in capacity shown by resin KFU, synthesized from phenoxyacetic acid and formaldehyde, supports the premise made in [8, 9] that phenol-formaldehyde resins are stable.

The data given in Table 2, showing the weight losses, and also the results of the experiments, plotted in Fig. 1, make it possible to calculate the total reduction in the capacity of the resins when irradiated.

Thus, for resin KU-2 (8% DVB) at a dose of 1.3×10^8 roentgens it is equal to 10.4%, while for KB-4P-2 it is equal to 42%.

It is interesting to mention that the total loss in capacity shown by resin KU-2 (8% DVB) is mainly due to dissolution of the cationite, while in the case of resin KB-4P-2 the loss in capacity is mainly due to destruction of the functional groups. This indicates that the sulfo and carboxyl groups show a different stability toward radiation.

As can be seen from Fig. 2, a reduction in the total capacity shown by resins KU-2 (8% DVB) and KU-1 when the radiation dose is increased is found to be in harmony with the amount of acid going into solution.

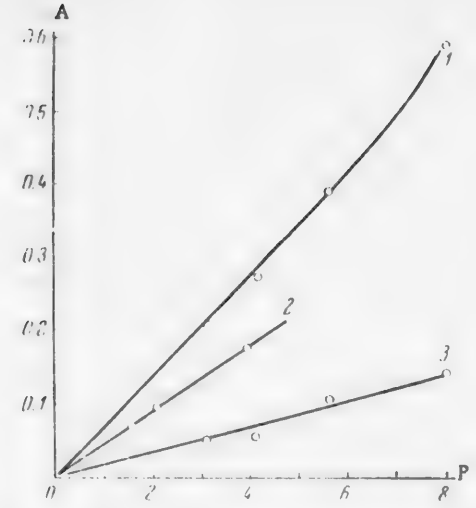

Fig. 2. Dependence of yield of acid on the dose. A) Yield of acid (in mg-equiv/g), B) dose (in ev/cc × 10^{21}). 1) KU-2-8, 2) K-2U-2-24, 3) KU-1.

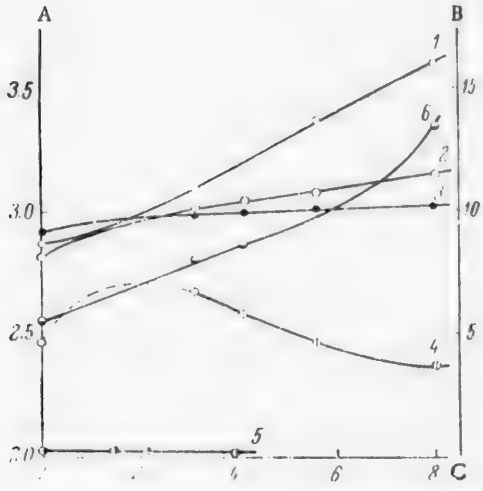

Fig. 3. Influence of γ-radiation on swelling of cationites in water. A) Swelling in water (in ml/g), B) swelling on 0.1N NaOH, C) dose (in ev/cc × 10^{21}). In water: 1) KU-2-8, 2) SBS-1, 3) KU-1, 4) KB-4P-2, 5) KU-2-24; in 0.1N NaOH solution: 6) KB-4P-2.

A study of the degree of swelling shown by ion-exchange resins permits judging to a certain degree the nature of the destruction processes suffered by resins when exposed to radiation. The degree of swelling shown by cationites depends on the nature of the sorbed ion, and on the ionic strength and pH of the solution. Proceeding from this, to ascertain the nature of the destruction processes or "crosslinking" suffered by the investigated resins, we determined the absolute swelling in water and in 0.1N NaOH solution, and also the density of the resin in the hydrated state. The data, characterizing the degree of swelling, are given in Table 2 and plotted in Fig. 3. The obtained results indicate that the swelling of sulfo- and carboxy-cationites in water at the given doses increases slightly, while for KU-1 and KU-2-24 it remains practically unchanged.

For cationite KB-4P-2, a reduction in the absolute swelling in water is observed at certain doses, which is probably associated with a loss of part of the ion-exchange groups. The swelling of this resin in 0.1N NaOH solution increases sharply with increase in the dose, due to the destruction of the chains of the methacrylic acid polymer.

Comparing the data obtained for the change in the physicochemical properties of the different kinds of cationites, it becomes possible to assume that the resistance shown by ion-exchange resins to the action of γ-radiation is determined mainly by their structure. Cationites KU-1, KU-2, SBS-1 and KFU are the most stable toward irradiation, since they contain aromatic rings in their composition, which are capable of absorbing the radiation energy without decomposition.

A comparison of the data, obtained by us in the irradiation of resins in water, with the results of exposing the dry cationites KU-2, KU-1, SBS-1 and KB-4P-2 to the action of γ-rays [7], reveals that the destruction processes and the loss in capacity are somewhat different in the dry and in the swollen resins.

From a comparison of our results with the literature data [9-11] it can be seen that not all ion-exchange resins showing a high resistance to the action of γ-radiation are characterized by a high chemical and thermal stability. For example, cationite KU-1 hardly changes its properties under the given irradiation conditions, and yet the thermal and chemical stability of this resin is somewhat below that of the other investigated sulfo-cationites. At the same time, cationite KU-2, containing more than 8-10% DVB, is a sorbent in which there is a coupling of both radiation and chemical stability.

SUMMARY

1. An investigation of the changes in the physicochemical properties of some cationites when exposed to Co^{60} γ-radiation revealed that the exchange capacity of resins KU-2, KB-4P-2, KFU and KMT is decreased by irradiation, whereas the capacity of resins KU-1 and SBS-1 remains practically constant with the given doses.

2. A comparative estimate of the stability of three types of carboxylic resins was made. It was established that cationites KB-4P-2 and KMT, synthesized from methacrylic acid, are less stable than the KFU resin, obtained by the polycondensation of phenoxyacetic acid with formaldehyde.

3. It was established that all of the investigated resins, when exposed to γ-radiation, suffer destruction of the polymer chains, which is expressed by increased swelling in water or in caustic.

4. It was shown that the amount of divinylbenzene in the KU-2 resin affects the solubility of the resin, but has little effect, at the given radiation doses, on the reduction in exchange capacity per gram of absolutely dry resin.

LITERATURE CITED

[1] E. Tompkins, J. Khym, and W. Cohn, J. Am. Chem. Soc. 69, 2769 (1947).

[2] D. E. Ferguson, Papers of Foreign Scientists at International Conference on World Utilization of Atomic Energy [Russian translation] (Goskhimizdat, Moscow, 1956)p. 243.

[3] E. Minami, M. Honda, and Y. Sasaki, Bull. Chem. Soc. Japan 31, No. 3, 372 (1958).

[4] G. Parker, J. Higgins, and J. Roberts, Ion-Exchange Technology (New York, 1956), p. 442.

[5] G. I. Cathers, Papers of Foreign Scientists at International Conference on World Utilization of Atomic Energy [Russian translation]. (Metallurgical Press, Moscow, 1956) p. 679.

[6] M. M. Senyavin, G. M. Kolosova, and V. A. Nikashina, Zhur. Neorg. Khim. 3, 104 (1958).

[7] A. P. Polevodov, V. A. Nikashina, A. V. Gordievskii, M. M. Senyavin, and A. Kh. Breger, Khim. i Khim. Tekhn. 4, 761 (1958).

[8] Chang Man-wei, A. I. Chernova, and M. A. Proskurnin, Atomnaya Énergiya 5, 573 (1958).

[9] K. M. Saldadze and Z. G. Demonterik, Supplement Investigations in the Domain of Ion-Exchange Chromatography [in Russian]. (Izd. AN SSSR, Moscow, 1957) p. 106.

[10] A. A. Vasil'ev, Supplement: Investigations in the Domain of Ion-Exchange Chromatography[in Russian](Izd. AN SSSR, Moscow, 1957) p. 89.

[11] N. G. Polyanskii, Zhur. Priklad. Khim. 32, No. 4, 735 (1959).*

Received January 29, 1959

* Original Russian pagination. See C. B. translation.

INVESTIGATION OF THE STEAM-DISTILLATION PROCESS*

É. K. Siirde and P. G. Romankov

Tallinn Polytechnical Institute

In steam distillation the weight ratio of water to distilled substance in the distillate is theoretically determined by the formula

$$\frac{G_1}{G_0} = \frac{M_1 P_1}{M_0 P_0}, \tag{1}$$

where G_1 is the weight amount of distilled substance, G_0 is the weight amount of steam, M_1 is the molecular weight of the distilled substance, and M_0 is the molecular weight of steam.

In view of the fact that complete equilibrium is actually not achieved in steam distillation, it becomes necessary to consider the excess consumption of introduced steam. Consequently, the actual consumption of steam G_0' can be expressed by the equation

$$G_0' = G_1 \frac{P_0 M_0}{P_1 M_1 \varphi}, \tag{2}$$

where φ is the saturation coefficient, which may be regarded as a measure of the degree to which steam is saturated with the distilling substance, and is expressed as the ratio

$$\varphi = \frac{P_1}{P_1^*}, \tag{3}$$

where P_1 is the actual partial vapor pressure of the distilling substance, and P_1^* is its equilibrium pressure at the distillation temperature.

In the literature [1-6] it is indicated that in practice the saturation coefficient φ fluctuates from 0.3 to 0.9, and depends on many factors, the main ones being the steam passage rate, the depth of the liquid layer, the diameter of the openings through which the steam is admitted into the still, and the physical properties of the substance being distilled.

Carey [4] found that this dependence is expressed by the following equation:

$$\varphi = \frac{P_1}{P_1^*} = 1 - e^{-\frac{KH}{d_0}}, \tag{4}$$

where d_0 is the diameter of the steam bubbles, H is the thickness of the liquid layer through which the steam passes, and K is a constant, characterizing the substance being distilled, and dependent on the diffusion rate of the substance in the vapor state.

*Communication II.

TABLE 1

Characteristics of Different Apparatus Used in the Experiments

Designation	Dimensions
Diameter of apparatus (in mm)	89, 100, 150, 255
Height of apparatus (in mm)	240, 400, 1500
Volume of apparatus (in liters)	from 1.89 to 76.8
Diameter of nozzle for introduction of steam (in mm)	6, 9, 11, 16, 1 × 19
Number of nozzles for introducing steam (pieces)	1, 2, 3
Amount of liquid consumed in experiment (in liters)	up to 25
Height of layer (in mm)	up to 820

TABLE 2

Physicochemical Properties of Substances Used in the Investigation of Distillation With Steam

Substance	Formula	Molecular wt.	Specific gravity at temp. (in °C)	Boiling point (in °C)	Viscosity (in cp.) at temp. (°C)	Surface tension of liquid (dyne/cm)
Carbon tetrachloride	CCl_4	153.8	1.595 (20°)	76.8	0.97 (20°)	26.8 (20°)
Benzene	C_6H_6	78.1	0.879 (20°)	80.1	0.65 (20°)	28.88 (20°)
Toluene	$C_6H_5CH_3$	92.1	0.866 (20°)	110.8	0.586 (20°)	28.43 (20°)
m-Xylene	$C_6H_4(CH_3)_2$	106.2	0.867 (17°)	139.3	0.61 (20°)	28.9 (20°)
Turpentine	—	136	0.878 (20°)	154—6	1.612 (20°)	21.2 (95°)
Aniline	$C_6H_5NH_2$	93.1	1.022 (20°)	184.4	4.40 (20°)	42.9 (20°)
Nitrobenzene	$C_6H_5NO_2$	123.1	1.205 (18°)	210.9	2.01 (20°)	42.6 (18°)
Naphthalene	$C_{10}H_8$	128.2	1.145 (20°)	217.9	0.776 (100°)	32.26 (80°)
β-Naphthol	$C_{10}H_7OH$	144.2	1.217 (4°)	285—6	—	—
Shale phenol	—	180	1.032 (20°)	240—260	27.8 (20°)	—
Shale tar	—	220	0.978 (20°)	300—320	—	—
Oleic acid	$CH_3(CH_2)_7CH=CH(CH_2)_7COOH$	282.5	0.900 (12°)	360 (decomposes)		

Some laboratory data on the steam distillation of aniline indicate that the effect of the depth of immersion of the bubbler can be expressed by equation (4), but there fails to be any data regarding the effect exerted by the size of the bubbles.

Starting with a material balance, it becomes possible to derive a theoretical expression for the saturation coefficient in the following manner. The material balance equation with respect to the substance being steam distilled can be the following:

$$k'\left(p_1^* - \bar{p}_1\right)dF = S_A \bar{w}_{cm} \gamma \frac{dp_1}{P}, \qquad (5)$$

where k is the mass-transfer coefficient, p_1 is the vapor pressure of the distilling liquid at its surface temperature, $\bar{p}_1$ is the average vapor pressure of the distilling liquid in the steam flow, F is the surface of mass transfer, S_A is the cross-section area of the apparatus, $\bar{w}_{cm}$ is the average rate of the vapor phase in this cross-section, γ is the specific gravity of the vapors of the liquid being distilled, and P is the total pressure.

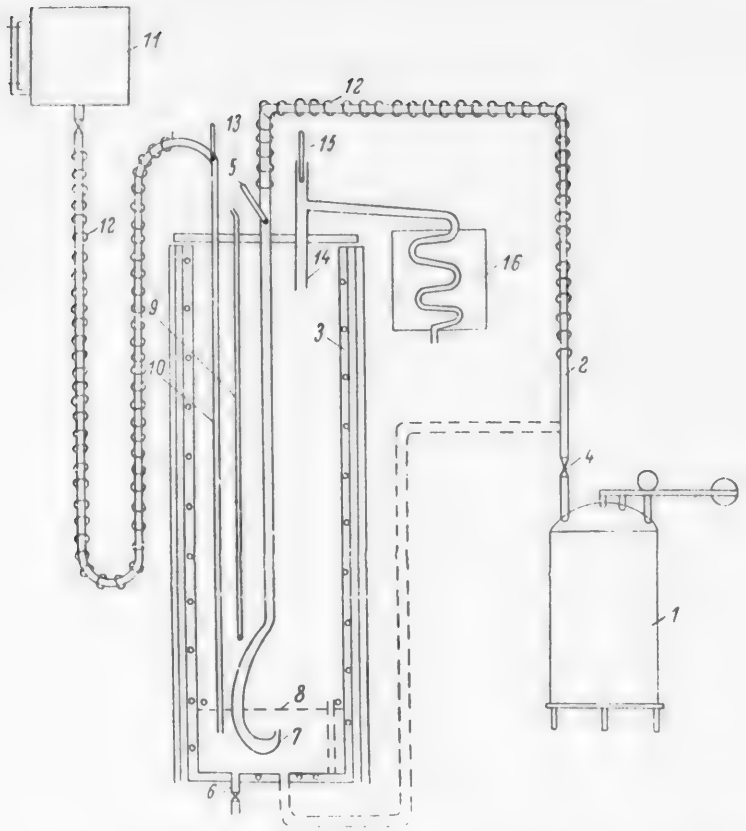

Fig. 1. Diagram of apparatus. 1) Steam kettle; 2) tube for admitting steam to still pot; 3) still pot; 4) valve for regulating steam flow; 5) thermometer; 6) valve for draining residue from still pot; 7) removable nozzle for admitting steam into liquid; 8) removable perforated baffle; 9) thermocouple; 10) tube for adding liquid to still pot; 11) supply tank; 12) heater; 13 and 15) thermometers; 14) tube for escape for distillate vapors from pot; 16) coil condenser.

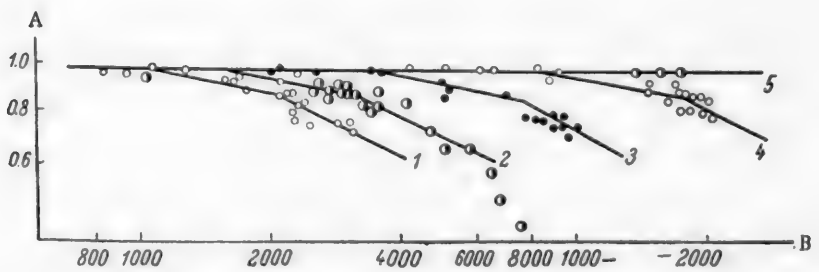

Fig. 2. Relation between saturation coefficient φ and the Fr criterion in steam distillation. A) Saturation coefficient φ; B) Freud criterion (Fr). 1) Carbon tetrachloride, $\frac{M_1P_1}{M_0P_0}$ = 22.3; 2) benzene, $\frac{M_1P_1}{M_0P_0}$ = 10.3; 3) toluene, $\frac{M_1P_1}{M_0P_0}$ = 4.1; 4) xylene, $\frac{M_1P_1}{M_0P_0}$ = 1.91; 5) nitrobenzene, $\frac{M_1P_1}{M_0P_0}$ = 0.18.

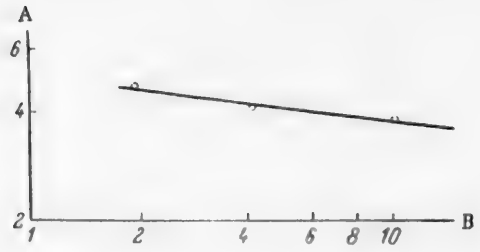

Fig. 3. Relation between ratio $\frac{\varphi}{Fr^{-0.12}}$ (A) and composition criterion (B) in the foam regime.

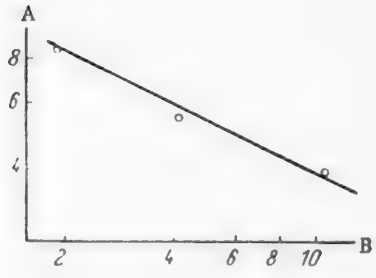

Fig. 4. Relation between ratio $\frac{\varphi}{Fr^{-0.48}}$ (A) and composition criterion (B) in the spray regime.

From this we obtain:

$$\frac{k'P}{S_A \bar{w}_{cm} \gamma} \int_0^F dF = \int_{p_1'}^{p_1''} \frac{dp_1}{p_1^* - p_1}. \qquad (6)$$

Integrating this equation with respect to the surface of mass transfer from O to F, and, in like manner, with respect to the vapor pressure of the liquid being distilled from p_1', corresponding to the entrance of the steam into the apparatus, to p_1'', corresponding to its escape from the apparatus, we obtain

$$\frac{k'FP}{S_A \bar{w}_{cm} \gamma} = \ln \frac{p_1^* - p_1''}{p_1^* - p_1'}. \qquad (7)$$

Assuming that $p_1' = 0$, i.e., that the vapors of the liquid being distilled are absent in the steam flow when the steam enters the apparatus, and taking into consideration the fact that saturation coefficient $\varphi = \frac{p_1''}{p_1^*}$, we find the value of φ by substituting as follows in equation (7):

$$\varphi = \frac{p_1''}{p_1^*} = 1 - e^{-\frac{k'FP}{S_A \bar{w}_{cm} \gamma}}. \qquad (8)$$

The obtained expression is a semilogarithmic function of different variables. However, it fails to give any important advantages over the criterial equations usually used in investigating mass- and heat-transfer processes.

In this paper, in which we investigated the dependence of the saturation coefficient on various factors, we resorted to the conventional technique of generalizing experimental material via the methods of the theory of similarity, expressing the results in the form of criterial equations, relating to different hydrodynamic regimes of the process.

According to equation (8), included in the principal factors that affect the saturation coefficient is the average velocity $\bar{w}_{cm}$ of the gas phase, which depends not only on the rate w_0 with which the steam is introduced into the liquid, but also on the rate of increase in the volume of the vapor phase due to the vapors of the substance being distilled, which in turn depends on the physical properties, characterized by the ratio $\frac{G_1}{G_0} = \frac{M_1 P_1}{M_0 P_0}$, of the distilling substance. The mass-transfer surface F, entering into equation (8), depends on the diameter d_0 of the bubbles and on their number n. The number of bubbles n in the liquid layer depends on the thickness h of the layer. Acting on the bubbles found in the liquid layer are Archimedes' force, the resistance force of the medium, and turbulent stresses. The surface tension force can be expressed by means of the bubble diameter d_0 and the surface tension coefficient σ. The saturation coefficient is also linked directly with the mass-transfer coefficient k'.

In mass-transfer it is necessary to take into consideration two different cases – the case of molecular and the case of turbulent mass-transfer. Under conditions of molecular mass-transfer, the mass-transfer coefficient k' can be expressed through the diffusion coefficient D_p and the thickness of the boundary film. When mass-transfer is turbulent, the mass-transfer proceeds via mass flow. The area of the openings on the steam nozzle and the cross section of the still serves as the geometric characteristic of the apparatus.

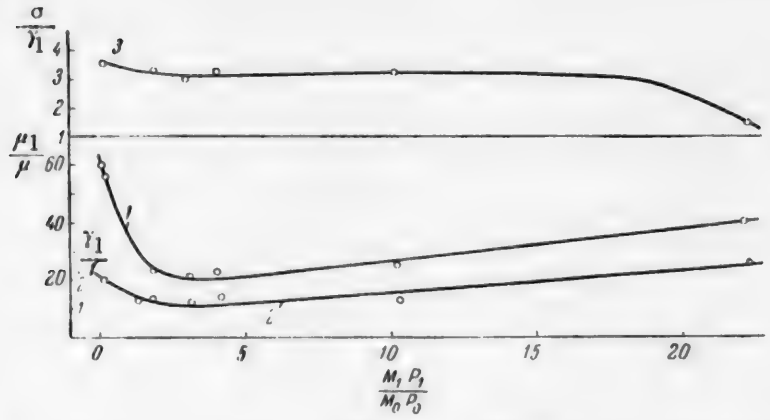

Fig. 5. Dependence of simplexes $\frac{\mu_1}{\mu}$ (1) and $\frac{\gamma_1}{\gamma}$ (2) and ratio $\frac{\sigma}{\gamma_1}$ (3) on the composition criterion.

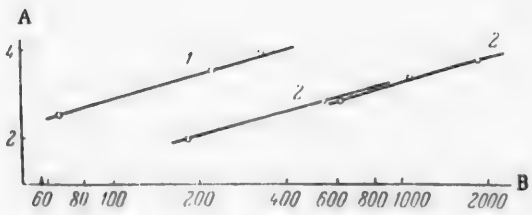

Fig. 6. Dependence of ratio $\frac{\varphi}{Fr^{-0.12}}$ (A) on the geometric simplex $\frac{S_A}{S_0}$ (B) for the foam regime. Apparatus diameter D_A (in mm): 1) 89; 2) 255.

Proceeding from all that has been said above, it becomes possible to write:

$$\varphi = f\left(w,\ \rho,\ \rho_1\ \ g,\ \sigma,\ \mu,\ \mu_1\ \ D_p,\ \frac{M_1P_1}{M_0P_0},\ d,\ h,\ D_A\right), \tag{9}$$

as a result of which the saturation coefficient can be written in the general form:

$$\varphi = f\left(Fr,\ \ Re_1\ \ Pr',\ We,\ \frac{M_1P_1}{M_0P_0},\ \frac{\rho}{\rho_1},\ \frac{\mu}{\mu_1},\ \frac{D_A}{h},\ \frac{D_A}{d}\right), \tag{10}$$

The simplex $\frac{D_A}{d}$ characterizes the flow density of the introduced steam. However, it would be more correct to characterize this value by the ratio $\frac{S_A}{S}$, where S_A is the cross-section area of the apparatus, and S is the cross-section area of the steam nozzle. If the steam is introduced through n nozzles, all having the same cross-section area, then the value of the corresponding area is equal to $S_0 = n \times S$, and the corresponding simplex is equal to $\frac{S_A}{S_0}$.

METHOD OF STUDY

Our study of steam distillation was made in apparatus with different geometric dimensions (Fig. 1). The characteristic dimensions of the different pieces of apparatus used are given in Table 1.

In removing samples of the distillate the following information was recorded: steam pressure in the pot; temperature of introduced steam; temperature of the steam and liquid in the still; temperature of the distillate; temperature of the added liquid; time required to collect the distillate sample; and volume of water and of distilled substance in the distillate.

In addition, the following values, relating to the process, were recorded: amount of liquid added to the still, amount of water condensed in the still pot, and the temperature of the walls of the still pot at the start and at the end of the measurements.

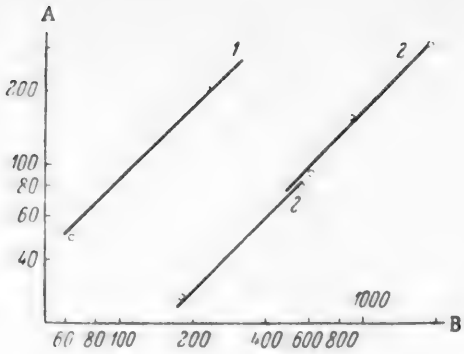

Fig. 7. Relation between ratio $\frac{\varphi}{Fr^{-0.12}}$ (A) and geometric simplex $\frac{S_A}{S_0}$ (B) in the spray regime. Apparatus diameter D_A (in mm): 1) 89; 2) 255.

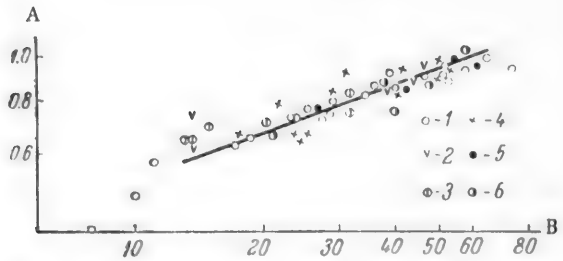

Fig. 8. Relation between the saturation coefficient and layer thickness of distilled liquid (Table 3). A) Saturation coefficient φ; B) layer thickness $\underline{h}$ (in mm). 1, 2, and 3) Toluene; 4) xylene; 5) nitrobenzene; 6) benzene.

To study the steam distillation of liquids we used substances with different chemical and physical properties. These substances are enumerated in Table 2, where we have listed their principal physicochemical properties. In this connection the steam distillation process was studied under the conditions of both two-phase and three-phase systems. The experimental data obtained in this manner are quite adequate for deriving a mathematical generalization of the experimental results.

TREATMENT OF EXPERIMENTAL DATA

The obtained experimental data were expressed by means of a criterial function. The numerical values of the constants in this function were obtained by employing the experimental data in such manner that the effect of each factor was considered separately, and here the other factors affecting the process were kept constant.

The dependence of the saturation coefficient on the Fr criterion (into which enters the linear velocity of the steam when escaping from the nozzle into the liquid) is shown in Fig. 2. From Fig. 2 it can be seen that in all cases, at comparatively small values of the Fr criterion, the numerical value of the saturation coefficient is close to one. With increase in the Fr criterion the numerical value of the saturation coefficient begins to decrease, in which connection the decrease continues uninterruptedly to a value of 0.88-0.86. A further increase in the Fr criterion causes the saturation coefficient to decrease further. In this connection, the decrease in the saturation coefficient with increase in the Fr criterion is relatively greater in this interval of values than in the preceding interval. This interval extends to saturation coefficient values equal to 0.60-0.55. As can be seen from Fig. 2, an even greater increase in the Fr criterion now results in a very sharp decrease in the saturation coefficient.

As a result, based on the experimental data it becomes possible to distingusih three regimes, which are characterized by a different change in the saturation coefficient as a function of the Fr criterion. These regimes are identical with those that were established by us when the bubbling was studied photographically. These three regimes, namely bubble, foam, and spray, are characterized by the same limiting steam velocities [7].

Employing the obtained experimental data (Fig. 2), it becomes possible to determine the analytical relationship between the saturation coefficient and the Fr criterion for the separate regimes.

In the bubble regime the numerical value of the saturation coefficient is equal to approximately 1, in which connection this value of the coefficient, within the limits of the given regime, is independent of the Fr criterion. Consequently, in this case the exponent of the Fr criterion in the criterial function is equal to zero.

In the foam regime the value of the saturation coefficient decreases as the Fr criterion increases. Mathematically, the relation between the saturation coefficient and the Fr criterion is expressed in this case by the equation

$$\varphi = CFr^{-0.12}. \qquad (11)$$

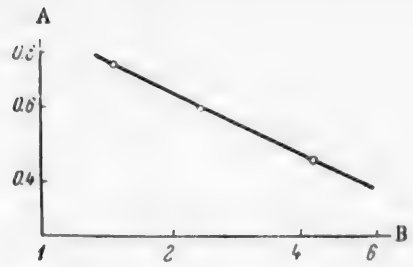

Fig. 9. Relation between ratio $\frac{\varphi}{Fr^{-0.12}\left(\frac{S_A}{S_0}\right)^{0.28}}$ (A) and geometric simplex $\frac{D_A}{h_0}$ (B) in the foam regime.

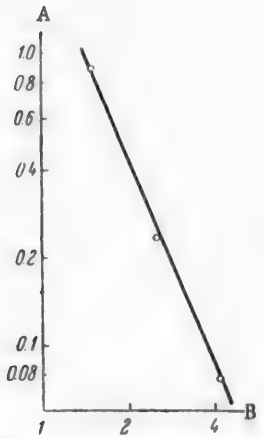

Fig. 10. Relation between ratio $\frac{\varphi}{Fr^{-0.48}\left(\frac{S_A}{S_0}\right)^{1.0}}$ (A) and geometric simplex $\frac{D_A}{h_0}$ (B) in the spray regime.

In the spray regime the relation between the saturation coefficient and the Fr criterion is expressed by the equation

$$\varphi = C_1 Fr^{-0.48}. \quad (12)$$

Passing to an elucidation of the relation between the saturation coefficient and the composition criterion, we will mention that in the future we will use the term "composition criterion" to designate the ratio $\frac{M_1P_1}{M_0P_0}$. This term received its name from the fact that it expresses the theoretical weight ratio of the components in the distillate mixture.

As can be seen from Fig. 2, a difference in the composition criteria is reflected on the saturation coefficient. The greater the composition criterion $\frac{M_1P_1}{M_0P_0}$, the smaller the value of the Fr criterion at which changes in the hydrodynamic regimes of bubbling occur.

The relation between the saturation coefficient and the value of the composition criterion for the case of different hydrodynamic regimes is shown in Figs. 3 and 4. It is characterized by the slope of the straight lines shown in these plots. Proceeding from this, the analytical relationship between the saturation coefficient and the composition criterion for the case of different regimes can be expressed by the following equations:
for the foam regime

$$\varphi = C_2\left(\frac{M_1P_1}{M_0P_0}\right)^{-0.13} \quad (13)$$

and for the spray regime

$$\varphi = C_3\left(\frac{M_1P_1}{M_0P_0}\right)^{-0.48}. \quad (14)$$

The specific gravity of the liquid being distilled, its viscosity, the surface tension, and also the characteristic diffusion criterion Pr', all fail to exert noticeable influence on the saturation coefficient, and consequently can be dropped from the criterial equation.

In this case we proceed in the same manner as is done in solving heat-transfer problems employing the method of approximate modeling [8]. Essentially this method consists in dropping from the general criterial function the terms containing second degree criteria, and in selecting as values characterizing the phenomenon such terms as are fit to reflect in a complex manner the properties of the substances [9, 10]. In our opinion, the value suitable for this purpose in the examined case is the composition criterion, since it contains two such parameters as molecular weight (M) and vapor pressure (P), which are found in close association with the other properties of liquids, and for this reason can reflect their influence in the criterial function. To verify such an assumption, we constructed the curves shown in Fig. 5, which reflect the dependence of the ratios $\frac{\mu_1}{\mu}$, $\frac{\gamma_1}{\gamma}$ and $\frac{\sigma}{\gamma_1}$ on the composition criterion $\frac{M_1P_1}{M_0P_0}$ for different substances at atmospheric pressure under steam distillation conditions.

The substances that we used for this were the following: hydrocarbons – benzene, toluene, xylene, octane, α-pinene, and naphthalene; halo derivatives – carbon tetrachloride; nitro compounds – nitrobenzene.

As the obtained curves show, our assumptions were fully justified.

The physical meaning of the geometric simplex $\frac{S_A}{S_0}$ consists in characterizing the uniformity of introducing the steam along the cross-section of the apparatus. The total area of the nozzle openings increases with increase in their number, and this is accompanied by an increase in the uniformity of distribution by the nozzles along the cross-section of the apparatus.

The experimental data on the dependence of φ on the geometric simplex are plotted in Figs. 6 and 7. The average rise of the experimental curves shown in Fig. 6, i.e., for the case of the foam regime, is 0.28, and consequently

$$\varphi = C_4 \left(\frac{S_A}{S_0}\right)^{0.28}. \tag{15}$$

For the case of the spray regime (Fig. 7), the average rise is 1.0, and consequently

$$\varphi = C_5 \left(\frac{S_A}{S_0}\right)^{1.0}. \tag{16}$$

The experimental data for steam distillation with a small thickness of the liquid layer are plotted in Fig. 8. The dependence of the saturation coefficient on the layer thickness of the liquid being distilled under various physical and hydrodynamic conditions is shown in this graph. Additional data, relating to these experiments, are given in Table 3. As can be seen from Fig. 8, under the conditions indicated in Table 3, a liquid layer thickness of 50-60 mm is fully adequate to saturate the steam with the vapors of the substance being distilled.

TABLE 3

Effect of Thickness of Liquid Layer

Compound	Composition criterion $\frac{M_1 P_1}{M_0 P_0}$	Simplex $\frac{S_A}{S_0}$	Limiting values of Fr criterion, referred to steam
Toluene	4.1	82.6	250
	4.1	259	3400
	4.1	278	470
Xylene	1.9	259	1900
Nitrobenzene	0.18	278	200000
Benzene	10.1	278	530

Based on these experimental results, which were obtained mainly under the conditions of a foam hydrodynamic regime, it becomes possible to express the geometric simplex $\frac{D_A}{h}$ in the form $\frac{D_A}{h_0}$. Here the liquid layer thickness h is replaced by the minimum layer thickness h_0 (the average value of which is taken equal to 60 mm), beginning from which the thickness of the liquid layer is without appreciable effect on the saturation coefficient.

The effect of the geometric simplex $\frac{D_A}{h_0}$ on the saturation coefficient is shown in Figs. 9 and 10. The rise of the straight line (Fig. 9) for the case of the foam regime leads to the following function:

$$\varphi = C_6 \left(\frac{D_A}{h_0}\right)^{-0.48} \tag{17}$$

and for the spray regime

$$\varphi = C_7 \left(\frac{D_A}{h_0}\right)^{-2.3} \tag{18}$$

In essence, this geometric simplex shows the dependence of the saturation coefficient on the diameter of the apparatus, since h_0 = const.

To sum up these investigations, it was established experimentally that three different formulas exist for the saturation coefficient, corresponding to the three hydrodynamic regimes.

In the case of the bubble regime

$$\varphi = 1.0. \tag{19}$$

In this case the hydrodynamic conditions and the structural dimensions of the apparatus exert very little effect on the saturation coefficient.

In the case of the form regime

$$\varphi = 1.17 Fr^{-0.12} \left(\frac{M_1 P_1}{M_0 P_0}\right)^{-0.13} \left(\frac{S_A}{S_0}\right)^{0.28} \left(\frac{D_A}{h_0}\right)^{-0.48} \tag{20}$$

and in the case of the spray regime

$$\varphi = 5.52 Fr^{-0.48} \left(\frac{M_1 P_1}{M_0 P_0}\right)^{-0.48} \left(\frac{S_A}{S_0}\right)^{1.0} \left(\frac{D_A}{h_0}\right)^{-2.3}. \tag{21}$$

The limits of the hydrodynamic regimes are characterized by the following conditions:

in the case of the bubble regime

$$Fr^{-0.12} \left(\frac{M_1 P_1}{M_0 P_0}\right)^{-0.13} \left(\frac{S_A}{S_0}\right)^{0.28} \left(\frac{D_A}{h_0}\right)^{-0.48} > 0.84, \tag{22}$$

in the case of the foam regime

$$0.84 > Fr^{-0.12} \left(\frac{M_1 P_1}{M_0 P_0}\right)^{-0.13} \left(\frac{S_A}{S_0}\right)^{0.28} \left(\frac{D_A}{h_0}\right)^{-0.48} > 0.735, \tag{23}$$

in the case of the spray regime

$$Fr^{-0.12} \left(\frac{M_1 P_1}{M_0 P_0}\right)^{-0.13} \left(\frac{S_A}{S_0}\right)^{0.28} \left(\frac{D_A}{h_0}\right)^{-0.48} < 0.735. \tag{24}$$

It is possible to consider these nonequalities as being experimentally justified within the limits of the following values for the criteria entering into them:

$$40 < \frac{S_A}{S_0} < 1785; \quad 1.485 < \frac{D_A}{h_0} < 4.25; \quad 0.18 < \frac{M_1 P_1}{M_0 P_0} < 22.4; \tag{25}$$

$$300 < Fr < 700\,000.$$

It is necessary to mention that the criterial function of the saturation coefficient in the case where a sieve was used to introduce the steam into the liquid proved to be completely identical with the function corresponding to the nozzles, and consequently equations (19), (20) and (21) are also applicable to this case, in which connection in calculating the simplex it is necessary to take the sum of the sieve openings as S_0.

SUMMARY

1. Based on a theoretical analysis and appropriate experiments, criterial functions for the saturation coefficient in steam distillation were obtained for the case of three different hydrodynamic injection regimes: bubble, foam, and spray. The method of approximate modeling was used in deriving the above mentioned criterial functions.

2. Into the criterial equations, characterizing the saturation coefficient, enter composition criteria that contain two such parameters as the molecular weight (M) and the vapor pressure (P), which are intimately linked with the other properties of liquids, and for this reason are capable of reflecting their effect in the criterial function.

LITERATURE CITED

[1] S. L. Libinson and A. B. Pakshver, Chem. Appl. 15, 277 (1928); 16, 25, 47, 71 (1929).

[2] L. G. Gurvich, Scientific Principles of Petroleum Processing [in Russian]. (Gostekhizdat, 1940).

[3] S. N. Obryadchikov, Principles of Petroleum Distillation [in Russian] (1940).

[4] J. H. Perry, Chemical Engineers' Handbook [in Russian]. (Moscow, 1937) 1st ed.

[5] Handbook of Chemistry [in Russian] (Goskhimizdat, 1952) Vol. III.

[6] M. G. Gonikberg (Editor), Distillation [in Russian] (IL, 1954).

[7] É. K. Siirde and P. G. Romankov, Zhur. Priklad. Khim. 31, No. 12, 1817 (1958).*

[8] A. I. Rychkov and A. N. Planovskii, Khim. Prom. 5, 31 (1955).

[9] A. A. Gukhman, Physical Principles of Heat Transfer [in Russian] (State Power Press, 1934).

[10] A. A. Gukhman, Zhur. Tekh. Fiz. 23, No. 6, 1064 (1953).

Received April 10, 1959

* Original Russian pagination. See C. B. translation.

A STUDY OF THE RATE OF CO_2 ABSORPTION BY MONOETHANOLAMINE SOLUTION IN A HORIZONTAL MECHANICAL ABSORBER

S. N. Ganz, S. B. Leibovich, N. A. Malyshevich

and M. A. Lokshin

Dnepropetrovsk Institute of Chemical Technology

Processes for the selective absorption of CO_2 from gases have found extensive use in industry. At the present time the following principal methods exist for the absorption of CO_2: absorption by water under pressure; absorption by aqueous potash solution with subsequent regeneration of the absorber; absorption by monoethanolamine (MEA) with subsequent regeneration of the solution; absorption by the alkalies Na_2CO_3, NaOH, and aqueous ammonia.

In order to accelerate the absorption rate of CO_2 by MEA solution we replaced the packed apparatus by horizontal mechanical absorbers with high speed agitation, a description of which was given earlier [1].

On the basis of our investigations [1-6], and in harmony with the general requirements of the theory and practice of absorption processes [7], we determined both the extent and the rate of CO_2 absorption by MEA solutions as a function of the peripheral speed of the disks or the number of revolutions of the shaft (n), the space velocity of the gas (W), the CO_2 concentration in the gas (C_g), the temperature, and the amount of MEA in the solution and the extent of its reprocessing (C_l).

Effect of the Peripheral Speed of the Disks. The experiments were run at a gas space velocity (W) = 400 cu m/cu m/hr, a CO_2 content in the gas of 20.3%, temperature 32°, pressure (P) = 752 mm Hg, and MEA concentration 30%.

As a result of the experiments it was established that a 100% absorption of carbon dioxide is achieved at a spindle speed (n) of 500 rpm, or a disk peripheral speed (v) of about 2 m/sec.

The absorption curve runs parallel to the abscissa when the peripheral speed of the disks is increased to 4 m/sec, and a smooth decrease in both the degree and rate of absorption begins after n > 1200 rpm (v = 5.15 m/sec) [1].

Effect of the Space Velocity of the Gas. In this series of experiments the absorption of CO_2 was investigated at disk peripheral speeds of 2 and 4 m/sec, with the following conditions kept constant: 30% monoethanolamine solution, t = 31°, CO_2 concentration 19.4%, and P = 755 mm Hg. The space velocities of the gas were varied from 200 to 700 cu m/cu m/hr.

The results of these experiments are plotted in Fig. 1, and from these results it follows that at gas space velocities exceeding 500 cu m/cu m/hr the degree of CO_2 absorption decreases due to a reduction in the contact time of the phases and an impairment of the hydrodynamic conditions in the apparatus.

In order to increase the degree of CO_2 absorption at W greater than 500 cu m/cu m/hr it is necessary to increase the peripheral speed of the disks. As can be seen from Fig. 1, a more complete absorption of CO_2 is achieved under these conditions.

Effect of the CO_2 Concentration. This function was investigated at W = 400 cu m/cu m/hr, n = 500 rpm, t = 31-32°, MEA concentration 30%, and P = 758 mm Hg.

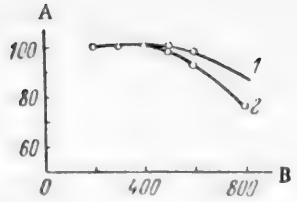

Fig. 1. Relation between the degree of CO_2 absorption by monoethanolamine solution and the space velocity of the gas. A) Degree of absorption (in %); B) gas space velocity W (cu m/cu m/hr). Absorption by monoethanolamine at n (in rpm): 1) 800-900; 2) 500.

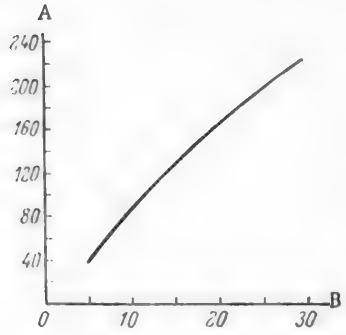

Fig. 3. Relation between the rate of CO_2 absorption by monoethanolamine solution and the CO_2 concentration. A) Absorption rate (in kg/cu m/hr); B) Co_2 concentration (in %).

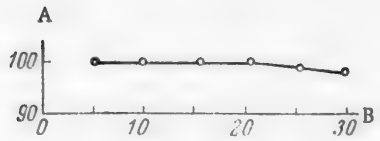

Fig. 2. Relation between the degree of CO_2 absorption by monoethanolamine solution and the CO_2 concentration. A) Degree of absorption (in %); B) CO_2 concentration (in %).

The results of these experiments are shown in Figs. 2 and 3. As can be seen from the given data, increasing the CO_2 concentration to 25% is practically without effect on the degree of absorption, and only when the CO_2 concentration is increased above 25% does the degree of absorption begin to diminish slightly. The curve shown in Fig. 3, characterizing the CO_2 absorption rate as a function of its concentration in the gas, indicates that increasing the CO_2 concentration leads to an increase in the absorption rate.

Effect of Temperature. Experiments revealed that raising the temperature to 50° fails to affect either the degree or the rate of CO_2 absorption by MEA solutions. Increasing the temperature above 50° causes first a slow, and then a rapid decrease in the degree of absorption. The investigated function is shown in Fig. 4.

Effect of MEA Concentration in Solution. In this series of experiments we investigated the absorption capacity of 10, 20, 30, 40 and 50% MEA solutions at W = 400 cu m/cu m/hr, n = 500 rpm, t = 37°, and a CO_2 concentration in the gas of 18.9%. The obtained results are plotted in Fig. 5, from which it can be seen that when the solution concentration of MEA is below 10% the degree of CO_2 absorption does not reach 90% because of the slow reaction rate under these conditions. When the MEA concentration is increased to 30% and higher, with all of the other conditions kept constant, the absorption rate increases rapidly and the degree of CO_2 absorption reaches 100%. Reasoning from these data, and taking into account the MEA losses due to drop entrainment with the gas, it must be assumed that the absorption process is best carried out using 30% MEA solution. To determine the degree of CO_2 absorption as a function of the degree of consumption of MEA solution with time, we used a MEA solution with an initial concentration of approximately 30%, and a gas with a CO_2 content of 19%. The spindle speed (n) in this experiment was 800 rpm, t = 22°, and space velocity (W) = 600 cu m/cu m/hr.

The results of these experiments are plotted in Fig. 6. From the graph it can be seen that saturation of the solution proceeds at a rapid rate at the start of the process and for the most part is completed in the first 5 minutes. After this, as the MEA concentration in the solution decreases, the degree of CO_2 absorption decreases sharply.

Comparative Rates of CO_2 Absorption by Potash and Monoethanolamine Solutions

In order to compare the intensity with which CO_2 is absorbed by potash and MEA solutions, we investigated the degree of CO_2 absorption by 20% potash solution as a function of the space velocity of the gas. The absorption was run at t = 23°, n = 800-900 rpm, and a CO_2 concentration in the gas of 18.6%. The results of this series of experiments are shown in Fig. 7. The data on the absorption of CO_2 by 30% aqueous MEA solution are also plotted

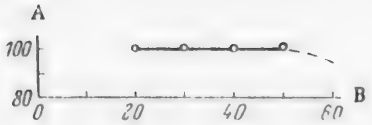

Fig. 4. Relation between degree of CO_2 absorption by monoethanolamine solution and the temperature of the absorbent. p = 754 mm Hg, W = 400 cu m/cu m/hr, n = 500 rpm, MEA concentration = 30%, and CO_2 concentration = 18%. A) Degree of absorption (in %); B) temperature of monoethanolamine (in °C).

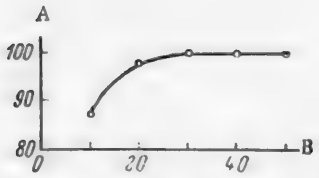

Fig. 5. Relation between degree of CO_2 absorption by monoethanolamine solution and solution concentration of monoethanolamine. A) Degree of absorption (in %); B) monoethanolamine concentration (in %).

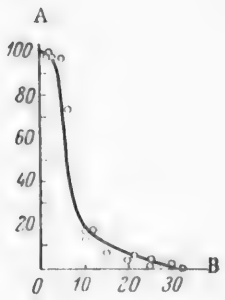

Fig. 6. Relation between degree of CO_2 absorption by monoethanolamine solution and duration of experiment. A) Degree of absorption (in %); B) duration of experiment (in min).

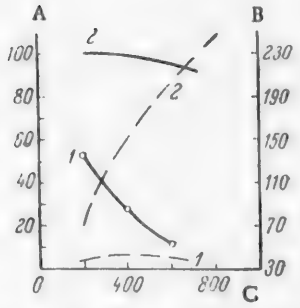

Fig. 7. Relation between degree of CO_2 absorption by potash and monoethanolamine solutions and the space velocity of the gas. A) Degree of absorption (in %); B) rate of absorption (in kg/cu m/hr); C) space velocity of the gas (in cu m/cu m/hr). Solid line – degree of absorption; broken line – rate of absorption. 1) Potash; 2) monoethanolamine.

in the same figure. The absorption rates of CO_2 by MEA (upper curve) and potash (lower curve) solutions are shown on the right by broken lines. From the given data it follows that even at low space velocities of the order of 200-250 cu m/cu m/hr the degree of CO_2 absorption by potash solution does not exceed 40-50%, whereas the use of 30% MEA solution results in the 100% absorption of CO_2 at space velocities twice as great, with the other conditions constant.

The absorption rate curves plotted in Fig. 7 are convincing evidence that MEA solution possesses important advantages, securing a higher intensity of the process.

SUMMARY

1. Our investigations revealed that the absorption of CO_2 by MEA solution in a mechanical absorber proceeds much more rapidly than in packed scrubbers.

2. The use of 30-35% MEA solution proves to be most suitable, in which connection the MEA solution possesses important advantages over 20% potash solution in that it has a much greater chemical capacity for CO_2 and a faster absorption rate.

LITERATURE CITED

[1] S. N. Ganz, Zhur. Priklad. Khim. 30, 1604 (1957).*

[2] S. N. Ganz and S. B. Kravchinskaya, Zhur. Priklad. Khim. 28, 2 (1955).*

[3] S. N. Ganz and S. I. Kapturova, Zhur. Priklad. Khim. 28, 6 (1955).*

[4] S. N. Ganz and M. A. Lokshin, Trudy Dnepropetrovsk (Khim.-Teknol. Inst. 1956) 5.

[5] S. N. Ganz, Zhur. Priklad. Khim. 30, 1311 (1957).*

[6] S. N. Ganz and M. A. Lokshin, Zhur. Priklad. Khim. 31, 191 (1958).*

[7] M. E. Pozin, Methods and Processes of Chemical Technology [in Russian] (Izd. AN SSSR, 1955)Vol. 1, p. 101.

Received September 25, 1958

* Original Russian pagination. See C. B. translation.

ENRICHMENT COEFFICIENT OF A SINGLE RECTIFICATION SIEVE PLATE

A. A. Noskov, G. V. Burova and P. Fel'desh

When the conventional technique of using the degree of change in the concentration (theoretical plates) is employed in the design of plate rectification columns, it is necessary to know the value of the enrichment coefficient, or the so-called plate efficiency of the designed equipment.

This value

$$\eta_1 = \frac{y_2 - y_1}{y_1^* - y_1}, \qquad (1)$$

as characterizing the process of mass transfer on the plate, was proposed by Murphree [1], where y_1 is the concentration (mole fraction) of the low-boiling component in the vapor entering the plate, y_2 is the concentration of the same component in the vapor leaving the plate and y_1^* is the concentration of the same component in the liquid flowing down from the plate.

Besides constructional factors, the efficiency of mass transfer in a rectification column depends primarily on the hydrodynamic conditions.

The investigations of Kirschbaum [2], Lewis [3], Evstaf'ev, Zykov and Karavaev [4], and Gautreaux and O'Connell [5], established that in plate columns with a lateral flow of the liquid the mixing of the liquid on the plate and the length of its path are important factors. The influence of the hydrodynamic conditions on mass transfer in rectification columns was shown in Kafarov's studies [6]. The effect of entrainment of liquid by the vapor was investigated in a number of studies; many authors mention the effect exerted by the physicochemical properties of the mixture being rectified, in particular, its viscosity [2, 7].

As a result, numerous variable factors of a geometric, hydrodynamic, and physicochemical character exert influence on the value of the enrichment coefficient of a rectification plate, which, naturally, makes it extremely difficult to derive a general equation for its calculation.

The calculation method proposed by Ju-Chin Chu [8], as well as the dimensionless equation derived by Anoshin [9] for sieve plates, do not reflect a number of conditions that affect the value of the enrichment coefvient of a plate.

For the case of complete mixing of the vapor, the absence of entrainment and loss of liquid by run back, and a constancy of the values $\underline{m}$ and η_1 along the plate, the theoretical equation derives [5]

$$\eta_1 = \frac{1}{K_m} \cdot \left[\left(1 + \eta_1 \frac{K_m}{n} \right)^n - 1 \right], \qquad (2)$$

in which $K_m = \frac{mG}{L}$ is the ratio of the slope coefficients of the equilibrium (m) and operating $\left(\frac{L}{G}\right)$ lines, η_1 is the local efficiency, determined by the equation [1, 7].

TABLE 1

Geometric Characteristics of Plates

	Experiment Numbers						
	1	2	3	4	5	6	7, 8, 9, 10
Diameter of plate D (in mm)	100	100	100	100	100	307	125
Height of overflow weir h (in mm)	80	40	40	40	12	40	17
Pitch and diameter of openings t/d (in mm)	6/2	6/2	4/1	10/4	6/2	6/2	7/2
Free area of plate (total area of openings) S_0 (in % of total area of plates)	5.9	5.9	3.0	9.6	5.9	5.9	6.0
Area of downspouts (two) F_{ds} (in % of total area of plate)	20	20	20	20	20	20	8
Circumference of downspout II (in mm)	72	72	72	72	72	220	79
Shape of downspout	Segment						Round

TABLE 2

Range in Physicochemical Constants

Viscosity of liquid $\mu_l \times 10^5$ (kg/sec/sq m)	3.6–6.2
Specific gravity of liquid γ_l (kg/cu m)	770–1370
Diffusion coefficient $D_l \times 10^9$ (sq m/sec)	1.26–4.0
Prandtl criterion (diffusion) for liquid, Pr_l	100–460
Surface tension, $\sigma \times 10^4$ (kg/m)	18.2–35.1
Viscosity of vapor, $\mu_v \times 10^6$ (kg/sec/sq m)	0.98–1.28
Specific gravity of vapor, γ_v (kg/cu m)	0.62–4.86
Diffusion coefficient, $D_v \times 10^4$ (sq m/sec)	0.041–0.26
Prandtl criterion (diffusion) for vapor, Pr_v	0.36–1.0

$$\eta_l = 1 - e^{-M}, \tag{3}$$

and n is a term (dimensionless), characterizing the degree of mixing of the liquid on the plate; the liquid is completely mixed when n = 1, and mixing is absent when n = ∞.

In equation 3, $M = \frac{k \cdot F \cdot \tau}{G_0}$, where k is the coefficient of mass transfer (in kg-mole/hr/sq m, $\Delta y = 1$), F is the surface of the elementary vapor volume (bubble), enclosing G_0 kg-mole of vapor (in sq m), τ is the time required for the bubble to pass through the bubbling layer on the plate (in hr), and e is the base of natural logarithms.

Not considering the difference between actual conditions and the theoretical, the degree of liquid mixing and the value of the local efficiency on a rectification plate still remain unknown at the present time. As a result, to determine theoretically the value of the enrichment coefficient η does not appear possible, and in practice its

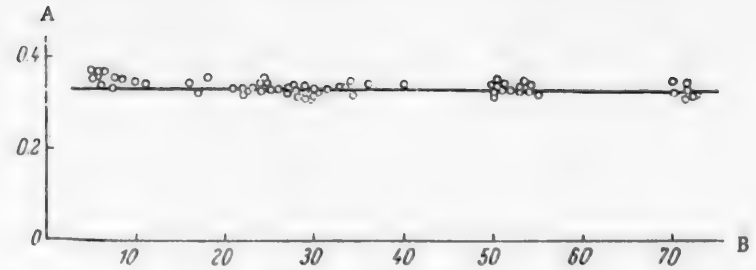

Fig. 1. Dependence of $\eta Fr^{0.1} \cdot Ga_l^{-0.04} \cdot H^{-0.1}$ on the composition of the liquid on the plate (experiment numbers 1-6). A) $\eta Fr^{0.1} \cdot Ga_l^{-0.04} \cdot H^{-0.1}$; B) average concentration of low-boiling component in the liquid on the plate, x_{av} (in mole %).

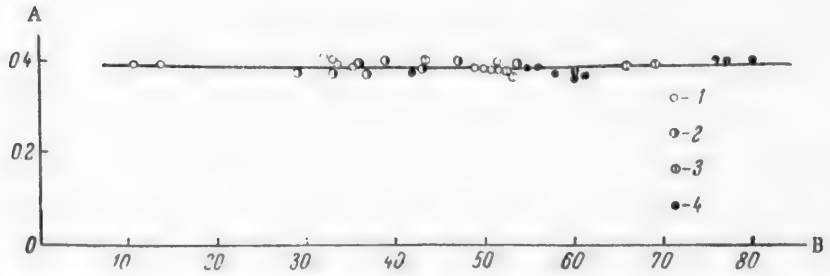

Fig. 2. Dependence of $\eta Fr^{0.1} \cdot Ga_l^{-0.04} \cdot H^{-0.1}$ on the composition of the liquid on the plate (experiment numbers 7-10). A) $\eta Fr^{0.1} \cdot Ga_l^{-0.04} \cdot H^{-0.1}$; B) average concentration of low-boiling component in the liquid on the plate, x_{av} (in mole %). 1) Ethyl alcohol–water; 2) methyl alcohol–water; 3) acetone–water; 4) carbon tetrachloride–toluene.

values are calculated either on the basis of experimental data or from empirical equations. With such a situation it is highly important to have a reliable generalization of the experimental data, which at the present time are quite voluminous.

It is possible to obtain the most fruitful and reliable generalization of the experimental data using the theory of similarity. However, applying this theory to the rectification process encounters serious difficulties, caused by the abundance of variable factors that affect both the hydrodynamics and mass transfer in a plate rectification column. For this reason, taking into complete consideration all of the conditions of similarity of rectification processes in plate columns proves to be an extremely complex problem, and to obtain fairly simple general equations, suitable for ordinary technical calculations, it becomes necessary to resort to an approximate method.

In making an experimental study of the rectification process in plate columns it seem logical first to make a study of mass transfer on a single plate in the absence of entrainment, i.e., under the simplest conditions possible, close to those for which equation (2) was derived. The second stage of the investigation will be a study of mass transfer under the more complex conditions prevailing in a multiplate column.

As is known, depending on the vapor rate in the column, it is possible for different hydrodynamic regimes to exist on a trickling sieve plate [10-13].

Based on the theory of similarity, an attempt was made in the present study to generalize the results of an experimental investigation of the enrichment coefficient of a single sieve rectification plate under the conditions of a foam regime, and in the absence of substantial run back of liquid through the openings of the plate.

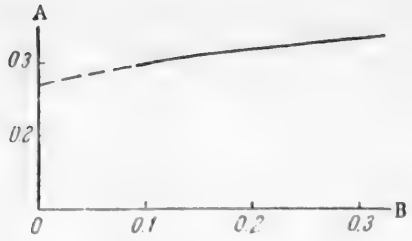

Fig. 3. Dependence of $\frac{\eta w^{0.2}}{h^{0.12}}\left(\frac{\mu_1}{\gamma_1}\right)^{0.08}$ on the plate diameter. A) $-\frac{\eta w^{0.2}}{h^{0.12}}\left(\frac{\mu_1}{\gamma_1}\right)^{0.08}$, B) plate diameter D (in m).

The experiments were run in three experimental stills, consisting of single-plate rectification columns with reflux splitters and steam-heated still pots. Each column was fitted with glass peepholes, making it possible to observe the operation of the plates. Samples were taken when completely steady conditions had been established; the concentration was determined from the specific gravity using a pycnometer. The geometric characteristics of the sieve plates used in our experiments are given in Table 1.

A total of ten experiments was run. In experiment numbers 1-7 we investigated the rectification of a mixture of ethyl alcohol and water, in experiment number 8 the rectification of a mixture of methyl alcohol and water, in experiment number 9 that of a mixture of acetone and water, and in experiment number 10 that of a mixture of carbon tetrachloride and toluene. All of the experiments were run at atmospheric pressure. The average concentration of the low-boiling component in the liquid on the plate ranged from 5 to 80 mole %.

The experiments were run at different values of $\frac{G}{L}$ (ratio of vapor and liquid flows), ranging from 1 to 1.5, and at different vapor rates in the column. The processed experimental data correspond to the limiting values of $\frac{G}{L}$, equal to 1 and 1.5 (reflux numbers ∞ and 2), and to vapor rates in the column ranging from 0.3 to 1.25 m/sec, although in a number of experiments the values of the vapor rates were outside these limits. The slowest vapor rate, where a substantial run back of liquid through the openings could still not be detected, differed for the plates with different geometric characteristics. Thus, in the number 3 series of experiments it was approximately 0.2 m/sec, in the number 4 series it was about 0.4 m/sec, and in the number 6 series it was approximately 0.6 m/sec. An insufficient number of experiments was run at vapor velocities exceeding 1.25 m/sec, but still it was possible to observe that at a vapor velocity in the column of the order of 1.5-2.0 m/sec the physicochemical properties of the mixing being rectified apparently failed to exert an effect on the value of the enrichment coefficient.

The experimentally obtained values for the enrichment coefficient η range from 0.65 to 1.17.

The range in the physicochemical properties of the mixtures studied are listed in Table 2.

To treat the study results in criterial form we obtained a system of criteria [14]. As the starting equations we took the following. The equation of motion and continuity for the liquid and vapor (at ρ_V = const):

$$g \cdot \rho_1 - \operatorname{grad} p_1 + \mu_1 \cdot \nabla^2 w_1 = \rho_1 \cdot \frac{Dw_1}{dz}, \tag{4}$$

$$\operatorname{div} w_1 = 0, \tag{5}$$

$$g \cdot \rho_V - \operatorname{grad} p_V + \mu_V \cdot \nabla^2 w_V = \rho_V \cdot \frac{Dw_V}{dz}, \tag{6}$$

$$\operatorname{div} w_V = 0. \tag{7}$$

The equation of convective diffusion in each of the phases:

$$\frac{Dx}{dz} = D_1 \cdot \nabla^2 x, \tag{8}$$

$$\frac{Dy}{dz} = D_V \cdot \nabla^2 y, \tag{9}$$

where x is the concentration of the low-boiling component in the liquid, y is the concentration of the same component in the vapor, and D_l and D_v are the corresponding molecular diffusion coefficients.

The equation of mass transfer

$$G_0 \cdot dy = k \cdot F \cdot (y^* - y) \cdot d\tau. \tag{10}$$

Limiting conditions:

$$w_{l,\,lim} = w_{l,\,lim} \tag{11}$$

$$\mu_l \operatorname{grad} w_l = \mu_v \operatorname{grad} w_v \tag{12}$$

$$p_v = p_l + \sigma\left(\frac{1}{R_1} + \frac{1}{R_2}\right). \tag{13}$$

The criteria of similarity may be obtained in conventional manner from equations (4)-(13); the rate of the liquid w_l enters into some of them, and the rate of the vapor w_v enters into others.

Neglecting the slight horizontal component of the liquid rate along the plate, it may be assumed that the rate of liquid movement on a sieve plate under foam conditions is determined completely by the vapor rate in the column. This permits substituting one vapor rate, as the determining rate, in all of the criteria containing w_l and w_v. From now on it will be designated by w. Then, taking as the determining linear dimension the height of the overflow weir h, we obtain for the stationary conditions from equations (4) and (6) the determining criteria:

$$Re_l = \frac{w \cdot h \cdot \gamma_l}{\mu_l \cdot g}, \quad Re_v = \frac{w \cdot h \cdot \gamma_v}{\mu_v \cdot g}, \quad Fr = \frac{w^2}{g \cdot h},$$

and from equations (8), (9), (10), (12) and (13) the corresponding criteria

$$Pe_l = \frac{w \cdot h}{D_l}, \quad Pe_v = \frac{w \cdot h}{D_v}, \quad M = \frac{k \cdot F \cdot \tau}{G_0}, \quad S_\mu = \frac{\mu_l}{\mu_v}, \quad K_{v-1} = \frac{\Delta p_{v-1} \cdot h}{\sigma}.$$

The obtained system of criteria gives the criterial function

$$M = f(Fr,\ Re_l,\ Re_v,\ Pe_l,\ Pe_v,\ S_\mu,\ K_{v-1}), \tag{14}$$

which is easily converted to the form

$$M = \varphi(Fr,\ Ga_l,\ Pr_l,\ Pr_v\ \ S_\gamma,\ S_\mu,\ K_{v-1}), \tag{15}$$

where

$$Ga_l = \frac{h^3 \cdot \gamma_l^2}{\mu_l^2 \cdot g}, \quad Pr_l = \frac{\mu_l}{D_l \cdot \rho_l}, \quad Pr_v = \frac{\mu_v}{D_v \cdot \rho_v}, \quad S_\gamma = \frac{\gamma_l}{\gamma_v}.$$

The geometric characteristics of sieve plates with downspouts of a given shape and a constant relative area F_{ds} are*: diameter of plate D, diameter of openings d, pitch of openings t, height of downspout above plate h. These variables give three geometric simplexes:

$$H_1 = \frac{D}{h}, \quad H_2 = \frac{d}{h}, \quad H_3 = \frac{t}{h},$$

which should be included in the general equation (15).

*Here we assume that the thickness of the plate has no influence on the mass-transfer.

From equations (2) and (3) it follows that

$$\eta = f(K_m,\ M,\ n). \tag{16}$$

Mixing of the liquid on the plate is determined by the hydrodynamic conditions, described by equations (4)-(7) and (11)-(13), and the geometric parameters of the plate. From this it follows that the dimensionless degree of mixing (n) will, in the final analysis, be characterized by those hydrodynamic criteria that enter into equation (14) or (15), and the geometric simplexes H_1, H_2 and H_3. Consequently, the desired general criterial function, based on equations (15) and (16), with the geometric simplexes taken into consideration, may be converted to the following form:

$$\eta = C \cdot Fr^a \cdot Ga_1^b \cdot Pr_1^e \cdot Pr_V^d \cdot S_\gamma^e \cdot S_\mu^f \cdot K_V^{g-1} \cdot K_m^h \cdot H_1^i \cdot H_2^j \cdot H_3^k. \tag{17}$$

The complexity of the last equation causes search for a simpler approximate solution. For this we will exclude from consideration the last limiting condition, namely, equation (13), or in other words, we will neglect the effect of surface tension on the value of the enrichment coefficient η, substituting exponent (g) in equation (17) equal to zero. With this condition, treating the experimental data in accordance with equation (17) leads, as will be shown below, to a much simpler criterial formula that at the same time is sufficiently accurate for all practical purposes.

Isolating the variable w, the value of exponent (a) for the Freud criterion in equation (17) may be determined from the experimental data. This value was found to be equal to 0.1. In a similar manner it was established that the plate enrichment coefficient η changes proportionally to the values $h^{0.12}$ and $D^{0.1}$ (D is the diameter of the column), and is practically independent of the relative area of the free section S_0 of the plate; when S_0 is increased from 3 to 9.6 (Table 1), with other conditions constant, the value of η hardly changes.

Further, based on the data of Anoshin [9], it may be assumed that, within the limits of our experiments, η is independent of the diameter d of the plate openings. This means that in equation (17) the exponent j is equal to zero, and, in addition, this shows that η is also independent of the pitch t of the openings, since $S_0 = f(d, t)$. Consequently, the exponent of H_3 is also equal to zero, and of the geometric simplexes in the equation there remains only H_1^i, whence i = 0.1, since the column diameter D does not enter into the other criteria and simplexes.*

After this, based on the proportionality $\eta \sim h^{0.12}$, it proves possible to determine the exponent b of the Ga_1 criterion: $-a + 3b - i = 0.12$, from which, substituting a = -0.1 and i = 0.1, we find b = 0.04.

As a result, equation (17) reduces to the form

$$\eta = CFr^{-0.1} \cdot Ga_1^{0.04} \cdot H^{0.1} \cdot X, \tag{18}$$

where

$$X = Pr_1^c \cdot Pr_V^d \cdot S_\gamma^e \cdot S_\mu^f \cdot K_m^h. \tag{19}$$

The value of X depends only on the physicochemical properties of the liquid and vapor, including the slope of the equilibrium line, and on the reflux ratio. To determine the effect of the liquid composition on the value of X we plotted the experimental data (Figs. 1 and 2), where the average concentration of the low-boiling component in the liquid on the plate, x_{av} (in mole %), is plotted along the abscissa, while the value $\eta Fr^{0.1} \cdot Ga_1^{-0.04} \cdot H^{-0.1}$ is plotted along the ordinate.

In Fig. 1 we show the results obtained using plates with a diameter of 100 and 307 mm, and having segmental downspouts with an area equal to 20% of the area of the plate (experiment numbers 1-6). The results, obtained using a plate with a diameter of 125 mm, and having circular downspouts with an area equal to 8% of the plate area, are shown in Fig. 2 (experiment numbers 7-10).

*From here on the index of the H_1 criterion is dropped.

From Figs. 1 and 2 it can be seen that the value $\eta Fr^{0.1} \cdot Ga_1^{-0.04} \cdot H^{-0.1}$ is, with sufficient accuracy, a constant. This indicates that the enrichment coefficient η of the plate is independent of all of the criterial variables entering into equation (19). Since both the density and the viscosity of the liquid already enter into the Galileo criterion Ga_1, then it follows that η is practically independent of the coefficients of diffusion in the liquid and in the vapor, the density and viscosity of the vapor, and also the value of $\frac{m \cdot G}{L}$.

From Fig. 1 we obtain:

$$\eta = 0.33 Fr^{-0.1} \cdot Ga_1^{0.04} \cdot H^{0.1}. \tag{20}$$

while from Fig. 2 we obtain:

$$\eta = 0.39 Fr^{-0.1} \cdot Ga_1^{0.04} \cdot H^{0.1}. \tag{21}$$

The difference in the numerical value of the coefficient is explained by the different conditions of liquid downflow. The area of the downspout in the column, D = 125 mm, was 2.5 times smaller than in the other two columns, which led to a substantial increase in the foam level on the plate in this column, observed through a sight glass.

As a result, a comparatively simple general equation was obtained, giving the relation between the enrichment coefficient of a single sieve plate and the principal criterial variables. As can be seen from Figs. 1 and 2, the correlation of the experimental data is quite good. In our experiments, the ranges in the criterial variables, determining, together with the above indicated restrictions, the range of application of the obtained equation, were the following:

$$Fr = 0.1\text{—}12.2, \quad Ga_1 \cdot 10^{-8} = 0.37\text{—}316,$$
$$H = 1.25\text{—}8.3.$$

Equation (20) in expanded form becomes:

$$\eta = 0.33 \frac{h^{0.12} \gamma_1^{0.08} D^{0.1} g^{0.06}}{w^{0.2} \mu_1^{0.08}}, \tag{22}$$

where h is the height of the overflow weir (in m), D is the column diameter (in m), w is the vapor velocity, referred to the complete cross section of the column (in m/sec), γ_1 is the specific gravity of the liquid (in kg/cu m), μ_1 is the viscosity of the liquid (in kg/sec/sq m), and g is the gravity factor (in m/sec^2). This equation shows the resultant effect of different variables on the enrichment coefficient of the plate.

From equation (22) it can be seen that this effect is small for all of the variables; the greatest effect is shown by the vapor velocity increasing, which causes η to decrease.

It should be mentioned that the term $\frac{mG}{L}$, which was varied from 0.15 to 5.0 in our experiments, does not affect the enrichment coefficient.

From Fig. 1 it can be seen that at values $x_{av} < 8\%$ the experimental points fall slightly above the straight line shown. This is apparently due to the negligible effect of the term $\frac{mG}{L}$, since at small values of x the slope m of the equilibrium curve for the mixture ethyl alcohol—water increases sharply. The absence of the term $\frac{mG}{L}$ affecting the value of the plate enrichment coefficient is in good agreement with the theoretical formula (2) when n has a value close to one.

The obtained results permit making an approximate calculation of the local efficiency on the sieve plates used by us. If equation (22) is written in the form

$$\frac{\eta_1 w^{0.2}}{h^{0.12}}\left(\frac{\mu_1}{\gamma_1}\right)^{0.08} = 0.379\,D^{0.1} \qquad (23)$$

and the last function is extrapolated to D = O (Fig. 3), then we obtain the following approximate equation for the local efficiency:

$$\eta_1 = 0.27\,\frac{h^{0.12}}{w^{0.2}}\cdot\left(\frac{\gamma_1}{\mu_1}\right)^{0.08} \qquad (24)$$

actually at h < 0.08 m, w > 0.3 m/sec, and $\frac{\gamma_1}{\mu_1} < 3 \times 10^7$ 1/m/sec.

SUMMARY

1. With some simplifying assumptions a criterial equation was obtained, giving a good correlation with the experimental data for a single sieve plate operating under foam conditions.

2. Under these conditions the plate enrichment coefficient is affected to the greatest degree by the vapor velocity in the column. The specific gravity and viscosity of the liquid also exert a slight influence on the enrichment coefficient. The effect of the molecular diffusion coefficients and of the vapor properties could not be shown.

3. Within the range of investigation, the enrichment coefficient is practically independent of the free cross-section area of the plate, the diameter and pitch of the openings, and also of the value of $\frac{m \cdot G}{L}$ (ratio of the slope coefficients of the equilibrium and operating lines), which is in harmony with the theoretical equation.

LITERATURE CITED

[1] E. V. Murphree, Ind. Eng. Chem. 17, 747 (1925).

[2] E. Kirschbaum, Distillation and Rectification Technology (Berlin, 1940).

[3] W. K. Lewis, Ind. Eng. Chem. 28, 399 (1936).

[4] A. G. Evstaf'ev, D. D. Zykov, and N. M. Karavaev, Izvest. Akad. Nauk SSSR, Otdel. Khim. Nauk 1955, No. 8, 119.*

[5] M. F. Gautreaux and H. E. O'Connell, Chem. Eng. Prog. 51, 232 (1955).

[6] V. V. Kafarov, Zhur. Priklad. Khim. 30, 1449 (1957); Khim. i Khim. Tekhnol. 3, 595 (1958).

[7] C. S. Robinson and E. R. Gilliland, Elements of Fractional Distillation (New York, 1950).

[8] Ju-Chin Chu, Petroleum Processing 6, 39, 154 (1951).

[9] I. M. Anoshin, Candidate's Dissertation [in Russian]. (MIPP, Moscow, 1952); Spirtovaya Prom., No. 4, 10 (1953).

[10] V. N. Stabnikov, Trudy Voronezh. KhTIPP, Nos. 3-4 (1939).

[11] M. E. Pozin, I. P. Mukhlenov, E. S. Tumarkina, and E. Ya. Tarat, Foam Method of Processing Gases and Liquids [in Russian]. Goskhimizdat, 1955.

[12] A. A. Noskov and V. N. Sokolov, Khim. Nauka i Prom. 3, 518 (1958).

[13] G. P. Solomakha and V. I. Matrozov, Trudy Moskov. Inst. Khim. Mashinostroeniya 13, 53 (1957).

[14] G. V. Burova and A. A. Noskov, Trudy Leningrad. Tekhnol. Inst. im. Lensoveta 41, 77 (1957).

Received February 27, 1959

* Original Russian pagination. See C. B. Translation.

HEAT TRANSFER FROM A FLUIDIZED CATALYST BED TO THE HEAT-EXCHANGE SURFACE*

V. B. Sarkits, D. G. Traber and I. P. Mukhlenov

Lensovet Technological Institute, Leningrad

In this communication we give the results of our investigations on determining the relation between the Nu criterion and the Re and Fr criteria, the latter characterizing the hydrodynamics of a fluidized bed. We also investigated the influence of such geometric parameters as the diameter of the apparatus and the initial height of the bed.

The investigations were run using the earlier described apparatus [1, 2]. In this series of experiments the diameter D of the apparatus was taken equal to 49, 73 and 100 mm, and the coil condenser used had a height of 80 mm and a heat-exchange surface of 0.00577 sq m.

The effect of the air velocity $\underline{w}$ (m/sec) and of the solid particle size $\underline{d}$ on the heat-transfer coefficient α (kcal/sq m/hr/deg) is characterized by the experimental data shown in Figs. 1 and 2. Only a portion of the data from a large number (approximately 1000) of experiments is shown here.

The experimental results are in good agreement with the earlier expressed theory regarding the nature of the relationship between the heat-transfer coefficient and the gas velocity [1], and they are also in good agreement with the mechanism proposed for the transfer of heat between a fluidized bed and the heat-exchange surface [3, 4].

Not even a single opinion exists in the literature on the mechanism of heat transfer from a fluidized bed. The various theories [5-8] that have been proposed were discussed by us earlier [3, 4].

We will examine the conditions under which the heat-transfer process takes place at the boundary.

It is known that in a filtering bed, because of its poor heat conductivity, there exist substantial temperature drops in different parts of the bed, while the temperature gradient at the interface of the bed with the heat-exchange surface is comparatively small. In a fluidized bed the convective transfer of heat by the solid particles and highly agitated gas phase leads to a practically complete equalization of the temperature in the main bulk of the bed, while sharp temperature gradients are observed near the heat-exchange surface, assuring high heat-transfer coefficients.

Here, under the conditions of a laminar character for the movement of the gas phase in the fluidized bed, the temperature gradient at the boundary with the heat-exchange surface will increase due to a sporadic exchange of the cold and hot particles, chaotically moving (and revolving) in different directions. Solid particles are agents for the transfer of heat from the main nucleus to the boundary heat-exchange portion [3], found near the cooling surface, where the heat is transmitted through the gas phase mainly by molecular heat conduction, in which connection the mechanical "purifying" [8] action manifested by the solid particles is very small.

In the examined case of a laminar regime, the average length of the path [3], along which the heat flow passes into the gas phase from the grains, found in the boundary heat-exchange portion, to the heat-exchange surface decreases with decrease in the size of the solid particles and increase in their concentration. This may be the reason for the fact that in the laminar and transition regions the maximum heat-transfer coefficients decrease

* Communication 2.

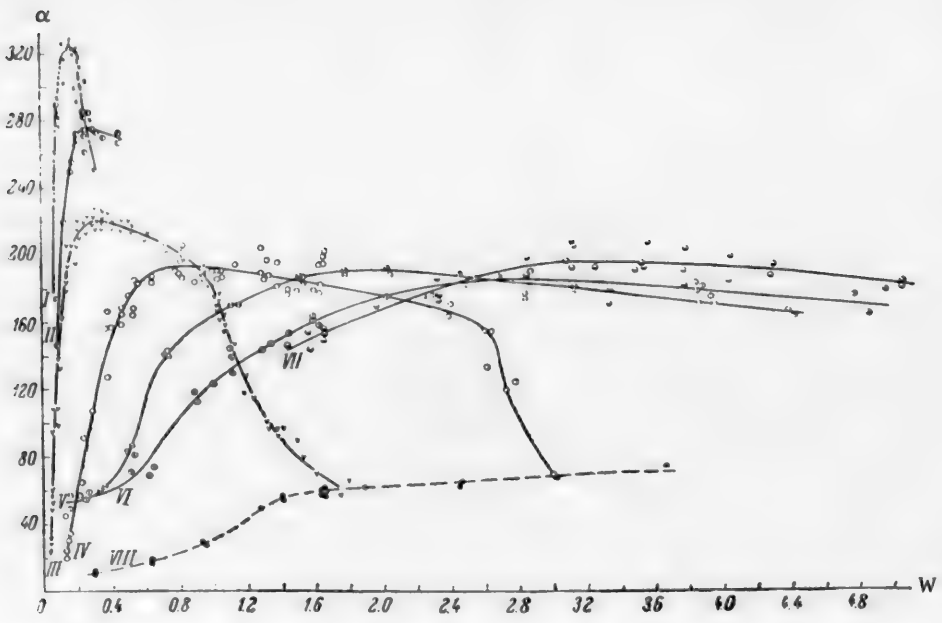

Fig. 1. Effect of air velocity and of solid particle size on the coefficient of heat transfer (D = 49 mm). Average size of catalyst BAV particles (in mm): I) 0.127, II) 0.257, III) 0.38, IV) 0.75, V) 1.5, VI) 2.5, VII) 3.5, and VIII) heat exchange in the apparatus without a solid phase present.

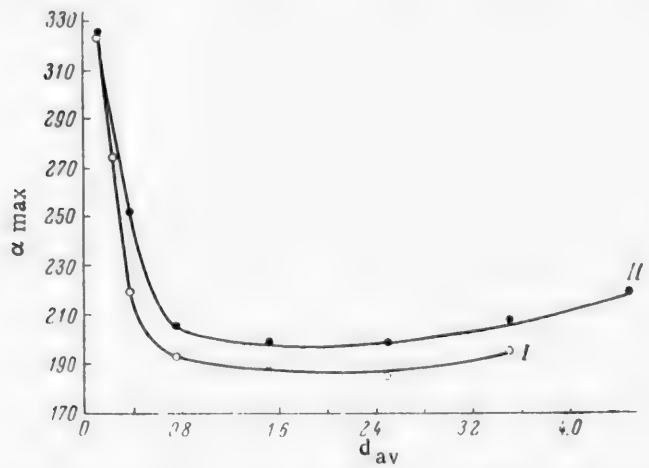

Fig. 2. Relation between the maximum coefficient of heat transfer and the grain size of catalyst BAV. I) D = 49 mm; II) D = 73 mm.

when the particle size of catalyst BAV is increased up to approximately 1.5 mm (Figs. 1 and 2). Such a character for the function $\alpha_{max} = \varphi(d)$ is emphasized in all of the existing investigations where different sized particles were used [1-4, 7-9]. However, such a relationship is valid only for the laminar and transition regions, where the thickness of the boundary heat-exchange portion is determined mainly by the size of the particles, their concentration, and their mobility (pulsation velocities).

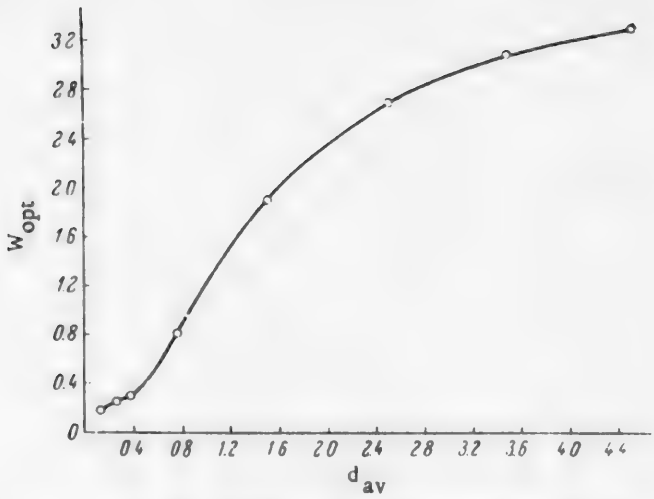

Fig. 3. Relation between the optimum air velocity and the particle size of catalyst BAV.

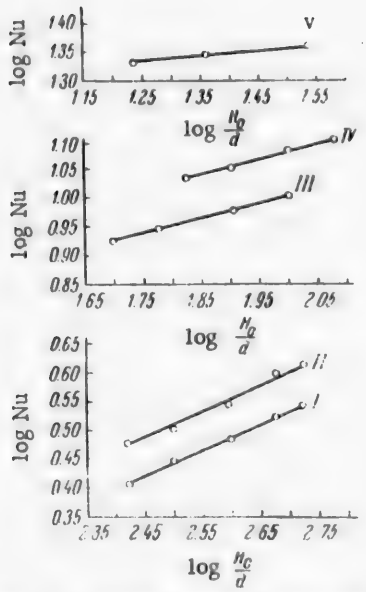

Fig. 4. Effect of initial bed height on the heat-transfer process. Average particle size of catalyst BAV (in mm): I) 0.38; III) 1.5; V) 3.5. Average particle size of conversion catalyst (in mm): II) 0.38; IV) 1.5.

With a turbulent movement of the gas, a boundary laminar layer of the gas always remains in the core of the flow at a heat-exchange surface, to which heat is transmitted from the turbulently moving gas phase and from the solid particles in contact with the layer. The average thickness of the boundary laminar layer depends on the linear velocity of the gas, its physical properties (viscosity, density), and the "purifying" action of the solid particles. In the turbulent region, where the thickness of the hydrodynamic laminar layer of gas and the thickness of the boundary heat-exchange portion apparently nearly coincide, the linear velocity of the gas stream should exert a constantly increasing influence on the thickness of these layers.

With increase in the size of the solid particles (or their density), constantly higher velocities of the gas are required to convert the bed into a fluidized state. Consequently, beginning with a certain particle size, a further increase in their size causes the maximum heat-transfer coefficient to rise. The validity of such a conclusion is illustrated by the experimental data given above for particle sizes d > 1.5 mm (Figs. 1 and 2).

As a result, the function $\alpha_{max} = \varphi(d)$ has a minimum, determined by the change in the hydrodynamic regime.

The relation between the optimum velocity of the gas flow (corresponding to α_{max}) and the particle size of catalyst BAV is shown in Fig. 3. The character of the curve, $w_{optimum} = \varphi(d)$, reflects the presence of different hydrodynamic regimes in the fluidized bed: laminary, transition, and turbulent.

To treat the obtained results in a power function of similarity criteria, it is necessary to first determine the effect of the relationships between the initial height H_0 of the bed, its diameter D, and the size $\underline{d}$ of the solid particles on the heat-transfer process.

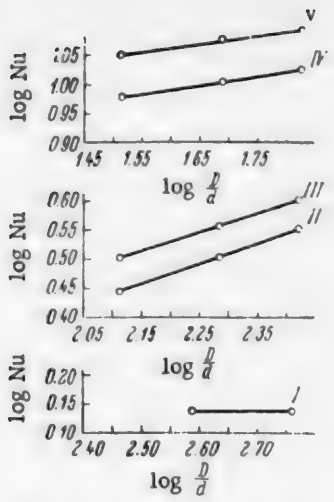

Fig. 5. Effect of apparatus diameter on the heat-transfer process. Average particle size of catalyst BAV (in mm): I) 0.127; II) 0.38; IV) 1.5. Average particle size of conversion catalyst (in mm): III) 0.38; V) 1.5.

The initial height H_0 of the bed, with the other conditions constant, determines the height of the fluidized bed and exerts considerable influence on its hydrodynamic characteristics. The literature data on the influence of the bed height on the heat-transfer coefficient are highly contradictory, which is apparently due to a difference in the experimental conditions used. It is obvious that the effect of the initial bed height, as a function of the hydrodynamic regime and numerical value of the simplex $\frac{H_0}{d}$, will be different. The results of our investigations for a laminar regime at $527 > \frac{H_0}{d} > 263$ and a turbulent regime at $120 > \frac{H_0}{d} > 17$ are shown in Fig. 4, where $Nu = \frac{\alpha \cdot d}{\lambda_g}$; λ_g is the heat conductivity of the gas phase.

Proceeding from the experimental results, the mean exponent of the simplex $\frac{H_0}{d}$ was taken equal to 0.45 for the laminar region, and equal to 0.16 for the turbulent region. As a result, for these two regimes we correspondingly have:

$$Nu = A_1 \cdot \left(\frac{H_0}{d}\right)^{0.45} \text{ and } Nu = A_2 \cdot \left(\frac{H_0}{d}\right)^{0.16}.$$

The diameter D of the apparatus also affects the hydrodynamics of the fluidized bed, and consequently, the heat-transfer process. From the data given below (Fig. 5), it follows that α_{max} increases with increase in the diameter of the apparatus, in which connection the rate of growth decreases as $\frac{D}{d}$ increases.

The contradictory nature of the literature data [5-10] on the influence of the apparatus diameter and of the bed height, and also on the location and dimensions of the heat-exchange surface, are due mainly to the lack of sameness in the experimental conditions.

The results of our investigations for a laminar regime at $575 > \frac{D}{d} > 129$ and a turbulent regime at $67 > \frac{D}{d} > 33$ are plotted in Fig. 5. The experiments were run at H_0 = 120 mm. Proceeding from the experimental results, the mean exponent of the simplex $\frac{D}{d}$ was taken equal to 0.16 for the laminar region, and equal to 0.13 for the turbulent region. As a result, for these two regimes we have:

$$Nu = B_1 \cdot \left(\frac{D}{d}\right)^{0.16} \text{ and } Nu = B_2 \cdot \left(\frac{D}{d}\right)^{0.13}$$

The heat-transfer equations were derived by processing the experimental data, plotted in Fig. 1, taking into account the data given above on the influence of the apparatus diameter and the initial bed height. The complex nature of the function $\alpha = \varphi(w)$ made it necessary to process the data for the two portions of the curves separately: from the gas velocity, corresponding to the formation of the fluidized bed (w_{cr}), to its optimum value, w_{opt}, and from w_{opt} to the start of escape of the solid phase from the apparatus.

The effect of the criterion $Re = \frac{w \cdot d}{\gamma}$ on the heat-transfer process ($Fr = \frac{d \cdot g}{w^2}$) is illustrated in Fig. 6, where, in accordance with what has been said above, the exponents of the geometric simplexes $\frac{D}{d}$ and $\frac{H_0}{d}$ are different for different regimes. The slope tangents of straight lines I, II, III and IV are respectively equal to 0.95, 0.84, 0.85 and ~1.0, which corresponds to the exponents of the Re criterion for different hydrodynamic regimes and corresponding sections of the curve, $\alpha = \varphi(w)$.

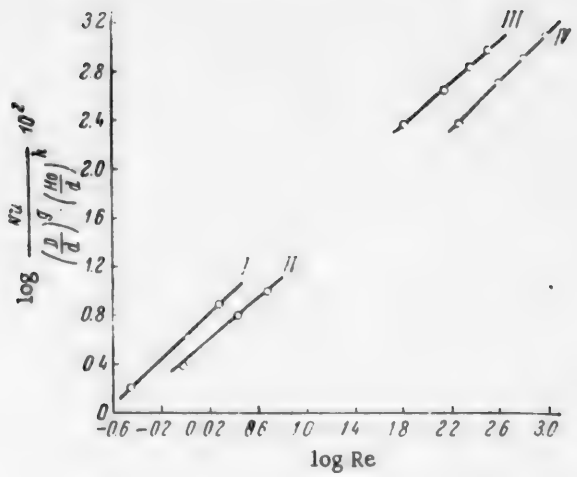

Fig. 6. Relation between the heat-transfer process and the Re criterion (Fr = const). Laminar region: I) from w_{cr} to w_{opt}; II) from w_{opt} to escape. Turbulent region: III) from w_{cr} to w_{opt}; IV) from w_{opt} to escape.

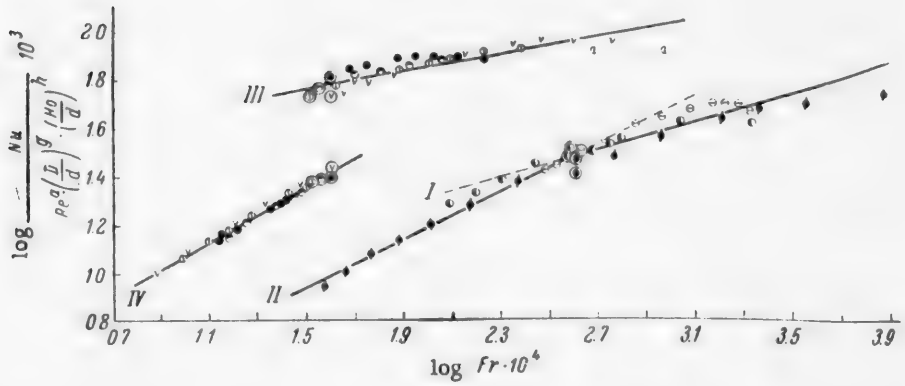

Fig. 7. Relation between the heat-transfer process and the Fr criterion. Laminar region: I) from w_{cr} to w_{opt}; II) from w_{opt} to escape. Turbulent region: III) from w_{cr} to w_{opt}; IV) from w_{opt} to escape. The different points indicate a change in the particle size of the BAV catalyst from 0.127 to 4.5 mm. The maximum values of α are designated by double symbols.

The exponent of the Fr criterion was determined by a graphical treatment of the experimental data, as shown in Fig. 7, where the numerical values of the exponents a, g and h are given above. The slope tangents of lines I, II, III and IV in Fig. 7 are respectively equal to 0.27, 0.49, 0.17 and 0.56.

As a result, the obtained experimental relationships, plotted in Fig. 1, may be described by the following four equations. In the limits of each hydrodynamic regime, equations (1) and (3) describe the portion of the curve from w_{cr} to w_{opt}, while equations (2) and (4) describe the portion from w_{opt} to w_{escape}.

Laminar region:

$$Nu = 0.065 \cdot Re^{0.95} \cdot Fr^{0.27} \cdot \left(\frac{D}{d}\right)^{0.16} \cdot \left(\frac{H_0}{d}\right)^{0.45}, \quad (1)$$

$$Nu = 0.15 \cdot Re^{0.84} \cdot Fr^{0.49} \cdot \left(\frac{D}{d}\right)^{0.16} \cdot \left(\frac{H_0}{d}\right)^{0.45}, \quad (2)$$

Turbulent region:

$$Nu = 0.14 \cdot Re^{0.85} \cdot Fr^{0.17} \cdot \left(\frac{D}{d}\right)^{0.13} \cdot \left(\frac{H_0}{d}\right)^{0.16}, \quad (3)$$

$$Nu = 0.56 \cdot Re^{1.0} \cdot Fr^{0.56} \cdot \left(\frac{D}{d}\right)^{0.13} \cdot \left(\frac{H_0}{d}\right)^{0.16}, \quad (4)$$

where

$$Nu = \frac{\alpha \cdot d}{\lambda_r}; \quad Re = \frac{w \cdot d}{\nu}; \quad Fr = \frac{g \cdot d}{w^2};$$

α is the heat-transfer coefficient; $\underline{d}$ is the particle size; $\underline{w}$, λ_g and ν are respectively the linear velocity in the free space of the apparatus, the heat conductivity, and the viscosity of the gas; $\underline{g}$ is acceleration due to gravity; D is the apparatus diameter; and H_0 is the initial bed height.

The values of the coefficients and exponents in equations (1)-(4) were verified for the given experimental conditions. Here the maximum error when the mean values were compared with the calculated did not exceed ±17% for equations (1) and (3), while for equations (2) and (4) it did not exceed ±10%.

In Fig. 7 the data, corresponding to the maximum heat-transfer coefficients, are designated by double symbols. As can be seen from the graph, the α_{max} for different particle sizes are observed at approximately the same value for the Fr criterion (for the laminar region at Fr ≈ 0.0415, and for the turbulent region at Fr ≈ 0.00374).

Consequently, the optimum velocities w_{opt} of air for different sizes of catalyst BAV may be determined from equations (5) and (6).

Laminar region:

$$w_{opt} = \sqrt{\frac{g \cdot d}{0.0415}} = 15.35 \cdot \sqrt{d}, \quad (5)$$

Turbulent region:

$$w_{opt} = \sqrt{\frac{g \cdot d}{0.00374}} = 51.2 \cdot \sqrt{d}. \quad (6)$$

The numerical values of the coefficients in equations (5) and (6) depend on the physical properties of the solid and gas phases. The deviations of the experimental data, plotted in Fig. 3, from the curves, described by equations (5) and (6), do not exceed ±2% for the laminar region, while for the turbulent region they do not exceed ±5%.

SUMMARY

1. An investigation of the function $Nu = \varphi\left(Re, Fr, \frac{D}{d}, \frac{H_0}{d}\right)$ for the process of heat transfer from a fluidized bed to the heat-exchange surface led to obtaining equations (1)-(4) for determining heat-transfer coefficients.

2. Equations (5) and (6) were derived for determining the optimum air velocity.

LITERATURE CITED

[1] I. P. Mukhlenov, D. G. Traber, V. B. Sarkits, and T. P. Bondarchuk, Zhur. Priklad. Khim. 32, No. 6, 1291 (1959).*

[2] I. P. Mukhlenov, D. G. Traber, and V. B. Sarkits, Trudy Leningrad Tekhnol. Inst. 54 (1959).

[3] V. B. Sarkits, D. G. Traber, and E. A. Protopopova, Trudy Leningrad Tekhnol. Inst. 54 (1959).

[4] V. B. Sarkits, D. G. Traber, and I. P. Mukhlenov, Scientific Technical Conference of Lensovet Technological Institute, Leningrad. Themes of Papers [in Russian] (Goskhimizdat, 1958).

[5] W. M. Dow and M. Jakob, Chem. Eng. Progr. 47, No. 12, 637 (1951).

[6] C. van Heerden, A. P. P. Nobel, and D. W. van Krevelen, Ind. Eng. Chem. 45, No. 6, 1237 (1953).

[7] Ju-Chin Chu, Fluidization (Editor-in-Chief, D. F. Othmer) (New York, 1956).

[8] M. Leva and coworkers, Chem. Eng. Progr. 45, No. 9, 563 (1949); 48, No. 6, 307 (1952).

[9] A. V. Chechetkin, High Temperature Heat-Transfer Agents [in Russian](State Power Press, 1957).

[10] N. I. Gel'perin, V. Ya. Kruglikov, and V. G. Ainshtein, Zhur. Priklad. Khim. No. 6 (1958).**

Received April 24, 1959

* Original Russian pagination. See C. B. translation.

** See C. B. translation

APPLICATION OF THE THERMAL DIFFUSION METHOD IN THE PURIFICATION OF DYES

B. M. Bogoslovskii, B. M. Yavorskii and A. D. Virnik

Laboratory of the Chemistry of Dyes of Moscow Textile Institute

Organic dyes are usually not chemically pure compounds but contain impurities, partially entrained with the starting intermediate products and partially formed in the process of obtaining the dye itself. These impurities (both organic and inorganic) differ from the dye itself in molecular weight, and in the size and shape of the molecule. In many investigations it is necessary to operate with chemically pure dyes. The preparation of pure dyes presents great difficulties and is associated with the expenditure of much labor and time. The methods used for the purification of different dyes are not the same [1].

Considering the complexity of the methods used at the present time for the purification of dyes, and taking into consideration the excellent results obtained using the thermal diffusion purification technique in various industrial operations (separation of isotopes, separation of molecular solutions, fractional separation of petroleum products), it seemed advisable to verify the possibility of using the thermal diffusion method to purify dye solutions. In case of success, the thermal diffusion method could become a universal method for the purification of dyes from inorganic and organic impurities.

The results of a preliminary study of the thermal-diffusion effect on dye solutions, and also on solutions of dye mixtures, are reported in this paper.

EXPERIMENTAL

Apparatus. Two thermal diffusion columns, one glass and the other metal, were used in the study. The glass column (Fig. 1) consisted of two concentric molybdenum glass tubes with external diameters of 26 and 30 mm and a wall thickness of 1.5 mm. These tubes were centered along their entire length in such manner that the gap between them did not exceed 0.4-0.5 mm. The gap at the ends of the column was 5 mm. The spaces (auxiliary reservoirs) created in this manner were destined to receive the fractions after thermal diffusion separation. The operating length of the column was 100 mm; the length of each auxiliary reservoir was 25 mm; the volume of the operating section was 4 ml; the volume of each auxiliary reservoir was 6.3 ml; the total volume was 16.6 ml. The column was heated with steam, which entered on the inside of the column. Tap water was circulated through the jacket for cooling. The auxiliary reservoirs were fitted with stopcocks to permit removal of fraction samples after thermal diffusion separation.

The metal column* (Fig. 2) consisted of two concentric stainless steel tubes with external diameters of 14 and 17 mm and a wall thickness of 1 mm. These tubes were centered along their entire length in such manner that the gap between them did not exceed 0.5±0.1 mm. In contrast to the glass apparatus, this apparatus did not have any auxiliary reservoirs. The operating length of the column was 1100 mm; the total volume was 25.64 ml. The outside tube was heated by an electric current, which passed through a nichrome wire wrapped on a sheet of mica; the resistance of the wire was 38 Ω. A LATR-1 automatic transformer was used to regulate the heat. Tap water, fed inside the column, served as the cooling agent. Both the heating and the cooling temperatures were measured by means of thermocouples, which were embedded in the internal and external tubes. Filling of the column with the investigated liquid was done by gravity from a vessel, located at the same level as the

*Our work in the metal column was done with the permission of A. V. Lykova in the Physics Laboratory of the Moscow Technological Institute of the Meat and Dairy Industry.

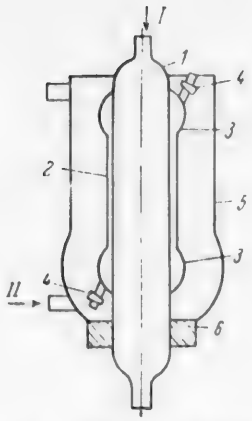

Fig. 1. Diagram of the glass column. 1) Inside tube, 2) outside tube, 3) auxiliary reservoirs, 4) stopcocks for removal of samples, 5) jacket for water cooling, 6) rubber stopper. I) Steam inlet, II) water inlet.

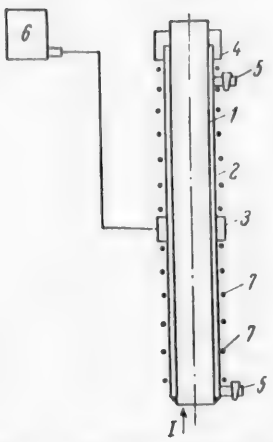

Fig. 2. Diagram of the metal column. 1) Inside tube, 2) outside tube, 3) feed mechanism, 4) centering packing gland, 5) stopcocks for removal of samples, 6) vessel for the investigated solution, 7) electric winding. I) Water inlet.

upper end of the column, through a feed mechanism, located at an equal distance from the ends of the column. This mechanism was a ring reservoir, assuring a uniform filling of the column with the investigated liquid through four openings with a diameter of 5 mm, arranged symmetrically in one plane around the circumference of the outside tube. The upper and lower ends of the column were fitted with stopcocks for the removal of liquid samples.

Description of Experiments. To study separation by thermal diffusion we took the following dyes: Congo red (content of chemically pure dye 82%, molecular weight 696), Acid Blue S (content of chemically pure dye 71.5%, molecular weight 695), and Acid Orange (content of chemically pure dye 84.4%, molecular weight 350).

The experiments in the glass column were run with 2% solutions of the dyes, Congo red and Acid Blue S, with the time of the thermal diffusion process ranging from 1 to 6 hours. The temperature of the steam used for heating was 100°. The temperature of the cooling water at the inlet side was 7°. The temperature of the water at the outlet side was 13°. A syringe was used to remove samples (5 ml) from the upper and lower auxiliary reservoirs immediately after the termination of heating and cooling.

The experiments in the metal column were run with 4% solutions of the dyes, Congo red and Acid Blue S, and also with 4% solutions of mixtures of the dyes. Mixture No. 1 consisted of 50% Acid Blue S and 50% Acid Orange, while mixture No. 2 consisted of 50% Acid Blue S and 50% of Congo red. When operating with solutions of the individual dyes, the time of the thermal diffusion process ranged from 0.5 to 3 hours, while in the experiments with solutions of mixtures it ranged from 1 to 2 hours. The temperature of the hot wall was 90°, and that of the cold wall was 6°. Samples (3 ml) were removed during the operation of the column, first from the upper portion, and then from the lower portion of the column.

Analysis Methods. The change in the concentration of the dye solutions was determined by measuring the optical density of the solution using a FEK-M photoelectric colorimeter, the sensitivity of which was within 1% of the absolute value of the concentration.

In the experiments where the individual dyes were processed through the metal column, the solutions for colorimetering were prepared in the following manner: 2-ml samples were removed with a pipet from both the upper and lower fractions, and also from the starting solution. Each sample was transferred to a 250-ml volumetric flask. The solution was made up to the mark with distilled water. When operating in the glass column, analogous samples (4 ml) were also removed by pipetting and transferred to a 250-ml volumetric flask. The solution was made up to the mark with distilled water. As a result, in all cases the dilution of the starting solution for colorimetering was brought to a dry dye content of 0.32 g/liter.

When studying the effect of thermal diffusion on solutions of dye mixtures, only 1-ml samples were removed with a pipet from the upper and lower fractions, and also from the starting solution. Each sample was transferred to a 250-ml volumetric flask. The solution was made up to the mark with distilled water. As a result, here the dilution of the starting solution for colorimetering was brought to a dry mixed dye content of 0.16 g/liter. The optical densities of the solutions, obtained by dilution, were determined by colorimetry, at first without a light-filter, and

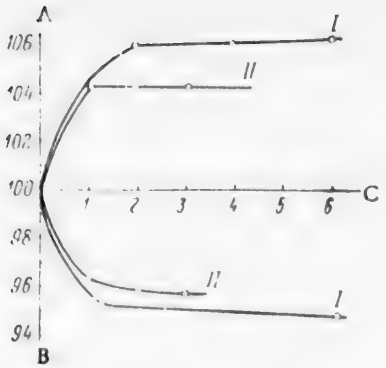

Fig. 3. Change in the concentration of Congo red solution. The concentration K of the starting solution was taken as 100%. A) Concentration of dye solution in the lower end of the column; B) the same in the upper end of the column; C) time (in hr). I) In the glass column; II) in the metal column.

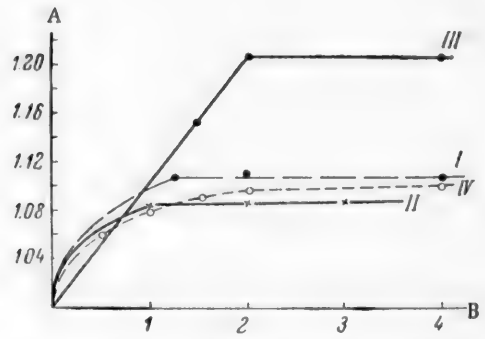

Fig. 4. Change in the coefficient of thermal-diffusion separation. A) Coefficient of separation (q); B) time (in hr). I) Congo red, glass column; II) Congo red, metal column; III) Acid Blue S, glass column; IV) Acid Blue S, metal column.

then in succession with three different light-filters. Parallel with this, we prepared standard solutions of the dyes, Congo red, Acid Blue S, and Acid Orange, all having the same concentration of 0.08 g/liter. These solutions were also colorimetered, at first without a light-filter, and then in succession with the same three light-filters. The concentrations of the mixture components in the solutions were determined for each sample using the formulas [2]:

$$K_1 = \frac{D_1B_2 - D_2B_1}{A_1B_2 - A_2B_1} \cdot n,$$

$$K_2 = \frac{D_2A_1 - D_1A_2}{A_1B_2 - A_2B_1} \cdot n,$$

where A_1 and A_2 are the optical densities of the standard solution of the first dye corresponding to light-filters No. 1 and No. 2, B_1 and B_2 are the optical densities of the standard solution of the second dye corresponding to light-filters No. 1 and No. 2, D_1 and D_2 are the optical densities of the investigated solution of mixed dyes with an unknown concentration of the components when using the same light-filters, K_1 is the concentration of the first dye (in g/liter), K_2 is the concentration of the second dye (in g/liter), and n is the concentration of the standard dye solutions (in g/liter).

The concentration of a mixture of dyes in solution is

$$K = K_1 + K_2.$$

EXPERIMENTAL RESULTS

The curves, characterizing the change in the concentration of the Congo red solution in the upper and lower ends of the column during the thermal diffusion process, are shown in Fig. 3. From these curves it can be seen that in all of the experiments there was an increase in the concentration of the dye molecule in the lower part of the column and a corresponding decrease in the upper part. The rate of change in the concentration was greatest at the start, for 1 to 2 hours, after which it dropped sharply, and further change in the concentration was slight. The rate of change in the concentration of Acid Blue S in the upper and lower ends of the column during the thermal diffusion bears a similar character.

The magnitude of thermal-diffusion separation is characterized by the coefficient of separation [3]:

$$q = \frac{[C_1 : C_2]_{II}}{[C_1 : C_2]_I},$$

where C_1 is the relative molar concentration of the dissolved substance (dye), and C_2 is the relative molar concentration of the solvent (water); indices: I) refers to the upper portion of the column, and II) refers to the lower portion.

On the basis of this formula we constructed the curves shown in Fig. 4, characterizing the change in the separation coefficient (q) for the experiments run by us. As the curves indicate, the separation coefficient increases rapidly at the start of the thermal-diffusion process, and then it changes very slowly, for all practical purposes approaching a constant value.

From the given curves it can be seen that in the glass column the separation coefficient for a 2% Congo red solution was 1.11, while for a 2% Acid Blue S solution it was 1.21. In the metal column, for a 4% Congo red solution, q = 1.09, and for a 4% Acid Blue S solution, q = 1.10. It should be mentioned that in the metal column, a close to the maximum thermal-diffusion separation coefficient is reached in 1 hour, whereas in the glass column the same effect is reached in 2 hours. However, as was found experimentally, we were able to obtain a larger separation coefficient in the glass column.

A study of the effect of thermal diffusion on solutions of mixed dyes also revealed an increase in the separate concentration of each component and of the mixture as a whole in the lower end of the column and a corresponding reduction in their concentrations in the upper end. The separation coefficient in the 2-hour experiment was 1.05 for mixture No. 1, and 1.07 for mixture No. 2. It is possible that in these experiments the separation coefficient didn't have time to reach a value close to the maximum.

Together with this, we observed a more rapid diffusion of one of the components of the mixture in the lower part of the column, as a result of which the ratio of the components in the mixture changed in both ends of the column. Thus, in the 2-hr experiment, mixture No. 1 was richer in Acid Orange in the lower portion of the column by a matter of 3% when compared with its original content in the mixture, and there was a corresponding decrease of 3% in the content of this component in the mixture in the upper part of the column. Mixture No. 2 was enriched in the lower portion of the column with Acid Blue S by a matter of 4.5% when compared with its original content in the mixture, and there was a corresponding decrease of 4.5% in the content of this component in the mixture in the upper part of the column. An increase in the separation coefficient may by achieved by using a multistage cascade composed of columns connected in series.

SUMMARY

1. An increase in the concentration of dye in the lower end of a thermal-diffusion column was observed.

2. A change in the concentration, close to the maximum, is reached in the first 1 to 2 hours, after which the rate of change in the concentration is much slower.

3. In studying the effect of thermal diffusion on solutions of dye mixtures, it was observed that, together with a general tendency for the concentration of the mixture to increase in the lower end of the column, there is a greater accumulation of the component with the relatively smaller molecular weight, in this portion, while when the molecular weights are the same, it is the component with the relatively shorter molecular length that shows the greater accumulation.

LITERATURE CITED

[1] B. M. Bogoslovskii, Zhur. Priklad. Khim. 28, 659 (1955).*

[2] T. Vickerstaff, The Physical Chemistry of Dyeing [Russian translation] (State Light Industry Press, 1956).

[3] R. C. Jones and W. H. Furry, Separation of Isotopes by Thermal Diffusion [Russian translation of review article in Revs. Modern Phys. 18, 151-224 (1946)] (IL, 1947).

Received November 28, 1958

* Original Russian pagination. See C. B. translation.

PLASTIC FILM LIGHT-FILTERS ABSORBING LONG-WAVE AND NEAR INFRARED REGIONS OF THE SPECTRUM*

E. A. Veller and B. A. Porai-Koshits

In different branches of industry it is necessary to use light filters made of plastic film to absorb the red and near infrared regions of the spectrum.

Of the organic compounds, other than the cyanine dyes, only several individual members are known whose absorption maxima lie in the region, λ = 680-700 mμ. These include: Naphthol Green, Filter Blue-Green, and Acid Green 2G Base [1, 2].

Cyanines of general formula $>N-\overset{|}{C}(=\overset{|}{C}-\overset{|}{C})_n=\overset{+}{N}$, classified as polymethine dyes, are used mainly as photographic sensitizers [3, 4]. Dyes of this type give a regular shift in the absorption maximum as n increases, with a simultaneous reduction in the light stability. They are quite soluble in organic solvents, but are extremely sensitive to the action of light, in which connection the color intensity of the film changes drastically with time. For this reason cyanine dyes possess little interest as filters.

Naphthol Green, being a complex iron salt of 1-nitroso-2-naphthol-6-sulfonic acid, is soluble in water, and for this reason is not suitable for the dyeing of films made from an organic plastic.

The dye, Filter Blue-Green, is obtained by the oxidation of 1,2-naphthalenediamine with ferric chloride; its structure has not been established. The dye is readily soluble in alcohol, but is insoluble in dichloroethane, and is not compatible with acetobutyrate film. The anthraquinone dye (Acid Anthraquinone Green 2G Base), extensively used by us to prepare film light-filters, does not give a sufficiently intense absorption of the red and near infrared portions of the spectrum. In connection with this, the preparation of film light-filters, showing maximum absorption in the far long-wave portion of the spectrum, from organic dyes appeared impossible.

Among colored inorganic compounds there are compounds the use of which could, in view of their spectra properties, solve the present problem. However, the blending of mineral compounds with plastics is difficult, and in some cases impossible. For this reason, the thought arose of synthesizing organic-mineral compounds, compatible with organic films of different composition, and at the same time, retaining the spectral properties of the inorganic compound.

Based on the data reported in the literature [5], we selected copper as the metal for combining with the organic radical, since mineral copper salts give a selective absorption in the long-wave and near infrared portions of the spectrum, with a fairly steep drop in the long-wave portion of the transmittance curve. The spectral characteristics of several copper compounds, namely, copper sulfate, copper acetate, and Schweizer's reagent, are given below (Figs. 1-3).

The combining of a metal with an organic radical may be depicted either as a complex of the metal with the organic compound (in particular, with dyes), or as a salt of the metal with the organic acid.

It has been shown in a number of studies devoted to the spectral properties of complexes that these compounds are soluble in weakly polar organic solvents [6-8], and, in addition, are compatible, for example, with acetobutyrate base. However, in most cases, the spectrophotometric characteristics of complexes do not depend on

*Communication IV in a series of papers devoted to a study of the physicochemical properties of hydrophobic dyes and their use in the preparation of light filters.

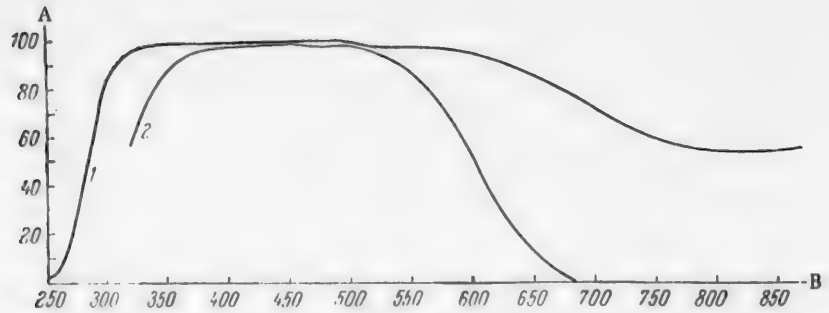

Fig. 1. Spectral characteristics of water solution of copper sulfate. A) Transmittance (in %); B) wave length λ (in mμ). Solution concentration (in %): 1) 0.635; 2) 8.57.

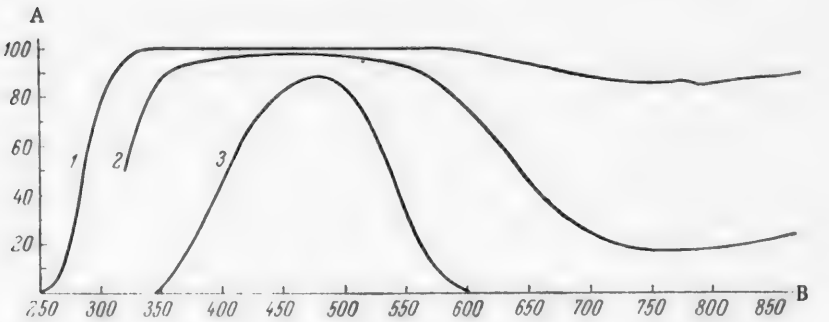

Fig. 2. Spectral characteristics of water solution of copper acetate. A) Transmittance (in %); B) wave length λ (in mμ). Solution concentration (in %): 1) 0.107; 2) 0.75; 3) 6.0.

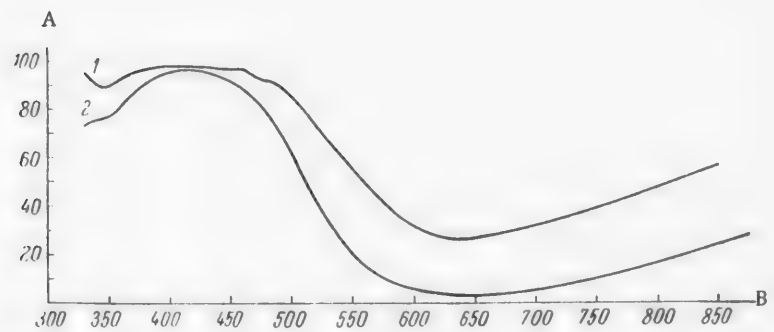

Fig. 3. Spectral characteristics of Schweizer's reagent. A) Transmittance (in %); B) wave length (in mμ). Solution of $Cu(OH)_2$ in concd. ammonia when diluted: 1) 30 times; 2) 3 times.

the nature of the metal, but instead depend on the nature of the dye with which the metal is linked. Our data, as well as the literature data [9, 10], indicate that in the ultraviolet region the spectra of metalized compounds fail to differ appreciably from the spectra of the corresponding dyes. A new absorption band appears in the visible region, but the principal absorption band proves to be nearly unchanged (the maximum shift is 5-10 mμ).

As a result, an attempt to use the complexes of dyes gave negative results.

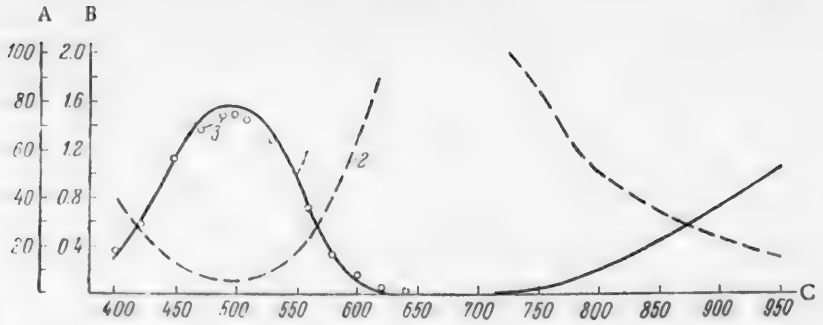

Fig. 4. Spectral characteristics of film light-filter prepared from plastic base and copper oleate. A) Transmittance (in %); B) density; C) wave length λ (in mμ). 1) Transmittance; 2) density; 3) transmittance of theoretically calculated light-filter.

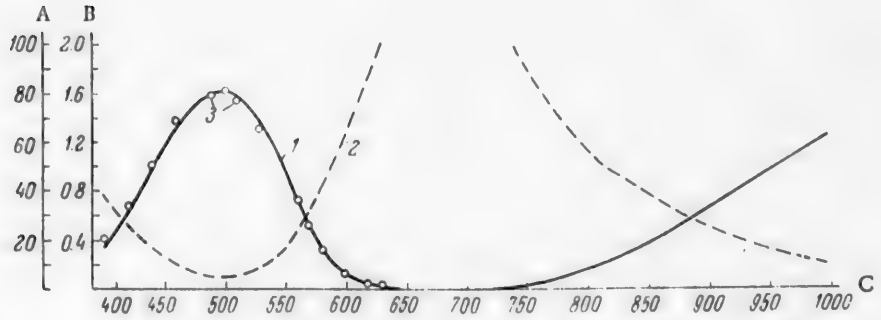

Fig. 5. Spectral characteristics of film light-filter prepared from plastic base and copper ricinoleate. A) Transmittance (in %); B) density; C) wave length λ (in mμ). 1) Transmittance; 2) density; 3) transmittance of theoretically calculated light-filter.

For this reason, in our work we concentrated mainly on the copper salts of unsaturated fatty and nephthenic acids. These salts are soluble in organic solvents [11], and, as our studies revealed, by retaining the optical properties of mineral copper salts, they absorb in the long-wave region of the spectrum. There still remained the problem of establishing the compatibility of these compounds with cellulose ester plastics.*

The first experiments in this direction revealed that the use of ethyl cellulose as a base permits obtaining a clear colored film when copper soaps are added. Neither by changing the soap concentration, nor the conditions of preparing the film itself (length of drying, time of exposure of the frame), were we able to obtain a clear filter based on acetobutyrate.

We have still been unable to establish whether this is due to a finer subdivision of the micelles in benzene, the solvent used when casting the ethyl cellulose films, when compared with the subdivision in dichloroethane, the solvent used for cellulose acetobutyrate, or whether it is due to the fact that in one case we are dealing with an ether (ethyl cellulose), and in the other case with an ester (cellulose acetobutyrate).

The work was done with oleic and ricinoleic acids. The copper salts of oleic acid were obtained from the sodium salts by double decomposition. In working out a method for the preparation of the copper salts, the sodium soaps of oleic acid were treated with the copper salts of mineral acids in either alcohol or water solution. The

*All of the experiments on casting the plastic films were performed by P. A. Medvedeva and Sh. G. Yanovskaya in the Department of Plastics of the Lensovet Technological Institute, Leningrad.

optimum conditions as regards yield and purity of product proved to be the method where an alcohol solution of sodium hydroxide is added to an alcohol solution of the copper salt and oleic acid. The copper soap formed in this manner was extracted with benzene.

To obtain better separation of the liquids, it proved helpful to add a small amount of water.

Equivalent amounts of oleic acid, sodium hydroxide, and copper salt of mineral acid were used in all cases. The solutions in organic solvent were dried over anhydrous sodium sulfate. To avoid oxidation, the solvent was distilled off in a stream of hydrogen.

Ricinoleic acid is usually obtained by the saponification of castor oil. The sodium soap obtained in the saponification is stable to the action of salts, and is salted out only with sodium hydroxide. According to Holde [11], the amount of sodium hydroxide in the liquor beneath the soap corresponds to the ratio 65:100. We ran the saponification by heating castor oil with caustic for 1 hour on the water bath, either in a porcelain dish or in a flask fitted with a reflux condenser. The obtained soap was filtered through glass wool, dissolved in hot water until completely clear, and then neutralized to methyl orange, at first with concentrated, and then with dilute hydrochloric acid.

The oil obtained from the neutralization was extracted with ether, and the ether layer was separated in a separatory funnel, washed with water, dried over anhydrous sodium sulfate, filtered, the ether distilled off in a stream of hydrogen, and the residual ricinoleic acid was dried in vacuo.

The ricinoleic acid was purified by us in order to remove saturated solid acids, the copper salts of which are insoluble in nonpolar solvents. The purification was made by the Varrentrapp method [12]. The method is based on the difficult solubility of the lead salts of saturated fatty acids in ether.

The copper salt of ricinoleic acid was obtained by one of the methods described above for the preparation of the copper soap of oleic acid, i.e., in alcohol, water or aqueous alcohol solution, in a separatory funnel under a layer of benzene. Close to the theoretical amount of 0.5N alcoholic KOH solution was consumed when the ricinoleic acid was titrated. The calculated amount of copper sulfate or copper nitrate was taken for converting the sodium soap to the copper salt.

In preparing the film light-filters, the concentration of copper oleate or ricinoleate in the solution or in the film was determined from the copper content (using the Kolthoff modification [13] of the Busse method).

To obtain the desired spectral characteristics for the filter, the copper salt concentration was calculated from the data of measuring a solution of known concentration, employing the method of calculating the light-filter when hydrophobic dyes are used [14]. The calculated amount of unsaturated fatty acid copper salt was added to a benzene solution of ethyl cellulose, and, then without adding a plasticizer, the film light-filter was prepared in conventional manner.

The spectral characteristics of the film light-filters prepared from a plastic base and copper oleate (Fig. 4), and from a plastic base and copper ricinoleate (Fig. 5), are given in Figs. 4 and 5.

Both light-filters have a maximum transmittance, $T_{\lambda 500\ m\mu}$, of about 80%, and a complete absence of transmission at λ = 620-730 mμ, which is in harmony with the theoretically calculated; consequently, they satisfy the requirement of absorbing the long-wave and near infrared regions of the spectrum.

SUMMARY

1. Known dyes and their metalized complexes cannot be used to obtain plastic film light-filters that absorb the long-wave and near infrared portions of the spectrum.

2. The spectral characteristics of the copper salts of unsaturated fatty and naphthenic acids correspond to the spectra of mineral copper salts.

3. Light filters, absorbing the long-wave and near infrared portions of the spectrum, can be obtained by adding the copper soaps of unsaturated fatty and naphthenic acids to ethyl cellulose film.

LITERATURE CITED

[1] S. S. Baranov, S. V. Khludov, and É. B. Shpol'skii, Atlas of Transmission Spectra of Transparent Colored Films [in Russian] Izd. AN SSSR, 1948.

[2] E. A. Veller and B. A. Porai-Koshits, "Some problems in the synthesis and application of dyes", Trudy Leningrad Tekhnol. Inst. im. Lensoveta (1956).

[3] The Chemistry of Synthetic Dyes and Pigments, Editor-in-Chief, H. A. Lubs, p. 248 (1955).

[4] Ya. Ts. Bokinik, Optical Sensitization [in Russian]. (State Art Press, 1957).

[5] F. Weigert, Optical Methods of Chemistry [Russian translation]. Goskhimtekhizdat, 1934.

[6] A. E. Martell and M. Calvin, Chemistry of the Metal Chelate Compounds (1952).

[7] L. M. Kul'berg, Organic Reagents in Analytical Chemistry [in Russian]. Goskhimizdat, 1950.

[8] N. I. Blok, Qualitative Chemical Analysis [in Russian]. Goskhimizdat, 1952.

[9] G. McP. Smith, and coworkers, J. Am. Chem. Soc. 61, 2624 (1939); 62, 1669 (1940); 63, 3071 (1941); 64, 1650 (1942).

[10] M. L. Ernsberger and W. R. Brode, J. Org. Chem. 6, 331 (1941).

[11] D. Holde, Fats and Oils [Russian translation], Vol. 2, pp. 251, 234 (1933).

[12] F. Varrentrapp, Ann. 35, 197 (1840).

[13] F. P. Treadwell and W. T. Hall, Analytical Chemistry [Russian translation] (ONTI, Chief Publishers of Chemical Literature, 1935)pp. 165-166.

[14] E. A. Veller and B. A. Porai-Koshits, Trudy Leningrad Tekhnol. Inst. im. Lensoveta 30, 3 (1955).

Received November 22, 1958

TECHNOLOGY OF THE ELECTROCHEMICAL DEPOSITION OF COBALT – TUNGSTEN ALLOY AND ITS PROPERTIES

N. P. Fedot'ev, P. M. Vyacheslavov, E. G. Kruglova and G. P. Andreeva

Among the few papers devoted to the deposition of tungsten alloys, the greatest interest is possessed by the studies of Gol'ts and Kharlamov [1], and also those of Brenner, Burkhead, and Seegmiller [2, 3].

Our preliminary experiments with various electrolytes, recommended by the above authors, revealed that electrolytes containing citric acid or potassium sodium tartrate are inferior to the electrolyte containing ammonium sulfate. Proceeding from these considerations, we took as the basis for further experiments an electrolyte with the following composition (g/liter): W 9, Co 3, $(NH_4)_2SO_4$ 150, NH_4OH (25%) 60.

The electrolyte was prepared by dissolving WO_3 in concentrated alkali solution, after which the ammonia and ammonium sulfate were added. The latter dissolves cobalt sulfate. In preparing the electrolyte it is important to obey the indicated order of dissolving the components, as otherwise it is possible to obtain an insoluble precipitate of tungsten compounds. The procedures for the chemical analysis of the electrolyte and the deposit were described earlier [4].

Effect of Various Factors on the Composition of the Deposit and the Current Efficiency

Effect of the Ratio of the Metals W : Co in the Electrolyte. The concentration ratio of the metals Co and W in the electrolyte is the main factor influencing the composition of the deposit.

The corresponding data are plotted in Fig. 1.

As an analysis of the curves reveals, increasing the concentration ratio of the metals W : Co in the electrolyte leads to an increase in the amount of tungsten in the deposit. The curves rise sharply as the W : Co ratio is increased up to 7, after which the rise becomes more gentle, and from values of W : Co = 11 the curves proceed nearly parallel to the horizontal axis, i.e., for all practical purposes there is no further increase in the amount of tungsten in the deposit.

As can be seen from Fig. 1, increasing the total amount of metals in the electrolyte causes both a steeper rise of the curve and an increase in the amount of W in the deposit. When the total amount of metals is 48 g/liter, the maximum amount of tungsten in the deposit is 56%, at 12 g/liter it is 52%, and at 10 g/liter it is 40%.

As Fig. 2 shows, the current efficiency drops sharply (from 70 to 15%) when the W : Co ratio in the electrolyte is increased from 1 to 7, then at W : Co = 9-11 the current efficiency changes but slightly, and when the values of the W : Co ratio exceed 11 the current efficiency remains practically constant (on the average, 10%).

Effect of $(NH_4)_2SO_4$ Concentration. The experiments were run in an electrolyte that contained Co 11 g/liter, W 9 g/liter, NH_4OH (25%) 60 g/liter, and $(NH_4)_2SO_4$ – variable amount; D_k = 6.0 amp/sq dm, t = 60°.

As the experiments revealed (Fig. 3), the ammonium sulfate concentration exerts substantial influence on both the composition and quality of the deposit. The amount of tungsten in the deposit increases sharply from 7 to 26% when the $(NH_4)_2SO_4$ concentration is increased from 10 to 150 g/liter; this increase becomes slight when

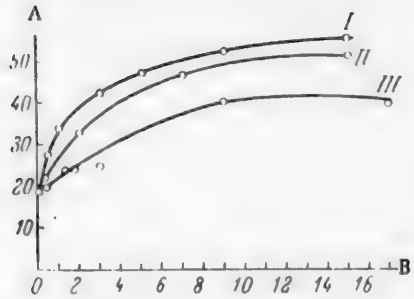

Fig. 1. Effect of ratio of W : Co in the electrolyte on the composition of the cathodic deposit. A) Amount of W (in %); B) ratio of W : Co in the electrolyte. Amounts of W and Co in the electrolyte (in g/liter): I) W 9, Co 0.5-30; II) W 1-45, Co 3; III) W + Co = 12.

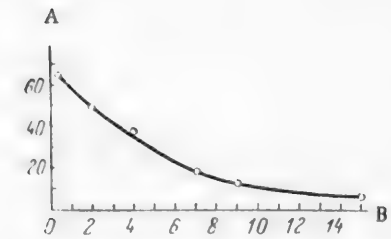

Fig. 2. Effect of ratio of W : Co in the electrolyte on the cathodic current efficiency. A) Current efficiency (in %); B) value of the W : Co ratio.

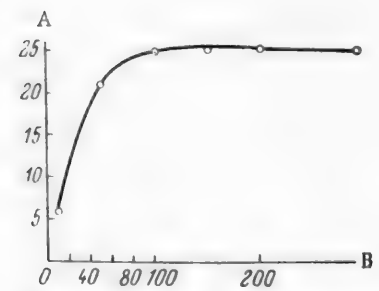

Fig. 3. Effect of $(NH_4)_2SO_4$ concentration on composition of cathodic deposit. A) Amount of W (in %); B) $(NH_4)_2SO_4$ concentration (in g/liter).

the $(NH_4)_2SO_4$ concentration is increased further (from 150 to 300 g/liter), but the quality of the deposit is greatly improved – it becomes light-colored, lustrous, and shows better bonding with the base.

With increase in the $(NH_4)_2SO_4$ concentration, the current efficiency changes along a curve whose maximum corresponds to a concentration of 150 g/liter. An $(NH_4)_2SO_4$ concentration of 200-250 g/liter must be recommended for operation, since in this case better quality deposits are obtained.

Effect of Ammonia Concentration. Ammonia fails to exert substantial influence on the composition of the deposit in the investigated range of 20 to 140 g/liter, but the quality of the deposit changes with increase in the NH_4OH content in that it becomes dark, and at 140 g/liter it turns black. The current efficiency changes correspondingly from 94 to 66%.

Effect of NaOH Concentration. Free caustic is without effect on the composition of the deposit, but its presence in large excess in the electrolyte leads to a darkening of the deposit.

The influence of the current density on the composition, quality of the deposit, and current efficiency was investigated for two electrolytes (Fig. 4).

As the shape of the curves indicates, the amount of tungsten in the alloy increases with increase in the current density. Of the two metals present in the electrolyte, tungsten is the less noble, and consequently the liberation of tungsten is facilitated when the current density is increased, whereas for cobalt the current density approaches the limiting value and the conditions for its liberation at the cathode become less favorable. Curve I corresponds to the higher W/Co ratio, and for this reason it lies above curve II.

The change in the current efficiencies is characterized by a maximum, corresponding to a current density of 10 amp/sq dm (Fig. 5) for curve I.

Increasing the total amount of metals increases the current efficiencies (curve I lies above curve II).

The quality of the deposit is impaired when the current density is increased, the luster is lost, a coarseness appears, and, beginning when D_k = 50 amp/sq dm, the deposit becomes brittle. The best appearing deposit was obtained at a current density of 10 amp/sq dm, and here the current efficiency was also high. Consequently, the preferred operating current density must be assumed to be D_k = 8-12 amp/sq dm, and in this range of densities the change in the amount of tungsten in the deposit corresponds to 1.5%.

In studying the effect of the temperature we used a bath containing (in g/liter): W 9 Co 11, $(NH_4)_2SO_4$ 150, NH_4OH 60, NaOH 9; D_k = 6 amp/sq dm.

The results of these experiments are plotted in Figs. 6 and 7.

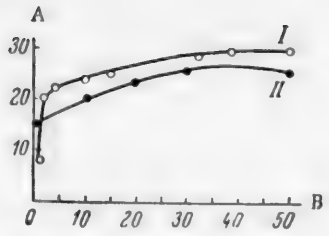

Fig. 4. Effect of cathodic current density on composition of cathodic deposit. A) Amount of W (in %); B) current density (in amp/sq dm).

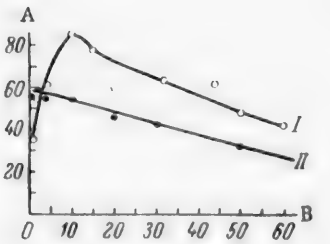

Fig. 5. Effect of the cathodic current density on the current efficiency. A) Current efficiency (in %); B) current density (in amp/sq dm).

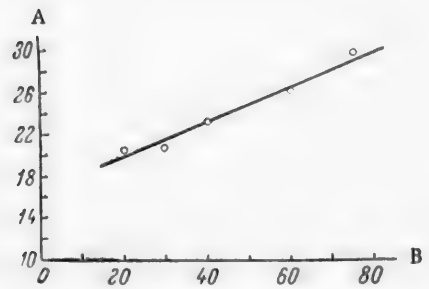

Fig. 6. Effect of electrolyte temperature on composition of deposit. A) Amount of W (in %); B) temperature (in °C).

As the graphs reveal, the amount of tungsten in the alloy increases slowly as the temperature is increased. The amount of W in the alloy increases by 0.6% for each 5° rise in the temperature.

Increasing the temperature of the electrolyte results in a substantial increase in the current efficiency. The efficiency increases by 2.5% for each 5° increase in the temperature. The quality of the deposit improves slightly (greater luster) with increase in the temperature. A temperature of 50° must be assumed to be the optimum.

The throwing power was determined from the weight increase of metal electrodeposited on cathodes located at different distances from the anode.

For comparison, we determined the throwing power of a nickel electrolyte with the composition (in g/liter): $NiSO_4 \cdot 7H_2O$ 165, H_3BO_3 30, $Na_2SO_4 \cdot 10H_2O$ 50, $MgSO_4 \cdot 7H_2O$ 20, NaCl – 20. The electrolyte for the deposition of the Co – W alloy contained (in g/liter): W 6 Co 6, $(NH_4)_2SO_4$ 300, NH_4OH (25%) 30.

The experimental data reveal that the throwing power of the electrolyte for the deposition of the Co – W alloy is substantially greater than the throwing power of the nickel electrolyte (30% instead of 17.5%).

When operating with a tungsten anode the dissolution goes uniformly with a current efficiency of 100%. The cathodic deposits were obtained even, smooth, and lustrous. The tungsten was electropolished to a mirror luster when dissolved.

The current density was raised to 65 amp/sq dm without any apparent passivation of the anode, and consequently the anodic surface can be 1/6 of the cathodic area when operating with tungsten anodes in production.

A low anodic current density (up to 0.3 amp/sq dm) must be used when operating with cobalt anodes, since otherwise the anodes become passivated and a black-brown deposit of cobalt hydroxide is formed on them, contaminating the electrolyte.

The use of an insoluble anode made from stainless steel gave negative results, since here the anode dissolved slowly.

Investigation of Mechanical Properties of Co – W Alloy

Internal Stresses in the Deposit. The earlier described method [5] was used to measure the internal stresses.

Measurement of the residual internal stresses revealed that they depend on the amount of tungsten in the deposit and decrease sharply with its increase to 35%, after which the decrease becomes less great (Fig. 8).

The internal stresses in deposits of Co – W alloy proved to be of the same sign and order of magnitude as the internal stresses in electrolytic deposits of chromium. The reason for the internal stretching stresses in the deposits of the alloy can be considered to be due to a reduction in the volume, occurring in the process of forming

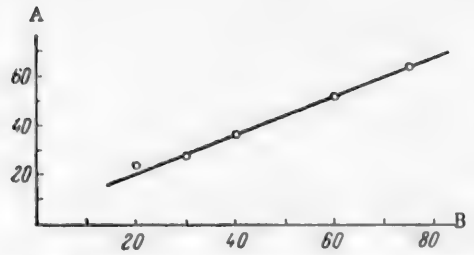

Fig. 7. Effect of temperature on the cathodic current efficiency. A) Current efficiency (in %); B) temperature (in °C).

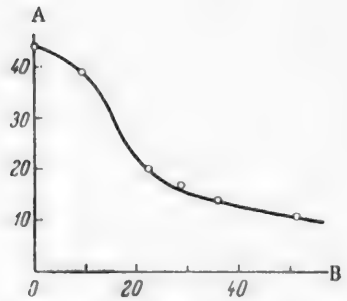

Fig. 8. Relation between internal stresses in the deposit and its composition. A) Internal stresses (in kg/sq mm); B) amount of W (in %).

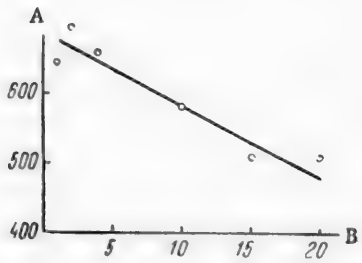

Fig. 9. Effect of cathodic current density on microhardness of deposit. A) Microhardness (in kg/sq mm); B) current density (in amp/sq dm).

the electrolytic deposit of the alloy and apparently associated with the formation of a solid solution.

Microhardness of Deposits of Co–W Alloy. A PMT-3 apparatus [6] was used to measure the microhardness. From an analysis of the obtained results it is clear that linear relationships exist between the hardness and the temperature, current density, and concentration of ammonium sulfate in the electrolyte.

The hardness is reduced by approximately 150 kg/sq mm when the current density is increased from 1 to 20 amp/sq dm (Fig. 9).

Measuring the hardness at a higher current density is difficult, since dull deposits are obtained, which require electropolishing. The hardness increases when the electrolysis temperature is increased (Fig. 10), which is apparently associated with a reduction in grain size.

Similar to the effect of raising the temperature, the hardness of the alloy deposit is affected but slightly when the ammonium sulfate concentration is increased (Fig. 11).

The deposits become duller, and consequently finely crystalline, when the $(NH_4)_2SO_4$ concentration is increased, and their hardness increases.

A highly interesting property of the electrolytic Co–W alloy is the great increase in its hardness after heat treatment (heat treatment for 1 hour at t = 600°). Metallurgically obtained Co–W alloy also shows an increase in hardness after heat treatment, but to a much smaller degree.

As can be seen from Fig. 12, the hardness of the alloy deposits is nearly doubled after heat treatment.

Testing for Abrasion Resistance. A special apparatus [4] with a reciprocating motion was used to run the abrasion resistance tests.

The rubber pair represented a firmly fixed stationary flat nickel plate and a brass disk, riding freely over the plate and coated with the alloy to a certain thickness (10 μ). Detachable weights were used to load the disk. The abrasion test was considered done when a stain of the base metal appeared, which stain was examined visually with a binocular lens, and also tested chemically by the usual procedure used to determine the porosity of galvanic coatings [4]. The abrasion resistance of the coating was estimated from the time of rubbing (in hours) required to show the bare metal.

To obtain comparative data, besides testing the main pair of metals, namely, (Co–W)–nickel, we also tested other pairs, for example: (Au–Cu)–nickel, white bronze–nickel, silver–nickel, and others. The tests were run with a constant load of 191.0 g/sq cm on the specimens.

The results of the tests are given in Table 1.

TABLE 1

Results of Abrasion Resistance Tests

Test pair		Number of hours to abrasion failure
Silver	Nickel	3.0
Gold–copper alloy: Au 60%, Cu 40%	Nickel	3.5
Gold–copper alloy: Au 85%, Cu 15%	Nickel	3.5
White bronze: Sn 40%, Cu 60%	Nickel	13.0
Cobalt–tungsten alloy: Co 65%, W 35%	Nickel	14.75
White bronze: Sn 40%, Cu 60%	White bronze: Sn 40%, Cu 60%	50 – 60
Cobalt–tungsten alloy: Co 65%, W 35%	Cobalt–tungsten alloy: Co 65%, W 35%	800 – 1000*

*The Co–W alloy was not heat treated.

TABLE 2

Results of Experiments on Chemical Resistance of the Alloy

Deposit	Weight loss (in mg/sq cm) per day		
	HNO_3	H_2SO_4	HCl
Ni	243	0.59	1.74
Co	1550	5.93	3.04
Co–W	110	0.165	1.68

Of the coatings tested, as may be judged from the data in Table 1, the greatest interest as regards abrasion resistance is possessed by the cobalt–tungsten alloy. When paired with nickel (based on the laboratory data), it proved to be 5 times as resistant as the silver–nickel pair.

Good results were also obtained for the pair in which the Co–W alloy was abraded on itself.

Testing the Chemical Resistance of the Electrolytic Co – W Alloy

The action of the acids H_2SO_4, HNO_3, and HCl, all taken at a 1 : 1 concentration, on the alloy containing 20% W, at 20°, was compared with the action of the same reagents on the electrodeposited metals, Ni and Co. The results of these experiments are given in Table 2.

From the data given in the table, it is obvious that the Co–W alloy, even with a low tungsten content, is much more acid resistant than either cobalt or nickel; in nitric acid it dissolves at a rate that is 2.2 times slower than that of nickel, and 14 times slower than that of cobalt; it is especially stable in sulfuric acid, and here its superiority is 3.6 times that of nickel, and 32 times that of cobalt.

Action of Some Aggressive Gases (NO_2 and SO_2). The alloy, deposited on a brass base, with a tungsten content of 35 and 45%, and a thickness of 5 and 10 μ, was tested in a desiccator containing conc. nitric acid.

The specimens were tested under different conditions: 8 hours at 60°, and 16 hours at 20°; the alloy containing 45% tungsten withstood 3 days of testing, and the alloy containing 35% tungsten lasted for 2 days.

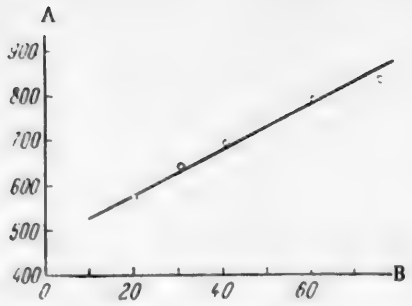

Fig. 10. Effect of electrolyte temperature on microhardness of deposit. A) Microhardness (in kg/sq mm); B) temperature (in °C).

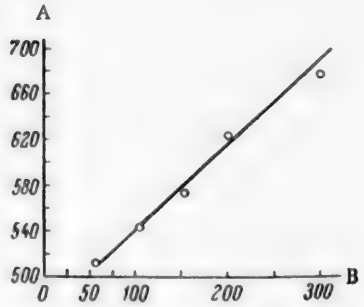

Fig. 11. Effect of $(NH_4)_2SO_4$ concentration on microhardness of deposit. A) Microhardness (in kg/sq mm); B) $(NH_4)_2SO_4$ concentration (in g/liter).

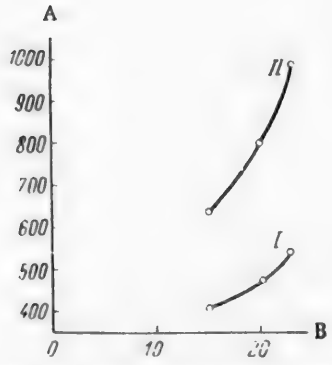

Fig. 12. Effect of heat treatment on microhardness of deposit. A). Microhardness (in kg/sq mm); B) amount of W (in %). Microhardness of deposit: I) before heat treatment; II) after heat treatment.

Alloys with a 35 and 45% tungsten content, and a thickness of 5 and 10 μ, deposited on a polished brass base, were also exposed to the action of sulfur dioxide (SO_2). The test conditions were: 8 hours at 60°, and 16 hours at 20°. Under these conditions all of the specimens lasted for 1 week without any visible changes, after which they darkened slightly.

The testing for porosity was done with an alloy containing 35% tungsten and having a thickness of 5 μ, deposited on a brass base.

Filter paper, moistened with a solution containing 20 g/liter of $K_3Fe(CN)_6$ and 20 g/liter of NaCl, was placed on the specimen and kept moist for 20 minutes. After repeated tests, in not a single instance did the reagent change color.

Testing of the Protective Ability and Corrosion Resistance of the Co–W Alloy. The testing was done by immersing the specimens in 3% sodium chloride solution at room temperature for 25 days. The alloys tested had a tungsten content of 25, 35, and 45%, and each composition was tested at a thickness of 5 and 10 μ (a total of 12 samples).

Within a day after immersion in sodium chloride solution, all of the samples became coated with a thin yellow film, which failed to change during the test period.

Of the three alloys tested, the alloy with a 35% tungsten content proved to be the best. It dissolved very slowly (0.1 g/sq m/day). The alloys containing 25% (0.178 g/sq m/day) and 45% tungsten (0.128/sq m/day) dissolved more rapidly.

If the standard scale is used in evaluating the corrosion resistance of the alloy, then under these conditions it is possible to consider the electrolytic Co–W alloy as belonging to the "completely stable" class.

SUMMARY

1. In working out the technology of depositing Co–W alloy, and based on an investigation of the effect of different factors on the composition of the deposit and the current efficiency, it was shown that the concentration ratio of the metals in the electrolyte exerts the greatest influence on the composition of the deposits; the amount of tungsten in the deposit increases as the W : Co ratio is increased, while the current efficiency decreases.

2. In investigating the dependence of the microhardness, internal stresses, and abrasion resistance of electrolytic coatings on various factors, it was shown that the hardness of Co–W coatings lies in the range of 500 to 700 kg/sq mm. Heat treatment for 1 hour at 600° nearly doubles the hardness of the Co–W deposits. The internal stresses decrease as the amount of tungsten in the coating increases.

The abrasion resistance of the pair (Co–W)–nickel is considerably greater than that of the pair silver–nickel. A high abrasion resistance was shown by the pair (Co–W)–(Co–W).

3. It was shown that the Co–W alloy is quite acid resistant, and stands up well in both a SO_2 and a NO_2 atmosphere.

4. The alloy containing 35% tungsten gave the best protection when testing was done in 3% NaCl solution.

5. The optimum electrolyte concentration and process conditions for the deposition of the alloy containing 35% W were established. Electrolyte (in g/liter): W 12, Co 4, $(NH_4)_2SO_4$ 250-300, NH_4OH (25%) 30-40, NaOH 10; D_k = 8-12 amp/sq dm; t = 50-60°; anodes–either platinum or tungsten.

LITERATURE CITED

[1] L. N. Gol'ts and V. N. Kharlamov, Soviet Author's Certificate, No. 46, 409.

[2] A. Brenner, P. Burkhead, and E. Seegmiller, J. Research Natl. Bur. Standards 39, 351 (1947).

[3] A. Brenner, P. Burkhead, and E. Seegmiller, Engineer 185, 209 (1948).

[4] N. P. Fedot'ev, P. M. Vyacheslavov, E. S. Kruglova, and G. P. Andreeva, Trudy Leningrad. Tekhnol. Inst. im. Lensoveta 53 (1959).

[5] L. A. Glikman, N. P. Fedot'ev, and P. L. Chernova, Zavodskaya Lab. No. 9 (1951).

[6] N. P. Fedot'ev and P. M. Vyacheslavov, Zavodskaya Lab. No. 7 (1952).

Received September 19, 1958

SOME PHYSICOCHEMICAL AND TECHNOLOGICAL PROPERTIES OF ELECTROLYTES FOR ELECTROCHEMICAL POLISHING OF STEEL

G. P. Maitak and G. S. Tret'yakova

Institute of General and Inorganic Chemistry of the Academy of Sciences of the Ukrainian SSR

In the previous paper [1] we described some new electrolytes for the electrochemical polishing of steel, composed of mixtures of sulfuric and phosphoric acids and containing the corrosion inhibitor "Unicol", proposed by Balezin, Barannik and Putilova [2] as an additive to etching solutions.

The results of investigating some of the physicochemical and technological properties of the mentioned electrolytes and the changes in these properties during electrolysis are described in this paper. The obtained results are compared with the results of similar investigations made using sulfuric-phosphoric-chromic acid electrolytes.

We determined the life span, density, viscosity, and electrical conductivity of the proposed electrolytes [1], the current efficiency in the anodic solution of steel in these electrolytes, and the change in the mentioned properties as the electrolyte was consumed. We also ran some experiments which enabled us to compare the throwing power of the proposed electrolytes with that of the sulfuric-phosphoric-chromic acid electrolytes.

All of the experiments described in this paper were run using anodes made of high-carbon steel ShKh-15 [3] and a mixed acid electrolyte with the following composition (in wt. %): H_3PO_4 35, H_2SO_4 50, and H_2O 15, and containing 2.5 volume % of Unicol MN-10, on the volume of the acid mixture, as inhibitor.

Anodic treatment of the steel was run at current densities of 1, 5, 10, 25, 50, 75 and 100 amp/sq dm. The earlier described [1, 3] apparatus and methods were employed in these experiments.

All of the tests were run in a freshly prepared, not agitated electrolyte, and after passing 75, 150, 250, 325, 400, 475, 550 and 600 amp-hr/liter through it during operation, i.e., at intervals of 75-100 amp-hr/liter, at a temperature of 18-25°, without a diaphragm, and without correcting the electrolyte composition.

According to Batashev [4], the life span of sulfuric-phosphoric-chromic acid electrolytes is 50-100 amp-hr/liter, and according to Popilov [5] it is 50-120 amp-hr/liter.

In the work of Fedot'ev, Kruglova, and Grilikhes [6, 7], when the sulfuric-phosphoric-chromic acid electrolyte was used in electropolishing, without separation of the cathodic and anodic areas by a diaphragm, and without correcting the composition, it ceased to function after the passage of 117 amp-hr/liter.

High-carbon steel ShKh-15 was electropolished in our investigated electrolyte, containing inhibitor Unicol MN-10 and having the above indicated composition, at anodic current densities of 75 and 100 amp/sq dm, both in freshly prepared electrolyte and after 75, 150, 250, and 325 amp-hr/liter had been passed through it during operation. The polishing power of the electrolyte decreased after the passage of 400 amp-hr/liter, and the surface became ribbed. Practically the same type of surface was also obtained in this electrolyte after longer operation, and specifically, after the passage of 475, 550, and 600 amp-hr/liter of current. After the passage of 600 amp-hr/liter, the electrolyte separated from the deposit and its composition was enriched. This correction led to restoring the polishing power of the electrolyte. As a result, when operation is without correction, the life of the electrolytes proposed by us is considerably longer than the life of sulfuric-phosphoric-chromic acid electrolytes, while a simple correction increases this life span.

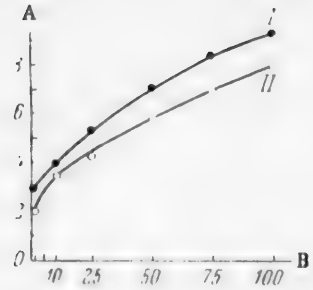

Fig. 1. Relation between the value of the voltage between the electrodes and the current density. A) Voltage between the electrodes (in v); B) anodic current density (in amp/sq dm). I) Freshly prepared electrolyte; II) the same electrolyte after the passage of 600 amp-hr/liter of current.

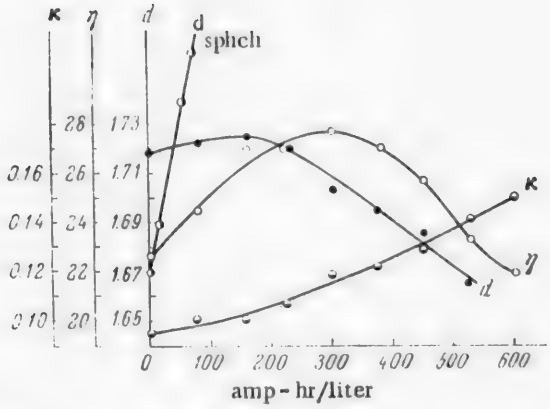

Fig. 2. Dependence of the density, viscosity and electroconductivity of investigated electrolyte for the electrochemical polishing of steel on the amount of electricity (in amp-hr/liter) passed through it in the electropolishing of high-carbon steel. d) Density (in g/cc); η) viscosity (in centipoises); κ) electroconductivity (in Ω^{-1} cm^{-1}); d_{sphch}) density of sulfuric-phosphoric-chromic acid electrolyte according to Batashev's data [4].

Some reduction in the current densities under which electropolishing occurs was observed as the electrolyte operated, but this reduction was considerably smaller than in sulfuric-phosphoric-chromic acid electrolytes [4]. The voltage values at the bath terminals, observed under the conditions of these experiments, are shown in Fig. 1. The voltages at the bath terminals are somewhat smaller in the operating electrolyte than in the freshly prepared electrolyte under the same conditions.

The density, viscosity and electroconductivity of the electrolyte were measured at 25° using conventional techniques. The results of these measurements are plotted in Fig. 2.

The density, viscosity and electroconductivity of the electrolytes proposed by us have values that lie close to their values for sulfuric-phosphoric-chromic acid electrolytes. This follows from their composition and can be seen from the comparison given below of the values of the density (d), viscosity (η) and electroconductivity (κ) of freshly prepared electrolytes, the one investigated by us, and the sulfuric-phosphoric-chromic acid electrolyte (based on Batashev's data [4]).

However, the direction of change in the density, viscosity, and electroconductivity of the proposed electrolytes and the sulfuric-phosphoric-chromic acid electrolytes during operation is different. This is due to the fact that in sulfuric-phosphoric-chromic acid electrolytes the electropolishing is conducted at high temperature, where the water evaporates, whereas in the electrolytes proposed by us the electropolishing is performed at room temperature, where the water vapors can be absorbed.

Both the density and the viscosity of sulfuric-phosphoric-chromic acid electrolytes increase in measure with their operation, while the electroconductivity decreases, which is explained by the evaporation of water and the binding of the sulfuric acid by the metals dissolving at the anode [4].

When operating with the electrolytes proposed by us, both the density and the viscosity increase at first, and then they decrease, while the electroconductivity increases in a monotonic manner (Fig. 2). This is apparently due to the following reasons. When operating with the electrolytes proposed by us there occurs moisture absorption, the accumulation of iron salts, and the salts of the other metals present in the steel, in the electrolyte, and the deposition of these salts in the precipitate when the solubility limit is reached. Only the first two factors, the absorption of moisture and the accumulation of salts, appear at the start. They operate in opposite directions. Under the conditions of our experiments the second factor, the accumulation of salts, suppressed the first factor at the start, as a result of

	d (g/cc)	η (centipoises)	κ ($\Omega^{-1} \cdot cm^{-1}$)
Electrolyte with inhibitor, investigated in the present paper (at 25°)	1.72	22.6	0.0945
Sulfuric-phosphoric-chromic acid electrolyte, investigated by Batashev [4] (at 20°)	1.67	20.0	0.0952

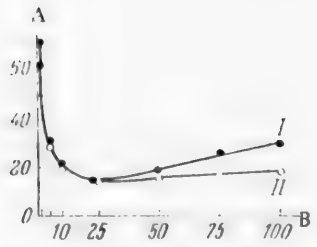

Fig. 3. Change in the current efficiency during the anodic solution of high-carbon steel (ShKh-15) in electrolyte for electrochemical polishing as a function of the current density. A) Current efficiency (in %); B) anodic current density (in amp/sq dm). I) Freshly prepared electrolyte; II) the same electrolyte after the passage of 600 amp-hr/liter of current.

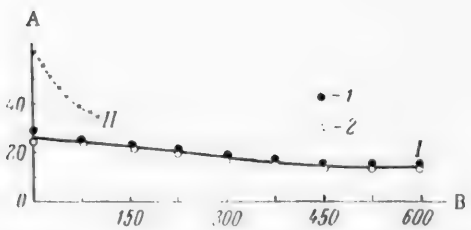

Fig. 4. Dependence of the current efficiency in the electrochemical polishing of high-carbon steel on the amount of electricity passed through the electrolyte. A) Current efficiency (in %); B) amount of electricity (in amp-hr/liter) passed through the electrolyte during operation. I) Electrolyte containing inhibitor, investigated in the present study, with extrapolation at an anodic current density (in amp/sq dm): 1) 75, and 2) 100; II) sulfuric-phosphoric-chromic acid electrolyte, based on Batashev's data [4].

which both the density and the viscosity increased in this portion of the plot (Fig. 1). However, due to the opposite effect of the first factor, namely, moisture absorption, both the density and the viscosity showed slight increase here when compared (Fig. 2) with the increase observed [4] when operating with the sulfuric-phosphoric-chromic acid electrolyte, where both of the factors determining the initial change, namely water evaporation and accumulation of salts, operate in the same direction. As soon as a precipitate begins to separate, the concentration of the metal ions in the electrolyte will also change as a result of a change in the solubility of the salts formed with continued change in the composition of the electrolyte, but at a slower rate. After this the solution also becomes diluted as the result of the effect of the third mentioned factor, namely, the deposition of acids in the precipitate as salts of the metals of the dissolved anode. As a result, the shape of the density and viscosity curves shown in Fig. 2 is apparently determined by the action of three factors: accumulation of metal ions in the electrolyte, moisture absorption, and the deposition of acids in the precipitate as the salts of the metals dissolving at the anode. Of these factors, the first causes the curves to rise, while the other two act in opposite directions. During electrolyte operation the first factor predominated at the start, and then the last two factors took over. For this reason the indicated curves pass through a maximum.

The electroconductivity of sulfuric-phosphoric-chromic acid electrolytes decreases sharply during operation [4, 6-8]. The electroconductivity of the electrolytes proposed by us increases during operation (Fig. 2) because of dilution due to moisture absorption and the deposition of acids in the precipitate of the metals dissolving at the anode. At the start, while the viscosity of the electrolyte is increasing during operation, the electroconductivity of the electrolyte increases but slightly in measure with its operation; when the viscosity begins to fall, the electroconductivity rises more rapidly.

In the experiments made to determine the current efficiency, or the coefficient of current consumption for the anodic solution of the metal, all of the conditions of anodic treatment of the steel were the same as in our earlier investigations [1, 3] and when determining the service life of the electrolyte, as described above.

The length of anodic treatment in each experiment was 10 minutes. The electrolyte was not agitated. Temperature 25°. The calculations were made in the same manner as in [4, 9], taking the electrochemical equivalents (in g/amp-hr): copper (in a coulometer) 1.186, and iron 1.042. The results of these experiments are plotted in Figs. 3 and 4.

The current efficiency drops sharply when the current density is increased (Fig. 3) in the region of relatively small values (1-10 amp/sq dm), it decreases slowly when the current density is increased in the region of somewhat higher values (10-25 amp/sq dm), and it increases in the region of higher values (25-100 amp/sq dm). Both passivation of the anode and the fraction of the current consumed for the anodic liberation of oxygen increase with increase in the current density, but the factors operating in the opposite direction, namely, destruction of the passive film by the direct action of the liberated oxygen gas, local hot spots, and the feeding caused by them of fresh electrolyte into the preanode layer, also increase at the higher current densities. For this reason, the current efficiency in an exhausted electrolyte operating for a long time is lower than in a freshly prepared electrolyte at the higher current densities. Curve 2 in Fig. 3, corresponding to the electrolyte that had operated for a long time, rises more slowly at the higher current densities than does curve 1, corresponding to the freshly prepared electrolyte, while the similar curve for the sulfuric-phosphoric-chromic acid electrolyte [4, 9], operating at a high temperature, does not rise, but instead has a minimum at the same current densities.

From Fig. 4 it can be seen that in measure with electrolyte operation the current efficiency at current densities of 75 and 100 amp/sq dm, at which steel is electropolished, decreases slightly and is practically linear. In the sulfuric-phosphoric-chromic acid electrolyte the current efficiency is higher [4, 9], and, in measure with its operation [4], the current efficiency shows a sharper decrease. The lower solubility of steel in the electrolytes proposed by us is apparently due to the fact that our electrolytes operate at a lower temperature, and besides this, the inhibitor exerts a protective action here.

To compare the throwing power of the electrolytes, we controlled the removal of the metal along the length of the anode, which was prepared from high-carbon steel rod and installed in the electrolyte perpendicular to the cathode surface.

The position of the anode was fixed by the other end of the rod, bent at a right angle to its operating portion and fastened in a vertical direction using a holder. The surface of the vertical portion of the rod, found in the electrolyte, was coated with Japan lacquer. The removal of metal was controlled by exact measurement of the rod diameter, which was equal to 3.5 mm. These experiments were run in the electrolyte containing inhibitor (at 25°), the composition of which was given above, and also in the sulfuric-phosphoric-chromic acid electrolyte (at 80 °C), containing (in wt. %): H_3PO_4 65, H_2SO_4 15, CrO_3 6, and H_2O 14, with the anodic current density kept constant at 75 amp/sq dm in both cases. The electrolytes were not agitated. The apparatus and all the other conditions of running the electrolysis in these experiments were the same as in the anodic electrochemical polishing experiments described above.

The experiments performed by us revealed that the electrolyte with inhibitor and the sulfuric-phosphoric-chromic acid electrolyte exhibit practically the same dispersing power.

SUMMARY

1. The service life of the investigated electrolyte, containing an inhibitor, in the electropolishing of high-carbon steel is considerably longer than that of the sulfuric-phosphoric-chromic acid electrolyte.

2. The density, viscosity, and electroconductivity of the freshly prepared electrolyte, containing inhibitor, are practically the same as those of the sulfuric-phosphoric-chromic acid electrolyte, but during operation they change less sharply and in a different manner: the density and viscosity increase at the start and then decrease, while the electroconductivity increases monotonically.

3. With increase in the current density, the current efficiency drops sharply at the start and then at a slower rate, while in going to higher current densities it shows some increase. The current efficiency drops as the electrolyte operates, but at a much slower rate than in the case of the sulfuric-phosphoric-chromic acid electrolyte.

LITERATURE CITED

[1] G. P. Maitak and G. S. Tret'yakova, Zhur. Priklad. Khim. 32, No. 5, 1060 (1959).*

[2] S. A. Balezin, V. P. Barannik, and I. N. Putilova, Utilization of Acid-Corrosion Inhibitors [in Russian]. Goskhimizdat, Moscow–Leningrad, 1948.

[3] G. P. Maitak, Ukrain. Khim. Zhur. 25, 385 (1959).

[4] K. P. Batashev, Trudy Leningrad. Polytekhn. Inst. 6, 121 (1953).

[5] L. Ya. Popilov, Technology of the Electropolishing of Metals [in Russian]. Mashgiz, Moscow–Leningrad, 1953, p. 120.

[6] N. P. Fedot'ev, E. G. Kruglova, and S. Ya. Grilikhes, Zhur. Priklad. Khim. 27, 157 (1954). *

[7] N. P. Fedot'ev and S. Ya. Grilikhes, Electrochemical Etching, Polishing and Oxidation of Metals [in Russian]. Mashgiz, Moscow–Leningrad, 1957, p. 75.

[8] L. Ya. Bogorad, S. Ya. Grilikhes, and R. S. Arson, Electrochemical Polishing of Steel [in Russian]. Leningrad Press, 1951, p. 46.

[9] K. A. Nesmeyanova, Monograph: Corrosion, Corrosion Protection, and Electrolysis [in Russian]. Mashgiz, Moscow, 1948, p. 139.

Received October 6, 1958

* Original Russian pagination. See C. B. translation.

FIRED AIR-DEPOLARIZATION ELECTRODES

N. I. Galkina, G. M. Popova, D. L. Kondrashov

and R. Kh. Burshtein

Institute of Electrochemistry of the Academy of Sciences of the USSR

Operation of the carbon air-depolarization electrode, used in the production of chemical sources of current, is accomplished through atmospheric oxygen, which, diffusing through the pores of the electrode, is reduced on its surface with the formation of hydrogen peroxide. The thus formed hydrogen peroxide then suffers catalytic decomposition on the carbon surface with the formation of water and oxygen [1].

As is known, the principal fault of the air-depolarization electrode is its wetting, since this prevents diffusion of the oxygen into the pores and leads to an impairment of the electrochemical characteristics of the carbon electrode. Wetting is also a function of the potential, and increases on either side of the point of zero charge on the carbon surface. Consequently, this phenomenon is determined by a change in the wetting of the surface when its charge is changed [1]. It was shown recently that the operation of the carbon air-depolarization electrode and its wetting depend essentially on its structure [2]. Based on the data obtained in investigating carbon electrodes prepared using binders it follows that reducing the pore radius leads to a decrease in the wetting of the electrode and an improvement in its electrochemical characteristics. This is due to the fact that in order for an electrolyte to penetrate into the pores of a hydrophobic electrode it is necessary to overcome the pressure, which is related to the pore radius by the equation

$$P = \frac{-2\sigma \cos\theta}{r},$$

where σ is the surface tension, r is the pore radius, and θ is the angle of contact between the carbon and the electrolyte.

The practicality of using fired air-depolarization electrodes prepared from activated charcoal was shown by Burshtein and Veselovskaya [1]. The binders in such electrodes are converted to activated carbon during activation, which makes it easier for the oxygen to reach the carbon surface when compared with the electrodes prepared using the binders proposed by either Spiridonov or Daniel-Bek [3, 4]. In addition, the electroconductivity of fired electrodes is greater than that of electrodes that contain binders. The indicated properties of fired electrodes should exert a favorable influence on the electrochemical characteristics of air-depolarization electrodes.

Another advantage of fired electrodes that should be mentioned is their greater mechanical strength. This type of electrodes should also be cheaper, since the use of organic solvents is not required in their preparation.

The purpose of the present study was to work out a method for the preparation of fired air-depolarization electrodes of known structure and to determine the effect of structure on the electrochemical properties of the fired air-depolarization electrode.

In order to select a rational technology for the preparation of fine-pored carbon electrodes we measured the pore distribution according to radius in several types of commercial electrocarbons. The mercury pressuring method [5] was used to measure the pore distribution according to size, using the apparatus described in a previous paper [2].

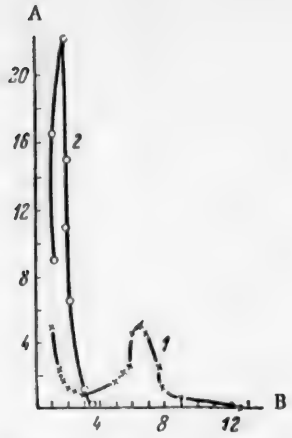

Fig. 1. Pore distribution according to radius. A) Value of $D(r) \times 10^5$; B) value of $r \times 10^{-3}$ A. 1) Spectral carbon; 2) 8/60 carbon.

As an example, the relations between the pore distribution and the radius for 8/60 carbons and spectral carbon are shown in Fig. 1. These experiments revealed that the 8/60 carbons possess a homogeneous and fine-pored structure, whereas the other carbons, for example, the spectral, have, besides narrow pores, a large amount of wide pores. For this reason it seemed expedient to utilize the technology of fabricating 8/60 carbons in the preparation of air-depolarization electrodes.

It is impossible to use 8/60 carbons directly in air-depolarization elements, since their electrochemical activity is extremely slight. The main reason for the low activity is the high burning temperature used, namely 1250°. In order to increase the activity of the carbons we ran the burning at 900°.

After burning, the carbons were activated in a carbon dioxide atmosphere at 900-950°. In the activation of these carbons, those for which the burning did not exceed 7% proved to have adequate mechanical strength. With the burning equal to 7%, it was possible to discharge a current of 5 ma/sq cm from the electrode at a potential of 1.2 v, relative to the zinc electrode.

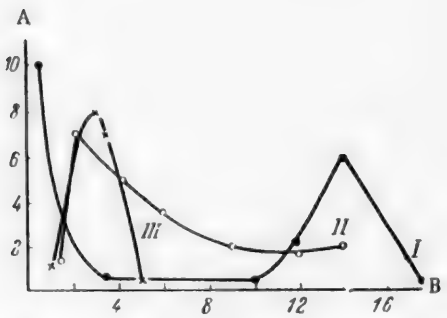

Fig. 2. Pore distribution in the electrodes according to radius. A) Value of $D(r) \times 10^5$; B) value of $r \times 10^{-3}$ A. I) BAC 100% + oil pitch; II) BAC 50% + soot 50% + coal tar; III) BAC 50% + lamp black 50% + coal tar.

It could be expected that the addition of activated charcoal, which has a true surface of 900-1000 sq m/g, will increase the activity of air-depolarization electrodes. Reasoning in this manner, we prepared three types of air-depolarization electrodes, each type composed of 50% birch activated charcoal (BAC), 50% soot, and binder. To reduce the amount of wide pores the carbon mass was subjected to repeated milling, and then electrodes were pressed from this mass at a pressure of 1000 kg/sq cm. The electrodes were burned and activated as described above. The percent of carbon burning was determined after activation. The degree of burning, as understood in the production of activated carbons, is a measure of their adsorption activity. After activation, the electrodes were paraffinized by dipping in a 2% solution of paraffin in gasoline. The pore distribution in these electrodes according to radius is shown in Fig. 2. From the obtained data it can be seen that besides having fine pores the specimens of types I and II have quite a large number of wide pores ranging in size from 18,000 to 5000 A, which makes the specimens from these materials less suitable for the preparation of air-depolarization electrodes. As can be seen from Fig. 2, pores with a radius exceeding 5000 A are absent in the type III electrodes, and here the maximum on the distribution curve lies at 3000 A.

In order to determine the effect of the binder on the structural and electrochemical characteristics of the electrodes, we prepared electrodes that contained either molasses, pitch or tar.

The curves for pore distribution according to radius for electrodes containing different binders are shown in Fig. 3. From the obtained data it can be seen that the electrodes prepared on a molasses base have a larger number of fine pores than the other types of electrodes. However, the type III electrodes differ but slightly in their structure from the electrodes prepared on a molasses base.

The dependence of the pore-radius distribution on the percent of burning was investigated for the type IV electrodes. Together with a large number of pores having a radius smaller than 3×10^3 A, the unactivated electrode also has a small amount of wider pores ranging in size from 5×10^3 to 8×10^3 A.

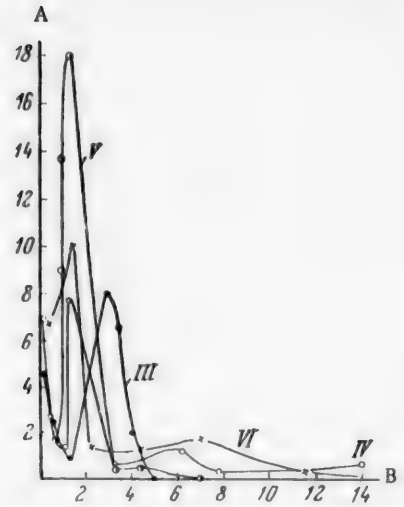

Fig. 3. Pore distribution according to radius for carbons prepared using different binders. A) Value of $D(r) \times 10^5$; B) value of $r \times 10^{-3}$ A. III) BAC 50% + lamp black 50% + coal tar; IV) BAC 50% + lamp black 50% + coal-oil pitch; V) BAC 50% + lamp black 50% + technical molasses; VI) BAC 50% + lamp black 50% + + coal-tar pitch.

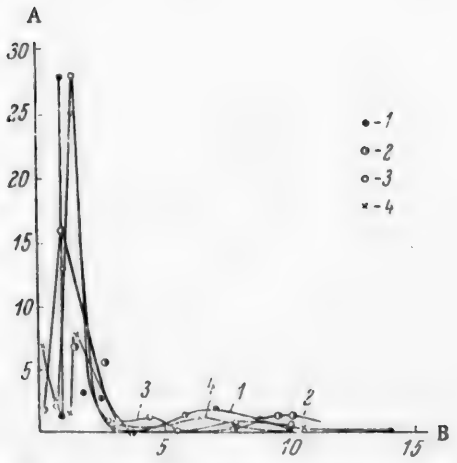

Fig. 4. Pore distribution according to radius in the type IV electrode as a function of the percent of burning. A) Value of $D(r) \times 10^5$; B) value of $r \times 10^{-3}$ A. Burning (in %): 1) 30; 2) 20; 3) 5; 4) unactivated.

As can be seen from the obtained data, activation of the electrodes causes the radius of the wider pores to increase slightly up to 12×10^3 A, while the radius of the narrow pores remains unchanged. Simultaneously with increase in activation, a more than 3-fold increase in the number of pores with radii ranging from 1.0×10^3 to 2.5×10^3 is observed. The results of these experiments are plotted in Fig. 4.

We also investigated the effect of the degree of burning of electrodes, prepared using different binders, on the electrochemical properties of air-depolarization electrodes.

The electrochemical studies were conducted in such manner that one side of the electrode was found in contact with the electrolyte, while the other side was exposed to the air. The electrode was polarized using an outside current source. The measure of electrochemical activity in our experiments was that current density at which the potential of the carbon electrode was equal to 1.2 v relative to the zinc electrode, which corresponds to a shift of 200 mv in the potential of the carbon electrode.

The results of these experiments are plotted in Fig. 5. From these data it follows that increasing the degree of burning in the activation of air-depolarization electrodes leads to an increase in their electrochemical activity. From Fig. 5 it can be seen that a linear relationship between the oxygen reduction rate at a carbon electrode and the activity of the latter is observed clear up to a carbon burning of 30%. From Fig. 5 it also follows that, at the same degree of activity, the greatest electrochemical activity is possessed by the electrodes with the finest pore structure.

The results obtained in investigating the relation between the potential and the current density are plotted in Figs. 6 and 7. From these data it can be seen that a linear relationship between the voltage and log i is observed up to current densities of 4.5×10^{-3} amp/sq cm. The slope of the linear portion of the curve corresponds to 0.062 v.

When the electrode were tested for length of operation at a potential of 1.2 v relative to the zinc electrode it was established that, with the same percent of burning, the electrodes with the smaller pores (types III and V) operate longer and have a greater specific capacity. Some of the results, obtained when the electrodes were allowed to operate for 240 hours, are plotted in Fig. 8.

A series of electrodes of the III and IV type were prepared for testing in iron–carbon elements. The testing was done with 4 elements composed of carbon

TABLE 1

Testing of Iron–Carbon Elements

Element No.	Discharge conditions	Final voltage (in v)	EMF	Initial voltage (in v)	Capacity (in amp hr)	Average temp. (in °C)
11	Continuous, 2.5 Ω	0.53	0.96	0.80	44.20	
17	Intermittent (for 6 hours per day)	0.63	0.97	0.82	45.00	
36		0.50	0.99	0.82	122	22
61		0.60	0.99	0.77	77	

TABLE 2

Potential of Carbon and Iron Electrodes

Element No.	Voltage of air-depolarization--Fe-50 element (in v)	Potential of carbon electrode relative to the zinc electrode (in v)	Potential of iron electrode relative to the zinc electrode (in v)
After 60 hours of discharge at a resistance of 2.5 Ω for 6 hours a day			
17	0.73	1.18	0.46
36	0.74	1.20	0.46
61	0.74	1.17	0.44
After 108 hours of discharge at a resistance of 2.5 Ω for 6 hours a day			
17	0.62	1.20	0.58
36	0.70	1.18	0.48
61	0.73	1.17	0.45

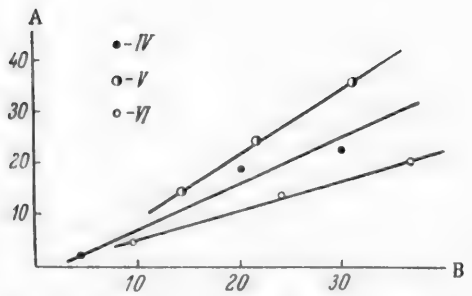

Fig. 5. Relation between the current density and the percent burning for different types of electrodes. A) Current density (ma/sq cm); B) burning (in %). IV) BAC 50% + lamp black 50% + coal-oil pitch; V) BAC 50% + lamp black 50% + technical molasses; VI) BAC 50% + + lamp black 50% + coal-tar pitch.

electrodes of the IV type and iron electrodes made of Suli porous iron. The test results are given in Table 1 and plotted in Fig. 9.

From the test results it follows that the element, discharging continuously, delivered 45 amp-hr, while with intermittent discharge the elements delivered from 45 to 120 amp-hr. The potentials of the carbon and iron electrodes relative to the zinc electrode were measured during the time of the intermittent discharge of the elements.

The results of these measurements are given in Table 2.

From these data it can be seen that the potential of the carbon electrode hardly changed after 108 hours of operation, whereas the potential of the iron electrode showed substantial shift to the positive side in this length of time. As a result, the capacities of elements No. 17 and No. 11 were apparently limited by the poor operation of the negative electrode. The carbon air-depolarization electrodes can operate for several cycles in in air-depolarization–iron elements.

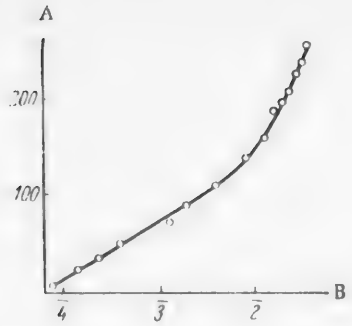

Fig. 6. Relation between the potential and the logarithm of the current density for type IV electrode. A) Potential (in mv); B) value of log i.

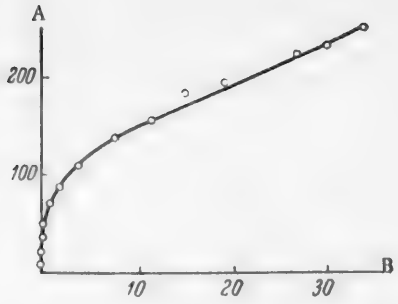

Fig. 7. Relation between the potential and the current density for type IV electrode. A) Potential (in mv); B) current density (in ma/sq cm).

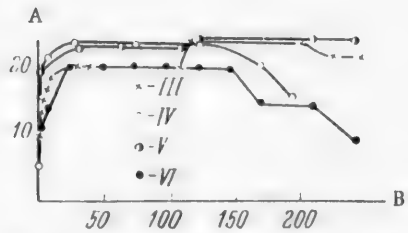

Fig. 8. Change in the specific capacity with time for different carbons. A) Current density (in ma/sq cm); B) time (in hr). III) BAC 50% + lamp black 50% + coal tar; IV) BAC 50% + lamp black 50% + coal-oil pitch; V) BAC 50% + + lamp black 50% + technical molasses; VI) BAC 50% + lamp balck 50% + coal-tar pitch.

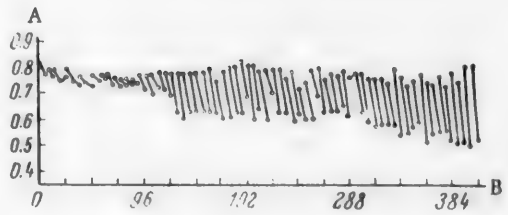

Fig. 9. Intermittent discharge of air-depolarization—Fe-50 element at a resistance of 2.5 Ω. A) Potential (in v); B) time (in hr.).

Preliminary testing of individual electrodes from an experimental batch, preparing using the type III technique, revealed that at a load of 1 amp the potential of carbon electrodes whose degree of burning exceeds 10% is equal to 1.16 v, which corresponds to a current density of 20 ma/sq cm.

From the obtained results it follows that fired carbon electrodes, having a fine-pored structure and containing activated carbon, are suitable for use in air-depolarization elements.

LITERATURE CITED

[1] R. Kh. Burshtein and I. E. Veselovskaya, Collection of Papers on Alkaline Elements for Air Depolarization [in Russian] Gosenergoizdat, 1947, p. 57.

[2] R. Kh. Burshtein and D. L. Kondrashov, Zhur. Priklad. Khim. 29, No. 9, 1691 (1956).*

[3] P. M. Spiridonov, Collection of Papers on Alkaline Elements for Air Depolarization [in Russian]. Gosenergoizdat, 1947, p. 5.

[4] V. G. Sochevanov, Galvanic Elements [in Russian]. Gosenergoizdat, 1951.

[5] H. L. Ritter and L. C. Drake, Ind. Eng. Chem., Anal. Ed. 17, 782, 787 (1945).

Received July 18, 1958

* Original Russian pagination. See C. B. translation.

PERMEABILITY OF CERTAIN ORGANIC POLYMER FILMS TO ATMOSPHERIC MOISTURE*

A. A. Berlin and K. P. Lesina

The use of certain organic polymer films as moisture-proof packaging material and protective coatings served as the reason for making a general study of the problem of film permeability [1, 2].

According to the modern concepts of the structure of high-molecular compounds the mechanism for the diffusion of vapor and gases through a polymer film is depicted as being a movement of the vapor or gas particles through temporary pores, that arise and disappear again due to chain flexibility [2, 3].

In this connection the movement rate of the vapor particles through the film depends on many factors, and specifically, on the size of the temporary pores and the dimensions of the migrating particles, on the solubility of the latter in the polymer, and also on the mobility of the polymer chains and the density of their packing.

The problem in the present study reduced to investigating the effect of a number of chemical and technological factors (chemical nature of the polymers, thickness and complexity of the film, nature of the plasticizer, etc.) on the permeability of certain organic polymer films to water vapor.

The method adopted to test the moisture penetration consisted in determining, by absorption in an adsorbent, the amount of moisture that had passed through a unit area of the film, placed in an atmosphere of 100% relative humidity at 18-20° for 24 hours [2]. As a result, the amount of moisture penetration was expressed in mg/sq cm per 24 hours. The comparative moisture resistance of a number of organic polymer films is shown in Table 1, from which it can be seen that of the tested specimens the films prepared from chlorinated poly(vinyl chloride) and the copolymer of vinylidene chloride (100 g) with vinyl chloride (VCC-40) show the least moisture penetration.

Apparently, the small tendency to absorb moisture and the high packing density of the macromolecules function to reduce the vapor permeability of these chlorine-containing polymers.

As regards poly(vinyl butyral), triacetylcellulose, and poly(methyl methacrylate), they all possess branched chains, which create substantial steric hindrance to the formation of a densely packed structure. In addition, the first of the mentioned polymers always contains a certain amount of free hydroxyl groups, tending to increase moisture sorption by the material.

The effect of film thickness on moisture penetration was determined for the films prepared from poly(methyl methacrylate) (PMM), Perchlorovinyl, and Copolymer VCC-40.

The curves in the figure show that in the case of materials with a relatively high moisture permeability (PMM), changing the film thickness exerts a strong influence on this property.

Decreasing the moisture permeability of a material reduces the dependence of moisture penetration on the film thickness to such an extent that for such polymers as VCC-40 it is possible to practically neglect this dependence in the interval of film thicknesses investigated by us ($\delta = 60-200\ \mu$) (see figure).

*Communication 13 in a series of investigations relating to the chemistry and technology of polymers.

TABLE 1

Moisture Permeability of Organic Polymer Films

Polymer	Film thickness (in μ)	Moisture penetration in 24 hr (in mg/sq cm)
Poly(vinyl butyral)	50–60	3.8–4.4
Poly(methyl methacrylate)	70–80	2.5
Triacetylcellulose	70–80	1.7–2.3
Poly(vinyl chloride)	70–300	0.7–1.0
Chlorinated poly(vinyl chloride) (Perchlorovinyl)	70–80	0.5–0.7
Copolymer of vinyl chloride with vinylidene chloride (Copolymer 40)	60–100	0.1–0.3

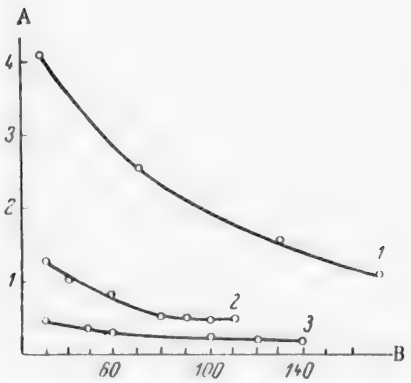

Effect of film thickness on moisture penetration. A) Moisture penetration in 24 hours (in mg/sq cm); B) film thickness (in μ). 1) Poly(methyl methacrylate); 2) Perchlorovinyl; 3) vinylidene chloride–vinyl chloride copolymer (VCC-40).

In the technology of preparing protective coatings it is recommended that a multilayer deposition of the lacquer solution be made, so that the defects of one film layer (open pores, graining, air bubbles, etc.) can be smoothed out by the deposition of the next layer.

In order to obtain an accurate idea as to the effect of layering on the moisture permeability of film materials we tested both one-layer and three-layer films, prepared from PMM, Perchlorovinyl, and VCC-40.

The results of these experiments, summarized in Table 2, reveal that when films are prepared by the method of casting from a lacquer solution, increasing the number of layers in the film does not reduce its moisture penetration. Increasing the flexibility of the plasticized polymer macromolecules can lead to an increase in the moisture penetration if solvation of the macromolecules by the plasticizer [3] does not reduce the ability of the material to sorb moisture. In connection with this the question arises as to the effect exerted by the chemical nature of the plasticizer on the moisture permeability of polymer films.

The data in Table 3 reveal that the 20% addition of the plasticizers tributyl phosphate, butyl stearate, and dibutyl phthalate impairs the moisture resistance of the Perchlorovinyl films, whereas the addition of the plasticizers dioctyl phthalate and ethyl acetoricinoleate permits obtaining materials with a very low permeability to atmospheric moisture.

Increasing the butyl stearate content from 20 to 40% raises the moisture permeability of Perchlorovinyl from 1.01 to 2.3%. Increasing the amount of such hydrophobic plasticizers as dioctyl phthalate and chlorinated paraffin from 20 to 60% not only fails to impair, but even improves somewhat the moisture resistance of Perchlorovinyl films (Table 4).

In the system polymer–plasticizer, the latter, filling the spaces between the polymer chains, affects the permeability value of the system in other ways besides weakening the intermolecular bonds and increasing the flexibility of the chains.

A plasticizer creates an additional medium in the system as a path for the migrating vapor or gas particles. Depending on the chemical natures of the plasticizer and diffusing particles, the rate of movement of the latter

TABLE 2

Effect of Number of Film Layers on Their Moisture Penetration

Polymer	Characteristics of film	Film thickness (in μ)	Moisture penetration in 24 hr (in mg/ sq cm)
Poly(methyl methacrylate) (plasticized)	One-layer	130—145	2.03
	Three-layer	160—180	2.05
Perchlorovinyl (plasticized)	One-layer	105—130	0.49
	Three-layer	90—135	0.51
Vinyl chloride-vinylene chloride copolymer (Copolymer 40) (unplasticized)	One-layer	70—90	0.23
	Two-layer	70—85	0.23

TABLE 3

Effect of Chemical Nature of Plasticizer on Mechanical Properties and Moisture Permeability of Perchlorovinyl Films. Plasticizer Content of Film = 20%

Plasticizer	Tensile strength (in kg/ sq mm)	Elongation at break (in %)	Moisture penetration in 24 hr (in mg/ sq cm)
Without plasticizer	4.1	5.4	0.6—0.7
Caster oil	3.7	9.2	0.65
Dibutyl phthalate	3.3	9.0	0.74
Ethyl acetoricinoleate	3.2	21.0	0.42
Tributyl phosphate	2.9	18	1.7
Dioctyl phthalate	2.3	95.0	0.41
Butyl stearate	2.1	26	1.01

TABLE 4

Dependence of the Strength and Elongation of Perchlorovinyl Films on the Amount of Added Dioctyl Phthalate

Amount of dibutyl phthalate (in %)	Tensile strength (in kg/sq mm) after air exposure at t = 20°		Elongation (in %) after air exposure at t = 20°	
	10 days	4 months	10 days	4 months
10	3.5	4.8	10.8	4.0
20	2.4	4.0	98.0	4.8
30	2.2	3.2	184.0	41.0
40	1.7	2.0	208.0	206.0

TABLE 5

Effect of Chemical Nature of Plasticizer on Moisture Permeability of Perchlorovinyl Film

Plasticizer	Amount of plasticizer (in %)	Film thickness (in μ)	Moisture penetration in 24 hr (in mg/sq cm)
Without plasticizer	0	60—70	0.6—0.7
Chlorinated paraffin	40	70—75	0.68
	60	75—77	0.41
Butyl stearate	10	60—80	0.78
	20	80—90	1.90
	40	80—90	2.29
Dioctyl phthalate	5	80—90	0.48
	10	80—90	0.74
	20	90—100	0.44
	30	80—90	0.43
	40	80—100	0.47

TABLE 6

Effect of Mechanical Orientation of Film on Its Properties

Polymer	Film characteristics	Tensile strength (in kg/sq cm)	Elongation (in %)	Bending 180° at temperature	
				−30°	−45°
Perchlorovinyl (unplasticized)	Ordinary	4.7	4.9	(+)	(−)
	Stretched at t = 130°	6.1	6.3	(+)	(+)
Perchlorovinyl, plasticized with dioctyl phthalate	Ordinary	1.8	202	(+)	(−)
	Stretched at t = 123°	2.0	215	(+)	(+)
Vinyl chloride—vinylidene chloride copolymer (VCC-40)	Ordinary	1.3	205	(−)	(−)
	Stretched at t = 127°	2.3	61	(+)	(+)

Note: The (+) sign denotes that the film withstood bending without failure, while the (−) sign denotes rupture of the film when bent.

in the system polymer—plasticizer can vary, and it can also differ to a variable degree from the rate of movement in the unplasticized polymer.

If the migrating particles and the plasticizer are mutually soluble, as, for example, in the case of moisture diffusing through a polymer plasticized with glycerin, the permeability of the polymer will be considerably higher than in the case where the plasticizer is not a solvent for the given gas or vapor. In the latter case, the plasticizer will function as an additional barrier in the path of the particles and the rate of movement of the latter in a given system will be slower the greater the amount of plasticizer present in the film (Table 5).

In the technology of preparing film materials with high elastic properties a special position is held by the process of mechanical orientation of the films while heated above their softening temperature [4, 5]. In the orientation process a partial straightening and orientation of the chains occurs, and the number of points at which

TABLE 7

Dependence of Heat Destruction of Vinyl Chloride–Vinylidene Chloride Copolymer on Chemical Nature and Amount of Some Stabilizers

Stabilizer	Amount of stabilizer on 100% of the copolymer	Rate of decomposition at t = 150°		
		ordinary films	films heated at 65° for 50 hours	films irradiated with quartz illumination for 100 hours
Without stabilizer	0	3 min 44 sec	3 min 10 sec	2 min 15 sec
1,2-Epoxy-3-phenoxypropane	3	35 min 35 sec	22 min 50 sec	1 min 25 sec
Tolylenediglycidylurethan	3	58 min 29 sec	40 min 35 sec	1 min 20 sec
	5	58 min 55 sec	–	5 min 37 sec
Hexamethylenediglycidylurethan	3	44 min	33 min 53 sec	4 min 10 sec

the chains crisscross decreases. Because of this the material becomes more pliable, which is reflected in a change in the film properties, in particular, an increase in their low-temperature resistance.

The effect of mechanical orientation on the low-temperature resistance of the films was checked on the two chlorine-containing polymers. The greatest effect of the indicated operation was observed for the films made from vinyl chloride–vinylidene chloride copolymer, where the film, incapable of being bent at -30° without breaking, acquired after mechanical orientation the ability to bend 180° without breaking, even when bent at a lower temperature (Table 6).

As a result, on comparing the principal characteristics of the studied films it was established that the films from the vinyl chloride–vinylidene chloride copolymer are characterized by having the greatest resistance to atmospheric moisture, and can be easily obtained by milling. Because of the high elastic properties of the copolymer, very little plasticizer has to be added (8-15%) to obtain suitable films.

A serious disadvantage, interfering with the industrial use of the polymer, was its low light and heat stability. The film of the copolymer quickly assumed a dark color when exposed to the action of light and heat, and a rapid chemical decomposition with the cleavage of HCl began at 150°. Encouraging results were obtained when a number of substances were tested as stabilizers, indicating that the addition of certain epoxide compounds, and, in particular, of tolylenediglycidylurethan [6] to the copolymer film could yield films that are quite stable to storage at room temperature, and even at somewhat higher temperatures, of the order of 50 to 60° (Table 7).

SUMMARY

1. Of a series of polymers that were investigated, it was established that the greatest resistance to moisture was possessed by vinyl chloride–vinylidene chloride copolymers, the moisture permeability of which is expressed by a value of 0.1-0.3 mg/sq cm in 24 hours, whereas a poly(vinyl chloride) film of even greater thickness allows 0.7-1 mg of moisture to penetrate in 24 hours.

2. It was shown experimentally that the chemical nature of the plasticizer, especially the extent to which the diffusing vapor particles dissolve in the plasticizer, has a very important bearing on the permeability value. As a result, for the chlorine-containing vinyl polymers and copolymers the best of the investigated commercial plasticizers is dioctyl phthalate, which gives a stable elasticity and does not affect the moisture resistance of the polymer film.

3. It was shown that both the heat stability and the light stability of films prepared from vinyl chloride–vinylidene chloride copolymers can be substantially improved by the use of epoxide stabilizers.

LITERATURE CITED

[1] S. A. Reitlinger, Uspekhi Khim. 20, 212 (1951).

[2] J. D. Edwards and D. B. Strohm, Modern Packaging 19, No. 2, 157, 190 (1940); C. A. 40, 1080 (1946).

[3] A. A. Tager, Uspekhi Khim. 18, 557 (1949).

[4] V. A. Kargin and G. A. Slonimskii, Zhur. Fiz. Khim. 23, 363 (1949).

[5] V. O. Sedlis, Transactions of First and Second Conferences on High-Molecular Compounds [in Russian]. (Izd. An SSSR, 1945).

[6] A. A. Berlin and A. K. Dobagova, Khim. Nauka i Prom. 2, No. 6, 808 (1957).

Received October 16, 1958

THE CATALYST CONCENTRATION DURING SYNTHESIS OF VINYL ACETATE OVER A HETEROGENEOUS CATALYST*

E. N. Rostovskii and I. A. Arbuzova

In our previous communications on the vapor-phase synthesis of vinyl acetate, we considered the results of study of a series of conditions of the process, the performance of the catalyst [1], the ratios of components [2], the residence time [3], and the possibility of different courses of reaction [4, 5].

In the present paper we submit experimental results for the influence of change of the content of catalytically active salt (zinc acetate) supported on active carbon on the efficiency of the catalyst. This problem has not hitherto been adequately studied in connection with the formation of vinyl esters. Relatively little work has been published on the quantitative evaluation of this aspect of analogous reactions.

Studies of the correlation of specific catalytic activity with surface concentration of catalyst were carried out by Kobozev and co-workers [4-9]. A maximum of specific activity was found in some cases in dependence on the degree of occupation of the surface (for example in the hydration [7] or polymerization [8] of acetylene); in other cases an increase in the quantity of supported catalyst led to an exponential fall in activity [9]. Adsorptive activation was also found to have a larger influence in ionic catalysis than in catalysis in presence of metals [7]. Kobozev made a study of concentrated layers and found that complications arose in the process of crystallization [6].

Widely divergent relations are reported by various authors in experimental studies of heterogeneous catalysis due to the complex nature of the over-all process. Studies of hydrogenation reactions, for example, have led to the following observations: a linear relation between increased reaction rate and increasing quantity of carbon-supported catalyst [10, 11], the absence of a clear relation between these factors [12], the existence of a minimum concentration of catalyst below which the process went very slowly, while the catalytic activity remained nearly constant when the catalyst content was considerably increased [13].

An increase in the quantity of catalyst on a support must result in alteration not only of the catalytic activity but also of the sorptive capacity. Inverse [14] and direct proportionality were observed in investigations of this aspect, as well as optimum activity at medium concentrations of salt deposited on the sorbent. The actual effect depended on the nature of the adsorbed molecules. In general the course of sorption of different substances must depend on the size of the molecules and the structural characteristics of the sorbent. This generalization is inadequate, however, as an explanation of the cause of the above-noted marked differences observed in studies of one and the same reaction, for example hydrogenation in presence of catalysts of similar compositions. Additional experimental material would therefore be of interest.

In a study of the synthesis of vinyl formate [16] we indicated the existence of an optimum concentration of zinc acetate, and the chief causes of this optimum were briefly considered.

The present work provides experimental material on the study of the catalytic activity of a series of catalysts. Sorptive activities and porosities are compared.

EXPERIMENTAL

Vinyl acetate was synthesized in the vapor phase under conditions similar to those previously described [1, 3]. Acetylene was admitted at a speed of 10 liter/hr into a thermostated vaporizer; it was saturated at 40° with

*Communication IV.

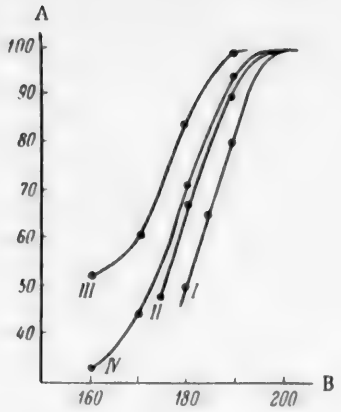

Fig. 1. Catalytic activity of different concentrations of zinc acetate on AG carbon. A) Acetic acid conversion (in %), B) reaction temperature (in °C). Zinc salt content (%): I) 9.2, II) 13.6, III) 17.7, IV) 25.6.

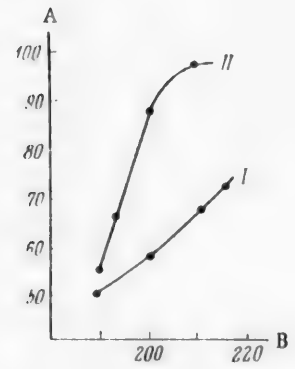

Fig. 2. Catalyst on active birch carbon. A) Acetic acid conversion (%), B) reaction temperature (°C). Zinc acetate content (%): I) 12.3, II) 22.4.

acetic acid vapor and then conducted into a reaction tube immersed in an air bath which was heated by an electric furnace. The acetylene/acid molar ratio was about 20:1. The process was regulated by the earlier method [1] whereby samples were withdrawn from the gas stream and analyzed for their content of acid and ester (in unit volume). The reaction temperature was kept constant and measured in the center of the catalyst bed. The temperature of the mixture reaching the catalyst was also measured. Catalysts were prepared with AG brand of active carbon (grain size 1-1.5 mm). The characteristic values of this carbon were somewhat higher than those of the sample of this grade of carbon previously used; the characteristics were determined by the previous techniques [3, 16]: The chlorine capacity was 52%; the relative specific surface in methylene blue sorption was 370 m^2/g. The total porosity, calculated with reference to the values of the apparent and true specific gravities [3], was 58%. Catalysts with zinc acetate contents of about 9 to 26% were prepared by deposition of this carbon. The catalytic activity was determined at several temperatures (between 170 and 200°) since due to the considerable variations in catalytic effect a certain temperature (say 200°) might be excessive for one catalyst but inadequate for another. The residence time of the reactants in the catalytic zone, calculated with allowance for the volume occupied by the carbon [3], was 3.7-3.9 seconds. Results of these experiments are plotted in Fig. 1 which shows that the most active catalyst was one containing about 18% of zinc acetate.

Figure 2 contains plots of measurements of the efficiency of catalysts prepared on another carbon – activated birch carbon – with a residence time of about 4 seconds. Again we note a strong influence of the zinc salt concentration on catalytic activity.

Catalysts deposited on AG carbon were investigated more closely with the objective of establishing the causes of the change of activity. Each sample was examined not only for its catalytic activity at various temperatures but also for its porosity and static sorptive activity for chlorine. A catalyst containing about 5% of zinc acetate was also studied.

Results of determinations of porosity (curve V), sorptive activity (curve VI) and catalytic activity (curves I, II, III and IV) are compared in Fig. 3 for a series of catalysts differing in zinc contents. These results indicate the existence of an optimum content of zinc salt corresponding to maximum catalytic activity. This maximum is very conspicuous at a reaction temperature of 190° or lower (curves II, III and IV). At 200° (curve I) the high activity of the catalysts slightly offsets the difference between them. Comparison of catalytic properties with porosity and sorptive activity shows that the optimum of activity is associated with decreasing porosity and sorptive activity of the catalyst with increasing quantity of salt on the carbon. This effect is accordingly the result of superposition of two factors when the concentration of zinc acetate on the carbon surface is increased – firstly the increased catalytic activity at higher salt concentrations, and secondly the decreased porosity and consequent decreased surface area of catalyst and decreased sorptive capacity.

The reaction rate is proportional to the quantity of catalytically active salt, while sorptive activity reflects the size of surface unoccupied by crystallites of salt. We can divide the diagram into three zones along the abscissas taking into account the inflections of curves V and VI: an increase in the quantity of zinc acetate causes the total porosity and sorptive activity at first, to fall rapidly (zone a in Fig. 3), then more slowly (zone b) and later again relatively sharply (zone c). The greater steepness of the curves in zone a evidently corresponds

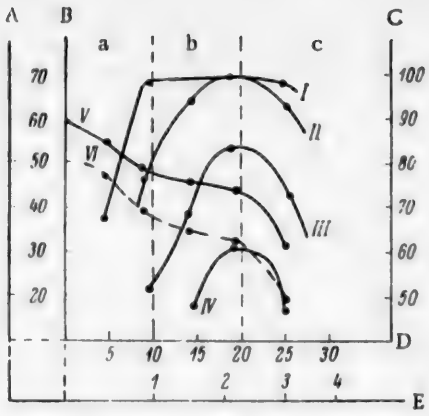

Fig. 3. Comparison of catalytic and sorptive activities and porosities of catalysts containing various amounts of zinc acetate. A) Total porosity (voidage) (curve V) of catalyst (in %), B) activity (curve VI) in chlorine sorption, C) acetic acid conversion (in %), I, II, III, IV catalytic activity at temperatures of 200, 190, 180 and 170° respectively, D) zinc acetate content (in %), E) number of molecules of zinc acetate occupying 100 A^2 of carbon surface.

to replacement by the zinc acetate of the more active portions of catalyst. In zones a and b the catalytic activity increases but the sorptive activity decreases, i.e., they are inversely proportional to one another. After the inflection of the isotherms, the catalytic and sorptive activities fall at nearly the same rate.

Figure 3 also includes a scale showing the approximate number of zinc acetate molecules occupying an area of 100 A^2 on the carbon surface. If a zinc acetate molecule is assumed (for the sake of simplicity) to be cubic, then it occupies an area of about 30 A^2. Uniform distribution of the salt will then correspond in zones a and b to a surface occupation of approximately 30 and 70% respectively. In the case of a catalyst containing 25-26% of zinc acetate, about 90% of the area will be occupied. Even long before occupation of the whole surface of the carbon, from the start of zone c, curves V and VI become steeper and this coincides with a fall in catalytic activity. The sharp drop in porosity and sorptive capacity when some of the surface is still unoccupied by zinc acetate indicates that some of the voids become enclosures not accessible to the sorbate. In zone b the increase in quantity of salt evidently corresponds to its relatively uniform distribution over the surface, while the greater steepness of the curves in zone c shows that subsequent introduction of relatively small quantities of salt removes a larger volume of catalyst voids from the sphere of reaction.

The foregoing data afford an explanation of the results reported in various publications, such as the direct or inverse proportionality between catalytic activity and quantity of catalyst (zones a and b correspond to the former and zone c to the latter). The specific conditions of preparation or utilization of the catalysts could mask the existence of an optimum concentration of salt on the carrier, such as occurred, for example, in the experiments at 200° plotted in curve I of Fig. 3.

SUMMARY

A study of a number of catalysts for the vapor-phase reaction of acetylene with acetic acid showed that existence of an optimum range of zinc salt concentrations on carbon is due to the superposition of two effects during increase in concentration of the salt: 1) increased catalytic activity and 2) decreased sorptive activity and porosity of the catalyst.

LITERATURE CITED

[1] S. N. Ushakov, E. N. Rostovskii and I. A. Arbuzova, Zhur. Priklad. Khim. 13, 1629 (1940).

[2] I. A. Arbuzova, S. N. Ushakov and E. N. Rostovskii, Zhur. Priklad. Khim. 31, 1704 (1958).*

[3] E. N. Rostovskii and S. N. Ushakov, Zhur. Priklad. Khim. 32, 2060 (1959).*

[4] E. N. Rostovskii and A. N. Barinova, Zhur. Priklad. Khim. 27, 1102 (1954). *

[5] E. N. Rostovskii, A. N. Barinova and A. I. Volkova, Izvest. Akad. Nauk SSSR, Otdel Khim. Nauk, 1379 (1957). *

[6] N. I. Kobozev, Zhur. Fiz. Khim. 13, 17 (1939).

[7] G. A. Pospelova, I. Ya. Shlyapintokh, N. I. Kobozev and L. A. Nikolaev, Zhur. Fiz. Khim. 21, 85 (1947).

[8] E. N. Martinson and N. I. Kobozev, Zhur. Fiz. Khim. 21, 85 (1947).

* Original Russian pagination. See C. B. translation.

[9] N. I. Kobozev, Uchenye Zapiski, Moscow State Univ., 86, 1, 13 (1946).

[10] C. Schuster, Z. phys. Ch., B, 14, 249 (1931).

[11] C. Schuster, Z. Elektroch. 38, 614 (1932).

[12] S. Josza, Z. ang. Ch. 41, 767 (1928).

[13] A. M. Rubinshtein, Kh. M. Minachev and N. I. Shuikin, Doklady Akad. Nauk SSSR, 62, 497 (1948).

[14] E. V. Alekseevskii and A. Musakin, Zhur. Obshchei Khim. 4, 669 (1934).

[15] H. Herbst, Kolloidchem. Beichefte, 21, 1, 36 (1925).

[16] S. N. Ushakov, I. A. Arbuzova and E. N. Rostovskii, Zhur. Priklad. Khim. 20, 1013 (1947).

Received July 17, 1958

THE AGING OF CABLE RUBBER

G. I. Dubrovin

Research Institute of the Cable Industry

Cable rubber ages both during storage and in course of use. Cable components are most usually exposed to a temperature of up to 65° in use. In some cases atmospheric conditions are a supplementary factor. Cable rubber is not exposed to the light when stored, nor is it then exposed to temperatures above normal.

In the present work consideration is given to the problem of determination of some constantly acting factors and of the kinetic characteristics of aging of insulating and hose rubber under natural (in store) and atmospheric conditions.

EXPERIMENTAL

Specimens of standard cuttings 2.0 mm thick were prepared from each rubber mix entering into cable manufacture. These specimens were heat-aged as specified in GOST 271-41 at 80° for 200 days and at 90° for 100 days. Specimens were prepared as specified in GOST 269-53; the mechanical characteristics of the rubber were determined as in GOST 270-53 and the electrical rupture strength as in GOST 2068-54 and GOST 6433-52.

Employment of Chemical Kinetic Equations to Describe the Aging of Rubber. It is suggested that rubber aging originates with oxidation of the rubber substance by atmospheric oxygen in presence of inhibitors and that the aging processes can be expressed by a chemical kinetic first order equation.

For a first order reaction it is permissible to insert in the equation any terms proportional to the concentration of the reacting substance. In the present case such a term is the specific elongation of rubber (ϵ). Then the formula can be represented by

$$K = \frac{2.3}{t} \lg \frac{\epsilon_0 - \epsilon_\infty}{\epsilon_t - \epsilon_\infty} \qquad (1)$$

or, when $\epsilon_{cr} = \epsilon_t$

$$K = \frac{2.3}{t_{cr}} \lg \frac{\epsilon_0 - \epsilon_\infty}{\epsilon_{cr} - \epsilon_\infty},$$

where K = the velocity constant of oxidation; ϵ_0 = specific elongation at rupture before aging (in %) ϵ_t = specific elongation at time t (in %); ϵ_{cr} = specific elongation at the end of the aging process under inhibitor conditions (in %); ϵ_∞ = limiting value of specific elongation during aging (in %); t = time of aging in days.

The relation between $\log \frac{\epsilon_0 - \epsilon_\infty}{\epsilon_t - \epsilon_\infty}$ and aging period t is represented for a first order reaction by a straight-line plot.

Our experimental results (Figs. 1 and 2) show that deviations from the linear relation occur at the start and end of the aging process; both of these periods are very short. The initial departures from linearity are ignored for the sake of simplicity in determining the period of service of cable rubber. The start of the second deviation is defined as the critical value of specific elongation ϵ_{cr}. Values found for type TS-35 SK-50 insulating rubber are ϵ = 70.0%, ϵ_{cr} = 290-350%.

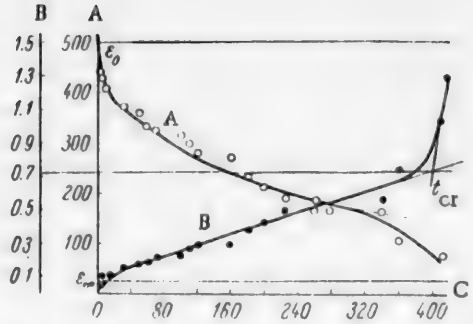

Fig. 1. Aging of ShN-40 hose rubber at 80°. A) Specific elongation (in %), B) value of $\lg \frac{\epsilon_0 - \epsilon_\infty}{\epsilon_t - \epsilon_\infty}$, C) aging period (in days).

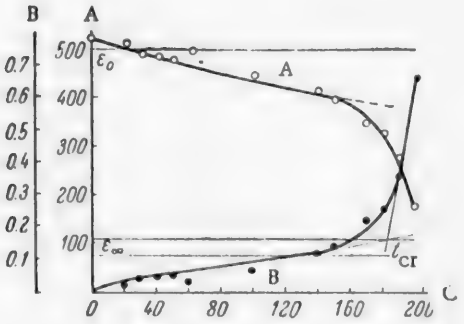

Fig. 2. Aging of TS-35 SK-50 insulating rubber at 90°. A) Specific elongation (in %), B) value of $\lg \frac{\epsilon_0 - \epsilon_\infty}{\epsilon_t - \epsilon_\infty}$, C) aging period (in days).

For ShN-40 hose rubber $\epsilon_\infty = 25\%$, $\epsilon_{cr} = 105\%$. These data are characteristic for rubber of the given composition.

The activation energy of the process can be calculated with the help of the Arrhenius equation from the experimental values of the oxidation velocity constants at two temperatures. If the activation energy is known, the Arrhenius equation can be used for calculation of oxidation velocity constants at the working temperature of cables in the following form:

$$\log K_X = \log K_1 - \frac{E}{4.6} \frac{(T_1 - T_x)}{T_1 \cdot T_x}, \qquad (2)$$

where K_1 and K_X = velocity constants of oxidation at T_1 and T_X, E = activation energy (in cal/mole), T_1 = absolute temperature corresponding to the artificial aging conditions, T_X = absolute temperature corresponding to natural aging in use.

The processes of oxidation of raw rubber present in vulcanized rubber under artificial conditions are not the same as those under normal conditions. In the determination of the service life of cable rubber by the Arrhenius equation it was therefore found that the calculated results were slightly higher than the experimental results. Since the mechanical properties of vulcanized rubber change more quickly under working conditions than under artificial conditions, the velocity constant of aging in equation (2), for the same reaction order, must be greater than the constant calculated from data for artificial aging.

For atmospheric and natural aging the values of the corrected constants K_s range between 1.0×10^{-4} and 6.0×10^{-4}.

Taking into consideration the corrected aging constants of cable rubber, K_s, the true aging constant K_{total} is expressed by the sum

$$K_{tot} = K_x + K_s. \qquad (3)$$

The working formula then acquires the form

$$\log (\varepsilon_t - \varepsilon_\infty) = \log (\varepsilon_0 - \varepsilon_\infty) - \left(\frac{K_x + K_s}{2.3}\right) t. \qquad (4)$$

The period of aging of cable rubber t_{cr} and the corresponding ϵ_{cr} can be determined with the help of equation (4) and the corresponding plots (Figs. 1 and 2).

Measurements were made of the specific elongation ϵ_t of specimens of ShN-40 hose rubber after aging at 70 and 80°, and of TS-35 SK-50 insulating rubber at 80-90° until the specimens had completely lost their elasticity. Results are presented in Table 1.

The mean value of activation energy E_{mean} is close to the analogous result obtained by Kuz'minskii and co-workers [1, 2] for the oxidation of raw rubber and vulcanized rubber.

TABLE 1

Calculated Values of the Velocity Constants of Oxidation K and of Activation Energy E at 70 and 80° for ShN-40 Rubber and at 80° For TS-35 SK-50 Rubber

	ShN-40 rubber	TS-35 SK-50 rubber
K_{70}	$2.3 \cdot 10^{-3}$	—
K_{80}	$5.6 \cdot 10^{-3}$	$2.55 \cdot 10^{-3}$
K_{90}	—	$5.62 \cdot 10^{-3}$
E_{mean} (in kcal)	22.6	22.4

TABLE 2

Change of Specific Elongation at Rupture During Aging of ShN-40 and TS-35 SK-50 Rubbers

Aging of ShN-40 rubber			Aging of TS-35 SK-50 rubber		
aging period (days)	at atmospheric pressure (in %)		aging period (in days)	during aging at 20 deg (in %)	
	experimental	calculated* from eq.(4)		experimental	calculated** from eq. (4)
0	476.0	476.0	0	556.0	556.0
60	451.0	466.0	183	521.0	535.0
90	387.0	462.0	365	516.0	515.0
120	375.0	457.0	548	494.0	495.0
210	370.0	442.0	731	470.0	477.0
270	388.0	433.0	915	466.0	466.0
360	376.0	420.0	1825	—	381.0
540	332.0	395.0	3650	—	260.0
600	377.0	377.0	—	—	—
720	373.0	371.0	—	—	—
1825	—	256.0	—	—	—
3650	—	141.0	—	—	—

*The following values were taken for the calculations: $\epsilon_0 = 476\%$, $\epsilon_\infty = 25.0\%$, $K_{80} = 5.6 \cdot 10^{-3}$, $K_{70} = 2.3 \cdot 10^{-3}$, E = 22.8 kcal, $K_{20} = 0.08 \cdot 10^{-4}$, $K_s = 3.95 \cdot 10^{-4}$.

**The following values were taken for the calculations: $\epsilon_0 = 556\%$, $\epsilon_\infty = 70\%$, $K_{100} = 5.62 \cdot 10^{-3}$, $K_{90} = 2.55 \cdot 10^{-3}$, $K_{20} = 0.05 \cdot 10^{-4}$, E = 22.4 kcal, $K_s = 2.41 \cdot 10^{-4}$.

Results of measurements of the specific elongation of aged ShN-40 rubber and TS-35 SK-50 rubber and results calculated from equation (4) are given in Table 2.

The method enables determination of the approximate working life of cable rubber. It is impossible to employ it for determination of guaranteed working lives of cable materials because other factors additional to those here considered affect the aging period. These are the design and dimensions of the cable, the material of construction of the outer hose, the migration susceptibility of the components of the batch, the relative humidity of the surrounding air, the biological characteristics of the medium, and the metal of the conducting core. These factors must be considered individually and appropriate corrections introduced during calculations.

We now go on to survey the factors influencing the process of aging of cable rubber with reference to the usual design of cable. This comprises three conducting cores (covered with insulating rubber) enclosed in a rubber hose.

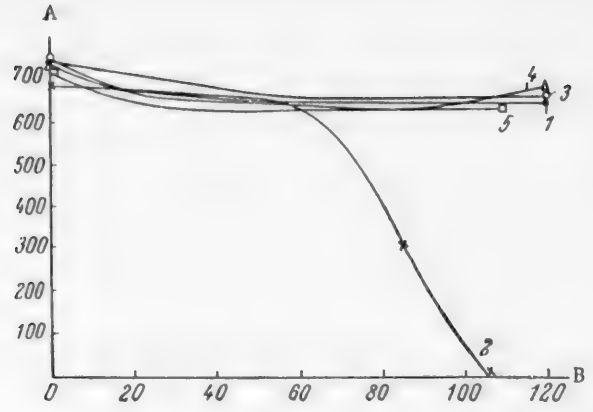

Fig. 3. Dependence of specific elongation of TSSh-35 SK-50 insulating rubber on period of aging at 100° and on period of contact with the surface of various metals. A) Specific elongation (in %), B) period of aging (days). 1) Control rubber. Metals: 2) copper, 3) iron, 4) aluminum, 5) tinned copper.

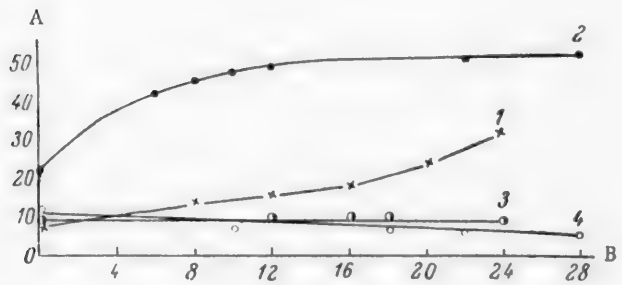

Fig. 4. Dependence of the equilibrium modulus on the period of aging at 100° of insulating and hose rubber in contact with each other. A) Equilibrium modulus ϵ_{∞} (in kg/cm^2), B) aging period (in days). Rubbers: 1) ShBM-40 (sulfur), 2) the same in contact with thiuram rubber, 3) TSSh-35 (thiuram), 4) the same in contact with ShBM-40 hose rubber.

Influence of Migrating Substances in Adjacent Parts of the Cable Structure on the Process of Rubber Aging. A large proportion of conductors and cables fabricated in Russia contains untinned conducting cores and an insulating coating of a rubber mix vulcanized with thiuram. It is assumed that thiuram rubber does not corrode the copper surface of the conducting core. It has been noted, however, that a small quantity of free sulfur is released from the insulating rubber during vulcanization and this sulfur actively participates in chemical reaction with copper with formation of sulfides: $2Cu + S \rightarrow Cu_2S$; $Cu_2S + S \rightarrow 2CuS$. Sulfur also reacts with the rubber hydrocarbon and vulcanizes it. The rubber insulation of the cable becomes enriched in this way with active radicals containing copper [3]:

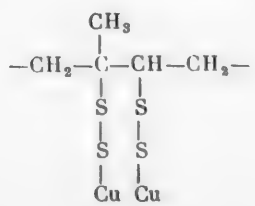

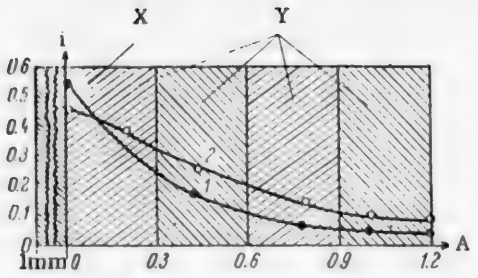

Fig. 5. Kinetics of diffusion of sulfur from hose rubber into rubber insulation during vulcanization and during aging: i = value of I_n/I_0 = ratio of radioactivities of hose rubber I_0 and insulating rubber I_n (in pulses/min.). A = thickness in mm, X = hose rubber, Y = insulating rubber.

The weakest point in this structure is the $-S-S^-$ bond [4, 5] so that the aging of insulating rubber is accompanied by rupture of the $-S\frac{|}{|}S-$ bonds with formation of active Cu—S— radicals which react with the rubber, at the same time as oxygen, and contribute to breakdown of the rubber chain molecules.

We see from Fig. 3 that the most intensive degradation of insulating rubber occurs when aging takes place in contact with the untinned copper surface. After insulating rubber 1.0 and 2.0 mm thick had been vulcanized, copper in amounts of 0.009 to 0.0027% was found. The experimental conditions were such that this copper could only have entered the rubber by migration.

Other substances, apart from copper compounds, that migrate into cable coverings are thiuram, sulfur, softeners, and plasticizers. It was established that thiuram migrates from the insulating rubber into hose covers.

It is known that the magnitude of the equilibrium modulus reflects the density of the space lattice, while gradual increase in the modulus indicates the occurrence of processes of structure formation; consequently enlargement of the space lattice of sulfur-containing hose rubber which ages in contact with insulating thiuram rubber can only be explained on the assumption that thiuram or its breakdown products migrate into the hose cover.

Additional bonds are formed in hose rubber under the influence of migration products [6, 7].

We see from Fig. 4 that the process of structure formation of hose rubber which is aging in contact with insulating rubber is considerably faster than the same process in blank specimens of the same rubber.

Migration of sulfur from hose rubber in the direction of the insulating rubber was investigated with the help of the radioactive isotope S^{35}. Results of this check are plotted in Fig. 5 in the form of a diagram of the distribution of radioactive sulfur in the rubber insulation divided into four parts to illustrate the process of migration of sulfur during vulcanization (curve 1) and after subsequent heating of the specimens for 6 days at 120° (curve 2) in contact with hose rubber containing S^{35}. We see from Fig. 5 that migration of sulfur goes with sufficient speed under the experimental conditions. There is no doubt that this is also true at a lower temperature although the speed would be lower [8].

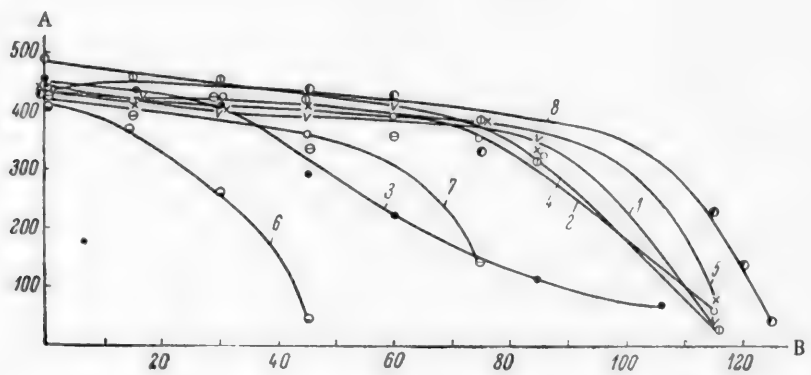

Fig. 6. Change of specific elongation of insulating rubber in course of aging at 100°, when aged in protective coverings fabricated from various materials. A) Specific elongation (in %), B) period of aging (days). 1) TSSh-35 rubber without casing. Casings: 2) ShN-40 rubber, 3) ShBM-40 (sulfur-vulcanized), 4) ShBM-40 (thiuram-vulcanized), 5) cotton tape, 6) the same, impregnated with an ozocerite composition, 7) polyvinyl chloride plastic P-239, 8) lead.

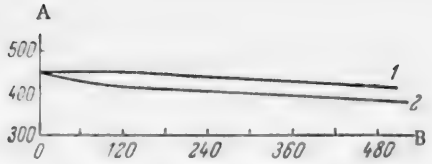

Fig. 7. Specific elongation of ShN-40 hose rubber as a function of the period of aging in storage and under atmospheric conditions. A) Specific elongation (in %); B) aging period (in days). Aging conditions: 1) in store; 2) in the open air.

Other materials can replace rubber as a protective sheath for insulation and conducting cores. These sheaths are fabricated from lead, polyvinyl chloride, and impregnated cotton tapes.

In order to determine the degree of protection of the insulating rubber by different coverings and the influence of these covers on the rubber insulation during the process of aging, tests were made of the aging of insulating rubber in hose coverings fabricated from various materials. The mechanical characteristics of the insulating rubber were also determined (Fig. 6).

We see from Fig. 6 that the greatest effect on the insulating rubber is exerted by the covering containing copper naphthenate (curve 6); this salt migrates from the ozocerite composition used for impregnation of the paper tapes round the conductors. The same rubber had the best mechanical properties after aging in a lead sheath.

Photodegradation of Cable Rubber. The insulating rubber was not subjected to light-aging, but the hose rubber of the sheath aged very slowly under the action of sunlight because the carbon black in the mixture acts as a light filter and protects the rubber against breakdown [9, 10]. Moreover polychloroprene rubber is a light-stable polymer [10]. Sheaths of other rubbers contain a high proportion of paraffin wax which migrates to the surface of the sheath and thereby protects the rubber against the action of solar radiation and ozone.

Figure 7 contains plots of results of experimental aging of rubber (on basis of "Nairit") in the dark and in sunlight under atmospheric conditions.

Moisture Absorption and Moisture Permeability of Cable Rubber. The electric breakdown strength of the rubber insulation of a cable depends on the thickness of the insulating rubber, on the thickness of the outer hose, on the rate of moisture uptake and penetration, on the operating temperature of the material, and on the chemistry of the rubber and the fillers in the mix.

Below a method is put forward for determining the permissible period of exposure of rubber to moisture in dependence on the temperature, the thickness of the outer hose and the electrical breakdown strength.

Discs 1 mm thick and 110 mm in diameter were prepared from the insulating rubber and placed in a casing of hose rubber 1 and 2 mm thick. The discs were placed in a desiccator containing water, and the desiccator was placed in a thermostat at a given constant temperature. At definite intervals of time the wetted rubber samples were removed from the desiccator, and the insulating rubber was detached from the hose and tested for breakdown strength in accordance with GOST 2068-54 and 6433-52.

The results of these tests are plotted in Fig. 8. We see that at the start of moisture exposure at 20° the breakdown strength of the insulating rubber rises, due to the moisture being absorbed by the hose cover both from outside and from the side of the insulating rubber.

After reaching a maximum, the curve of breakdown strength starts to fall; this signifies that the process of sorption of moisture from the insulating rubber side is complete. This is followed, after a short equilibrium period, by penetration of moisture through the hose cover and its absorption by the insulating rubber. Attainment of the maximum permissible uptake of moisture of the insulating rubber is determined from the elastic breakdown strength for the grade of rubber in question in accordance with GOST 2068-54.

In the tests at 70° (curves 4, 5 and 6 in Fig. 8) the process of moisture uptake through the hose coverings is accelerated, and the quantity of moisture passing through the cover increases. Deterioration in electrical breakdown strength at 70° therefore goes very much faster than at 20°.

SUMMARY

1. A systematic method of calculation is put forward which enables determination of the approximate period of aging of cable rubber. A new formula for calculation of the specific elongation of rubber during aging is checked.

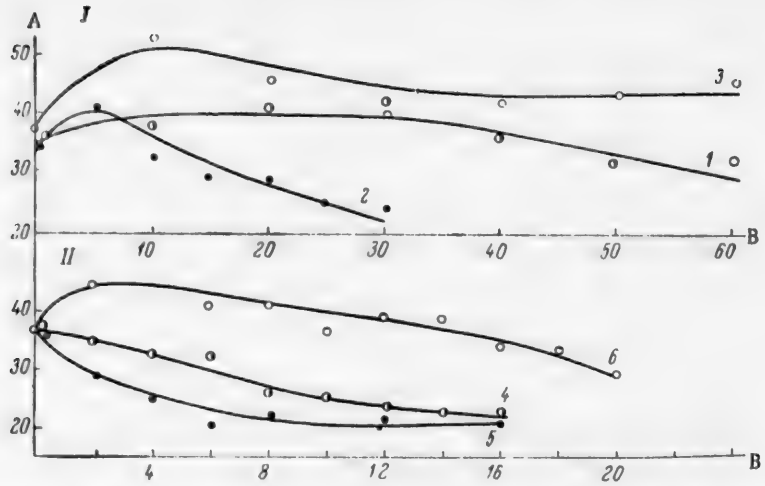

Fig. 8. Relation between electrical breakdown strength of insulating rubber and the period of moisture penetration through hose covering with a thickness of 1 mm at 20 and 70°. A) Breakdown strength (kV/mm), B) period of exposure to moisture (in days). Coverings at 20°: 1) ShN-40 rubber, 2) ShBM-40 rubber, 3) butyl rubber composition; at 70°, 4) ShN-40, 5) ShBM-40, 6) butyl rubber. Moistening: I) at 20°, II) at 70°.

2. Compounds of copper, which migrate from the current-conducting core, activate the process of aging of insulating rubber.

3. Thiuram, as a result of migration from the rubber insulation, activates the process of aging of sulfur-containing hose rubber.

4. A method is advanced for determination of the permissible period of humidification of hose coverings from the change in the electrical breakdown strength of insulating rubber in dependence on the composition of the rubber and the thickness of the protective covering.

I make special acknowledgement and extend thanks to S. I. Sokolov for his guidance throughout this work, and also to L. I. Lyubanskaya and A. S. Kuz'minskii for valuable advice.

LITERATURE CITED

[1] A. S. Kuz'minskii, N. N. Lezhnev, and Yu. S. Zuev, Oxidation of Raw Rubber and Vulcanized Rubber [in Russian] (State Chemical Press, 1957).

[2] A. S. Kuz'minskii and L. I. Lyubchanskaya, Kauchuk i Rezina 6, 3 (1958).

[3] N. V. Stepanyuk, Trudy NIIRP [Sci. Research Inst. Rubber Industry] 1, 109 (1955).

[4] N. N. Semenov, Some Problems of Chemical Kinetics and Reactivity [in Russian] (Acad. Sci. USSR Press, 1954).

[5] Cottrell, The Strength of the Chemical Bond [Russian translation] (For. Lit. Press, 1956).

[6] G. M. Bartenev, Zhur. Tekh. Fiz. 22, 11 (1952).

[7] L. A. Vishnitskaya, Trudy NIIRP 1, 53 (1954).

[8] J. Auerbach and C. D. Gehman, Anal. Chem. 4, 685 (1954).

[9] F. F. Koshelev and N. S. Klimov, General Technology of Rubber [in Russian] (State Chem. Press, 1958).

[10] J. T. Blake, Synthetic Rubber [Russian translation] (State Chem. Press, 1957) p. 552.

Received June 25, 1959

THE DEIONIZATION OF ACID PROTEIN HYDROLYZATES WITH ANION-EXCHANGING RESINS

A. B. Davankov, A. N. Oratynskaya, V. M. Laufer and A. G. Lipinskii

In recent years numerous high-molecular substances containing various functional groups have been prepared which are capable of entering into chemical reactions similar to those that take place between reacting substances in solutions.

Solid substances of this type, which are insoluble in water and organic solvents, are known as high-molecular electrolytes. To this group of substances belong the important general class of ion-exchanging resins [1] which have come into extensive use in a variety of applications in adsorption technology [2].

One of the most important and promising fields of application of ion-exchanging resins is the separation of amino acids and the elimination of various impurities from protein hydrolyzates. Such impurities are inorganic acids and salts and humic substances.

Separation of the components of a complex mixture of amino acids by simple methods is of great scientific value for the development of protein chemistry, and for the study of the mechanism of nitrogen metabolism in living organisms, plants, microflora and microfauna; amino acids serve as an efficient means of treatment of complex diseases, while ion-exchanging materials are new diagnostic agents.

Numerous publications [3] have been devoted to the separation of amino acids by ion-exchange and to their selective adsorption. The literature on the removal of impurities from protein hydrolyzates is much smaller. Yet the latter problem is of great practical importance; without a solution to this problem, it is difficult to separate and obtain amino acids in the pure state.

The potential value of ion-exchangers for this purpose is obvious, especially since definite progress has been made recently in the field of separation, and the process of hydrolysis itself has been effected with the help of ion-exchanging resins.

It is well-known that considerable difficulties attend the isolation of amino acids from their hydrochlorides or sulfates and their preparation as the free bases. Residues of chloride ions are especially difficult to remove from amino acids. At the same time the complete elimination of chloride ions or the ions of other acids from amino acids is absolutely essential. This requirement arises not only in preparative work but also on the industrial scale, as for example in the production of new types of chemical fibers (such as enanthin and pelargone from the appropriate amino acids.

The majority of the methods described in the literature for freeing amino acids of chloride ions are for preparative use and therefore hardly can be applied in industry. They include the treatment of amino acid hydrochlorides with solutions of salts of heavy metals followed by precipitation of the excess of ions of these metals with hydrogen sulfide.

Treatment of amino acid hydrochlorides with ethylene oxide (method of Rodionov and Yartseva [4]) is a lengthy operation and necessitates removal of secondary products of reaction (ethylene chlorohydrin and ethylene glycol).

TABLE 1

Results of Extraction of Cl^- and SO_4^{2-} Ions from Acid Casein Hydrolyzates with Anion-Exchange Resins under Dynamic Conditions

Expt. no.	Cycle no.	Anion exchange resin	Wt. of air-dry resin in adsorption col., g	Amt. of solution filtered through resin (in ml)	pH of original sol.	Chlorine content (%)	Total N content (in mg %)	Original content of amino N (in mg %)	Content of amino nitrogen (in mg %)	Extraction of chlorine		
										in g	in milli equiv/g	in % of original quantity in solution
1	1	AN-2F	10	80	1.4	5.80	2230	1660	1666 *	2.36	6.62	50.86
2	1	AN-2F	40	425 **	1.0	5.35	2440	1620	1613	9.83	6.88	43.22
	2	AN-2F	40	250	1.0	5.35	2440	1620	1655	9.67	6.77	72.27
	3	AN-2F	40	250	1.0	5.35	2440	1620	1614	9.10	6.36	68.01
3	1	AV-16	10	80	1.4	5.80	2230	1660	1596	2.66	7.47	57.32
4	1	EDE-10P	10	80	1.4	5.80	2230	1660	1592	2.15	6.02	46.34
5	1	N-O	10	100	1.0	5.35	2440	1620	1600	0.70	4.78	13.09
6	1	EDE-10P	10	100	0.92	8.67 ***	2170	1262	1192	5.19 ****	10.78 ****	59.86 ****
7	1	AV-16	10	100	0.92	8.67	2170	1262	1366	5.14	11.30	62.77

* Mean of all of the samples with allowance for volume of water poured into the column at start of the experiment.

** In Expt. No. 2, 25 ml samples of filtrate were taken; in all of the remaining experiments 10 ml samples were taken.

*** SO_4^{2-} content.

**** SO_4^{2-} extracted.

TABLE 2

Results of Extraction of Cl^- Ions During Filtration of Hydrolyzate

Volume of filtration fraction (in ml)	Hydrochloric acid hydrolyzates of casein											
	N-O, weight 100 g, moisture content 47.5%			MMG-1 wt. 100 g, moisture cont. 37.6%		AN-2F, weight 100 g, moisture content 23.5%			EDE-10P, weight 100 g, moisture content 10.9%		
	Cl^- (in %)	amino nitrogen (in mg%)	pH	Cl^- (in %)	amino nitrogen (in mg%)	Cl^- (in %)	amino nitrogen (in mg%)	pH	Cl^- (in %)	amino nitrogen (in mg%)	pH
Original hydrolyzate	5.02	1400	1.03	5.44	1600	5.12	1450	1.03	5.12	1450	1.03
100	1.24	1300	4.09	1.90	1380	0	1460	8.14	0	1150	9.50
100	3.10	1400	2.60	3.67	1570	0	1410	6.92	0	1421	8.20
100	3.90	1390	1.67	4.49	1585	0.99	1470	4.30	0	1870	5.93
100	4.13	1380	1.40	4.70	1600	2.38	1440	2.12	1.73	1630	4.99
100	—	—	—	5.20	1600	—	—	—	3.60	1400	1.99
100	—	—	—	—	—	—	—	—	3.94	1420	1.59

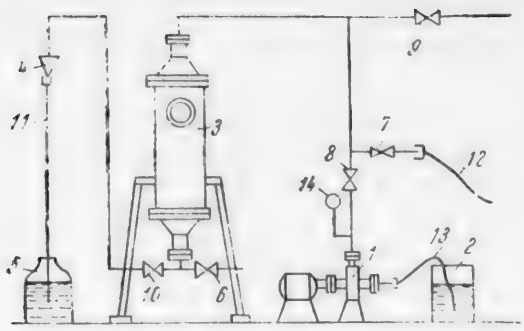

Pilot plant for deionization of protein hydrolyzates. 1) Centrifugal pump, 2) capacity vessel, 3) ion-exchange column, 4) funnel, 5) bottle, 6-10) valves, 11-13) flexible hoses, 14) pressure gange.

TABLE 3

Amino Nitrogen Contents of Fractions

Fraction number	Vol. of fraction (ml)	Amino nitrogen (in g)	Fraction number	Vol. of fraction (ml)	Amino nitrogen (in g)
1	100	0.12	6	100	1.61
2	100	1.05	7	100	1.50
3	100	1.61	8	100	0.99
4	100	1.94	9	100	0.06
5	100	1.81	10	100	0.03

The hydrochloride, the electrochemical,and the extractive methods do not ensure complete freedom of amino acids from chloride ions.

An additional method of complete removal of chloride ions from mixtures of amino acids was put forward by Davankov and Laufer [5]. It is based on the use of amphoteric ion-exchange resins previously "charged" with ions of heavy metals that react with chloride ions to form insoluble precipitates adsorbable by the ion-exchange resin. This method offers the possibility of preparing ω-aminoenanthic acid and ω-aminopelargonic acid entirely free of chloride ions without the need for dilution of solutions of these acids.

The conditions of the present work with protein hydrolyzates were less rigorous. It was therefore to be expected that solution of the problem of removal of mineral acids from these hydrolyzates could be effected with anion-exchanging resins.

In the present work we studied the conditions necessary for solution of the above problem on the industrial scale. For this purpose it was necessary to find select suitable grades of ion-exchangers of Russian manufacture for freeing amino acids of traces of mineral acids used as catalysts in the acid hydrolysis of proteins. Results obtained in the laboratory were tried out in a pilot plant.

Some operating troubles were encountered when we carried out this process for the first time on a fairly large scale. These have now been overcome, and in our opinion the process is acceptable for industrial purification of amino acids from unwanted impurities with the help of ion-exchange adsorption.

Removal of the hydrolyzing agent from protein hydrolyzates with the help of ion-exchanging resins is a particular aspect of the general problem of demineralization of various biological liquids and extracts.

Deionization was applied to hydrochloric and sulfuric acid hydrolyzates of casein. These consisted of a mobile dark-brown liquid with a characteristic odor. It was composed of amino acids contaminated with certain products of incomplete hydrolysis of the protein—peptides.

TABLE 4

Results of Experiments on Deionization of Sulfate Hydrolyzates of Casein

AN-2F, wt. 100 g, H_2O content 23.5%			EDE-10 P, wt. 100 g, moisture 10.9%		
Volume of filtrate (ml)	SO_4^{--} content (in %)	Amino nitrogen (mg %)	Volume of filtrate (ml)	SO_4^{--} content (in %)	Amino nitrogen (mg %)
Original . .	8.80	1400	Original	8.80	1400
100 *	0	60	200 *	0	0
	0	877	100	0	380
	0.25	1100		0	1287
	0.88	1230		0	1415
	3.04	1360		0.50	1440
	5.45	1425		2.02	1783
	7.02	1400		4.75	1443
				6.72	1380

* Volume of water in column

TABLE 5

Yield and Composition of Products after Filtration of Casein Hydrolyzates

	AN-2F resin, wt. 2.5 kg, moisture 23.5%							EDE-S0P resin, wt. 3-5 kg, moisture 10 %			
	hydrochloric acid				sulfuric acid			hydrochloric acid			
	volume of filtrate (l.)	Cl^- content (%)	amino nitrogen (in mg %)	pH	Cl^- content (%)	amino nitrogen (in mg %)	pH	volume of filtrate (l.)	Cl^- content (%)	amino nitrogen (in mg %)	pH
Original hydrolyzate	—	5.31	1500	1.05	8.80	1360	0.99	—	5.31	1500	1.05
Volume of displaced water . . .	7.0	0.01	147	6.07	0.04	226	7.70	7.0	0	5.0	9.00
	4.0	0.62	784	4.01	0.75	980	4.30	7.0	0.007	600	9.53
	4.0	1.47	1375	3.20	2.18	1150	2.76	7.0	0.033	1150	8.80
	4.0	2.62	1490	2.68	5.32	1236	1.71	6.0	1.68	1700	4.61
	4.0	3.68	1514	1.81	7.01	1360	1.23	4.0	3.66	1500	2.16

It is known that at low pH values (1-2) of the medium, a large proportion of the amino acids is present in solution in the form of $[HOOCRNH_3]^+$ cations. Possible exceptions to this rule are the monoaminodicarboxylic acids. On this basis we can assume that filtration of a solution of amino acids through an adsorption column filled with anion-exchanging resin will result in preferential adsorption of Cl^- and SO_4^{--} anions, while the amino acids will remain in solution.

Of course we cannot altogether rule out the possibility of molecular adsorption of amino acids by the resin, so that the total nitrogen balance in the hydrolyzates before and after the experiments is inevitably upset. However, molecular adsorption plays a subsidiary part during ion-exchange processes and is unlikely to have a serious effect on the process of deionization of protein hydrolyzates.

Laboratory experiments on extraction of Cl^- and SO_4^{--} ions from protein hydrolyzates were performed in glass columns with an internal diameter of 10 and 20 mm and containing 10 and 40 g respectively of air-dry resin. The height of the bed of resin in the columns was 160, 270, and 365 mm; the solutions were filtered at the rate of 30 and 59 ml/hour.

Glass columns of larger diameter (20-25 mm) were used in the next series of experiments with charges of air-dry anion-exchange resins of 100-200 g. The rate of passage of the solution was 50 ml/hour.

For analysis 50-100 ml samples of filtrate were taken. The pH was determined potentiometrically, Cl^- ion by the Volhard method, SO_4^{--} ion by precipitation as $BaSO_4$, and amino nitrogen (NH_2) by Sörensen-Gavrilov titration.

Prior to use, the anion-exchange resins were treated with 4% HCl solution and then with distilled water until neutral. The resins had the following size distribution: 85% of ÉDÉ-10P resin was in the 0.25-0.50 mm range; 70-90% of N O, MMG-1 and AN-2F resins consisted of particles in the 0.25-2.0 mm range.

Resins were regenerated for re-use by treatment with 3-5% NaOH solution. Completeness of removal of Cl^- and SO_4^{--} ions from the resin was checked during regeneration with the aid of $AgNO_3$ and $BaCl_2$ solutions respectively.

The adsorbents used were weakly basic (MMG-1 and AN-2F), medium-basic (N- O) and ÉDÉ-10P) and strongly basic (AV-16) anion exchange resins.

Table 1 contains results of extraction of Cl^- and SO_4^{--} ions from acid casein hydrolyzates in small-diameter columns at a filtration rate of the solution of 38 ml/hour · cm^2; Table 2 contains results of extraction of Cl^- ions during filtration through a 20 mm diameter column at a relatively low rate (16 ml/hour · cm^2).

It follows from the results set forth in Tables 1 and 2 that resins ÉDÉ-10P, AN-2F and AV-16 give better results as demineralizers of proteins than resins N- O and MMG-1. The same is true in regard to the loss of nitrogenous substances in the hydrolyzate.

It is interesting to note that some of the anion-exchangers, and particularly ÉDÉ-10P, exhibit a maximum of amino nitrogen concentration in some fractions of filtrate whose amino nitrogen content exceeded that in the original hydrolyzate.

This phenomenon may be explained by the fact that a certain quantity of nitrogen compounds is taken up initially by resin ÉDÉ-10P, and subsequently at a certain stage the ion with a lower affinity to the resin (for example the ion of amino acid) is displaced by the more strongly sorbed ion (for example the chloride ion). This process leads to enrichment of fractions of hydrolyzate with amino nitrogen.

The following experiment was run to check the foregoing explanation. Seven hundred ml of casein hydrolyzate was filtered through a column packed with ÉDÉ-10P resin. The residues of hydrolyzate were displaced with water. Ten fractions (each of 100 ml) were collected in all, and the amino nitrogen was determined in each. The original hydrolyzate contained 1600 mg % so that a total of 11.2 g of amino nitrogen was filtered. Table 3 shows that the quantity of amino nitrogen taken in the experiment is equal to the quantity of amino nitrogen found in the fractions. It becomes evident that the amino nitrogen "increment" in some fractions of filtrate is a consequence of the special exchange characteristics of ÉDÉ-10P resin.

The original hydrolyzate contained 11.2 g amino nitrogen, while the amount found was 10.72 g or 95.7%.

Additional evidence of the selective adsorption of hydrolysis products by ÉDÉ-10P resin at the start of the process is provided by the change of hydrogen ion concentration of the filtrate. The very high pH of the earlier fractions (close to the pH value of diamino acids) indicates that amino acids of basic character predominate in them.

The fraction with maximum content of amino nitrogen has a pH of 5.93, although break-through of inorganic acid has not yet started (chloride ion absent). In all probability the increased acidity of this fraction is associated with desorption of acid products of hydrolysis from the resin.

The results of experiments on the deionization of sulfuric acid hydrolyzates (Table 4) confirm the presence of a maximum of amino nitrogen in filtrates obtained with ÉDÉ-10P resin. The yield of deionized material with these hydrolyzates is approximately the same as with the hydrochloric acid hydrolyzates. The initial concentration of sulfate ion in the hydrolyzate was 1.5-2 times that of chloride ion. The results of laboratory experiments were checked in a stainless steel pilot plant. Experiments in a stainless steel column were carried out only with ÉDÉ-10P and AN-2F resins which had given better results in deionization of protein hydrolyzates in glass columns.

The stainless steel ion-exchange column was designed for 5 kg of dry resin. It consists of a cylindrical vessel closed at top and bottom by conical stoppers. Perforated plates are located at top and bottom and are intended for uniform distribution of the liquid stream through the cross-section of the column. A sight-glass is fixed in the upper part of the column to enable observation of the process.

A centrifugal pump and a pipeline system were provided to facilitate the various operations of the process of hydrolyzate demineralization. The column, pump, and pipeline system are illustrated in the accompanying diagram.

The pilot plant was operated as follows. Hydrolyzate was taken from reservoir 2 by pump 1 and forced into column 3. After deionization, the liquid passed through funnel 4 into the 20-liter bottle 5.

After the resin had been saturated with acidic anions, the residue of hydrolyzate was displaced with water. The resins were regenerated with 4-5% sodium hydroxide solution admitted through pump 1. A reverse stream of water removed the alkali from the column after regeneration. Water for washing and loosening the resin was passed up from below through valve 6 and discharged to the drain through valve 7.

Filtration of protein hydrolyzate was effected at a rate of 0.15 liter/hr · cm^2.

Twenty experiments with AN-2F resin and ten experiments with ÉDÉ-10P resin were run in the stainless steel column.

The data from these experiments are presented in Table 5. This table gives the yield and composition of casein hydrolyzates after filtration through a stainless steel column packed with ion-exchanging resin. The first filtrate fractions are hydrolyzate diluted with water. The yield of fully demineralized hydrolyzate is higher after treatment with ÉDÉ-10P resin than with AN-2F resin. The amino nitrogen content of filtrates in the ÉDÉ-10P runs also has a maximum. The first fractions with this resin have a strongly alkaline reaction. It is seen that the results in the stainless steel column are substantially the same as those obtained in glass columns.

The pattern of change of hydrogen ion concentration in the filtrate is of very great practical interest because pH determination is the quickest means of control of the finished product in a flow process. Measurements reveal that pH values of less than 5.5 in the filtrates indicate nearly complete deionization of the hydrolyzate; pH values between 5.5 and 3.5 correspond to chloride ion contents in the filtrate of not more than 2.0%. pH values of less than 3 indicate inadequate demineralization of the hydrolyzate.

SUMMARY

1. Grades ÉDÉ-10P and AN-2F of anion-exchanging resins were shown to be applicable for removal of the hydrolyzing agent from protein hydrolyzates.

2. Utilization of ion-exchanging resins (AN-2F and ÉDÉ-10P) is not accompanied by serious losses of the amino nitrogen of the hydrolyzate.

LITERATURE CITED

[1] E. B. Trostyanskaya and A. B. Pashkov, Khim. Nauka i Prom. 11, 5, 593 (1957).

[2] A. B. Davankov and V. M. Laufer, Zhur. Priklad. Khim. 29, 1952 (1956); 29, 1029 (1956); 30, 839 (1957); 31, 494 (1958). •

[3] V. V. Rachinskii and T. B. Gapon, Chromatography in Biology [in Russian] (Acad. Sci. USSR Press, 1953).

[4] V. M. Rodionov and N. G. Yartseva, Izvest. Akad. Nauk SSSR, Otdel. Khim. Nauk, 1, 108 (1950).

[5] A. B. Davankov and V. M. Laufer, Avtor. Svid. No. 107254, December 13, 1956.

Received July 21, 1958

• Original Russian pagination. See C. B. translation.

INVESTIGATION OF THE CATALYTIC CONVERSION OF METHANOL TO FORMALDEHYDE IN A FLUIDIZED CATALYST BED

M. V. Polyakov, V. V. Shalya and Z. Z. Vysotskii

On the industrial scale methanol is now converted to formaldehyde [1-4] by direct oxidation over catalysts of the molybdenum oxide type [1, 2] starting from a methanol–air mixture containing 5-10% of methanol, or by combined oxidation and dehydrogenation over silver catalysts [2] starting from a methanol–air mixture with an optimum CH_3OH content of 37-45% [3]. All of the existing industrial plants operate with a fixed bed of catalyst supported on pumice or another similar carrier. Copper was previously used as a catalyst in this reaction but has been replaced by silver due to the low yields of formaldehyde over a fixed bed of copper.

The ranges of methanol contents in the process mixture mentioned above are fairly narrow and fix the lower and upper explosion limits of methanol–air mixtures under normal conditions.

It was previously shown [4] that the reaction in question is a chain process with a heterogeneous–homogeneous mechanism [5] which is very common in thermal gaseous reactions. There are grounds for assuming that the character of the process, in particular the catalytic selectivity, is profoundly governed by the ratio of the initiating (surface) and successive homogeneous steps of the process. In this connection the possibility of changing the distance between the catalyst grains during an experiment is an important requirement for the study of such reactions. If the other conditions of the heterogeneous step were kept constant, it would then be possible to change the conditions of development of the homogeneous steps of the process. This requirement can be most conveniently satisfied by carrying out the reaction in a fluidized bed of catalyst.

The application of fluidized catalysis to this reaction would appear expedient also because it would very greatly facilitate the study of the hitherto neglected explosive region of the methanol–air mixture. Finally, a fluidized bed of catalyst might be expected to give better results with our selected catalyst–copper–than a fixed bed.

The aim of the present work was to study the conversion of methanol to formaldehyde in presence of a fluidized bed of copper catalysts with special consideration of the course of the process in the explosive region and of the occurrence of homogeneous reaction steps at the catalyst surface and inside the bed itself (between the grains of catalyst).

EXPERIMENTAL

Preparation of Catalysts. Powdered catalysts of the following types were prepared and tested: 1) Nonporous copper in the form of filings from a piece of pure copper; 2) porous copper prepared by reduction of copper oxide powder with hydrogen; 3) nonporous copper in the form of regular microspheres (obtained by passing copper filings, pieces of cut wire or nonporous copper powder through the flame of an oxygen torch and allowing the products to fall into water in a beaker where all of the particles solidified to small regular spheres whose diameter could easily be regulated by starting with copper particles of suitable dimensions); 4) microspheres of copper–silver alloys (1, 5, 10 and 25% Ag); 5) copper deposited on pumice from aqueous or aqueous methanolic solutions of copper nitrate or formate; 6) copper deposited by the same method on silica gel (during catalysis at above 300°, copper is oxidized by atmospheric oxygen and reacts with the silica gel to form copper silicate which retains a considerable proportion of the porosity of the original silica gel and functions in turn as a good carrier).

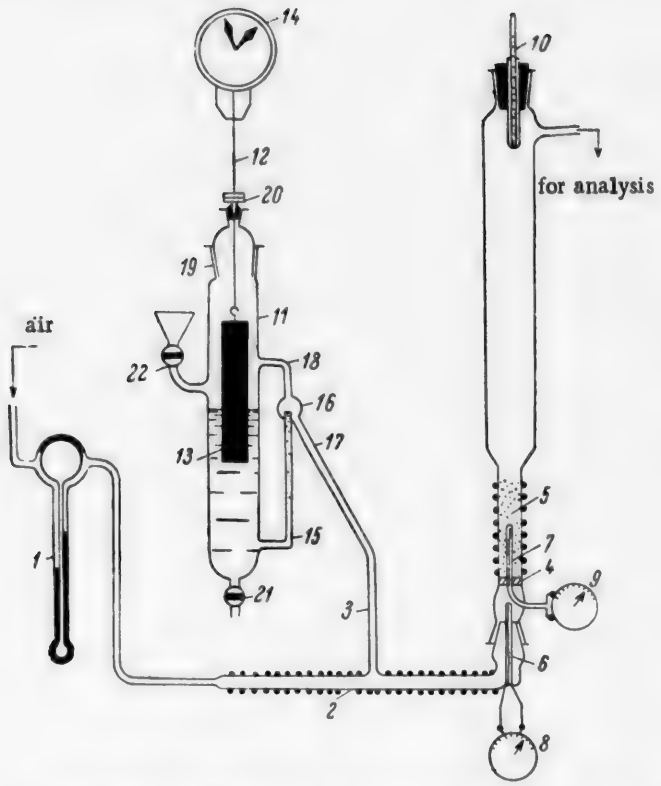

Fig. 1. Diagram of apparatus for investigation of the conversion of methanol to formaldehyde in a fluidized catalyst bed.

The prepared catalysts were screened on sieves to fractions of the required sizes before being charged into the reactor.

Apparatus. Experiments were run in a dynamic apparatus (Fig. 1). Air from flowmeter 1 entered vaporizer 2 from which it took up methanol vapor (methanol was admitted from a proportionator via tube 3). The methanol–air mixture passed through porous quartz screen 4 into a bed of powder catalyst 5. Temperature at the reactor inlet in the bed and at the outlet were measured with chromel–alumel thermocouples 6 and 7 (provided with pyrometers 8 and 9) and with an ordinary thermometer 10 respectively. The upper widened part of the reactor served to slow down the gas rate and so avoid entrainment of catalyst particles. The vaporizer and reactor were fabricated of quartz and fitted with regulatable electric heaters.

Proportioning of the Methanol. The proportionator takes the form of a cylindrical glass vessel 11 (Fig. 1) with a diameter of about 70 mm. In this is suspended (by wire 12) a cylinder 13 which displaces liquid methanol from vessel 11. The rate of immersion of cylinder 11 is regulated by the clockwork mechanism 14. The displaced methanol passes through elbow 15, bulb 16, and outlet 17 into pipe 3 and then into the vaporizer. Tube 18 serves to maintain a constant pressure over the liquid in vessel 11 and in bulb 16 in the event of pressure fluctuations in the vaporizer. The tightness of the system is ensured by the ground-glass closure 19 and the gasket 20. Taps 21 and 22 are intended for admission and run-off of liquid. The rate of admission is varied either by changing the rate of immersion of cylinder 13 or by replacing cylinder 13 by one of another diameter while keeping the rate of immersion unchanged. The proportionator operated satisfactorily with admission rates of 0.3 to 11.0 cm^3 of methanol or aqueous methanol per minute under an excess pressure in the system of 30-50 cm water.

Analysis of Products. The mixture of products discharged from the reactor consisted of CH_2O, CH_3OH, CO_2, CO, H_2, H_2O, CH_4, and (in some experiments) O_2. It was passed through traps containing distilled water in

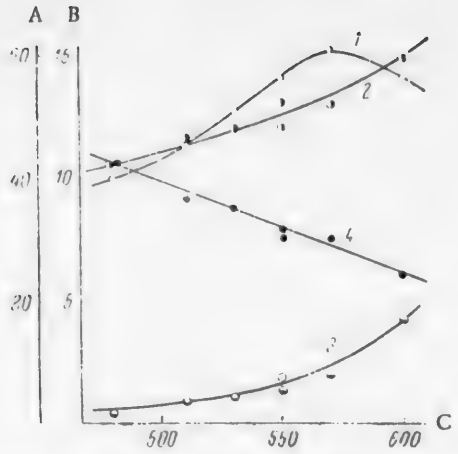

Fig. 2. Yield of reaction products as a function of the temperature. Space velocity $\underline{v}$ = 2.17 liter/min, CH_3OH content of mixture 38%. A) Yield (in %) of CH_2O (1); B) yield (in %) of H_2 (2); CO (3), CO_2 (4); C) temperature (°C).

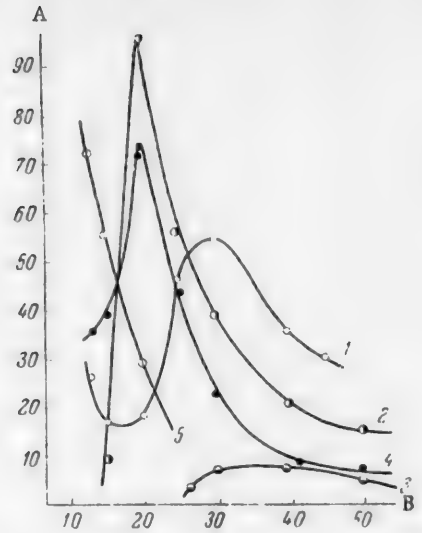

Fig. 3. Yield of products as a function of the CH_3OH content of the mixture at 520°. A) Yield (in %) of CH_2O (1), H_2 (2), CO (3), CO_2 (4), O_2 (5); B) CH_3OH content (in %).

Yield of Products of Oxidation of CH_3OH Under Boiling-Bed and Fixed-Bed Conditions Starting From a Mixture Containing 3% CH_3OH, Space Velocity 2940 cm^3/min.

Quantity of catalyst (ml)	State of bed	Temp. of experiment (°C)	Yield of CH_2O (as % of CH_3OH)	% composition of exit gases*		
				CO_2	O_2	CO
3	"Boiling"	550	12.0	2.2	17.3	0.2
		530	16.5	2.2	17.6	0.2
		510	14.4	2.3	17.2	0.1
	Fixed	550	2.5	2.6	16.6	—
		530	7.0	2.4	16.6	1.1
		510	8.7	2.5	17.2	0.7
6	"Boiling"	550	16.2	2.4	17.0	0.4
		530	21.0	2.3	17.3	0.3
		510	22.8	2.4	17.2	0.2
	Fixed	550	3.7	2.7	16.5	0.3
		530	10.3	2.5	16.8	0.8
		510	12.3	2.8	16.6	0.4

* Hydrogen and other gases were not determined in the analysis.

which the water vapor condensed and CH_2O and CH_3OH dissolved. The solution in the traps was analyzed by standard methods in an Orsat apparatus.

EXPERIMENTS WITH UNSUPPORTED METAL CATALYSTS

The first experiments were run with pure copper filings with particle sizes of less than 150-200 μ. Maintenance of this catalyst in the suspended state calls for high linear flow rates of the order of 3 m/sec. These catalysts fluidized satisfactorily but they balled up [6] when the temperature of the bed was raised to 300-350° and the bed ceased to "boil".

We next prepared and tested microspheres of pure copper. Results of these experiments show that the bed continues to boil even at temperatures of up to 500°, i.e., they show that the shape of the particles affects their

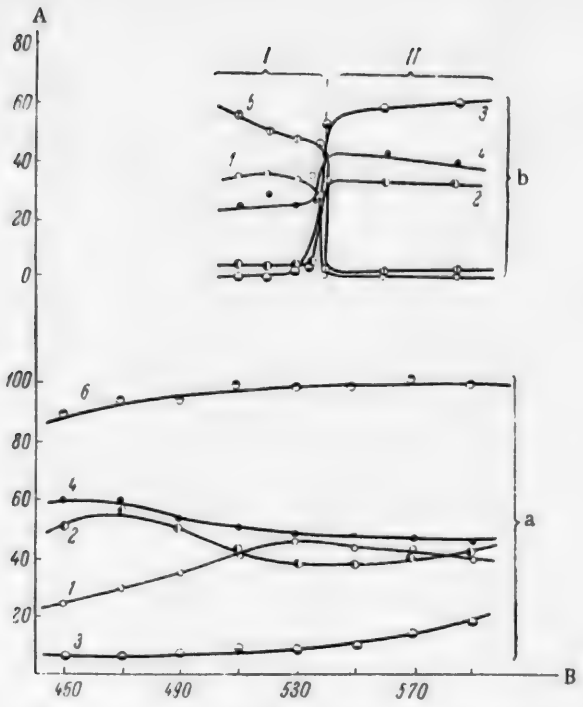

Fig. 4. Yield of products as a function of the temperature for highly active (a) and less active (b) catalysts. a) 20% CH_3OH, v = 2.21 l./min., 25 cm^3 of catalyst; b) 16.8% CH_3OH, v = 4.69 l./min., 6 cm^3 of catalyst. A) Yield (in %): 1) CH_2O, 2) H_2, 3) CO, 4) CO_2, 5) O_2, 6) over-all conversion of CH_3OH; B) temperature (in °C). I) No flame, II) flame over catalyst.

susceptibility to form aggregates. However, even these specimens balled up and even fused at 500° and higher. Similar results were obtained with spherical copper–silver catalysts.

EXPERIMENTS WITH SUPPORTED CATALYSTS

Employment of porous supports (pumice, silica gel) prevented balling-up and fusion of the catalysts and at the same time increased their specific surface. Catalysts of this type were studied with reference to the dependence of yield on quantity of copper on the support, on the reaction temperature, on the quantity of catalyst in the reactor, on the rate of the gas stream, on the methanol content of the starting mixture, and on the additions of water to the methanol. In this connection special attention was paid to the methanol concentration range in which a flame appeared at a bed of not too active catalyst. This is the harmful homogeneous tail-off region. In some experiments a comparison was also made of the results for a fluidized and a fixed bed of a catalyst of the same composition.

During the investigation we established that the maximum yield of CH_2O corresponds to 24 mg copper per cm^3 of carrier in all cases. It should also be noted that the yield of CH_2O at a "boiling" bed of supported copper catalyst slightly exceeded, even in the first experiments, that previously obtained in industry at a fixed bed of copper catalyst (54-58%).

Typical curves of yield of products as a function of the temperature in the region of compositions of starting mixture outside the explosive limits are presented in Fig. 2. It is especially noteworthy that the course of the CH_2O curve, whose maximum is usually in the 540-580° region, corresponds to a temperature lower than that under fixed-bed conditions in industry (700-750°). Lowering of the CH_2O yield with rising temperature is accompanied by rapid rise of the CO and H_2 contents of the exit gases, reflecting the start of thermal breakdown of the formaldehyde.

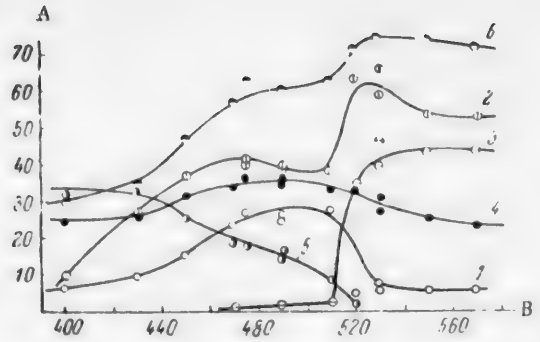

Fig. 5. Yield of products as a function of temperature for a catalyst of intermediate activity; 25% CH_3OH, v = 2.21 l./min., 10.5 cm^3 of catalyst. A) Yield (in %) of 1) CH_2O, 2) H_2, 3) CO, 4) CO_2, 5) O_2, 6) degree of conversion; B) temperature (in °C).

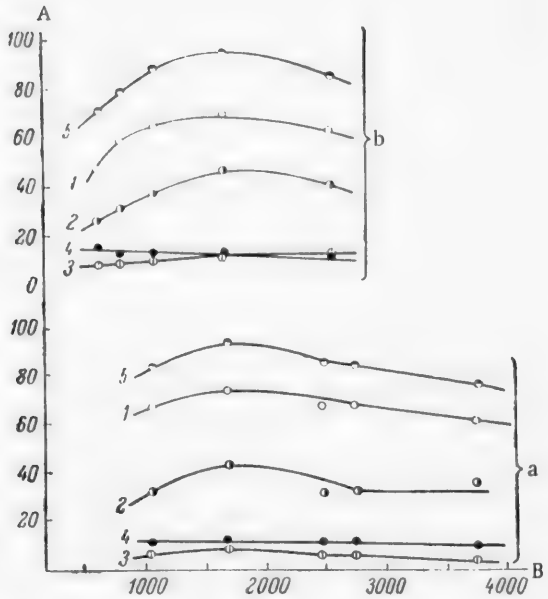

Fig. 6. Yield of products as a function of the gas velocity at 590°, starting from a mixture containing 32% CH_3OH in presence of various catalyst quantities in the reactor: a) 15 cm^3, b) 25 cm^3. A) Yield (in %) of 1) CH_2O, 2) H_2, 3) CO, 4) CO_2, 5) degree of conversion of CH_3OH; B) gas velocity (cm^3/min).

Figure 3 contains curves of yield of products as a function of the methanol content of the starting mixture in a wide range of concentrations. These curves show that in the explosive region the CH_2O yield drops sharply at the same time as the CO_2 and H_2 yields rise appreciably (and also the CO yield at higher temperatures). With closer approach to the lower explosive limit (7%) the CH_2O yield again rises. Similar curves were obtained for temperatures of 540, 560 and 580°. In all of the cases the maximum of yield corresponded to 30% CH_3OH in the mixture. In isolated cases a stationary flame was observed in the 9-20% CH_3OH range in the methanol–air mixture over the catalyst bed; in other cases a rapid flash or even a detonation occurred. For this reason the explosive region and the adjacent regions of compositions of the mixture were investigated more closely.

Curves of the temperature dependence of product yields for highly active and less active catalysts are compared in Fig. 4. In the case of a less active catalyst the curves suddenly change direction when 540-545° is reached; at this point a stationary flame is developed at the catalyst.

Similar curves are plotted in Fig. 5; their course resembles that of the curves for the less active catalyst, but in this case no flame was observed at the catalyst bed when the activity of the catalyst and its quantity were altered. Comparison of Figs. 4 and 5 indicates that the homogeneous step of the process (accompanied by a flame at the bed) is a sequel to preceding homogeneous steps which proceed at the bed and evidently also between catalyst grains without development of a flame.

Similar results were obtained for a whole series of compositions of the alcohol–air mixture containing from 17 to 36% of CH_3OH. These data (and other data not presented here due to lack of space) are evidence that the curve of degree of conversion of CH_3OH versus temperature changes in a regular manner with the composition of the mixture.

Further confirmation of the existence of homogeneous steps was obtained in later comparative experiments in which, other conditions being kept constant, in one case the catalyst was kept fluidized while in another case the "boiling" bed was artificially compressed and changed into the usual fixed bed. The results (see table) show that under fluidized bed conditions the yield of CH_2O is higher than in the case of the fixed bed. Starting from these data and from earlier data obtained by the method calorimetric determinations [7] in our laboratory which showed that the predominating proportion of the CH_2O is formed in a homogeneous step of the process, we can conclude that compression of the bed (which results in shortening of the distance between the catalyst particles) is unfavorable to the occurrence of such homogeneous steps and therefore leads to a lower yield of CH_2O.

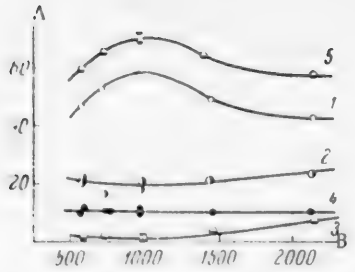

Fig. 7. Yield of products as a function of the gas velocity in presence of copper supported on nonporous quartz at 570°; 37% CH_3OH; 15 cm^3 catalyst. A) Yield (in %) of 1) CH_2O, 2) H_2, 3) CO, 4) CO_2, 5) degree of conversion; B) velocity of stream (in cm^3/min).

In connection with the foregoing considerations, great interest is attached to the results of a study of the relation between the yield of products and the speed of the gas stream (Figs. 6 and 7).

Typical results with different amounts of catalyst are plotted in Fig. 6. The different plots are noteworthy for the characteristic course of the curves of yield of CH_2O and H_2 and of the over-all conversion; they all exhibit a maximum at a certain gas rate. Each of these curves has a right-hand descending branch because with increasing gas rate the proportion of unreacted methanol also increases. The left-hand descending branch of each curve is more unusual. It is not logically accounted for within the framework of the usual theory of heterogeneous catalysis. On the basis, however, of the theory of heterogeneous-homogeneous catalysis, we can interpret the fall in yield of CH_2O and H_2 and the simultaneous fall in degree of CH_3OH conversion with falling gas rate as the result of gradual compression of the bed. This process would lead to a less well-developed homogeneous reaction step in the space between the catalyst grains and would accordingly lower the intensity of the over-all reaction.

Corresponding results are plotted in Fig. 7 for copper on nonporous quartz. Here we see that also in this case the general law applies, and the yield of CH_2O is nearly equal to the yield on pumice–supported copper.

DISCUSSION OF RESULTS

Existing methods of detection and study of the homogeneous steps of complex heterogeneous-homogeneous processes [7-13] are only applicable when a reaction takes place in a fairly wide vessel on the walls (or in the central part) of which the catalyst is distributed. Under the usual conditions of catalytic reactions, when the entire volume of the reaction zone is filled with particles of catalyst, these methods are unsuitable.

On the other hand, the fluidized method, which we employed with the objective of investigating the homogeneous steps under conditions approximating to those of ordinary catalysis in a fixed bed, enabled us to obtain new data which support the hypothesis of the occurrence of homogeneous steps between the particles in the catalyst bed.

The formation of flames at the catalyst bed, often observed also at a fixed bed (the harmful "homogeneous tails" at the bed) are actually evidence that homogeneous steps can occur to a considerable extent under favorable conditions. These steps originate at the surface of the catalyst as in our case, but under other conditions [14], when the reactor surface at the catalyst bed is overheated, they can also be initiated by the surface of the reactor constructional material.

The occurrence of such less intensive homogeneous steps between the catalyst grains (which also result in a more selective reaction) is supported by the following experimental observations in the course of the present work: 1) Gradual change of form of the product yield versus temperature curves (Figs. 4 and 5) up to the stage of appearance of a flame at the bed (it is evident that the homogeneous flame at the bed is the sequel to the primary homogeneous steps that occur in the voids between the catalyst particles); 2) fall of CH_2O yield on transition from a "boiling" to a fixed bed of the same catalyst (see table); in this case the compression of the particles, which reduces the voids between the particles, introduces less favorable conditions in the voids for the homogeneous step during which most of the formaldehyde is formed; 3) decrease in yields of CH_2O and H_2 and of the over-all conversion with falling gas rate; this can only be explained by the gradual contraction in the volume of the bed when the gas rate is reduced and, as in the preceding case, by less intensive development of homogeneous steps in the catalyst bed; 4) identical mechanism (and yield of products) with a porous support (pumice) and a nonporous support (quartz), demonstrating that only the outer layer of catalyst grain is active and thus providing indirect evidence for the heterogeneous-homogeneous mechanism of the catalytic reaction.

During the investigation we frequently observed that reaction in a "boiling" bed of catalyst apparently lowers the explosive risk with mixtures of methanol and air. There are two reasons for this. Firstly, the design of the apparatus in the fluidized process is such that the reaction mixture always enters the catalyst bed from below by way of a porous plate without passing through the free space of the reactor. Secondly, the free space inevitably contains suspended particles of the finest fraction of catalyst on which the gas-phase chains can be broken. At the same time we could not altogether prevent explosions. In the region of mixtures poor in methanol, the oxygen is not fully consumed, and under certain conditions a highly explosive mixture containing oxygen and reaction product (hydrogen) is present at the bed. An explosion of this mixture cannot be prevented by the small quantities of fine particles from the catalyst bed suspended in the reactor space.

The results of the work demonstrate that pure, unsupported metallic catalysts are unsuitable for operation of this process in a fluidized bed. At the same time (see Figs. 6 and 7), the results show that the yield of CH_2O on pumice- or quartz-supported copper reaches 70% and higher, which considerably exceeds the earlier yield on a fixed bed of copper catalyst. Moreover the reaction temperature is appreciably lowered. These data indicate that supported copper catalysts in a fluidized beds are of potential interest from the industrial aspect.

SUMMARY

1. The technique of catalysis in a fluidized bed is employed in a study of the conversion of methanol to formaldehyde in presence of a copper catalyst. A wide range of compositions of methanol–air mixtures was studied, including the explosive region.

2. A number of experimental results are obtained that lend support to the hypothesis of the occurrence of the homogeneous steps of the over-all heterogeneous-homogeneous conversion of CH_3OH to CH_2O not only at the catalyst bed but also inside it, i.e., between the catalyst particles.

3. It is shown that a catalyst in the form of copper deposited on a porous support (pumice) or on a non-porous support (quartz) enables a considerable increase in the yield of CH_2O (to 70-74%) calculated on the CH_3OH passed through the bed. This is of practical interest.

LITERATURE CITED

[1] H. Adkins and W. R. Peterson, J. Am. Chem. Soc. 53, 1512 (1931).

[2] R. N. Hader, R. D. Wallace and R. W. McKinney, Ind. Eng. Ch. 44, 1508 (1952).

[3] E. Jones and G. G. Fowlie, J. Appl. Chem. 3, 206 (1953).

[4] I. M. Loos and M. V. Polyakov, Ukrain. Khim. Zhur. 24, 190 (1958).

[5] M. V. Polyakov, Uspekhi Khim. 17, 351 (1948).

[6] M. É. Aérov, Zhur. Khim. Prom. 5, 227 (1951).

[7] M. L. Bogoyavlenskaya and A. A. Koval'skii, Zhur. Fiz. Khim. 20, 1326 (1946).

[8] F. M. Vainshtein and M. V. Polyakov, Zhur. Fiz. Khim. 15, 164 (1941).

[9] P. Yu. Butyagin and S. Yu. Elovich, Doklady Akad. Nauk SSSR 54, 607 (1946).

[10] Dim. Vladov, Yearbook of Phys. Math. Faculty Univ. Sofia, Book 2 (Chemistry), Part II (1953/1954); Doklady Akad. Nauk SSSR 109, 561 (1956).

[11] M. Vanpee, Bl. Soc. chim. Belges 62, 468 (1953).

[12] A. M. Markevich, Zhur. Fiz. Khim. 30, 735 (1956).

[13] P. G. Ivanov and A. A. Balandin, Doklady Akad. Nauk SSSR, 119, 4, 727 (1958).*

[14] P. M. Stadnik and M. I. Golovei, Ukrain. Khim. Zhur. 23, 728 (1957).

Received August 15, 1958

* Original Russian pagination. See C. B. translation.

POLYAMIDE POWDER SORBENTS FOR DETERMINATION OF TANNIDES

P. Ya. Frenkel' and A. N. Mikhailov

In 1954-1955 in the tanning materials laboratory of the Central Scientific Research Institute of the Leather Industry (TsNIKP), a new method was evolved for determination of tannides and their substitutes with the help of a polyamide sorbent in place of hide powder.

The new analytical method is based on the fact that polyamides obtained in the form of highly dispersed powders after hydrolysis and reprecipitation are characterized by intensified ability to absorb natural tannides and other sulfoaromatic tanning substances. Polyamides bind tannides because, like proteins, they contain active peptide groups $-CONH-$ and a certain number of free amino groups $-NH_2$ [1, 2]. For analytical purposes an efficient method of preparation of standard samples of powdered sorbents from polyamide resins was developed. The special features of the method are direct precipitation of finely dispersed, highly absorbent powders not requiring further pulverization, and enrichment of the preparations during hydrolysis with free amino groups. These procedural features ensure high sorptive properties of the polyamide sorbents obtained by the TsNIKP method. Preparation of the polyamide powder sorbents is characterized by simplicity and cheapness.

Formation of the sorbents directly after reprecipitation in the form of highly dispersed powders by the TsNIKP method is in fundamental contrast to foreign methods whereby the polyamides are obtained after reprecipitation in the form of clots or a solid fibrous material which requires pulverization. The heat generated during grinding in a ball mill, as reported in an earlier paper [3], evidently diminishes the reactivity of the active groups of the polyamide and lowers the sorptive capacity, especially for the tanning fractions of syntans [4].

The method developed by the TsNIKP gives fine, highly dispersed powders directly after reprecipitation. The particle size of our polyamide powders is below the resolving power of the microscope. Electron-microscopic studies of preparations of caprone powders were carried out.* Electron microphotographs of the thoroughly triturated aqueous dispersion were obtained. The contrast was improved by rubbing with chromium. The instrument was a UM-100 electron microscope operating on 60 kv. The electron micrographs (diagram, a and b) of the polyamide (capron) sorbert show that the particles are predominantly oblong and not more than a few microns in radius. The electron micrographs therefore demonstrate the high degree of dispersity of the prepared powders.

The size of particles of capron polyamide sorbent was characterized by the method of determination of the end groups by titration of the polyamide as an amphoteric compound with 0.01 N solutions of acid and alkali (in separate samples). This procedure is based on the assumption that the functional end groups remain intact after reprecipitation [5]. The structure of capron resin (product of condensation of caprolactam) is:

$$H_2N-(CH_2)_5-CO-[-NH-(CH_2)_5-CO-]_n-NH-(CH_2)_5-COOH.$$

This simple method was applicable because of the adequate wettability in association with the complete insolubility of the polyamide preparations in water.

The molecular weight of capron polyamide before and after reprecipitation (according to the technique of end-groups determination) is given on the following page:

*The electron microphotographs were taken by A. L. Zaides.

Preparation	Molecular weight
Capron resin ("crumb" for stocking rayon), mechanically pulverized	13,300
Capron powder preparations obtained by hydrolysis under following conditions:	
3 days and 20°	6600
6 days and 20°	5900
0.25 day and 65-70°	4570

TABLE 1

Sorption of Tannides from Solutions of Vegetable Tanning Extracts

Extract	Using polyamide sorbent		Using hide powder (GOST method)	
	in % of wt. of extract	efficiency (in %)	in % of wt. of extract	efficiency (in %)
Russian				
Oak (tannides of oak bark), specimen:				
I	53.2	60.7	52.8	60.1
II	46.0	55.1	45.4	54.4
III	42.9	56.7	42.7	56.4
IV	46.9	57.7	47.3	58.3
Willow (tannides of willow root), specimen:				
I	44.7	52.7	44.5	51.9
II	40.0	49.5	40.7	50.4
	38.3	54.2	37.4	53.0
Fir (tannides of fir bark)	41.8	47.6	40.8	46.6
Snakeweed (tannides of snakeweed root)	44.3	51.7	42.9	50.6
Imported				
Oak (tannides of oak galls)	66.5	84.6	64.6	82.6
Quebracho (tannides of quebracho wood)	69.9	89.5	70.2	89.9
Chestnut (tannides of chestnut wood)	64.8	78.0	63.3	76.0

The molecular weight of capron resin is usually determined at artificial fiber plants from the viscosity of a 1% solution of the polymer in cresol or sulfuric acid [6] and amounts to approximately 16,000.

The increase in the number of end groups after the resin had been held in acid for several days showed that partial hydrolysis evidently took place throughout the chain. Rise of hydrolysis temperature to 65-70° had an unfavorable influence on the sorptive capacity of the preparations. It was found desirable to keep the temperature of dissolution of the resins within the limits of 25 ± 3°.

Numerous exploratory analyses (over 1000) showed that polyamide powder preparations easily absorb tannides and their substitutes from solutions of various plant extracts, synthetic tanning agents, and commercial tan liquors. The use of a polyamide sorbent does not call for introduction of correction or conversion factors. Results have been published of test analyses in comparison with BEM analyses, together with curves of sorption of tanning agents by different amounts of polyamide [3]. The same publication described a series of undoubted advantages of the analytical polyamide method as confirmed in practice. The most outstanding of these advantages are the simplicity and relative speed of the analyses [3].

After extensive trials, the polyamide method was accepted in the industry at the start of 1956 and since then it has been continuously applied to the analysis of industrial tanning liquors.

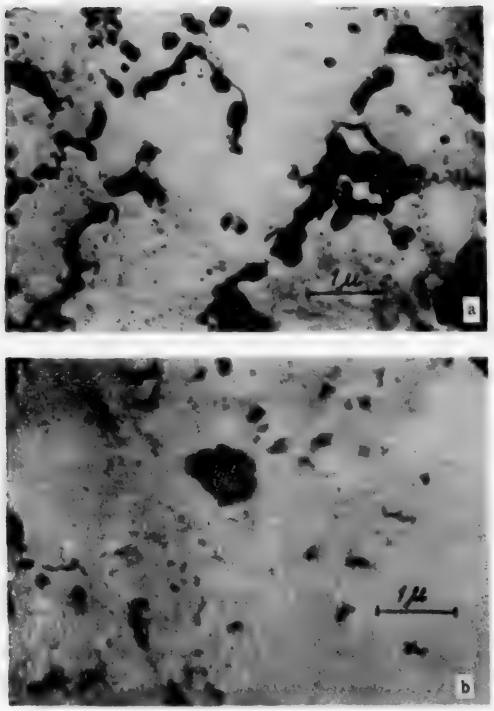

Electron photomicrograph of capron polyamide sorbents.

Shortly afterwards, in July 1956, an investigation of the TsNIKP polyamide sorbent led the Ukrainian Scientific Research Institute of the Leather Industry (UkrNIKP) to recommend the method to laboratories in the industry for the determination of tannides in tanning extracts.

Typical results set forth in Tables 1 and 2 show the similarity between the values of sorption of tannides and their synthetic substitutes from solutions of various tanning preparations obtained with polyamide sorbent (in suitable proportions) and the values obtained in GOST analyses with the help of hide powder.

The similarity of absorption of tannides in both of the cases is noteworthy since it indicates the possibility of replacement of hide powder (pulverized hide tissue) by the polyamide sorbent. The natural protein material (containing collagen) is thus replaced by a powder preparation of a polyamide which functions in sorption of tannides as a synthetic analog of protein.

The mean accuracy of the new method, calculated for various tanning agents, meets the GOST specification [3]. Sorption curves of tannides and their substitutes were reproducible with different preparations of capron sorbent [3]. The sorbent was used in determination of tannides in the proportion of 2.5 g dry powder for 25 ml of analyzed solution, since this amount is within the saturation region of the polyamide [3]. Analyses by both of the methods were carried out in solutions of vegetable extracts at the natural pH value (4.5-5.0) and with a tanning agent concentration in the analytical solutions of 7.5-9.0 g/liter. Synthetic tannins were analyzed at pH = 3.5-4.0 and a concentration of 4.0-4.5 g/liter. Complete absorption of the tannides (detannization) was effected in 10 minutes.

Auxiliary syntans AN and NK (sulfoaromatic acids of anthracene and naphthalene) were sorbed more weakly than the other tanning agents by the polyamide sorbent because their only active groups are SO_3H groups and they are bound only at the amino groups of the sorbent, whereas other syntans contain OH and SO_3H groups. Lignosulfonic acids and their salts (sulfite cellulose extracts) contain, in addition to SO_3H groups, a negligible number of hydroxyl groups and are likewise weakly sorbed by polyamide powders.

The objective of universal adoption of the polyamide method of determination of tannides in our tanning extract and leather industries will be realized only when supplies of polyamide sorbent are available on the industrial scale. The efficient method of preparation of the sorbent developed at the TsNIKP enables the powder preparations to be obtained both from acid-soluble polyamide resins of regular structure and from alcohol-soluble modified resins. Good powder sorbents have thus been obtained from polyamides of various structures: from the acid-soluble resin capron, from products of polycondensation of caprolactam with AG salt and also with AZG salts (salts of adipic or azelaic acid and hexamethylenediamine).

The similar sorptive properties of the various polyamide sorbents is demonstrated by analyses of willow extract carried out in the analytical laboratory of TsNIKP using two samples of sorbent: a sorbent on a capron basis (I) and a sorbent on the basis of an alcohol-soluble modified resin (II). Deviations from the results of analyses with hide powder are insignificant and lie within the limits of accuracy of the analysis (Table 3).

Numerous experiments showed that the determination of the free amino groups by the polyamide titration method (acid capacity) is an important criterion which correlates with the sorbent properties of the preparation. For normally sorbing powders the acid capacity is between 7.5 and 8.5 ml of 0.01 N HCl per 1 g of dry sorbent. There is an optimum range of acid capacities which is reached under certain technological conditions (hydrolysis temperature, drying temperature) and sorption of tannides is at an optimum in that region (Table 4).

TABLE 2

Sorption of Tanning From Solutions of Synthetic Tanning Agents

Syntan	Materials from which synthesized	Active groups of the syntan	Sorption (in % of dry substance of syntan)	
			using polyamide sorbent	using hide powder (GSTU method)
Syntans – substitutes for tannides				
PL	From bituminous coal polyphenols, formaldehyde and lignosulfonates	OH, HSO_3	51.5	50.2
SPS	From shale polyphenols, formaldehyde and lignosulfonates	OH, HSO_3	47.0	46.5
PS	From bituminous coal polyphenols, sulfite and formaldehyde	OH, HSO_3	63.5	63.9
Syntan No. 4	From bituminous coal polyphenols, β-naphthol, formaldehyde and sulfuric acid	OH, HSO_3	70.6	70.0
Amphoteric type MPK	From shale polyphenols, formaldehyde and urea	OH, NH_2	56.2	56.4
Auxiliary syntans				
AN	From crude anthracene and sulfuric acid	HSO_3	36.0	38.1
NK	From naphthalene, sulfuric acid and formaldehyde	HSO_3	39.7	43.4
	Sulfite cellulose extract	HSO_3	30.0	33.7

It was established that the normal polyamide powder preparations from polyamides of various structures mentioned in Table 3 – capron (I) and copolymer (II) – had similar acid capacities in the region of 7.5-8.5 ml of 0.01 N HCl per 1 g of dry substance.

A study of the influence of the moisture content of the preparations on the sorption of tannides was very valuable. It was found that the optimum moisture content for sorption is 20 ± 2%.

The effect of the final moisture content of the sorbent on the sorption of tannides is shown on the following page.

The moisture content of polyamide powders (both capron and alcohol-soluble copolymer) must be brought to the indicated limits by gentle drying at room temperature or in a stream of air at a temperature of not higher than 35°.

The selection of optimum moisture content of the sorbents within the indicated limits is a fundamental point of difference between our method and foreign methods [4, 9]. It not only led to the attainment of a high

TABLE 3

Results of Analyses of Willow Extracts

Data for	Analytical data (in %) and pH value					
	with hide powder		with polyamide sorbents			
			I		II	
	normally moist substance	absolutely dry substance	normally moist substance	absolutely dry substance	normally moist substance	absolutely dry substance
Moisture	19.2	0	19.2	0	19.2	0
Dry residue	80.8	100.0	80.8	100.0	80.8	100.0
Solubles	77.7	96.2	77.0	96.2	77.7	96.2
Insolubles	3.1	3.8	3.1	3.8	3.1	3.8
Non-tannides (stirring)	37.0	45.4	37.7	46.7	37.9	46.9
Tannides	40.7	50.4	40.0	49.5	39.8	49.3
Grading	52.4	52.4	51.5	51.5	51.3	51.3
pH of analytical solution	5.3	5.3	5.3	5.3	5.3	5.3
Color of detannized solutions of non-tannides	Similar in all cases					

TABLE 4

Acid Capacity and Sorption of Tannides

Form of preparation	Hydrolysis conditions		Acid capacity (in ml 0.1 N HCl per 1 g of dry sorbent)	Sorption of tannides under conditions of analysis (in % of content in solution)
	period (in days)	temperature (°C)		
Mechanically pulverized capron fiber and resin	—	—	1.2–1.4	0
Powder preparations				
I	3	20	6.0–6.2	85–90
II	6	20	7.5–8.5	100
III	10	20	7.5–8.5	100
IV	0.25	65–70	14.6	70–75

Moisture content (%)	Sorption of tannides under conditions of analysis (in % of the content in the analytical solution)
3.5	87
7.0	91
18	100
20	100
22	100

sorptive capacity but also made the method practicable for series of routine analyses in industry. In foreign investigations [4] polyamide powders are used at very low moisture contents (3-8%) at which sorption is very low; another preparation [9], with 80% water content giving a paste, was impracticable for long series of routine analyses.

TABLE 5

Characteristics of the Hygroscopic Properties of the Polyamide Sorbent Capron

Relative humidity of air in desiccator (in %)	Humidity of sorbent aft. dehyd. (%, natural wt.) after expiration of following periods (days)					
	2	26	36	43	62	73
0	0.5	0.5	0.4	0.4	0.5	0.4
	0.6	0.7	0.5	0.5	0.6	0.6
20	1.8	1.9	1.9	1.9	1.8	1.8
	1.9	2.0	1.9	2.0	1.9	1.9
43	3.7	3.5	3.6	3.6	3.5	3.4
	3.6	3.5	3.5	3.5	3.5	3.3
66	7.9	7.2	7.2	7.3	7.2	6.8
	8.3	7.6	7.7	7.6	7.4	7.1
78	9.7	9.0	9.4	9.5	8.7	8.5
	10.7	8.4	8.2	8.2	7.5	7.2
91	17.2	13.9	14.5	14.4	13.3	12.3
	18.1	14.4	15.1	15.1	13.8	12.4
100	27.6	27.4	27.5	27.5	27.0	27.6
	27.9	27.1	27.4	27.0	27.1	27.8

Note: The moisture content of the original sorbent (before dehydration), determined by drying at 105°, was 28.9% of the natural weight.

Studies of the hygroscopic properties * of polyamide sorbent and practical experience showed that polyamide powders easily lose moisture. A preparation containing 28.9% moisture was dehydrated by keeping over solutions of various desiccants and was also kept under conditions of 100% relative humidity (over water). The relative humidity of the air in the desiccators was 0, 20, 43, 66, 78, 91 and 100%.

The investigations reported in Table 5 showed that the moisture content of a polyamide powder fell from 28.9 to 17-18% after the sample had been held for two days at a relative humidity of the air over the desiccant solution of 91%. Consequently, it is technologically desirable for attainment of the optimum moisture content of the sorbent (20 ± 2%) under the conditions of analysis of the tannides for the powder to be kept at the indicated relative air humidity (91%) for about 48 hours after pressing in the filter press or after drying in the air. When a sorbent is being used under plant conditions, it should be stored in closed desiccators or tightly closed containers in a cool, damp place; these containers are best placed in desiccators containing water. The experiments showed (Table 5) that the moisture content of the powder remained substantially constant when kept for 73 days at a relative atmospheric humidity of 100%.

There are definitely great potentialities for the application of polyamide sorbents which afford the possibility of a simply operated, convenient, and less time-consuming method of analysis of tannides.

Polyamide sorbents can also be successfully employed in column chromatography for such purposes as the fractionation of tan liquors and phenol mixtures, and for the isolation of materials containing phenolic hydroxyls or sulfonic acids such as lignosulfonic and sulfoaromatic acids. These sorbents can therefore find diverse and extensive application in analytical and applied chemistry.

LITERATURE CITED

[1] K. H. Gustavson, JALCA 47, 11, 700 (1952); J. Pol. Sci. 12, 316 (1954).

* Hygroscopic properties of polyamide sorbent (capron) were determined by Yu. B. Kavkazov and Z. A. Shilova.

[2] A. N. Mikhailov, Chemistry of Tanning Materials and Tanning Processes [in Russian] (State Light Industry Press, 1953) p. 485.

[3] P. Ya. Frenkel' and A. N. Mikhailov, Nauchno-Issled. Trudy TsNIKP 26, 26 (1956).

[4] H. Batzer, Makromol. Ch. 8, 183 (1952); "Leder" 8, 169 (1951); 2, 25 (1954).

[5] V. A. Zamyatina and V. V. Korshak, Izvest. Akad. Nauk SSSR 5, 480 (1945).

[6] Z. A. Rogovin, Chemistry and Technology of Artificial Fibers [in Russian] (State Light Industry Press, 1957).

[7] A. B. Pashkver and E. E. Mankash, Chemistry and Physical Chemistry of High-Molecular Compounds [in Russian] (Acad. Sci. USSR Press, 1952) p. 188.

[8] V. V. Korshak, Chemistry of High-Molecular Compounds [in Russian] (Acad. Sci. USSR Press, 1953) p. 481.

[9] M. Boix, AQEIC 5, 182 (1954); "Leder" 2, 38 (1956); abstract from Spanish.

Received March 10, 1958

HIGH-PRESSURE DESTRUCTIVE HYDROGENATION OF TUIMAZIN PETROLEUM

Ya. R. Katsobashvili and N. P. Volynskii

Institute of Petroleum AN SSSR

Work at the Institute of Petroleum AN SSSR [1] has shown that during the destructive hydrogenation of petroleum and petroleum residuums at low pressure (10-30 atm) and over an active catalyst, the temperature coefficient and the rate constant for the cracking reaction at temperatures of 410-450° are 1.3 and 0.05-0.20, respectively, while the rate constant for desulfurization is 0.36-1.06.

The low values of the temperature coefficient and cracking rate constant and the high value of the rate constant for desulfurization suggest that with an increase in reaction temperature, the desulfurization rate should increase to a greater extent than the cracking rate. This is important in the production of diesel fuels and fuels for reaction motors from high-sulfur crudes in a single-step process.

It was possible to avoid the acceleration of undesired reactions (aromatization, gas formation, and coke formation) associated with an increase in temperature by increasing the space rate, which, moreover, generally increased the conversion.

In the present work, we investigated the effect of temperature (500-540°), space rate (2-5 kg/liter/hour), and amount of feed charged per unit volume of catalyst on the hydrocracking of petroleum at a pressure of 30 atm. over a fixed bed of catalyst in a flow-type apparatus.

The catalyst used was No. 7360 commercial molybdena-alumina catalyst containing 14% MoO_3.

For the feed, we selected a Tuimazin crude having the following physicochemical properties: density (d^{20}_4), 0.8470; sulfur content, 1.34%; 46.7 wt. % boiling up to 300°.

The stainless steel reactor was charged with 0.8 liter of fresh catalyst (particle size $\approx 2 \times 2 \times 2$ mm). The mixture of feed stock and hydrogen was preheated to 400-420° and passed into the lower part of the reactor. The reactor was heated by a four-section electric furnace, which permitted us to maintain a uniform temperature along the height of the reactor. The reaction products and excess hydrogen were discharged into a condenser, and were then passed to a separator. After a predetermined amount of feed had been charged, the catalyst was purged with steam to remove adsorbed product.

The amount of coke on the catalyst was determined by elemental analysis.

A study of the dependence of catalyst activity on the length of the experiment (or on the amount of feed charged) showed that under the conditions used (a temperature of 520° and a space rate of 4 kg/liter/hour), it is advantageous to charge about 5 kg of feed per volume of catalyst (Figs. 1 and 2). When more than 7 kg of feed was charged, activity of the catalyst began to drop owing to coke formation, as may be seen from the increase in sulfur content of the liquid products; when 3.5 kg or less feed was passed over the catalyst, there was a greater effect on the adsorptive properties of the catalyst – coke formation and gas formation were accelerated, and, in connection with this, there was a decrease in the yield of liquid products. Therefore, in the experiments carried out to study the effects of temperature and space rate on the hydrocracking of petroleum, the amount of feed charged was constant at 5.1 kg per liter of catalyst.

Yields and Properties of the Products of Catalytic Hydrocracking of Tuimazin Crude Under Various Conditions. Operating Pressure – 30 Atm; Amount of Crude Fed – 5 kg per Liter of Catalyst

Expt. conditions		Yield (in wt. % of the crude)						Physicochemical properties of the products													
								total liquid products					1bp-180° fraction			180-300° fraction			residue > 300°	
temp. (°C)	space rate, kg/liter/hr	total liq. prods.	1bp-180° fraction	180-300° fraction	residue > 300°	300-400° fraction	residue > 400°	coke	density, d_4^{20}	sulfur cont. (%)	degree of desulf. hyr. %	unsaturates content (wt. %)	density, d_4^{20}	sulfur cont. (%)	unsaturates content (wt. %)	density, d_4^{20}	sulfur cont. (%)	unsaturates content (wt. %)	density, d_4^{20}	sulfur content (%)
450	1.0	89.6	29.5	32.9	27.2	—	—	3.10	0.8101	0.24	84.0	6	0.7283	0.020	5	0.8252	0.18	4	0.895	0.39
500	1.9	88.0	30.2	36.1	21.7	19.0	2.7	2.76	0.8050	0.19	87.5	7	0.7225	0.008	6	0.8257	0.21	6	0.910	0.47
	3.0	88.6	27.8	36.0	24.8	18.9	5.9	2.63	0.8106	0.28	81.5	11	0.7225	0.006	10	0.8227	0.22	8	0.912	0.56
	4.0	91.5	27.4	35.7	28.4	20.6	7.8	2.58	0.8174	0.39	73.4	12	0.7283	0.016	10	0.8263	0.35	8	0.907	0.73
520	1.9	85.1	36.2	33.5	15.4	11.8	3.6	2.71	0.7949	0.23	85.4	8	0.7195	0.010	7	0.8316	0.24	5	0.946	0.63
	3.0	88.3	34.8	34.2	19.3	15.4	3.9	2.69	0.8047	0.25	83.5	9	0.7219	0.006	10	0.8267	0.25	8	0.933	0.64
	4.0	86.7	29.7	33.7	23.3	18.7	4.6	2.79	0.8121	0.29	81.2	12	0.7287	0.016	11	0.8287	0.28	8	0.912	0.65
540	1.9	80.1	39.2	30.5	10.4	7.5	2.9	2.69	0.7976	0.16	90.5	7	0.7207	0.008	9	0.8402	0.18	7	0.989	0.61
	3.0	83.9	36.8	33.6	13.5	10.8	2.7	2.74	0.7973	0.20	87.5	10	0.7270	0.076	10	0.8369	0.25	8	0.964	0.63
	4.0	85.0	36.6	33.1	15.3	11.4	3.9	2.48	0.8076	0.25	84.1	12	0.7255	0.007	15	0.8363	0.30	10	0.953	0.69
	4.9	86.5	31.8	33.5	21.2	16.2	5.0	2.57	0.8173	0.34	78.1	15	0.7284	0.014	15	0.8315	0.34	11	0.927	0.78

In spite of the high temperatures of the process, an increase in space rate made it possible to obtain high yields of liquid products – 85-92 wt. % (see table).

As may be seen from the data in the table, the yield of coke was practically independent of space rate (2-5 kg/liter/hour) and temperature (500-540°) and comprised 2.6-2.8% calculated on the crude charged. The yield of the fraction boiling above 400° did not exceed 3-5 wt. % in the majority of the cases, which indicates a high degree of conversion of the high molecular weight fraction of the petroleum under the conditions studied.

The density of the fraction boiling above 300° increased appreciably with an increase in temperature and a decrease in space rate.

Turning our attention now to the increase in the degree of conversion of the high molecular weight hydrocarbons under these conditions, the conclusion is inescapable that the increase in density of the high-boiling fractions of the liquid products is explained not only by aromatization reactions, but also by the simple accumulation in these fractions of the aromatic hydrocarbons formed during the hydrocracking process and which have the greatest resistance toward hydrogenation.

The densities of the total liquid products and the fractions boiling up to 180° and from 180° to 300° change only insignificantly with a change in the temperature and in the space rate.

With a change in the space rate from 2 to 5 kg/liter/hour, the sulfur content of the total liquid products and of the 180-300° fraction increased only very slightly – from 0.2 to 0.3%; the sulfur content of the fractions boiling above 300°, which amounted to 0.6-0.8%, also depended but little on the space rate, especially at the higher temperatures (520-540°). This indicates a high desulfurization reaction rate, and this is determined by the activity of the catalyst and by the temperature of the process.

Hydrogenation reactions also proceeded to a considerable extent, as may be seen from the unsaturates content of the light and intermediate fractions. In spite of high space rates and, consequently, short contact times, the contents of unsaturates were not high at any of the temperatures and space rates studied, and they amounted to 7-15% in the fraction boiling from the initial boiling point of the product to 180° and 5-11% in the 180-300° fraction.

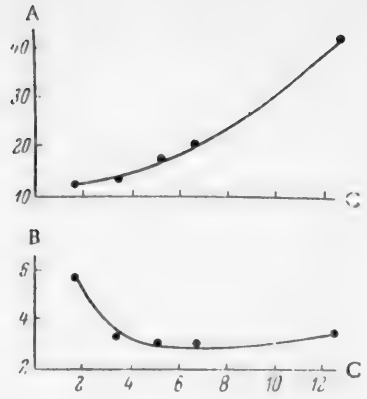

Fig. 1. Amount of coke on the catalyst and yield of coke as a function of the amount of feed charged per unit volume of catalyst. Temperature, 520°; space rate, 4 kg/liter/hour. A) Amount of coke on the catalyst (in %); B) yield of coke (in % of the crude); C) amount of feed (in kg of crude per liter of catalyst).

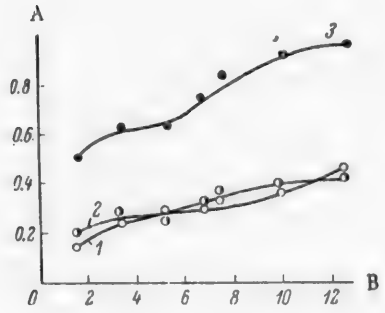

Fig. 2. Sulfur content of the total liquid products and of the fractions as a function of the amount of crude charged per unit volume of catalyst. Temperature, 520°; space rate, 4 kg/liter/hour. A) Sulfur content (in %); B) amount of feed (in kg of crude per liter of catalyst). 1) Total liquid products, 2) 180-300° fraction, 3) residue boiling above 300°.

The contents of aromatic hydrocarbons in the fractions boiling from the initial boiling point of the product to 180° and from 180° to 300° increased with an increase in temperature and with a decrease in space rate, and they amounted to 10-15% and 28-40 weight %, respectively, at all of the temperatures and space rates studied in the present work.

The increase in the yield of aromatic hydrocarbons with an increase in temperature and with an increase in contact time can be explained both by aromatization and dehydrocyclization reactions and by an increase in the degree of conversion of the high molecular weight hydrocarbons; the more difficultly hydrogenatable smaller molecules produced by the latter process go into the intermediate and, particularly, the lighter fractions.

SUMMARY

During an investigation of the conversion of Tuimazin crude by hydrocracking over commercial molybdena-alumina catalyst No. 7360 under a pressure of 30 atm , at a temperature of 500-540°, and at a space rate of 2-5 kg/liter/hour in a flow-type apparatus, it was shown that at an elevated temperature of 500-540°, the space rate can be increased to 5 kg/liter/hour while retaining sufficient depth of hydrogenation and desulfurization.

2. At the optimum space rate, a high yield of liquid products is maintained, 85-92 wt. %, and the degree of conversion of the high molecular weight fractions of the crude is high; the yield of the fraction boiling above 400° amounts to 3-5 wt. % of the crude.

LITERATURE CITED

[1] N. S. Kurkova, Candidate's Dissertation, (Moscow, 1956).

EMULSION COPOLYMERIZATION OF HEXAFLUOROBUTADIENE WITH DIENE COMPOUNDS*

A. L. Klebanskii and O. A. Timofeev

As is well known, the emulsion polymerization process has a number of features peculiar to it as compared to mass and dispersion polymerization, and it differs from the latter in complexity and in being a polyphase system. This complexity of the system has caused doubts that the rules governing copolymerization could be transferred to emulsion copolymerization. The literature contains only a few examples of the determination of copolymerization ratios in any monomer system , mass or emulsion [1], and these data are in disagreement in the individual cases. In addition, some authors have asserted that the method by which polymerization is carried out has no effect on the reactivity ratios.

This promoted us to investigate the extent to which reactivity ratios established during solution copolymerization of chloroprene and hexafluorobutadiene are applicable to the copolymerization of these monomers in an emulsion. Since the introduction of a second component, even in very small amounts, into polymerization to form a copolymer sharply changes the properties of the homopolymer as compared to those of the copolymer, it appeared to be of interest to study the effect of hexafluorobutadiene on the properties of copolymers with the indicated monomers.

The experimental method has been described previously [2].

The Effect of a Number of Basic Factors on the Rate of the Emulsion Copolymerization of Chloroprene and Hexafluorobutadiene and on the Composition of the Copolymers

The copolymerization process was carried out at an initial monomer ratio of 7 : 3 (at 40°) and an initial water-monomer ratio of 3 : 1; the initiator was $K_2S_2O_8$ (0.6%), the emulsifier was esteramine** (5%), and the pH of the aqueous phase was 3 except for those cases when the effect of one factor or another or the effect of concentration was being investigated.

Nature of the Emulsifier. It was established that, as in the case of the polymerization of hexafluorobutadiene, the most suitable of the emulsifiers tested was the cationic emulsifier esteramine. In contrast to the polymerization of hexafluorobutadiene alone, we obtained here a considerably more stable emulsion which retained its homogeneity to the end of the polymerization.

The Effect of Emulsifier Concentration (Fig. 1). The optimum emulsifier concentration was 5% esteramine. An increase in the emulsifier concentration from 5 to 15% had little effect on the rate of the process, while a decrease in the concentration to 2% sharply decreased the rate of the process as a result of a decrease in the total surface of the polymerizing particles (both micelles and polymer-monomer particles).

*Communication II.

**Ester of diethylaminoethanol and lauric acid.

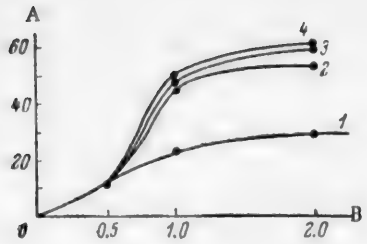

Fig. 1. Dependence of copolymerization rate on emulsifier concentration. A) Extent of polymerization (in %), B) time (in hours). Emulsifier concentration (in %): 1) 2, 2) 5, 3) 10, 4) 15.

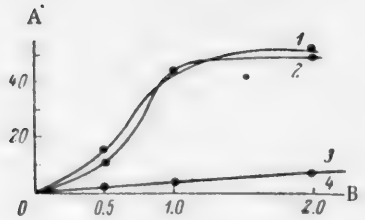

Fig. 2. Dependence of copolymerization rate on pH of the aqueous phase. A) Extent of polymerization (in %), B) time (in hours). pH values: 1) 1, 2) 3, 3) 5, 4) 7.

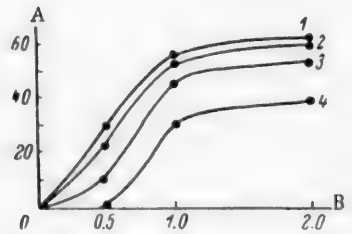

Fig. 3. Dependence of copolymerization rate on water-monomer ratio. A) Extent of polymerization (in %), B) time (in hours). Ratios of phases: 1) 2 : 1; 2) 3 : 1; 3) 5 : 1; 4) 10 : 1.

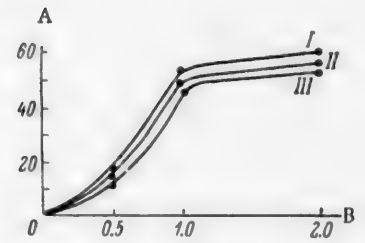

Fig. 4. Dependence of copolymerization rate on the nature of the initiator. A) Extent of polymerization, B) time (in hours). Initiators: I) $K_2S_2O_8$, II) cumene hydroperoxide, III) tertiary butylcumene hydroperoxide.

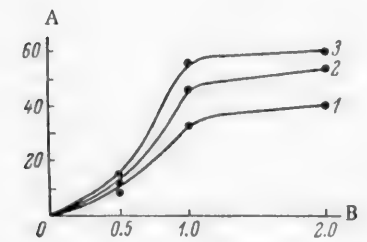

Fig. 5. Dependence of copolymerization rate on the concentration of potassium persulfate. A) Extent of polymerization (in %), B) time (in hours). $K_2S_2O_8$ concentration (in mole %): 1) 0.3, 2) 0.6, 3) 0.9.

The Effect of pH of the Aqueous Phase (Fig. 2). As is apparent in Fig. 2, the pH of the aqueous phase had a considerable effect on the rate of the copolymerization process. The process was accelerated by a more acid medium. There was no reaction at all at a pH of 7, at a pH of 5 the process proceeded at a very low rate, while at a pH of 3 there was a sharp increase in the rate of the process. A further decrease in pH from 3 to 1 had almost no effect on the copolymerization rate.

Effect of the Ratio of Aqueous Phase to Monomer Phase (Fig. 3). The highest rate of the process was attained at a water-monomer mixture ratio of 2 : 1. With an increase in this ratio, there was a gradual decrease in the copolymerization rate.

Effect of the Nature of the Initiator (Fig. 4). Both a water-soluble initiator ($K_2S_2O_8$) and initiators soluble in organic media (cumene hydroperoxide and tertiary butylcumene hydroperoxide) were tested. The initiators were used in a concentration of 0.4 mole % with respect to the mixture of monomers.

Effect of Initiator Concentration. As is apparent from Fig. 5, the copolymerization rate increased with an increase in initiator concentration.

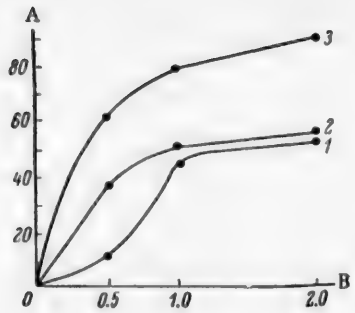

Fig. 6. Dependence of copolymerization rate on the nature of the redox system. A) Extent of polymerization (in %), B) time (in hours). Redox system: 1) no redox system, 2) II, 3) I.

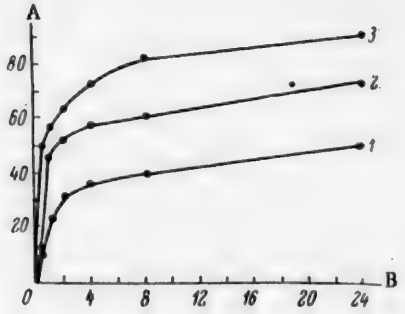

Fig. 7. Dependence of copolymerization rate on initial monomer ratio. A) Extent of polymerization (in %), B) time (in hours). Ratios: 1) 5:5; 2) 7:3; 3) 9:1.

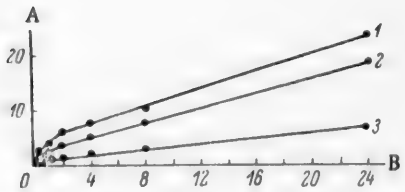

Fig. 8. Change in the composition of the copolymer during the course of copolymerization as a function of the initial monomer ratio. A) Amount of hexafluorobutadiene in the copolymer (in moles), B) time (in hours). Component ratios: 1) 5:5; 2) 7:3; 3) 9:1.

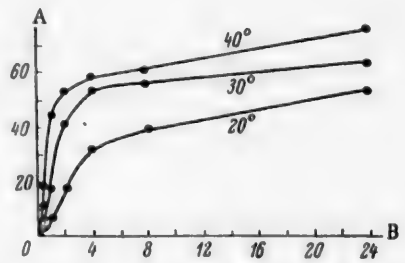

Fig. 9. Dependence of polymerization rate on polymerization temperature. A) Extent of polymerization (in %), B) time (in hours).

Effect on the Oxidation – Reduction System. The following redox systems were tested:

I		II	
1) $K_2S_2O_8$	— 0.60 g	1) $K_2S_2O_8$	— 0.60 g
2) $FeSO_4$	— 0.05 g	2) $FeSO_4$	— 0.05 g
3) $Na_4P_2O_7$	— 0.15 g	3) $Na_4P_2O_7$	— 0.15 g
4) DHMA*	— 0.30 g	4) Invert sugar	— 1.00 g

The amounts of the oxidation – reduction components were calculated on the basis of 100 g of monomers.

As may be seen from Fig. 6, oxidation system I accelerated the copolymerization process to a significant extent, while system II had only an insignificant effect on the rate of the process.

Effect of Initial Monomer Ratio on the Rate of the Copolymerization Process and on the Composition of the Copolymers. The following initial monomer ratios (mole) of chloroprene to hexafluorobutadiene were studied: 9:1, 7:3, and 5:5.

*DHMA – dihydroxymaleic acid.

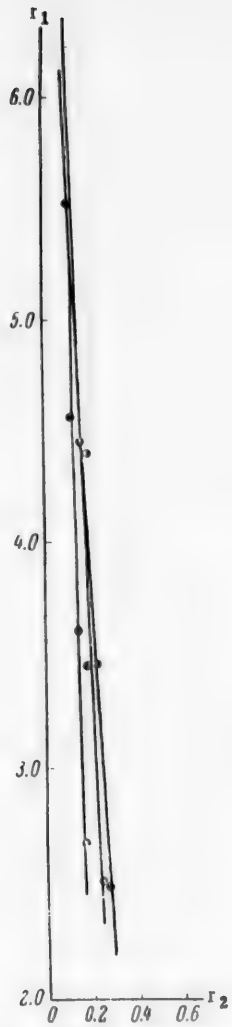

Fig. 10. Determination of the copolymerization ratios (r_1 and r_2) for the emulsion copolymerization of chloroprene and hexafluorobutadiene.

As Fig. 7 shows, the copolymerization rate depended on the initial monomer ratio. The copolymerization process slowed down with an increase in the concentration of hexafluorobutadiene in the mixture of monomers. An increase in the amount of hexafluorobutadiene in the copolymer was observed with an increase in its concentration in the initial mixture (Fig. 8).

Effect of Polymerization Temperature. As is apparent from Fig. 9, the polymerization temperature had some effect on the copolymerization rate. The rate of the process increased with an increase in temperature.

On the basis of the study of the effects of all of the factors under consideration on the rate of copolymerization of chloroprene with hexafluorobutadiene, a recipe was developed, and conditions for carrying out the process were established: monomer – 100.00 g, water – 291.15 g, esteramine – 5.00 g, hydrochloric acid (36%) – 3.25 g, and potassium persulfate – 0.60 g; pH of the aqueous phase – 3.0, temperature – 40°.

The copolymerization ratios for the emulsion polymerization of chloroprene and hexafluorobutadiene were calculated from the experimental data using the integral composition equation [3].*

On the basis of the experimental results, it is possible to compare the copolymerization ratios for emulsion and solution copolymerization of chloroprene and hexafluorobutadiene (Fig. 10). The ratios for solution copolymerization were: $r_1 = 5.47$ and $r_2 = 0.10$.

The ratios for emulsion copolymerization were: $r_1 = 5.52$ and $r_2 = 0.10$.

A comparison of the two sets of ratios shows that the ratios for copolymerization of chloroprene and hexafluorobutadiene in homogeneous solution are very close to those for emulsion copolymerization, and the discrepancy between these ratios may be explained by experimental error. This confirms the assumption that the copolymerization ratio does not depend on the method by which the process is carried out.

The probabilities of the types of bonds occurring in the copolymer and the distribution of average lengths of monomer chains in the copolymer were determined from the copolymerization ratios [4].

It was established that with a low concentration of hexafluorobutadiene in the monomer mixture (9 : 1), the resulting copolymer was chiefly composed of a combination of chloroprene units with each other. Hexafluorobutadiene units occurred joined together only when polymerization proceeded to a great extent, when the concentration of chloroprene in the monomer mixture had become considerably decreased. The maximum probability for the combination of hexafluorobutadiene units was 1.18 in this case. With an increase in the hexafluorobutadiene concentration in the initial monomer mixture (7 : 3 and 5 : 5), there was an increase in the probability for the combination of hexafluorobutadiene units with each other in the copolymer, and this probability was greater the greater the concentration of hexafluorobutadiene in the initial monomer mixture and the greater the extent of polymerization, i.e., as the chloroprene was used up and the concentration of hexafluorobutadiene in the monomer mixture increased correspondingly. Thus, for example, with an initial monomer ratio of 7 : 3 and an extent of polymerization of 74%, the probability for the joining of hexafluorobutadiene units with each other was 2.09, while with an initial monomer ratio of 5 : 5 and an extent of polymerization of 51.1% this probability was 2.45.

*These constants were also determined for copolymerization in benzene solution.

This indicates that with an increase in the concentration of hexafluorobutadiene in the initial monomer mixture, there is a tendency toward an increase in alteration of chloroprene and hexafluorobutadiene molecules, and there is also an increase in the tendency for hexafluorobutadiene molecules to join together.

Copolymer properties

Using the recipe and the process conditions developed in the present work, copolymer samples were prepared on a larger scale.*

Copolymers of chloroprene with hexafluorobutadiene were studied in greater detail; only a few data were obtained for copolymers of fluoroprene with hexafluorobutadiene and isoprene with hexafluorobutadiene.

The tests showed that the introduction of a small amount (12%) of hexafluorobutadiene into the chloroprene copolymer composition prevented crystallization, which is the cause of the considerable hardening of polymers during storage and which makes processing difficult. The brittle point was improved somewhat (-45° in place of -39 or -40° for chloroprene homopolymer). The presence of hexafluorobutadiene in the copolymer also brought about a certain improvement in the stability toward gasoline, particularly with respect to swelling in aromatic solvents (benzene). Swelling of chloroprene homopolymer in benzene is 150-170% in 24 hours, but it was 108% for the chloroprene-hexafluorobutadiene copolymer. Thus, only a small amount of hexafluorobutadiene in the chloroprene copolymer brings about some improvement in brittle point and gasoline stability and prevents crystallization. The mechanical indexes of the copolymer are somewhat lower than those of chloroprene homopolymer.

A further increase in the amount of hexafluorobutadiene in the chloroprene copolymer (up to 28% and higher) did not cause any appreciable improvement in the physical properties discussed above, while the mechanical properties suffered significantly. The copolymer of fluoroprene with hexafluorobutadiene did not have any advantages over fluoroprene homopolymer, and the mechanical properties were relatively poor. Tests of an isoprene-hexafluorobutadiene copolymer prepared with a monomer mixture having a high hexafluorobutadiene content showed that the high content of hexafluorobutadiene brought about a sharp decrease in strength, but the other properties, except for gasoline stability, were little changed in comparison with polyisoprene.

It should be remarked that copolymers of chloroprene with hexafluorobutadiene are characterized by a high vulcanization rate. It was established previously that polychloroprene prepared without the use of sulfur as a modifier is characterized by a very low vulcanization rate. Vulcanization of copolymers of chloroprene and hexafluorobutadiene proceeds at a high rate and without an accelerator.

This same high vulcanization rate was exhibited by copolymers of fluoroprene with hexafluorobutadiene and isoprene with hexafluorobutadiene (vulcanization temperature, 134°; time, 10 minutes).

In connection with the above, it appeared to be of interest to study the question of whether it would be possible to vulcanize fluoroolefin polymers by introducing into the polymer chain very small amounts of hexafluorobutadiene, which would provide sites at which the vulcanization process could take place. Apparently, the introduction of this compound must be in minimum quantity in order to make vulcanization possible without disturbing the basic properties of the polymer.

SUMMARY

1. A comparison of the calculated copolymerization ratios for solution and emulsion copolymerization of chloroprene and hexafluorobutadiene showed these ratios to have very close to the same values, and the earlier proposal that copolymerization ratios are independent of the method by which the copolymerization is carried out was thereby confirmed.

2. Copolymers of hexafluorobutadiene with the monomers considered have high vulcanization rates; therefore, hexafluorobutadiene may be of interest as a monomer for copolymerization with fluoroolefins to make possible vulcanization of these copolymers.

LITERATURE CITED

[1] F. R. Mayo and C. Walling, Chem. Rev. 46, 2, 191 (1950).

*The tests were carried out by V. N. Kartsev and F. E. Berman in the VNIISK [All-Union Scientific Research Institute of Synthetic Rubber].

[2] A. L. Klebanskii, Zhur. Priklad. Khim. 32, 9 (1959).*

[3] S. N. Ushakov, S. P. Mitsengendler and G. A. Shtraikhman, Uspekhi Khim. 19, 3, 265 (1950).

[4] L. Gindin, A. Abkin and S. Medvedev, Zhur. Fiz. Khim. 21, 11, 1269 (1947).

Received August 9, 1958

* See C. B. Translation.

THE BEHAVIOR OF SULFUR DURING THE CHLORINATION OF COAL

B. I. Losev, N. S. Vorob'eva, V. K. Ninin and E. A. Zimakova

Until the past few years, a comparatively small amount of work had been carried out in the field of coal chlorination. The work that had been done was directed to: 1) a study of the chemical structure of coal by means of chlorination [1-4] and 2) the production of valuable chemical products (CCl_4, C_2Cl_6, etc.) [5]. More recently, we have done some work for the purpose of investigating the chlorination of lignite and determining the effect of process conditions on the degree of chlorination [6, 7]. All of this work has shown that coal adds a considerable amount of halogen, and this produces extensive changes in its chemical composition – solubility in various organic solvents is increased. Not only do deep-seated changes in the organic matter of the coal occur during the chlorination, but de-ashing of the coal is also clearly evident. Moreover, the decreased sulfur content of the coal after chlorination is of great interest. For this reason, Donets coal was chlorinated.

TABLE 1

Characteristics of the Original Coals

Rank	Content (in wt. %)					
	M^*	A^d*	S_t^e*	V^g*	C^c*	H^c*
G. (Dobropol'e) . . .	7.41	7.58	1.45	36.49	82.29	5.52
PZh (Nikitovka) . .	9.65	7.42	2.59	29.34	85.32	5.23
K (Avdakova) . . .	8.86	7.70	2.67	23.08	87.48	4.84
PS (Chumakovo). . .	5.70	7.33	1.89	16.31	88.52	4.41

* M – moisture; A^d – ash, dry basis; S_t^e – total sulfur expressed as the element; V^g – volatiles; C^c – combustible carbon; H^c – hydrogen in combustible material.

EXPERIMENTAL

First of all, it was necessary to determine how coals of various ranks behave during chlorination, to determine which coal is the most active during its interaction with chlorine giving the greatest percentage decrease in ash and sulfur, so that it can be further used as a chlorinating additive. Coals of the following ranks were investigated: PS (Chumakovo), PZh (Nikitovka), K (Avdakova), and G (Dobropol'e).* The results of the investigation are presented in Tables 1-5.

The chlorination was carried out in a three-necked flask fitted with a stirrer, a liquid seal, a bubbler, a reflux condenser, and a thermometer. The coal was first powdered and sieved through an 0.25-mm sieve; it was then mixed with a 7-fold amount of water and charged to the flask; the chlorine was fed at a rate of 70-80 cc/minute. At the conclusion of the chlorination, the coal was filtered, separated in a Buchner funnel, and dried at a temperature of 80°. This treatment was considered sufficient to prepare the coal for analysis. Determination of the amount of chlorine added was carried out by the method developed in the IGI [Institute of Minerral Fuels] AN SSSR. This method is as follows: a weighed amount of the chlorinated coal, 6-12 mg, is

* Transliteration of Russian – Publisher's note.

TABLE 2

Results of Experiments on the Chlorination of Coal

Expt. No.	Rank	Exptl. Conds		Content (in wt. %)					Degree (%)	
		time (in hours)	temp. (in °C)	A^d	S_t^e	C^c	H^c	Cl	deashing	desulfurization
1	G (Dobropol'e)	10	0	3.30	0.80	65.52	2.96	15.70	56.5	43.1
2	P S (Chumakovo)	10	0	5.03	1.16	82.00	3.58	5.30	31.4	38.5
3	K (Avdakovo)	10	0	6.90	1.90	82.10	4.10	1.80	10.5	28.8
4	PZh (Nikitovka)	10	0	5.04	1.14	79.3	3.94	5.60	32.1	56.0
5		6	0	6.65	1.89	77.65	4.79	2.70	12.3	26.0
6		10	0	4.03	0.48	53.2	3.17	25.79	46.2	78.5
7		6	20	6.16	1.42	72.4	2.97	4.65	18.7	45.0
8		6	20	4.34	0.51	54.1	3.15	25.75	58.0	80.0

TABLE 3

Results of Experiments on the Chlorination of Coal

Rank of coal and Expt. No.	Content (in %)				
	Cl^v	S_t^e	S_{pyr}	S_{sulf}	S_{org}
PZh (Nikitovka, Donets Basin)	—	2.59	1.143	0.093	1.33
Expt. No. 24	1.65	1.79	0.815	0.0	0.93
Expt. No. 31	15.50	1.32	0.55	0.0	0.77
Expt. No. 40	5.25	1.90	0.76	0	1.14
"Komsomolets" pit coal (Kizelov basin)	—	2.22	0.46	0.04	1.72
Expt. No. 2	8.45	1.61	0.01	0	1.55
Expt. No. 3	9.46	1.51	0.0	0	1.45
Expt. No. 4	16.17	1.35	0	0	1.29

TABLE 4

Results of Experiments on the Stepwise Chlorination of Coal

Coal sample	Content (in wt. %)				
	Cl^v	S_t^e	S_{pyr}	S_{sulf}	S_{org}
Original PZh coal (Nikitovka)	—	2.59	1.143	0.093	0.91
Chlorinated coal	9.36	1.41	0.50	0	0.91
Chlorinated coal:					
from Expt. No. 1	17.42	1.15	0.29	0	0.85
from Expt. No. 2	20.50	0.90	0.182	0	0.72
from Expt. No. 3	22.24	0.80	0.172	0	0.63
from Expt. No. 4	24.0	0.55	0.15	0	0.39
from Expt. No. 5	24.8	0.55	0.15	0	0.39

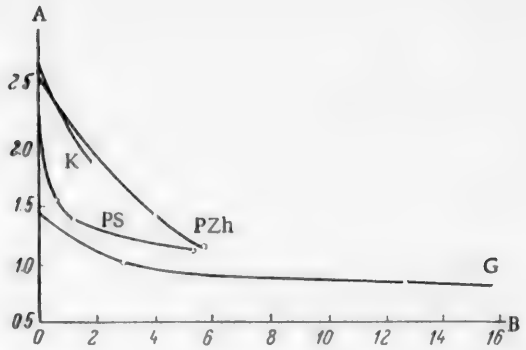

Fig. 1. Dependence of the change in sulfur content of coals of different ranks on the amount of added chlorine. A) Sulfur content, S_t^c, (in wt. %); B) amount of chlorine (in %).

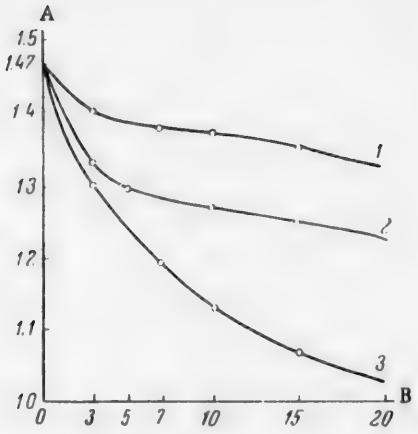

Fig. 2. Dependence of the sulfur content of coke on the addition of chlorinated "PZh" rank coal to the charge. A) Sulfur content of coke (in %), B) amount of chlorinated coal (in %). Chlorine content (in %): 1) 1.6, 2) 3.93, 3) 5.6.

burned in a quartz tube in a current of oxygen. The combustion products are absorbed in a solution of KOH and H_2O_2, and the amount of halogen is determined in the solution by Volhard titration. The sulfur is determined by the Eschka method. In order that the results be comparable, all of the coals were chlorinated under the same conditions: time, 10 hours; temperature, 0°; chlorine feed rate, 70 cc/ minute (Table 2, Experiments Nos. 1-4).

During the chlorination of coal in water, it was noticed that the decrease in the sulfur content of the coal depended directly on the chlorine content, which, in turn, depended on the degree of pulverization of the coal, the rate at which chlorine was fed, the length of the experiment, and the temperature, as is apparent from Table 2 (Experiments 5-8).

Figure 1 shows the manner in which the change in the sulfur content of coals of various ranks depends on the amount of chlorine added. As may be seen from Figure 1, the greatest degree of desulfurization occurred with "PZh" rank coal (56% of the total amount of sulfur in the coal). Since sulfur is present in coal in the form of sulfates, sulfides, and organic compounds, and also in the free state, each of these various forms of coal behaves differently during chlorination of coal (Table 3). The content of pyrite sulfur decreased up to 40%, and the sulfate sulfur was removed completely. The decrease in organic sulfur was less.

Successive chlorinations were carried out in order to obtain more complete removal of sulfur from the coal.

All experiments were carried out at room temperature with a chlorination time of 6 hours and a chlorine feed rate of 70 cc/ minute.

As may be seen from the data of Table 4, the stepwise method of chlorinating coal can lead to the removal of up to 80% of the sulfur in the coal.

In addition, we carried out an investigation of the possibility of decreasing the sulfur content of coke by the addition of chlorine-containing additives to the coal charge*. Chlorinated coal with a chlorine content of 1-20% was used as the chlorine-containing additive; the chlorinated coal was added to the charge in different percentage ratios, replacing similar ranks of coal. The coking coal, which had a particle size of 0-2 mm, was carefully mixed and charged to the iron container in a manner such that the bulk density was the same in all experiments (0.73-0.75 g/ cc). The coking was carried out under laboratory conditions in a 2-kilogram furnace; the heating rate was 10°/ minute. The composition of the charge was (in %): PZh (Nikitovka) – 37, PZh (Trudovaya) – 10, G (Dobropol'e) – 14, PS (Chumakovo) – 18, and K (Avdakovo) – 21.

* The amount of chlorine introduced did not have any effect on the fire brick with which the furnace was constructed.

TABLE 5

Results of Experiments on Decreasing the Sulfur Content of Coke

Expt. No.	Chlorine content in mix (in %)	Coke analysis: content (in wt. %) S_t^e	A^d	Cl^v	strength index (in kg/dm²)	yield of coke of the class (in %): >2.5 mm	<0.5 mm
1	—	1.47	10.62	None	14.2	76.9	14.9
2	0.4	1.39	10.30	None	14.5	79.6	13.0
3	0.9	1.36	10.22	None	15.3	80.5	12.1
4	1.3	1.35	10.15	None	15.2	79.8	12.8
5	1.95	1.30	10.03	None	13.6	76.0	14.0
6	2.6	1.28	10.01	None	11.3	74.1	14.8

As the data of Table 5 show, the addition of chlorinated coal to the charge led to a decrease in the sulfur content of the coke by 10-15%. While during the ordinary coking of a Krovoi Rog charge desulfurization occurs to the extent of 30%, during coking of this same charge with the addition of chlorinated coal, the desulfurization was 40% (Figure 2). This same desulfurization effect was obtained during pot coking of a charge with the addition of chlorinated coal under commerical conditions.

SUMMARY

1. The chlorination of coal of different ranks ("G", "PZh", "K", and "PS") in water led to a decrease in the sulfur and ash contents of the coal. Moreover, it was shown that a simultaneous decrease in both pyrite and organic sulfur occurs. Sulfate sulfur was removed completely.

2. Chlorinated coal can be used as a chlorinating additive to a coal charge. The addition of chlorinated coal (chlorine content 1-10%) causes a decrease in the sulfur content of the coke by 10-15%; the mechanical properties of the coke are not harmed by this treatment.

LITERATURE CITED

[1] E. J. Bevan and C. F. Cross, Ch. News 44, 185 (1881).

[2] J. A. Smythe. Brit. Assoc. Advancement Sci. Rept. 343-346 (1896).

[3] A. Marsch, A. McCulloch and E. Parrisch, J. Soc. Chem. Ind. 48, 167-174 T (1929).

[4] H. Eccles and A. McCulloch, J. Soc. Chem. Ind. 49, 377-382 T, 383-386 T (1930).

[5] Combes, German Pat. 204912 (1909).

[6] V. A. Alekseeva, Ukrain. Khim. Zhur. 20, 3, 319 (1954).

[7] M. I. Shenbor, Candidate's Dissertation (Moscow, 1954).

Received December 8, 1958

ISOMERIZATION OF TETRAHYDRONAPHTHALENE

V. V. Tishchenko and Yu. I. Perin

A. A. Zhdanov State University, Leningrad

Studies of thermocatalytic polymerization of aromatic and naphthenic hydrocarbons, present in petroleum, over natural aluminosilicate catalysts at temperatures consistent with the theory of isosterism (not above 250°) revealed a number of principles governing their behavior in relation to the structure and number of carbon atoms in the alkyl radical chains [1-4]. While the number of investigations dealing with this problem is relatively large, the conversion of the hybrid hydrocarbon tetrahydronaphthalene (tetralin), present in amounts of up to 0.2-0.3% in petroleum, has been hardly studied at all. However, investigation of the thermocatalytic conversion of tetrahydronaphthalene is of undoubted interest because of the peculiar structure and properties of compounds of this type, and would give an indication of the possible conversions in petroleum in the course of natural metamorphism in oil-bearing rocks*.

The literature presently available contains a paper by Bloch and Thomas, describing the conversion of tetralin in the vapor phase over a zirconia–alumina catalyst at 400-500° [6]. They found that the main conversion product of tetralin is naphthalene. Scission of the hydrogenated ring yielded benzene, toluene, xylenes, and high-boiling alkylbenzenes. Part of the tetralin was converted into decalins and their isomers. In addition, at 400° they isolated small amounts of hydrocarbons of the methane and monocyclic naphthene series, the composition of which was not investigated. Tetralin and its isomers comprise about 73% of the main bulk of isomerization products. At 500° a small amount of olefins is formed.

Earlier Ipat'ev and Klyukvin showed that in hydrogenation of naphthalene over a mixed catalyst of aluminum and nickel oxides at a temperature above 400° the hydrogenation products are decomposed with formation of considerable amounts of benzene hydrocarbons and naphthalene (~ 50%) [7]. The isomerization products of tetralin isolated by Block and Thomas are very similar in nature to those obtained by Ipat'ev and Klyukvin, and are pyrogenic in character, and therefore the mechanism of their formation cannot be taken into consideration in relation to the metamorphism of petroleum.

The present investigation shows that the result of low-temperature conversion of tetralin over activated clay (gumbrin) differs significantly from the results of Bloch and Thomas. At low temperatures the yield of aromatic hydrocarbons is considerably lower, since cracking is excluded, while the yield of naphthenic hydrocarbons is considerably higher, so that it was possible to isolate and investigate them. No olefin hydrocarbons were present in the gas.

Investigation of the resultant isomerization products leads to the conclusion that the conversion of tetralin in presence of gumbrin proceeds in two principal directions. First, conjugated hydrogenation takes place with formation of decalin, dihydronaphthalene, and naphthalene. At the same time, the hydrogenated part of the naphthalene undergoes scission with formation of diethyl- and butylbenzene. The secondary reaction may be assumed to be isomerization of decalin with narrowing of the ring and formation, on the one hand, of dimethylbicyclooctane, and on the other, of methylcyclopentane by way of methylhydrindane which is converted, with scission of the five-membered ring under the influence of hydrogen liberated during formation of tars and carboids, into butylcyclohexane; removal of the radical gives cyclohexane, which is then isomerized to methylcyclopentane. Another secondary reaction is formation of benzene from diethyl- and butylbenzene, from which the radicals are split off in the form of ethane and butane, which were found in the gas together with hydrogen, the amount of ethane being nearly five times as much as butane. This ratio indicates that scission of the hydrogenated

* Correlation of laboratory experiments on catalytic conversion of hydrocarbons over activated clays with the natural metamorphism of petroleum has been justified by Frost [6].

tetralin ring occurs mainly at the bond between the second and third carbon atoms and to a lesser extent between C_9 and C_1 or between C_4 and C_{10}. Benzene was not found in the products formed by isomerization of tetralin at 205-206°; hence it may be assumed that, as the experiments showed, the radicals are split off at a temperature close to 225°. Butylcyclohexane was not isolated either, but its presence in the isomerization product could be assumed, because in adsorption separation of the 175-185° fraction the first portions had a much lower refractive index than the methylhydrindane isolated from this fraction; the respective values were n_D^{20} 1.4598 for the first portions and n_D^{20} 1.4693 for methylhydrindane. The refractive index of butylcyclohexane is n_D^{20} 1.4412.

From the foregoing the following scheme may be postulated for isomerization of tetrahydronaphthalene:

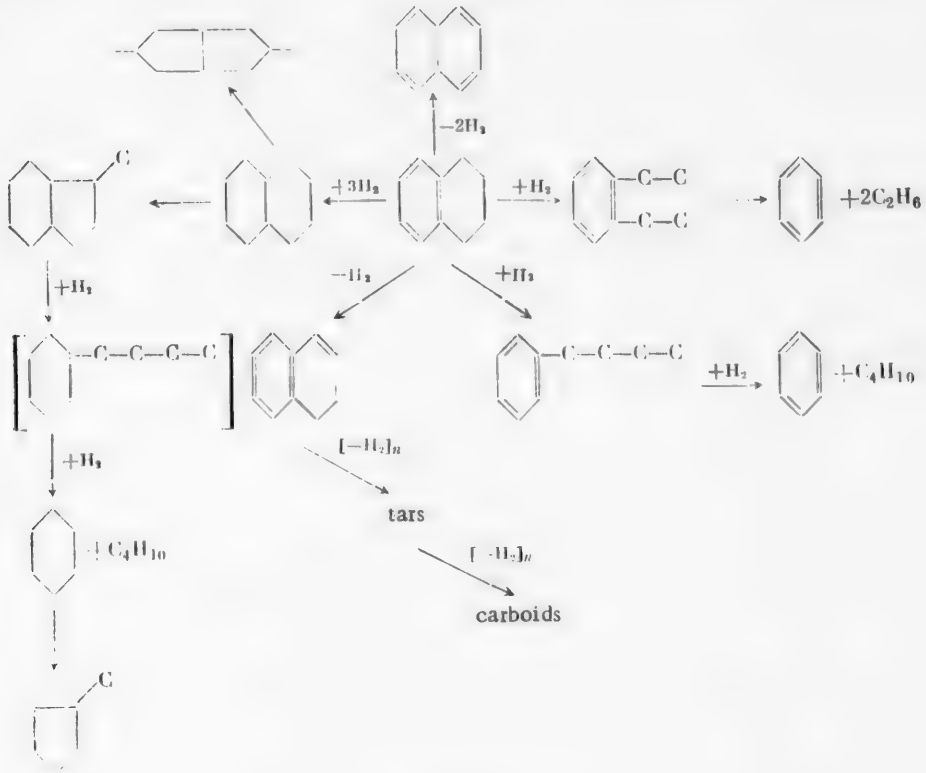

EXPERIMENTAL

The tetralin used for the experiments had the following constants: b. p. 203-207°, d_4^{20} 0.9728, n_D^{20} 1.5411. Naphthalene was not detected analytically. The catalyst used was gumbrin activated by 10% hydrochloric acid. Since it was impossible to determine the instant when equilibrium was reached during the experiments, it was assumed that "nominal equilibrium" had been reached when the refractive index of the liquid, determined at intervals, ceased to change. The justification for this was that, as was shown in preliminary experiments in an open vessel (flask with a condenser set for reflux) the vapor temperature of the boiling liquid ceased to vary at the same time as the refractive index. Attempts to effect isomerization of tetralin at its boiling point in an open vessel with 25 and 35% of catalyst resulted in appreciable, but,in practice,small changes in the hydrocarbon, giving values of n_D^{20} 1.5498 and 1.5514, respectively. For more distinct results the subsequent experiments were performed in an autoclave with 50% of catalyst at 225-250°, with durations of 20 and 25 hours. These conditions corresponded to the most complete isomerization of tetralin. Increase of the heating time from 20 to 25 hours raised the yield of light fractions, boiling up to 190°, by a factor of 1.5, with a slight increase of the amount of heavy fractions, boiling above 225°. Under these conditions the conversion of tetralin reached 62-63%. The material balance for one experiment (temperature 250°, heating time 25 hours) is given below in illustration of the quantitative yields of the products. Gas obtained, 1.25%; liquid product decanted, 61.93%; amount of product retained by the catalyst and distilled in steam 14.60%; tars extracted in acetone from the catalyst, 12.50%; carbonaceous fractions

(carboids), 4.05%; loss, 5.62%. The gas composition was: hydrogen 49.7%, ethane 40.8%, butane 8.3%. After each experiment the steam distillate was separated from water, dried, and combined with the part of the isomerization product decanted from the catalyst. The product was then separated into five-degree fractions with the aid of a column and the density and refractive index of each fraction were determined. Since the refractive indices of fractions of the same boiling ranges differed relatively little in the experiments, these fractions were combined and after fourfold fractionation through a column of 20 theoretical plates they were ultimately separated into the following fractions: 73-80° (3.60 g), 80-85° (2.17 g), 85-125° (two drops), 125-160° (0.45 g), 160-170° (1.63 g), 170-175° (0.23 g), 175-177° (2.00 g), 177-179° (0.43 g), 179-181° (0.55 g), 181-183° (6.12 g), 183-185° (1.68 g), 185-195° (0.32 g), 195-200° (6.32 g), 207-211° (3.85 g), 211-214° (9.20 g), 214-225° (2.17 g). The 200-207° fraction, which consisted of tetralin, was not refractionated or investigated. The refractive index and, when possible, the density of each fraction were determined.

Investigation of Fractions

Fraction 1 (3.60 g), b. p. 73-80°, d_4^{20} 0.8652, n_D^{20} 1.4926. The physical constants and freezing point (+3.5°) show that this fraction could contain benzene, cyclohexane, and methylcyclopentane. After removal of benzene by 100% sulfuric acid there remained 0.13 g of naphthene hydrocarbons with the following constants: b. p. 73-79.5° (by Sivoloboff's method [8] and n_D^{20} 1.4208. The remaining mixture of naphthenes was found, by means of an interpolation graph, to contain 35% methylcyclopentane and 65% cyclohexane. This ratio corresponds to the equilibrium between these hydrocarbons at 250° [9]. Thus, the fraction consisted of 89.2% benzene, 7.0% cyclohexane, and 3.8% methylcyclopentane.

Fraction 2 (2.17 g), b. p. 80-85°, d_4^{20} 0.8665, n_D^{20} 1.4924. By its constants it was close to Fraction 1, and consisted of 88% benzene and 12% cyclohexane.

Fraction 3. Not investigated.

Fraction 4 (0.45 g), b. p. 125-160°, n_D^{20} 1.4642. After treatment with 100% sulfuric acid the refractive index decreased to n_D^{20} 1.4508 (close to the refractive index of dimethylbicyclooctane).

Fraction 5 (1.63 g), b. p. 160-170°, d_4^{20} 0.8409, n_D^{20} 1.4517. Distillation from a 3 ml flask with a small column yielded a fraction boiling at 165-168°. Removal of aromatic hydrocarbons left 0.42 g of liquid product of b. p. 165-167° (by Sivoloboff's method) and refractive index n_D^{20} 1.4476. These constants exactly correspond to dimethylbicyclooctane.

Found %: C 87.05; H 13.35; mol. wt. 139.

$C_{10}H_{18}$. Calc. %: C 86.95; H 13.05; mol. wt. 138.

Fraction 6 (0.23 g), b. p. 170-175°, n_D^{20} 1.4689. Not investigated.

Fraction 7 (2.00 g), b. p. 175-177°, n_D^{20} 1.4792. This apparently contained cis- and trans-decalin, as treatment with 100% sulfuric acid changed the refractive index very little—to n_D^{20} 1.4787. It was not studied further, because it was subsequently added to the decalin distillate from the adsorption separation of fractions boiling in the 177-185° range.

Fraction 8 (0.43 g), b. p. 177-179°, n_D^{20} 1.4801; and Fractions 9 (0.55 g) b. p. 179-181°, n_D^{20} 1.4803; 10 (5.85 g), b. p. 181-183°, d_4^{20} 0.8782, n_D^{20} 1.4828; and 11 (1.43 g), b. p. 183-185°, d_4^{20} 0.8788, n_D^{20} 1.4943 were combined and separated by the American Petroleum Institute chromatographic method [10] into three fractions. The separation was checked by determination of the refractive indices of the eluates. The weight of hydrocarbon mixture taken for the separation was 6.4 g. Three fractions were obtained by adsorption separation (a. s.): Fraction 1 (0.48 g), n_D^{20} 1.4612-1.4694, consisting of "isodecalins;" Fraction 2 (4.19 g), n_D^{20} 1.4694-1.4849, contained cis- and trans-decalin, and Fraction 3 (0.75 g) was a mixture of aromatic hydrocarbons.

Fraction 1 (a. s.) had b. p. 179-180° (by Sivoloboff's method). After treatment with 100% sulfuric acid the refractive index remained almost unchanged (n_D^{20} 1.4677), and therefore the fraction was free from aromatic hydrocarbons; its physical constants were very close to those of methylhydrindane.

Fraction 2 (a. s.) was dehydrogenated by Zelinskii's method over a nickel—aluminum catalyst. From the catalyzate (2.1 g) a white crystalline substance with a naphthalene odor was isolated by freezing out. The substance after recrystallization melted at 79.8°, and its picrate at 147.5°. The residue after isolation of naphthalene

was dearomatized, and its constants then became: b. p. 181-182°, d_4^{20} 0.8758, n_D^{20} 1.4677, which are in good agreement with those of 1-methylhydrindane. The presence of 1-methylhydrindane in the dehydrogenation product is difficult to explain; it is probably due to the presence in its molecule of a five-membered naphthene ring which retards dehydrogenation.

Fraction 3 (a. s.) had b. p. 177-185°, d_4^{20} 0.8719, n_D^{20} 1.4976. The high refractive index and density indicate that the hydrocarbons of this fraction are of aromatic character and the constants suggest that they are a mixture of diethyl- and butylbenzene. Investigation of the fraction was difficult because of the small amount available, and therefore the aromatic fraction obtained by adsorption separation from the 175-185° fraction of the material-balance experiment. The combined aromatic fractions (a. s.) were oxidized by alkaline permanganate solution. The amount taken for oxidation was 1.18 g. Oxidation yielded 0.1650 g of acids. The basicity of the acids, calculated from titration data, was 1.56, which corresponds to a mixture of 44% benzoic and 56% phthalic acids, or 44% butylbenzene and 56% ethylbenzene. From a part of the acid mixture benzoic acid in the form of long needles melting at 120.6° was obtained by sublimation.

Fraction 12 (0.28 g) had b. p. 185-195°, n_D^{20} 1.4956. Because of the small amount this was not investigated.

Fractions 13 (6.30 g), d_4^{20} 0.9692, n_D^{20} 1.5348 and 14 (3.85 g), b. p. 207-211°, were not investigated, as they consisted mainly of tetralin.

Fraction 15 (9.20 g) had b. p. 211-214°, d_4^{20} 0.9954, n_D^{20} 1.5783. The constants of this fraction are very close to those of 1,2-dihydronaphthalene. Crystals of m. p. −7.8° were frozen out at −17°. The somewhat low refractive index and density are most likely due to the presence of 1,4-dihydronaphthalene (b. p. 112°, d_4^{20} 0.9926, n_D^{20} 1.5593).

Fraction 16 (2.14 g) had b. p. 214-225°, d_4^{20} 0.9686, n_D^{20} 1.5731. The fraction should have contained naphthalene and dihydronaphthalenes. Naphthalene was isolated by freezing out and filtration at room temperature on a funnel with a porous plate. The isolated naphthalene melted at 80° after recrystallization from alcohol, and the picrate melted at 148°.

Fractions boiling above 225° were not investigated.

SUMMARY

1. In a study of the conversion of tetralin in presence of gumbrin at 206, 225, and 250° it was shown that at 225 and 250° tetralin undergoes extensive conversion with formation of aromatic and naphthenic hydrocarbons. The naphthenic hydrocarbons are isomerized with narrowing of the ring.

2. Aromatic hydrocarbons are formed as the result of hydrogen disproportionation (naphthalene, dihydronaphthalene) and by scission of the hydrogenated part of the tetralin molecule (diethyl- and butylbenzene).

3. In presence of hydrogen the radicals of diethyl- and butylbenzene are split off with formation of benzene, butane, and ethane.

LITERATURE CITED

[1] B. S. Grinsfeld, H. H. Voge, and G. M. Good, Ind. Eng. Ch. 37, 1168 (1945).

[2] A. F. Dobryanskii and B. G. Gavrilov, Uch. Zap. LGU, ser. khim. 11, 155 (1957).

[3] V. V. Tishchenko and S. G. Chepurina, Uch. Zap. LGU, ser. khim. 15, 211 (1957).

[4] F. G. Chiapetta, Ind. Eng. Ch. 45, 147 (1953).

[5] A. V. Frost, Usp. Khim. 14, 6 (1945).

[6] H. S. Bloch and C. L. Thomas, J. Am. Chem. Soc. 66, 1589 (1944).

[7] V. N. Ipat'ev and N. A. Klyukvin, Zhur. Russ. Fiz.-Khim. Obshch. 56, 245 (1925).

[8] A. Sivoloboff, Ber. Deut. Chem. Ges. 19, 795 (1866).

[9] V. V. Tishchenko and N. V. Petrova, Uch. Zap. LGU, ser. khim. 15, 147 (1957).

[10] F. D. Rossini, Hydrocarbons From Petroleum [Russian translation] (State Fuel Technology Press, Leningrad, 1957) p. 132.

Received June 28, 1958

CONTRIBUTION TO THE QUESTION OF THE CHARACTERISTICS OF BENZENE IN THE CHEMICAL INDUSTRY

M. Illyukevich

The world use of benzene in industrial organic synthesis (aniline, phenol, ethylbenzene, etc.) has now reached a value of more than a million tons a year.

The quality of industrial benzene is controlled through the use of standards which have been adopted by the various countries and which differ from country to country only in details.

The properties used as controls include boiling point, density, color reaction with sulfuric acid and measured on the Spilker-Cramer scale, bromine number, freezing point, and content of sulfur and sulfur-containing compounds (preeminently, carbon disulfide and thiophene).

The number of compounds which can be detected not only in raw, but also in commercial benzene is very large, although their total amount by weight is small and, for example, amounts to approximately 1% in "nitration-grade" benzene.

Aromatic compounds (predominantly toluene), paraffins, naphthenes, olefins and cycloolefins, and sulfur-containing compounds are among the contaminants of benzene.

The presence of one contaminant or another in benzene is determined by 3 conditions: 1) the source of the benzene (nature of the coal from which the benzene was obtained), 2) the coking method, and 3) the method used to purify the raw benzene.

Thus, the major impurities in European benzenes are naphthenes, chiefly methylcyclohexane.

Thiophene is a very important, as well as harmful impurity in benzene.

Of the relatively recent works studying saturated hydrocarbon contaminants of benzene, the work of Anderson and Engelder [2] may be mentioned; these authors analyzed a typical American "nitration-grade" benzene by both condensation temperature and index of refraction, and established the presence of cyclohexane, methylcyclohexane, 3-methylhexane or 3-ethylhexane or both, n-heptane or 2,2,4-trimethylpentane or both, 1,1-dimethylcyclopentane, and trans-1,2-dimethylcyclopentane or trans-1,3-dimethylcyclopentane or both.

In the opinion of the authors, the presence of any paraffins, cyclopentanes, and cyclohexanes,the boiling points of which are in the region of the condensation temperature of the sample,is possible. The authors estimated the total amount of saturated hydrocarbons at 0.6%. With respect to aromatic impurities, the authors established the presence of toluene and p-cymene.

When benzene is used in high-temperature processes or in the presence of catalysts, certain ordinarily inert impurities become active and cause complication of the process.

The poisoning effect of even small traces of sulfur on catalysts during certain reactions is well known.

As a result of the action of sulfuric acid on hydrocarbons during the sulfonation of benzene, there are a number of reactions involving benzene, its contaminants, and the products of their conversion [3], of which the major ones are: sulfonation, oxidation, condensation, isomerization, and hydrogen exchange.

TABLE 1

Benzene sample	Reduction coefficient (in ml)	Color with H_2SO_4 Schpiller-Cramer scale	Bromine number	Crystallization temp.
№ 1	11—28	0.2	0.064—0.11	5.4
№ 2	27—31	0.2—0.3	0.13—0.12	5.4
№ 3	22—52	—	—	5.35—5.45
Experimental sulfonation grade	52—54	—	—	5.25
Moscow gas plant	35—75	0.2—0.3	0.1—0.2	5.0—5.3
Cryoscopically pure benzene	2.5	0	0	5.5

TABLE 2

Benzene	Reduction coefficient			
	170°	190°	220°	250°
Cryoscopically pure	1.1	2.3	3.1	4.5
Experimental sulfonation grade	18	53	85	121
No. 3				
I	18	68	—	123
II	—	22	—	91

As is well known, the reactivity of saturated hydrocarbons is determined by their structure, particularly by the accumulation of branched chains and tertiary carbon atoms.

During the vapor-phase sulfonation of benzene, there can occur an increased evolution of sulfur dioxide with all of the ensuing consequences, so that benzene which satisfies the requirements for "nitration-grade" benzene is unsatisfactory in this reaction. At high temperatures, sulfuric acid is a rather strong oxidizing agent for hydrocarbons, being reduced to some extent to sulfurous acid and bringing about a whole series of further reactions, for example:

$$H_2SO_4 \longrightarrow O + SO_2 + H_2O,$$

$$C_nH_{2n+2} + O \text{ (atomic)} \longrightarrow C_nH_{2n} \xrightarrow{H_2SO_4} (C_nH_{2n})_m,$$

$$R{-}CH{=}CH_2 \begin{cases} \rightarrow RCH(OSO_3H)CH_3 \\ \rightarrow RCH(OH)CH_2SO_3H \end{cases} \rightleftarrows RCH(OSO_3H)CH_2SO_3H.$$

It is evident that this ability to reduce sulfuric acid at high temperatures, which is intrinsic though possessed to a totally different extent by all of the benzene contaminants, can be used to evaluate benzene quality if the reaction is carried out under specific standard conditions.

During an experimental investigation, it was found that the amount of sulfur dioxide liberated during the reaction, as expressed in milliliters of an 0.1 N solution of iodine, is quite constant for the same benzene, and is actually characteristic of the quality of the benzene and of its reducing power with respect to sulfuric acid. The quality of a benzene as expressed by its reduction coefficient corresponds in general to the quality evaluated by ordinary standard indices. Benzenes with high color numbers with sulfuric acid and with low melting points have, as a rule, higher reduction coefficients, and the reduction number is higher, the darker (blacker) the color of the reaction mixture; the color can also be considered and evaluated on a comparative scale during sulfonation.

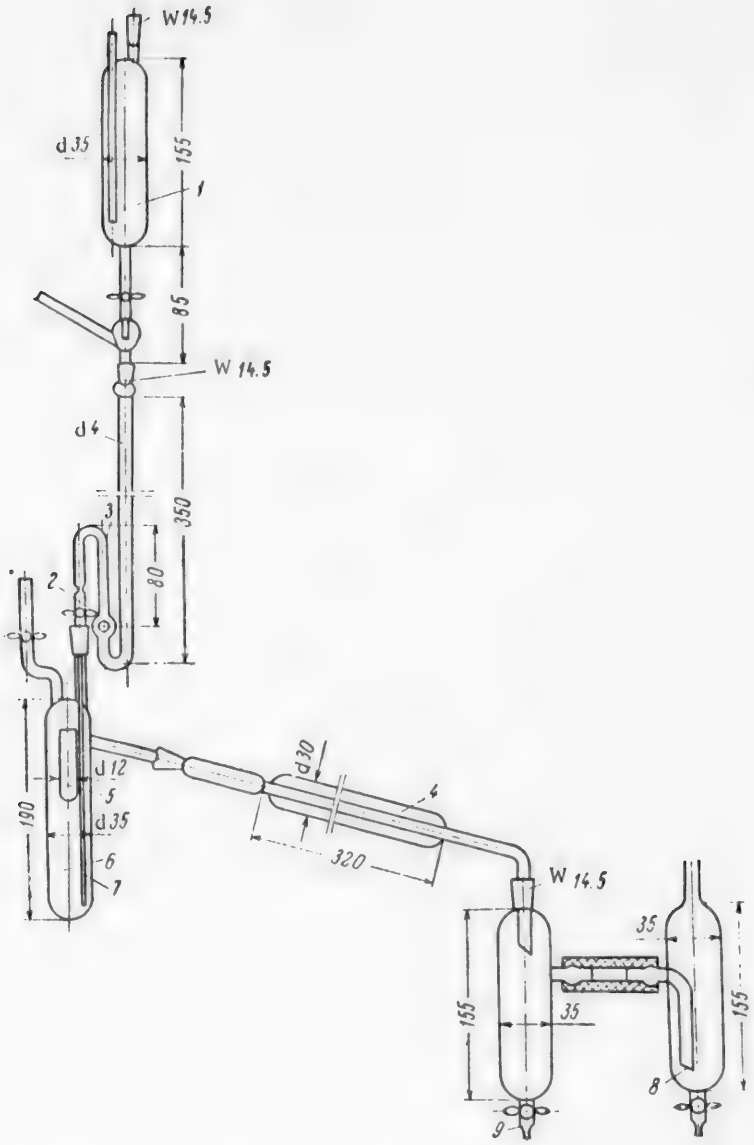

Apparatus for the determination of the reduction coefficient of benzene.
1) Calibrated benzene container, 2) valve, 3) liquid seal, 4) condenser,
5) thermometer tube, 6) sulfonator, 7) capillary, 8) trap, 9) receiver.

The characterization of benzene by means of its reduction coefficient in sulfonation is of the greatest interest for evaluation of the quality of benzene destined for sulfonation. The Spilker-Cramer color index with sulfuric acid is not only coarse (having practical significance at scale points of −0.1, −0.2, and −0.3), but it detects the presence of only the impurities which are the most unstable toward sulfuric acid.

In Tables 1 and 2 are presented the reduction coefficients of samples of benzenes of different origins. It may be remarked that while the data for Sample No. 1 and the Moscow benzenes* are quite statistical, the figures presented for the remaining benzenes has a random character.

* Recently, the Moscow coke-gas plant has produced benzene with higher indices than those cited in Table 1.

TABLE 3

Compound	Amount per 100 ml of solution in benzene (in ml)	Reduction coefficient (in ml)
Carbon disulfide	1	4.1
n-Heptane	1	4.5
iso-Octane	1	13.8
Cyclohexane*	1	21
	1	360
Thiophene	0.0547 g	68.7**
	0.0514 g	66.4**

*During the sulfonation of cyclohexane with oleum (25% SO_3) at a temperature of 20-25°, Menshutkin and Vol'f [4] obtained the sulfonic acid in 70% yield.

**In solution in benzene with a reduction coefficient of 41.3 ml.

The high indices of eastern benzenes merit attention. Benzenes from the Moscow gas plant, which operates with coals of various orgins, have indices which vary within wide limits.

The reduction coefficients increase sharply with an increase in sulfonation temperature.

A number of compounds out of the group of possible contaminants of benzene were examined in mixtures with cryoscopically pure benzene (Table 3).

If it is assumed that the oxidation of thiophene by sulfuric acid proceeds without side reactions according to the equation:

$$SC_4H_4 + 12O = 4CO_2 + 2H_2O + SO_2,$$

the oxidation of thiophene requires 12 moles of sulfuric acid and liberates 13 moles of sulfurous acid, which corresponds to 3290 ml of 0.1 N iodine solution per ml of thiophene; this figure is 9 times greater than that actually obtained at a temperature of 190° (360 ml) and almost 3 times greater than that obtained at a temperature of 250° (~1000 ml). As a matter of fact, the reaction is more complex and includes the formation of tar and the condensation of intermediate products, not to mention the formation of hydrogen sulfide.

It is evident that the relationship between the various figures for the same benzene contaminant and the corresponding reduction coefficients is not necessarily linear.

Another sulfur containing contaminant of benzene – carbon disulfide – is quite stable under our conditions and has essentially no effect on the sulfonation process. Cyclohexane is appreciably more active; methylcyclohexane, which is a characteristic contaminant of benzene, should have still greater activity. Saturated normal hydrocarbons with a small number of carbon atoms per molecule are characterized by a small, but nevertheless appreciable activity.

The method can be used for rapid qualitative evaluation of benzenes of even a high degree of purity.

When benzene is gradually washed with sulfuric acid, the bromine number drops, as does the reduction coefficient; the reduction coefficient is still appreciable, 5-10 ml, when the bromine number has decreased to zero. Whether the values of the reduction coefficient for a given sample of benzene are stable depends on the accuracy with which the sulfonation conditions are observed; practically parallel determinations agree satisfactorily, as a rule, with deviations from the average of 5-10%.

Determination of the reduction coefficient of benzene under standard sulfonation conditions. 100 ml of the benzene tested was passed through 50 ml of concentrated sulfuric acid (96-97%) over a period of two hours and at a temperature of 190°. The vapors leaving the sulfonator were condensed, the condensate was washed several times with a dilute solution of sodium hydroxide (5-10%) until there was no longer a reaction with iodine for sulfurous acid, and the latter was determined iodometrically. The number of milliliters of the 0.1 N iodine solution required for the oxidation of the sulfurous acid formed during the reaction characterizes the benzene tested. The apparatus used for the determination of the reduction coefficient of benzene is shown in the figure. Although the determination can be carried out using the usual system for vapor-phase sulfonation (benzene vaporizer – benzene preheater – sulfonator), the apparatus is more compact when the benzene is heated at a single point.

SUMMARY

1. It was established that it is possible to characterize commercial benzene samples by their ability to reduce sulfuric acid at a high temperature (170-250°).

2. It is proposed to express the reduction coefficients for the different grades of benzene in milliliters of 0.1 N iodine solution consumed by oxidation of the sulfurous acid which is formed during the sulfonation of the benzene under standard conditions (temperature, 190°).

3. Reduction coefficients were established for a number of compounds – benzene contaminants – added to pure benzene (cryoscopic grade).

LITERATURE CITED

[1] H. Stinzendorfer, Oel u. Kohle, 38, 193 (1942).

[2] J. R. Anderson and C. J. Engelder, Ind. Eng. Ch. 37, 541 (1945).

[3] P. S. Panyutin. The Chemistry of Fuel and Oil Materials. Military Academy of Mechanization and Motorization of the RKKA [Workers' and Peasants' Red Army], 1, 49 (1939); T. D. Stewart and D. Harman, J. Am. Chem. Soc. 68, 1135 (1946); G. S. Gordon and A. L. Burwell, J. Am. Chem. Soc. 71, 2355 (1949); R. F. Marschner and D. R. Carmody, J. Am. Chem. Soc., 73, 604 (1951); R. L. Burwell, R. B. Scott, L. G. Maury, and A. S. Hussey, J. Am. Chem. Soc. 76, 5822 (1954); J. W. Otvos, D. P. Stevenson, C. D. Wagner, and O. Beeck, J. Am. Chem. Soc. 73, 5741 (1951); V. N. Setkina, D. N. Kursanov, O. D. Streligov, and A. L. Liberman, Doklady Akad. Nauk SSSR, 85, 1045 (1952); D. N. Kursanov, V. N. Setkina, and O. D. Sterligov, Izvest. Akad. Nauk. Otdel, Khim. Nauk, 1035 (1953); D. N. Kursanov and V. V. Voevodskii, Uspekhi Khim., 23, 641 (1954).

[4] B. N. Menshutkin and Vol'f, Neftyan. Khoz., 13, 340 (1927).

Received April 1, 1958

---

* Original Russian pagination. See C. B. translation.

OXALATE METHOD FOR THE DETERMINATION OF ALKALOIDS IN EPHEDRA*

M. I. Goryaev, S. A. Moshkevich, R. N. Sazonova and I. M. Shabanov

Ephedrine and pseudoephedrine are usually associated in ephedra, but only the first of these alkaloids has therapeutic value; pseudoephedrine can be converted to ephedrine by isomerization, though with considerable loss (about 50%).

From an industrial point of view, ephedra is of great interest, since the ephedrine content of the ephedra alkaloids is high. In mountain ephedra, which is collected in Kazakhstan for the production of ephedrine, the ephedrine content frequently reaches 1.5% of the total alkaloids. At the present time, ephedra is inspected at the factories for total alkaloid content (not below 2%), which causes misunderstandings with the collecting organizations; ephedra with a relatively high ephedrine content but a low percentage of total alkaloids (1.5-2.0%) is frequently of greater value for production than is ephedra with a high total alkaloid content (more than 2%) but a low ephedrine content.

Up to the present time, it has not been possible to resolve this contradiction owing to the lack of a satisfactory method for the determination of the individual alkaloids in ephedra.

There is now a GOST [All-Union State Standard] method for the determination of the individual alkaloids in ephedra; the method was developed by the VNIKhFI [All-Union Chemicopharmaceutical Scientific Research Institute], and is based on the differing solubilities of the alkaloids in petroleum ether. Ephedrine is readily soluble in petroleum ether, while pseudoephedrine is very slightly soluble. According to this method, the alkaloids are extracted from ephedra by the usual standard method [1]; after evaporation of the ethyl ether, the alkaloids are dissolved in petroleum ether, and the insoluble pseudoephedrine is filtered and weighed. Gaseous hydrogen chloride is then passed into the petroleum ether, and the precipitated ephedrine hydrochloride is filtered, washed with chloroform, and determined gravimetrically.

In checking this method, we noted the following disadvantages: 1) the method requires too much time for routine production analysis, since the results are obtained only in 3-4 days; 2) it is impossible to determine the total alkaloid content of the raw material, since the formula used for the calculation does not take into account the amount of pseudoephedrine hydrochloride which goes into solution when the total alkaloid hydrochlorides are washed with chloroform; 3) it is difficult to carry out the work at temperatures above 20°, considering that when the solution is poured slowly through the glass filter (without switching on the vacuum pump), the solvent evaporates rapidly from the surface.

Analytical data from the determination of the individual alkaloids by this method are presented in Table 1. As may be seen from Table 1, in all cases the total alkaloids as calculated from the individual alkaloid contents is significantly less than the true value, and only after the addition of the amount of pseudoephedrine hydrochloride extracted from the chloroform solution does the sum approach the true alkaloid content of the raw material.

In the present paper, we propose two variants of the oxalate method for the determination of the individual alkaloids in ephedra. In neither variant are such solvents as chloroform and petroleum ether required, with the exception of the ether used for the separation of the total alkaloids from the plant. This method is quite suitable for routine analyses of mountain ephedra both in the plants and in the supply depots of Kazakhstan and Central

* Communication III of a series of papers on the quantitative determination of alkaloids.

TABLE 1

Determination of the Alkaloids in a Synthetic Mixture and in Ephedra on the Basis of Their Different Solubilities in Petroleum Ether (VNIKhFI Method)

Sample	Total alkaloids in mixture by standard method for ephedra	Sample wt. (in mg)		Obtained (in mg)		Total alkaloids from the individual determinations (in mg)	Amount of pseudoephedrine unaccounted for (in mg)	Actual total alkaloids (in mg)	Content (in %)				
		ephedrine	pseudoephedrine	ephedrine	pseudoephedrine				ephedrine	pseudoephedrine	sum	pseudoephedrine unaccounted for	total
				51.98	104.40	156.38	68.55	224.93	0.52	1.04	1.56	0.68	2.24
Synthetic alkaloid mixture . .	200 mg	40	160	54.69	125.90	180.59	26.10	206.69	0.55	1.26	1.81	0.26	2.07
				34.19	117.40	151.60	57.50	209.10	0.34	1.17	1.51	0.58	2.09
				25.91	111.20	137.11	63.14	200.25	0.26	1.11	1.37	0.63	2.00
Mountain ephedra, Kugalinsk region	2.18—2.22%	—	—	—	—	—	—	—	0.56	1.04	1.60	1.94	2.54
Mountain ephedra, Uigursk region	2.34%	—	—	—	—	—	—	—	0.31	1.26	1.57	0.50	2.07
Mountain ephedra, Kurgalinsk region	1.30%	—	—	—	—	—	—	—	0.44	0.61	1.05	0.52	1.57
	1.30%	—	—	—	—	—	—	—	0.41	0.55	0.96	0.65	1.61
Mountain ephedra, Sarkand region	2.20%	—	—	—	—	—	—	—	0.51	0.42	0.93	0.65	1.58
Mountain ephedra, Krasnogorsk region	2.14%	—	—	—	—	—	—	—	0.31	0.81	1.12	0.66	1.78
	2.14%	—	—	—	—	—	—	—	0.32	0.92	1.24	0.77	2.01

TABLE 2

Effect of Total Alkaloids on the Solubility of Ephedrine

Wt. of alkaloid sample (mg)			Obtained (in mg)				Dissolved ephedrine oxalate calc'd on ephedrine basis	Content of dissolved ephedrine in total alkaloids (%)	Alkaloids separated, as the bases		Total alkaloids without water of crystallization of ephedrine (%)
pseudo-ephedrine	ephedrine		oxalate		base						
	in mg	in %	ephedrine	pseudo-ephedrine	ephedrine	pseudo-ephedrine			in mg	in %	
250	50	16.67	42.6	304.1	36.35	239.00	13.65	4.55	275.35	91.78	92.6
225	75	25.00	78.7	278.6	61.9	219.00	13.10	4.37	280.90	93.63	94.86
200	100	33.33	108.7	230.3	85.45	181.02	14.55	4.95	266.47	88.82	90.40
150	150	50.00	173.1	186.7	136.03	146.76	13.97	4.66	280.79	93.59	96.00

TABLE 3

Determination of Alkaloids by Variant I of the Oxalate Method

Source of ephedra	Moisture (%)	Alkaloid content by standard method (%)	Alkaloid content by titration with 2% oxalic acid (%)	Found by oxalate method (in %)		
				ephedrine	pseudo-ephedrine	total
Mountain ephedra, Krasnogorsk region	3.6	2.35	2.52	1.03	1.42	2.45
	3.6	2.35	2.56	1.05	1.38	2.43
	3.6	2.35	2.52	1.00	1.45	2.45
	7.6	2.14	2.34	0.83	1.47	2.30
	7.6	2.14	2.35	0.83	1.41	2.24
	4.8	2.35	2.29	0.83	1.25	2.08
	4.8	2.35	2.29	0.83	1.40	2.23
	5.6	2.34	2.30	0.79	1.40	2.19
	5.6	2.34	2.30	0.78	1.43	2.21
	5.4	2.85	2.63	1.00	1.43	2.43
	5.4	2.85	2.65	0.77	1.74	2.51
Mountain ephedra, Sarkand region	4.0	2.14	2.00	0.74	1.37	2.11
	4.0	2.14	2.11	0.81	1.19	2.06
Mountain ephedra, Andreev region	3.8	2.24	—	1.53	0.99	2.52
Mountain ephedra, Alakul' region	5.0	1.86	—	0.70	1.30	2.00
	5.0	1.86	—	0.67	1.42	2.09

Asia. The method is not new in principle. Oxalates have previously been used for the qualitative separation and identification of ephedra alkaloids [2-4]. Pseudoephedrine oxalate is very readily soluble in cold water, while ephedrine oxalate is almost insoluble. Black and Kelly [5], on the basis of some observations by Shou [2, 3], consider the separation of these alkaloids through the oxalates to be convenient and effective.

While carrying out determinations of the individual alkaloids as the oxalates, we noted that: 1) excess oxalic acid increases the solubility of ephedrine oxalates; 2) the amount of solvent (water) and the amount of pseudoephedrine in the solution have an effect on the solubility of ephedrine oxalate. Consequently, as we established, the alkaloids must be accurately back-titrated with 2% oxalic acid to a neutral reaction (using litmus as the indicator).

The titrated solution, which is contained in a small flask, is evaporated slightly on a hot plate for better precipitation of the ephedrine oxalate after the solution has been cooled. In this case, the solubility of the ephedrine amounts to about 5% of the total amount of alkaloids.

Data on the effect of the total alkaloids on the solubility of the oxalates in a synthetic mixture of ephedrine and pseudoephedrine during titration with 2% oxalic acid are shown in Table 2.

TABLE 4

Determination of Alkaloids by Variant II of the Oxalate Method

Source of ephedrin	Moisture (%)	Alkaloid content by standard method (%)	Alkaloid content by method B (in %)	Found by oxalate method (in %)		
				ephedrine	pseudoephedrine	total
Mountain ephedra, Krasnogorsk region	3.6	2.35	2.86	1.08	1.60	2.68
	3.6	2.35	2.86	1.20	1.45	2.65
	3.6	2.35	2.86	1.07	1.71	2.78
	3.6	2.35	2.86	1.05	1.71	2.76
	7.6	2.14	2.37	0.82	1.43	2.25
	7.6	2.14	2.38	0.81	1.46	2.27
	4.8	2.35	2.42	0.89	1.26	2.15
	4.8	2.35	2.39	0.81	1.34	2.15
	5.6	2.34	2.37	0.76	1.31	2.17
	5.6	2.34	2.34	0.82	1.34	2.16
	5.4	2.85	2.78	0.99	1.52	2.51
	5.4	2.85	2.75	0.92	1.53	2.45
Mountain ephedra, Sarkand region	4.0	2.14	2.24	0.71	1.29	2.00
	4.0	2.14	2.20	0.76	1.24	2.00
Mountain ephedra, Andreev region	3.8	2.24	2.32	1.71	0.75	2.46
	3.8	2.24	2.36	1.44	0.85	2.29

It may be seen from an inspection of Table 2 that, with a correction of not more than 5% for solubility, ephedrine can be determined as the oxalate with high accuracy by precipitation with 2% oxalic acid. As regards the pseudoephedrine, the error in its determination will be from ±0.05 to ±0.10%, i.e., within the ordinary limits of accuracy for the determination of alkaloids in ephedra.

These results on the determination of individual alkaloids in pure mixtures were transferred to the determination of the individual alkaloids in ephedra.

Two variants were developed for the determination of the individual alkaloids: 1) with separation of the total alkaloids from the ephedra by the standard method, 2) with separation of the total alkaloids by distillation with superheated steam.

Determination of the Individual Alkaloids in Ephedra

Variant I. To the mixture of alkaloids, which had been separated from ephedra by the standard method [1], was added, from a microburet, a 2% solution of oxalic acid*; the addition was continued until the mixture was neutral to litmus paper. The solution was evaporated in the flask on asbestos gauze on a hot plate to half its volume, and was then allowed to stand in a cold cabinet at a temperature of 3-5° until ephidrine oxalate no longer precipitated. The ephedrine oxalate was then vacuum filtered through a No. 2 porous (Schott) filter, and the precipitate was dried on the filter at 105° to constant weight.

Usually, 200 ml of the filtrate from the separation of the alkaloids by the standard method was used for the determination of ephedrine and pseudoephedrine. In this case, the ephedrine in the 200 ml of filtrate (from 20 g of ephedra) was calculated as the percentage content (x) of the absolutely dry ephedra by the following formula:

$$x = \frac{(a \cdot 0.786) + 5\% \text{ (of the total alkaloids in 20 g of ephedra)}}{(100 - b)\,2},$$

where a is the weight of oxalate (from 20 g of ephedra), b is the per cent moisture in the given sample, and 0.786 is a factor for converting ephedrine oxalate to ephedrine.

* The 2% oxalic acid solution was prepared by dissolving 20 g of ordinary chemically pure acid (HOOCCOOH · $\cdot 2H_2O$) in 600-700 ml of water and bringing the total volume of the solution to one liter. Titration of 10 ml of this solution required 32 ml of 0.1 N NaOH (phenolphthalein indicator).

TABLE 5

Comparative Data on the Content of Alkaloids in Ephedra as Determined by Variants I and II of the Method

Source of ephedra	Determined (in %)				Variant I		Variant II	
	ephedrine base		pseudo-ephedrine base					
	Variant				total alkaloids (in %)	amount of ephedrine in % of total alkaloids	total alkaloids (in %)	amount of ephedrine in % of total alkaloids
	II	I	II	I				
Mountain ephedra, Krasnogorsk region	1.03	1.08	1.42	1.60	2.45	—	2.68	—
	1.05	1.20	1.38	1.45	2.43	—	2.65	—
	1.00	1.07	1.45	1.71	2.45	—	2.78	—
	—	1.05	—	1.71	—	—	2.76	—
Average	1.03	1.10	1.42	1.62	2.45	42.05	2.72	40.50
Mountain ephedra, Krasnogorsk region	0.83	0.82	1.47	1.43	2.30	—	—	—
	0.83	0.81	1.41	1.46	2.24	—	—	—
Average	0.83	0.81	1.44	1.45	2.27	36.60	2.26	35.80
Mountain ephedra, Krasnogorsk region	0.83	0.89	1.25	1.26	2.08	—	2.15	—
	0.83	0.81	1.40	1.34	2.23	—	2.15	—
Average	0.83	0.85	1.32	1.30	2.15	38.60	2.15	39.54
Mountain ephedra, Krasnogorsk region	0.79	0.76	1.40	1.31	2.19	—	2.17	—
	0.78	0.82	1.43	1.34	2.21	—	2.16	—
Average	0.78	0.79	1.42	1.33	2.20	35.46	2.16	36.6
Mountain ephedra, Krasnogorsk region	1.00	0.99	1.43	1.52	2.43	—	2.51	—
	0.77	0.92	1.74	1.53	2.51	—	2.45	—
Average	0.88	0.95	1.58	1.52	2.47	35.63	2.48	38.62
Mountain ephedra, Sarkand region	0.74	0.71	1.37	1.29	2.11	—	2.00	—
	0.81	0.76	1.19	1.24	2.00	—	2.00	—
Average	0.77	0.73	1.28	1.26	2.05	37.60	2.00	36.50
Mountain ephedra, Alakul' region	1.53	1.71	0.99	0.75	2.52	—	2.46	—
	—	1.44	—	0.85	—	—	2.29	—
Average	1.53	1.57	0.99	0.80	2.52	60.7	2.37	66.2

Example. The total alkaloids in the ephedra amounted to 2% of the air-dried sample (400 mg of alkaloids in a 20 g sample or 200 ml of filtrate). 200 mg of ephedrine oxalate was obtained with a moisture content of 10%. Consequently, the percentage content (x) of ephedrine in the absolutely dry material was:

$$x = \frac{(200 \cdot 0.786) + 5\% \text{ (from 400 mg of alkaloids)}}{(100 - 10)\,2} = \frac{157 + 20}{180} = 0.98\%.$$

The pseudoephedrine was determined in the filtrate; for this purpose, the filtrate was evaporated to dryness in a drying cabinet at a temperature of 105° and then weighed.

The percentage content (x) of pseudoephedrine in the absolutely dry material was calculated according to the formula:

$$x = \frac{(a \cdot 0.786) - 5\% \text{ (of the total alkaloids in 20 g of ephedra)}}{(100 - b)\,2}.$$

Results of separate determinations of ephedrine and pseudoephedrine in ephedra by Variant I are presented in Table 3.

As may be seen from Table 3, the total amount of ephedrine and pseudoephedrine was in rather good agreement with the total alkaloids as determined by the standard method. Thus, this method for the determination of the individual alkaloids in ephedra is reliable and rather rapid.

In case the total alkaloids are determined by the standard method in one sample, and only the ephedrine is determined in another sample, the pseudoephedrine content in the ephedra can be calculated as the difference between the total alkaloids according to the standard method and the amount of ephedrine found by the oxalate method.

Under this condition, the percentage content (x) of ephedrine in the absolutely dry sample is determined by the formula:

$$x = \left[\frac{a \cdot 0.786}{(100 - b)\,2}\right] + \frac{5\%\ (\text{of the total alkaloids in the absolutely dry sample})}{200},$$

where a is the weight of ephedrine oxalate (from 20 g of ephedra), b is the per cent moisture in the given sample of ephedra, and 0.786 is a factor for converting ephedrine oxalate to ephedrine base.

Example. The total alkaloids in the ephedra amounted to 2% of the air-dried material (400 mg in the 20 g sample, i.e., in 200 ml of filtrate) or 2.22% of the absolutely dry material (444 mg in a 20-g sample, i.e., 200 ml of filtrate). 200 mg of ephedrine oxalate was obtained. Consequently, the percentage content (x) of ephedrine in the absolutely dry ephedrine:

$$x = \left[\frac{200 \cdot 0.786}{(100 - 10)\,2}\right] + \frac{5\%\ (\text{of } 444 \text{ mg of alkaloids})}{200} = \frac{157}{180} + 0.11 = 0.98\%.$$

A third form of calculation is used when the total alkaloids are determined by titration with 2% oxalic acid, from a microburet, to a neutral reaction toward litmus paper.

When 2% oxalic acid is used, the percentage content (x) of total alkaloids in the absolutely dry sample is calculated by the formula:

$$x = \frac{V \cdot 52.8}{(100 - a)\,2}$$

where V is the amount of 2% oxalic acid (in ml) consumed in the titration of the total alkaloids (in a 20 g sample of ephedra) and a is the moisture in the given sample (in %).

The percentage contents of ephedrine and pseudoephedrine are calculated by the formulas presented above.

Determination of the Individual Alkaloids in Ephedrine by the Oxalate Method with Separation of the Alkaloids from the Ephedra with Superheated Steam

Variant II. The alkaloids are distilled from the ephedra with superheated steam at a temperature of 127-142°; 4 g of NaCl and 20 ml of 10% NaOH are added according to Method B previously developed by us [6]. The resulting distillate (1500 ml), which contains the alkaloids and ammonia, is titrated with 0.1 N hydrochloric or sulfuric acid (with methyl red indicator); from the amount of 0.1 N acid consumed in the titration is subtracted 8.24 ml of 0.1 N acid which is consumed in the titration of the ammonia. More correct results are obtained if a small excess of 0.1 N acid is added, to a rose coloration, and the solution is back-titrated with 0.1 N base to a weak yellow color.

The percentage content of alkaloids (x) in the ephedra is calculated on a dry basis according to the formula:

$$x = \frac{(V - 8.24) \cdot 16.5}{(100 - a)}.$$

where V is the amount of 0.1 N solution of hydrochloric or sulfuric acid consumed in the titration of the total alkaloids and ammonia, and a is the moisture in the given sample (in %).

After the titration, the distillate (1500 ml) is evaporated to 100 ml, and rock salt is then added to saturation followed by 20 ml of 30% NaOH. The mixture is washed with ether (10-11 times) until the alkaloids are completely extracted; 150-200 ml of ether is required. The ether solution is dried over sodium sulfate and distilled. The resulting total alkaloids are titrated with 2% oxalic acid (litmus paper indicator).

The solution is evaporated on a hot plate to slightly less volume and allowed to stand in a cold cabinet for crystallization (at a temperature of 3-5°). The precipitated crystals are filtered on a No. 2 porous (Schott) filter. The remaining procedure is as described above for Variant I.

The percentage content of ephedrine in the absolutely dry ephedra is calculated by the formula:

$$x = \frac{(a \cdot 0.786) + 5\%\ (\text{of the total alkaloids})}{(100 - b)},$$

where a is the weight of ephedrine oxalate and b is the moisture in the given sample (in %).

Example. A 10 g sample of ephedra was used. The total alkaloids in the ephedra were determined to be 2%, i.e., 200 mg (in the 10 g sample); the moisture was 10%; the weight of ephedrine oxalate was 100 mg. The percentage content (x) of ephedrine in the ephedra, calculated on an absolutely dry basis, was:

$$x = \frac{(100 \cdot 0.786) + 5\%\ (\text{of } 200\ \text{mg})}{(100 - 10)} = \frac{78.6 + 10}{90} = 0.98\%.$$

The percentage content (x) of pseudoephedrine in the absolutely dry material was calculated by the formula

$$x = \frac{(a \cdot 0.786) - 5\%\ (\text{of the total alkaloids})}{(100 - b)}.$$

Results of determinations by Variant II of the method are presented in Table 4.

As the data of Tables 3 and 4 show, the determinations by the two variants of the method of the amount of ephedrine in any one sample are in good agreement.

Deviations between the amount of total alkaloids as determined by the oxalate method and by the standard method, on the one hand, and the amount as determined by steam distillation, on the other hand, are explained by the different degrees of accuracy of the methods, which are difficult to eliminate during routine analyses of the material. In particular, the inaccuracies of the standard method for the determination of the total alkaloids in ephedra were discussed in detail in our earlier paper [7].

In addition to ephedrine and pseudoephedrine, the mixture of alkaloids undoubtedly contains other bases, but the amount of these bases is very insignificant. Amoung these secondary alkaloids, L-norephedrine and L-N-methylephedrine have been found in insignificant amounts in the European and Asiatic species of ephedra [8-11]. There is still no basis to relate the discrepancies between the results obtained by the various methods for the determination of total alkaloids in ephedra to the presence of these secondary alkaloids in the plant.

Ephedrine base was isolated from the ephedrine oxalate from several samples of ephedra, which had been used for the determination of individual alkaloids. The hydrochloride of this ephedrine melted at a temperature of 215-216°. A mixture with a known sample of ephedrine hydrochloride melted without depression of the melting point.

According to the data of a number of authors, ephedrine hydrochloride melts at a temperature of 215 to 218° [12, 13].

The ephedrine hydrochloride had $[\alpha]_D^{20} - 34.3°$ (in water), which is in good agreement with the literature value [12, 14].

Comparative data from the determination of ephedrine and pseudoephedrine in several samples of ephedra, by both methods, I and II, are presented in Table 5.

It may be seen from the data in Table 5 that both methods give good results in the determination of ephedrine, and, moreover, in contrast to the standard method for the determination of individual alkaloids, both methods make possible the accurate determination of pseudoephedrine in ephedra.

In conclusion, the authors wish to express their appreciation to E. A. Khorenko, who took part in the development of this method.

SUMMARY

1. A method was developed for the quantitative determination of ephedrine and pseudoephedrine in ephedra. The separation is based on the different solubilities in water of ephedrine and pseudoephedrine oxalates.

2. The determination of ephedrine and pseudoephedrine may be carried out by either of two variants which depend on the method used to separate the alkaloids from the ephedra. In the first variant, the total alkaloids are separated by the usual standard method by digestion with 1% sulfuric acid and subsequent extraction with ether. In the second variant, separation of the total alkaloids from the plant is accomplished by distillation with superheated steam.

LITERATURE CITED

[1] Medicinal-Technical Raw Material (Standartgiz [State Standards Publishing House], 19 3).

[2] T. Q. Shou, J. Biol. Chem. 70, 109 (1926).

[3] T. Q. Shou, Zbl. 1, 5, 75 (1900).

[4] Chin - Tung, Chinese J. Physiol. 3, 397 (1927).

[5] O. F. Black and J. W. Kelley, Am. J. Pharm. 99, 12, 748 (1927).

[6] M. I. Goryaev, R.N. Sazonova, and I. M. Shabanov, Vestnik Acad. Nauk, KazSSR, 1, 71 (1958).

[7] M. I. Goraev, R. N. Sazonova, and I. M. Shabanov, Zhur. Priklad. Khim. 31, 289 (1958).*

[8] O. Wolves, Arch. Pharm. 268, H5, 337 (1930).

[9] Nagai and Kanao, J. Pharm. Soc. Japan. 48, 101 (1928).

[10] S. Smith, J. Chem. Soc. 2056 (1927).

[11] S. Kanao, Ber. 63, 95 (1930).

[12] A. P. Orekhov. The Chemistry of Alkaloids (in Russian) (Acad. Sci. Press, Moscow, 1955).

[13] V. Grignard. Traite de Chimie organique. Masson et C^ie, Paris (1950).

[14] T. A. Henry. The Chemistry of Plant Alkaloids [The Plant Alkaloids] (Russian translation) (Scientific-Technical Press, Moscow, 1956).

Received May 23, 1958

* Original Russian pagination. See C. B. translation.

PREPARATION OF ETHERS OF ALKYLENE CHLOROHYDRINS

N. P. Smetankina and V. S. Étlis

The β-halo ethers are the least studied of the halogenated ethers [1]. Several methods exist for the preparation of β-chloro ethers: through the chloroamides [2-4]; by the action of chlorine on olefins in the presence of alcoholic alkali [5-7], by the addition of free alkyl hypochlorites to olefins [8], and by liquid-phase chloroalkoxylation of olefins through the action of chlorine on olefins in an alcoholic medium [9-11]; the last method is the least studied. The literature contains only a few brief reports of the synthesis of certain β-chloro ethers by the last method.

The aim of the present work was to investigate the effect of the individual factors on the process. The study was carried out on the preparation of the methyl ether of propylene chlorohydrin. When the process was carried out with ethyl and isopropyl alcohols, similar results were obtained.

EXPERIMENTAL

The investigation of process conditions was carried out using a reactor with a diameter of 80 mm and a height of 500 mm and fitted with a reflux condenser and a thermometer. Prior to the start of the reaction, the reactor was charged with 1 kg of alcohol, which was then cooled to the required temperature with a mixture of ice and salt. The chlorine was fed through a porous disperser which extended to the bottom of the reactor. The propylene was fed in a similar manner at a distance of 60 mm above the point of introduction of the chlorine. The feed rates and gas consumption were measured with gas flow meters. The unreacted gases were passed from the upper part of the reactor to a control flask containing a starch–KI solution for the detection of chlorine in the effluent gas, and the gas was then vented to the atmosphere. The process was carried out in a manner such that there was no chlorine in the effluent gases.

At the conclusion of the synthesis, the reaction mixture was analyzed for HCl content and, in certain cases, for propylene chlorohydrin content by dehydrochlorination with excess alkali and back titration. The product was then neutralized with soda, washed free of unreacted alcohol, dried, and distilled. The chloro ether-dichloropropane fraction was analyzed for chlorine content by the Stepanov method using mercurimetric titration, and the composition of the product was calculated on the basis of these data. In order to isolate the pure methyl ether of propylene chlorohydrin, the mixture was cooled and treated with concentrated sulfuric acid [6]. The dichloropropane layer was separated, and the oxonium compound was treated with ice water; the product was washed, dried, and distilled. The resulting methyl ether of propylene chlorohydrin (probably a mixture of isomers) had a b.p. of 100-102° and n_D^{20} 1.4145.

Found %: C 44.06; H 8.33; Cl 31.98. C_4H_9OCl. Calculated %: C 44.25; H 8.35, Cl 32.65.

Literature data [4]: $CH_2ClCH(OCH_3)CH_3$, b.p. 104-105°, n_D^{15} 1.429; $CH_2(OCH_3)CHClCH_3$, b.p. 98-99°, n_D^{15} 1.408.

The process was also investigated using a propane-propylene fraction from the cracking of petroleum; the fraction had the following composition (in %): C_3H_6, 85.1; C_2H_4, 1.1; C_3H_8, 10.00; C_2H_6, 1.3; i-C_2H_{10}, 0.34; O_2, 0.40; CO, 0.04; N_2, 1.6. Commercial (cylinder) chlorine was used, and it was given a preliminary drying with concentrated H_2SO_4. The methyl alcohol (0.2% moisture) was used without additional treatment, except in experiments for the determination of the effect of the addition of water on the process, in which case completely anhydrous methyl alcohol was used; the anhydrous alcohol was obtained by treating commercial methanol with magnesium.

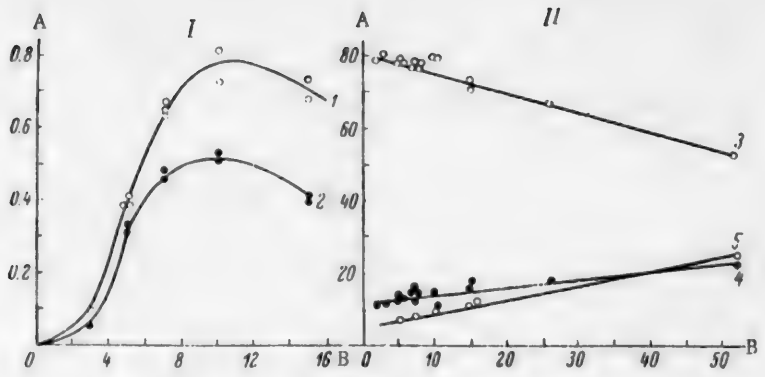

Fig. 1. Effect of synthesis time on the composition of the reaction products. Synthesis conditions: 1000 g of CH_3OH; 1 cc H_2O; temperature from -5 to +5°; mole ratio of Cl_2 to C_3H_6, 1 : 4 at a chlorine rate of 0.5 mole/ hour. A) Fraction (I) and per cent (II), B) synthesis time (in hours). 1) Mole ratio of chloro ether to HCl, 2) chloro ether yield based on chlorine, 3) chloro ether content in reaction products, 4) dichloropropane content in reaction products, 5) high-boiling residue in reaction products.

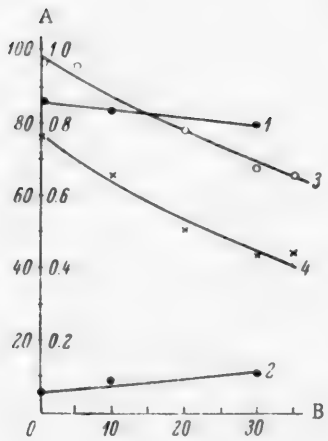

Fig. 2. The effect of temperature on the composition of the reaction products. Synthesis conditions: 1000 g of CH_3OH; 1 cc of H_2O; synthesis time, 10 hours; mole ratio of Cl_2 to C_3H_6, 1 : 4 at a chlorine feed rate of 0.5 mole/ hour. A) Per cent and fraction, B) temperature (in °C). 1) Chloro ether content in the reaction products, 2) dichloropropane content in the reaction products, 3) mole ratio of chloro ether to HCl, 4) chloro ether yield based on chlorine.

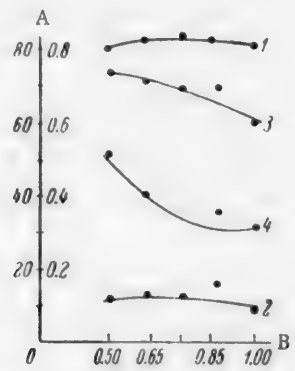

Fig. 3. Effect of gas feed rates on the composition of the reaction products. Synthesis conditions: 1000 g of CH_3OH; 1 cc of H_2O; synthesis time, 7 hours; mole ratio of Cl_2 to C_3H_6, 1 : 4. A) Per cent and fraction, B) chlorine rate in mole/ hour. 1) Chloro ether content of reaction products, 2) dichloropropane content of reaction products, 3) mole ratio, chloro ether : HCl, 4) chloro ether yield with respect to chlorine.

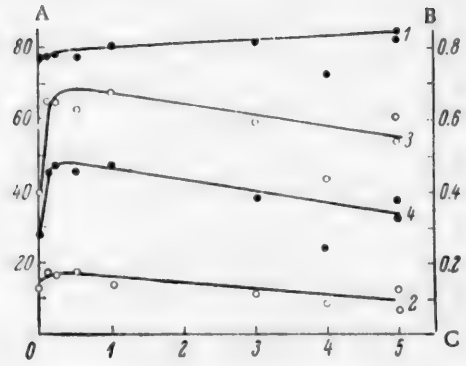

Fig. 4. Effect of water content of the original alcohol on the composition of the reaction products. Synthesis conditions: 1000 g of CH_3OH; synthesis time, 7 hours; temperature, from -5 to +5°; mole ratio of Cl_2 to C_3H_6, 1:4 at a chlorine feed rate of 0.5 mole/hour. A) Per cent, B) amount of water in the original alcohol (in %). 1) Chloro ether content of reaction products, 2) dichloropropane content of reaction products, 3) mole ratio, chloro ether : HCl, 4) chloro ether yield with respect to chlorine.

TABLE

The Effect of Mole Ratio of Propylene to Chlorine on the Process

Mole ratio C_3H_6 : : Cl_2	Composition of resulting mixture (in %)		
	chloro ether	dichloro-propane	high-boiling res.
2	83	7	10
3	84.7	7.5	8
4	86.8	5.4	7.8

DISCUSSION OF RESULTS

The interaction of propylene, alcohol, and chlorine proceeded mainly in accordance with the following reactions:

$$C_3H_6 + Cl_2 + CH_3OH \rightarrow CH_2ClCH(OCH_3)CH_3 + HCl; \quad (A)$$

$$C_3H_6 + Cl_2 \rightarrow CH_2ClCHClCH_3. \quad (B)$$

The predominance of one reaction over the other depends on the reaction conditions. We investigated the effects of temperature, synthesis time, gas feed rates, and the addition of water to the starting alcohol with the aim of determining whether it is possible to obtain a product with a high chloro ether content.

The results of the investigation of the effect of synthesis time on the process under otherwise uniform conditions are presented in Figure 1; it may be seen from Figure 1 that an increase in synthesis time had an undesirable effect on the composition of the resulting mixture and on the yield of chloro ether. With an increase in synthesis, time, the chloro ether content of the reaction products dropped, and the amount of dichloropropane and high-boiling residue increased.

The occurrence of reaction (A) is made difficult by the accumulation of HCl in the reaction mixture. Theoretically, 1 mole of hydrogen chloride should be formed for each mole of chloro ether; however, as shown by the curve of the mole ratio of chloro ether to hydrogen chloride (Figure 1, I), this ratio is always less than unity. Some of the additional amount of HCl probably results from the formation of bis-2-chloroisopropyl ether, which was found in the reaction products (b.p. 186, d_4^{20} 1.1116), and other highly chlorinated products.

An increase in temperature decreased the solubility of the gases in the reaction medium and, consequently, had an undesirable effect on the entire course of the synthesis.

From the results presented in Figure 2 it may be seen that with a decrease in the temperature to 0°, the percentage of chloro ether in the resulting reaction mixture decreased, as did the yield with respect to chlorine.

The results of the investigation of the effect of chlorine and propylene feed rates on the chloroalkoxylation process are presented in Figure 3.

Chlorine feed rates of 0.5, 0.65, 0.75, 0.85, and 1.0 mole/hour were tested. As may be seen from the graph, the composition of the mixture underwent almost no change with an increase in the gas feed rates; however, the yield of the desired product decreased sharply.

The results of the investigation of the effect of the mole ratio of propylene to chlorine are shown in the table. The yield of product increased and its composition improved somewhat with an increase in the mole ratio of propylene to chlorine.

The synthesis conditions were: CH_3OH, 1000 g; H_2O, 1 cc; synthesis time, 7 hours; temperature, from -5 to +5°; chlorine feed rate, 0.5 mole/hour.

Data, presented in Table 4 show that the addition of water catalyzes the chloroalkoxylation process.

Even the presence of just 0.1% H_2O in the starting alcohol significantly activated the process. However, the use of alcohol with higher water contents is undesirable, since, although the content of the methyl ether of propylene chlorohydrin in the mixture remains high (82.02%), its yield is significantly decreased owing to the reaction

$$CH_2 = CH - CH_3 + Cl_2 + H_2O \rightarrow CH_2ClCH(OH)CH_3 + HCl,$$

as is evident from the fact that 5.1 g (1.37% based on the chlorine) of propylene chlorohydrin was formed in the mixture when the concentration of water in the original alcohol was 0.1%. An increase in the added water to 0.2% increased the propylene chlorohydrin content of the mixture to 9.3 g (2.9% based on the chlorine), while the presence of 1% H_2O increased the content to 25.1 g (7.72%). At a water content in the methyl alcohol of 5%, 51.4 g (15.5% based on the chlorine) of propylene chlorohydrin was formed; consequently, 15.5% of the chlorine was consumed by this side reaction. The corresponding yields of chloro ether are presented graphically (Figure 4).

On the basis of these data, it is evident that it is desirable to add from 0.1 to 1.0% water to the original alcohol as a catalyst.

SUMMARY

Optimum conditions were found for the production of the methyl ether of propylene chlorohydrin with a methanol charge of 1000 g; temperature, from -5 to +5°; synthesis time, 10 hours at a propylene: chlorine mole ratio of 1:4; a chlorine feed rate of 0.5 mole/hour; and a catalytic amount of water, 0.1-1% of the weight of the alcohol charge.

LITERATURE CITED

[1] V. I. Isagulyants and P. S. Belov, Uspekhi Khim. 27, 4, 488 (1958).

[2] M. V. Likhosherstov and T. V. Shalaeva, Zhur, Obshchei Khim. 8, 4, 370 (1938).

[3] M. V. Likhosherstov and V. A. Sklyarov, Trudy Voronezh., Univ. 8, II (1935).

[4] V. A. Sklyarov, Zhur. Obshchei Khim. 23, 2121 (1939).

[5] M. V. Likhosherstov and A. A. Petrov, Zhur. Obshchei Khim., 5, 10, 1348 (1935).

[6] A. K. Seleznev, Zhur. Priklad. Khim. 27, 3, 327 (1954);* Zhur. Priklad. Khim. 30, 6, 965 (1957).*

[7] A. K. Seleznev and I. S. Maksimova, Zhur. Priklad. Khim. 25, 78 (1952).*

[8] M. V. Likhosherstov and S. V. Alekseev, Zhur. Obshchei Khim. 9, 1279 (1934).

[9] A. K. Seleznev, Zhur. Priklad. Khim. 31, 4, 620 (1958).*

[10] P. Ernst, Ger. Pat. 537636.

[11] L. N. Lapin and R. Kh. Zamanov, Zhur. Anal. Khim. 10, 6, 364 (1955).*

Received August 12, 1958

* Original Russian pagination. See C. B. translation.

PRODUCTION OF INDIVIDUAL ALCOHOLS FROM SPERM WHALE OIL

P. S. Ugryumov

Alcohols obtained from sperm whale oil, lauryl, myristyl, cetyl, and others, are required for the production of a number of medicinal preparations and for the production of higher alkyl and alkylene halides [1]. The body oil of the sperm whale contains, on the average, up to 40% aliphatic alcohols in the form of esters; 70% of these alcohols are unsaturated (oleyl alcohol). Cetyl alcohol is the major component of the saturated alcohols in the body oil. Sperm whale oil is inedible, since it contains approximately 66% waxy esters and only 34% triglycerides.

Sperm whale oil was formerly consumed exclusively as an oily material. The article "A new method for the convenient and rapid purification of blubber" [2], published in Russian, is among the early works on the processing of whale oil. In its unrefined form, sperm whale oil cannot be used in other industries. The yearly extraction of sperm whale oil in the USSR is about 8-9 thousand tons. The yearly world catch of whales over the period of 1950-1953 was 43,439-55,795. In 1951, 18,264 head of sperm whales were processed, and in 1956, the number amounted to 18,590. In other years, beginning with 1948, the number of whales processed never dropped below 10-15 thousand a year.

For the production of saturated alcohols, sperm whale oil can be catalytically hydrogenated under elevated pressure and high temperatures.

Aliphatic alcohols can also be obtained by reduction of sperm whale oil with metallic sodium by the Bouveault-Blanc method. In older methods used in plants, the metallic sodium was charged in large bars (4 kg each) in the amount calculated to give 4 g-atoms of sodium per mole of acid. However, these processes have now been improved. The unsaturated bonds in natural oils are not touched in the Bouveault-Blanc reduction process.

Sperm whale oil can be processed by still a third method – by saponification and subsequent distillation of the aliphatic alcohols. The composition of the fatty acids and aliphatic alcohols formed during the saponification of sperm whale oil has been discussed in some detail in the literature [3].

The wax separated from the case oil of the sperm whale has acquired the name "Spermaceti". The composition of spermaceti is: 11% crude sperm whale oil and 89% cetyl palmitate. In the pure form, spermaceti is a white, lustrous, coarsely lamellar mass with a crystalline structure, a melting point of 42-47°, and a density of 0.945-0.970. On the average, 3 thousand tons of alcohols derived from sperm whale oil are produced each year in the USSR. Unfortunately, we have not developed the production of spermaceti.

The percentage composition of sperm whale oil with respect to its major components is presented below.

	From the case	From the body
Wax	74	66
Triglycerides	26	34

Oil from the head of the whale contains 48.85% saturated fatty acids in the form of triglycerides. Among these acids are (in %): C_{10}, 6.88; C_{12}, 22.66; C_{14}, 15.31; C_{16}, 3.94; and C_{18}, 0.26. The remaining 51.15% are unsaturated fatty acids in the form of monoesters (in %): C_{12}, 13.79; C_{14}, 14.85; C_{16}, 13.02; C_{18}, 7.12; and C_{20}, 2.37. The body oil contains 12.5% saturated and 87.5% unsaturated fatty acids.

The content of oil in the various parts of the sperm whale body has been studied in some detail [4]. The ratio of case oil to body oil in the sperm whale averages 1:7.

Only the glyceride fraction of the oil can undergo saponification; the wax remains untouched. Industrial apparatus for the complex processing of sperm whale oil to wax and aliphatic alcohols has been created in the USSR. An article by Petrov [5] was devoted to this question. Liquid waxes are unsuitable for the production of cosmetics. Therefore, N. A. Petrov first hydrogenated the sperm whale oil at 180° under a pressure of 10-15 atm in the presence of copper-nickel catalyst, and then separated the solid wax. Deep-seated hydrogenation of sperm whale oil, or of the wax separated from it, yields three fractions of higher aliphatic alcohols with a yield of 96-97% of the oil charged.

However, our interest lies in another scheme for the processing of sperm whale oil. The new scheme includes the use of processes for reduction of the oil by means of metallic sodium [6].

The present article reports a new system for the processing of sperm whale oil to higher aliphatic alcohols using methylisobutylcarbinol or Ethyl Cellosolve as a reaction promoter, and decomposition of the alcoholates with urea. Carrying out this reaction in a medium of furfural in an autoclave and subsequent decomposition of the alcoholates with water is considered less satisfactory. Separation of the resulting alcohols by pressing leads to quantitative separation of lauryl and myristyl alcohols in the liquid fraction, from which they are separated by vacuum distillation. Separation of sperm whale alcohols into saturated and unsaturated fractions is carried out with the corresponding bromides by crystallization at temperatures from -8 to -20° from dichloroethane, n-hexane, acetone, or petroleum ether (b.r. 50-60°). Separation of the alcohols by centrifugation of the emulsion gave two fractions, solid and a liquid.

The resulting sperm whale alcohols can again be converted into wax of the required quality of transesterification with plant and animal oils.

EXPERIMENTAL

Starting materials. The sperm whale oil had the following properties: acid number, 6-13; saponification number, 123-147, iodine number, 63.0-84.0; hydroxyl number, 3.7; Reichert-Meissl number, 1.6; unsaponifiable content, 38.59; fatty acid content, 60.38; glycerine content, 2.2%; and density, 0.8781-0.8835.

A mixture of esters was separated from the sperm whale oil by molecular distillation in a film-type apparatus at 200-250° and a pressure of 10^{-3} mm Hg. 300 g of a mixture of these esters (fatty acids with an iodine number of 80 and higher alcohols) and 600 g of a mixture of ligroin and xylene in a ratio of 2:1 were charged to a glass vessel. The solution was gradually cooled to 5°. The solid product which precipitated was filtered and the solvent was evaporated. The yield of solid esters was 30 g; m.p. 48.3°, iodine number 73. The yield of liquid esters was 270 g; m.p. 5°, iodine number 87.3. Inasmuch as both fractions had a high iodine number, the method did not attain its purpose with respect to the separation of saturated compounds.

The alcohols obtained by saponification of the sperm whale oil had the following constants: hydroxyl number, 212.5-218-5; iodine number, 67.5-67.3; acid number, 0.99-0.87; and saponification number, 1.25-2.98. 10% of the alcohols derived from the sperm whale oil distilled at 115-145° at 10 mm, 40% distilled at 145-180°, 40% distilled at 180-200°, and 7% distilled at 200-220°.

Reduction with metallic sodium. 97 g of metallic sodium (4.2 g-atoms) and 50 ml of xylene were charged to an apparatus fitted with a reflux condenser, and nitrogen was passed into the reactor. The apparatus was heated to the point at which the xylene began to boil. After the metallic sodium had melted, the mechanical stirrer was switched on at a rate of 100-150 rpm. The metallic sodium was dispersed. Stirring was continued, and a mixture of 424 g of dry sperm whale case oil (with a moisture content not exceeding 0.1-0.03%), 10 ml of pyridine, and 212 g of methylisobutylcarbinol (2 moles) diluted with 100 ml of xylene was gradually introduced portionwise into the vessel. The addition was carried out at a rate such that violent boiling was maintained at all times. Upon completion of the addition of the mixture of sperm whale oil and methylisobutylcarbinol, stirring was continued

for another 15 minutes. Completion of the reaction was determined by the disappearance of the balls of metallic sodium. 218 g of dry, crystalline urea was introduced into the apparatus while the temperature was maintained at below 200° and stirrer operation was continued. Gradual evolution of ammonia was observed during the addition. Sodium cyanate precipitated. Heating of the apparatus and stirring was continued over a period of several additional hours until the evolution of ammonia was complete. The sodium cyanate was filtered at 80-100°, washed with a hot mixture of xylene and methylisobutylcarbinol, and dried at 100°. Filtration was sometimes made difficult by the formation of an emulsion. The filtrate and the wash liquids were washed in turn with large volumes of water. The emulsion which formed was broken by acidification and subsequent neutralization. The solvent was evaporated. The yield of liquid alcohols was 370 g; f.p. 25°, iodine number 43.8. The yield of sodium cyanate was 236 g. 90% of the methylisobutylcarbinol was recovered. Decomposition of the alcoholates with urea provides for safe operation and, simultaneously, the production of a valuable by-product sodium cyanate.

Separation of the aliphatic alcohols into solid and liquid alcohols. The alcohols were separated into two fractions (solid and liquid) at room temperature by pressing at 60 atmospheres with a hydraulic press and a temperature of 0 to 15°. The resulting solid sperm whale alcohols had a solidification temperature of 40-50°, a b.p. of 300-350° (200-220° at 20 mm), an iodine number of 30, a hydroxyl number of 218, an acid number of 0.74, and a saponification number of 1.6. The yield of solid alcohols from the sperm whale body oil varied from 15 to 25%. The liquid alcohols obtained from sperm whale body oil had a freezing point of 16°, an iodine number of 70-80, and a hydroxyl number of 210-240. The yield of liquid alcohols from the sperm whale body oil varied from 75 to 85% of the total aliphatic alcohols.

Pressing of 4 kg of the alcohols from the case oil yielded 1.8 kg of solid sperm whale case alcohols. Under the same conditions, 0.8 kg of solid sperm whale body oil alcohols was obtained from 4 kg of the alcohols.

The liquid fraction of the sperm whale case oil alcohols obtained by reduction of the oil with metallic sodium was used for the separation of lauryl and myristyl alcohols.

Distillation of the liquid fraction of the alcohols obtained from sperm whale oil. 500 g of the liquid sperm whale oil alcohols derived from the case oil were distilled under water-aspirator vacuum from a Claisen flask fitted with an adapter, and this gave approximately 350 g of a fraction with an average molecular weight of 187, a melting point of 22-23°, a boiling range of 258-278° (151-173° at 20 mm), a hydroxyl number of 285-300, and a density of 0.833. The residue in the flask was technical oleyl alcohol with an iodine number of 76. A second distillation separated 116 g of technical lauryl alcohol with a b.p. of 150-155° at 21 mm and a m.p. of 18-21°. The residue from the second distillation was technical myristyl alcohol.

Separation of the aliphatic alcohols from the products of the saponification of sperm whale oil. The saponified sperm whale oil was extracted with benzene. The higher aliphatic alcohols went into the benzene phase. The soap remained in the aqueous mother liquor. Then, after evaporation of the solvent, the whale oil alcohols were separated by pressing into solid and liquid fractions. Vacuum distillation of 500 g of the liquid whale oil alcohols obtained by saponification gave approximately 100 g of a fraction with an m.p. of 7°, a b.r. of 255-285° (160-180° at 20 mm), a hydroxyl number of 250-270, and an iodine number of 2-10. The residue in the flask was technical oleyl alcohol with an iodine number of 76. A second vacuum distillation isolated 19 g of technical lauryl alcohol with an m.p. of 14-16°, and a b.p. of about 160° at 21 mm. The distillation residue was a mixture of technical alcohols – myristyl, zoomaryl, and physeteryl. The soap was saponified, and approximately 10% lauric and myristic acids and 33% C_{16} fatty acids were found in the resulting acids in the form of fatty acid salts of amines.

The product obtained from the liquid fractions of the alcohols derived from sperm whale oil by two-fold vacuum distillation had the composition: 2.6% decanol, 61.0% dodecanol, 23.0% tetradecanol, 11.2% hexadecanol, and 2.2% octadecanol.

Catalytic reduction of the fatty acids from sperm whale oil without reduction of the double bond. 2 kg of oleic acid (iodine number 79), 75 g of copper carbonate, and 25 g of cadmium acetate were charged to an autoclave. The mixture was heated to 120°. Hydrogen was then added to a pressure of 232 atmospheres at 290°. The yield of oleyl alcohol was 89%; the alcohol had an iodine number of 75 and a hydroxyl number of 208. Whale oil fatty acids (iodine number 67) in methanol at a ratio of 1:2, together with a 100-fold excess of hydrogen, was passed through a tubular reactor in the presence of a zinc-barium-chromium catalyst; the temperature and pressure conditions were the same as above. In this case, the yield of aliphatic alcohols was 98% of theoretical, the iodine number was 68, and the hydroxyl number was 222.

Amidation. Free aliphatic alcohols and fatty acid amides were obtained by the action of ethanolamine at 180-190° on sperm whale oil.

Purification of the solid fraction of the whale oil alcohols. The solid fraction of the whale oil alcohols in a 3-fold volume of carbon tetrachloride was treated at 0° with bromine in a 3-fold volume in carbon tetrachloride. Upon dilution of the solution with cold petroleum ether, the bromides precipitated. After removal of the bromides, cetyl alcohol with an m.p. of 48-49° was obtained by distillation of the solvent from the mother liquid; the boiling range was: first drop at 310°, 5% at 312°, and 95% at 316°; the hydroxyl number was 229. After a second distillation, the hexadecyl alcohol boiled at 192° (15 mm) and had m.p. of 48°. The residue from the distillation, which amounted to 4-5% of the original alcohols, was stearyl alcohol.

Hydrogenation of the whale oil alcohols. The hydrogenation was carried out in an autoclave under a hydrogen pressure of 20 atmospheres at a temperature of 170-180° and in the presence of copper-nickel catalyst. Upon completion of the hydrogenation, the iodine number of the product did not exceed 2. The catalyst was removed by filtration. The hydrogenated whale oil alcohols were distilled under reduced pressure. The cetyl alcohol distilled at 190-192° at 15 mm (freezing point, 45-49°), and the stearyl alcohol distilled at 210° at 15 mm (freezing point, 49-55°). Distillation was also used for the isolation of lauryl and myristyl alcohols. However, complete separation of the cetyl and stearyl alcohols was not obtained.

Separation of the whale oil alcohols into saturated and unsaturated fractions. 275 g of whale oil alcohols was dissolved in 100 ml of dichloroethane. The mixture was allowed to standat at -20° for a day. The precipitated crystals of saturated aliphatic alcohols (iodine number, 1.5) were filtered at -15°. The solvent was distilled from the filtrate with live steam. The unsaturated alcohols (iodine number, 94) were obtained in the form of a light oil. The separation was controlled by iodine number. 91 g of saturated alcohols and 168 g of unsaturated alcohols were obtained. The content of saturated alcohols in the liquid whale oil alcohols separated by pressing was 7-10% as determined by iodine number.

Isolation of oleyl alcohol. 23 g of bromine was added to 250 ml of dichloroethane. The mixture was stirred, and 5.2 ml of redistilled pyridine was gradually added from a dropping funnel at 13-14°. The solution was stirred for 30 minutes, and was then used to brominate the unsaturated aliphatic alcohols.

Alcohol	Temperature (in °C)		Iodine number
	b. p.	f. p.	
Lauryl	150—152 (21mm) 255—259	18—21 24	—
Cetyl	190—192 (15mm) 318—320	45—49	—
Stearyl	210 (15mm) 344	—	—
Oleyl	178—180 (7mm) 340		92—94 95

A solution of 60 g of the total whale oil alcohols in 300 ml of carbon tetrachloride was cooled with an ice-salt mixture to -15°, and the solution of pyridine tetrabromide was then added at this temperature over a period of 4 hours with constant stirring. Stirring was continued at -15° for an additional 2 hours after the addition of the solution had been completed. The bromides precipitated upon dilution of the solution with cold petroleum ether.

An acetic acid solution of the bromides was placed in a 2-liter jar fitted with a stirrer, a dropping funnel, and a device for sprinkling in the zinc dust, and 40 ml of acetic acid and 100 ml of water were added for washing the flask. 40 g of zinc dust was then added in small portions over a period of 40-50 minutes to the reaction mixture, which was at a temperature of 16-17°, and the mixture was stirred for 7 hours at 20-23°. The yield of oleyl alcohol from the whale oil was 11%; the alcohol had a b.p. of 178-180° at 7 mm and a hydroxyl number of 208.

Separation of cetyl and oleyl alcohols. 10 g of whale oil alcohols from the saponified oil and 5 g of liquid ammonia was charged to a metal vessel. The vessel was tightly closed by tightening the bolts, and was shaken at 0° for 15 minutes. Cooling was continued while the vessel was opened. 3 g of the insoluble cetyl alcohol was separated. The ammonia was evaporated and 6-7 g of pure oleyl alcohol was obtained.

Separation of lauryl and myristyl alcohols. From a mixture of saturated whale oil alcohols, obtained by crystallization from a solvent at low temperatures, the lauryl and myristyl alcohols were separated by vacuum distillation. A mixture of lauryl and myristyl alcohols was obtained from the mixture of liquid whale oil alcohols (obtained by pressing the whale oil alcohols) by drying the mixture over anhydrous sodium sulfate followed by low-temperature crystallization from organic solvents.

The constants of these whale oil alcohols and, for comparison, the literature values [3] are presented in the table (the values above the line are those of the present author, and those below the line are the literature values).

SUMMARY

1. Alcohols obtained by saponification of sperm whale body oil were separated into the following components (in %): stearyl alcohol, 5; cetyl alcohol, 20; oleyl alcohol, 65; and lauryl and myristyl alcohols, 10. The fatty acids included 10% C_{12}-C_{14} acids and 33% C_{16} acids.

2. Whale oil alcohols obtained by reduction of the case oil with metallic sodium were separated into the following components (in %): stearyl alcohol, 4; cetyl alcohol, 30; oleyl alcohol, 26; and lauryl and myristyl alcohols, 40.

LITERATURE CITED

[1] P. S. Ugryumov, Med. Prom. 4 (1953); 13, 4, 15 (1956); Russ. Pats. Nos. 98,797, 99,567, and 111,198; Application MZ SSSR No. 1820 (1951).

[2] Supplement to the Technological Journal, consisting of scientific reports having as their subject the application of scientific discoveries to practical uses, published by the Academy of Sciences, Vol. 1, Part III, 42 (1816).

[3] L. Schon, Soap Perfumery and Cosmetics, 25, 1, 65 (1952).

[4] E. Wahuon, Jugr chimiste, 38, 205, 107 (1956).

[5] N. A. Petrov, Masloboino-Zhirovaya Prom. 12, 6 (1952).

[6] F. O. Barrett, J. D. Fitzpatrick and R. G. Kadesch, Ind. Eng. Ch. 45, 1114 (1953).

Received October 21, 1958

SYNTHESIS OF 3,3'-DINITROBENZIDINE AND THE ANALYTICAL REAGENTS ARSENAZO II, TORON II, AND PHENAZO

V. I. Kuznetsov and S. B. Zavvin

Biphenyl-4,4'-diarsono-3,3'-bis[<-azo-2>-1,8-dihydroxynaphthalene-3,6-disulfonic acid] (arsenazo II) and biphenyl-4,4'-diarsono-3,3'-bis[<-azo-1>-2-hydroxynaphthalene-3,6-disulfonic acid] (toron II) are valuable analytical reagents for uranium, thorium, and the rare earth and certain other elements [1]. 3,3'-Dinitrobiphenyl-4,4'bis[<-azo-4>phenol] (phenazo) is an interesting reagent for magnesium [2]. 3,3'-Dinitrobenzidine is necessary both for the synthesis of these compounds and for the synthesis of certain others, for example, 3,3'-diaminobenzidine, a valuable reagent for selenium [3].

The method for the synthesis of arsenazo II and toron II is published here for the first time. The method for the synthesis of 3,3'-dinitrobenzidine constitutes a substantial improvement over the method described in the literature.

3,3'-Dinitrobenzidine.

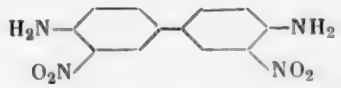

In the preparation of 3,3'-dinitrobenzidine, the amino groups in the benzidine must first be "protected" by an acetate [4] or formate [5] radical, and the resulting diacetylbenzidine is then nitrated with concentrated nitric acid, specific gravity 1.48, at 0° [4], a mixture of acetic and nitric acids, specific gravity 1.50, at room temperature [6], or a mixture of acetic anhydride and nitric acid, specific gravity 1.52, at a temperature of from -12 to -16° [7]. The acetyl groups are removed from the product with a mixture of KOH and ethyl alcohol [6, 8] or dilute, 4:1, sulfuric acid [7].

This method was found to be insufficiently reproducible. In a number of cases, when insignificant changes were made in the conditions, low-melting products were obtained, evidently a mixture of 3,3'-dinitrobenzidine, 3-nitrobenzidine, and other nitro and polynitro substituted benzidines.

In the method described below, the acetylation and nitration steps are combined into one operation. The nitration is carried out at 100° in a medium of acetic acid and acetic anhydride using ordinary nitric acid with a specific gravity of 1.35.

Method of synthesis. 50 g (0.27 mole) of finely powdered benzidine (base) was added, with vigorous stirring, to a mixture of 250 ml of acetic anhydride and 350 ml of glacial acetic acid in a three-necked flask fitted with a stirrer and a reflux condenser. The mixture was heated on a boiling water bath for 2-3 hours. It was then cooled to 60-70°, and, after 15-20 minutes, 50 ml of HNO_3 with a specific gravity of 1.35 (0.6 mole) was added. The mixture acquired a dark orange color. It was again heated to 100°, and vigorous stirring was continued for an additional 20-30 minutes. The mixture became bright orange. It was cooled to 20-30°, filtered, and washed with 20-50 ml of acetic acid and 100-200 ml of water.

The orange-yellow 3,3'-dinitro-N,N'-diacetylbenzidine was returned to the same flask, 200-300 ml of ethyl alcohol was added, and the mixture was stirred until a homogeneous mass was obtained. The mixture was heated to 70-80°, and, with as vigorous stirring as possible, 80 ml of a 40% solution of NaOH was added at one time.

The suspended precipitate slowly dissolved, and from the resulting dark orange solution separated bright red 3,3'-dinitrobenzidine. The mixture was stirred for another 30-40 minutes. It was then cooled to 10-20°, filtered, and the precipitate washed with 30-50 ml of ethyl alcohol and 200-400 ml of warm water. It was dried at a temperature not exceeding 70°.

The yield was 70 g; m.p. 275° (literature value of recrystallized 3,3'-dinitrobenzidine, 260-275° [4-8]).

3,3'-Diaminobiphenyl-4,4'-diarsonic acid.

This product was prepared from 3,3'-dinitrobenzidine by bis-diazotization followed by arsonation (Bart reaction) and reduction of the nitro groups to amino groups.

The 3,3'-dinitrobenzidine was bis-diazotized with nitrosylsulfuric acid in a medium of concentrated H_2SO_4 [6, 8]. Reaction of the comparatively unstable 3,3'-dinitro-4,4'-bisdiazobiphenyl with arsenious acid was carried out in a medium of $NaHCO_3$ cooled to 0°. The resulting 3,3'-dinitrobiphenyl-4,4'-diarsonic acid was reduced with ferrous salts in an alkaline medium.

Method of synthesis. Preparation of the nitrosylsulfuric acid solution: 18 g (0.26 mole) of $NaNO_2$ was added very slowly and with stirring to 70 ml of concentrated H_2SO_4 heated to 60-80°. The solution was cooled to room temperature, and added portionwise to a solution of 30 g (0.11 mole) of 3,3'-dinitrobenzidine in 60 ml of concentrated H_2SO_4. From time to time, a test for completion of the bis-diazotization was made. For this purpose, a drop of the solution was placed in a test tube with 2-5 ml of water. The appearance of a reddish color indicated incomplete diazotization. If the solution remained colorless or only slightly yellowish, it was considered that diazotization was complete.

The dark orange bis-diazo solution was poured onto 1-2 kg of ice, and was then rapidly filtered from chance impurities.

50 g of As_2O_3 was dissolved in 50-100 ml of a 40% solution of NaOH; the solution was diluted to 1 liter with water, and 1 g of $CuCl_2 \cdot 2H_2O$ in 100-200 ml of water (the catalyst) was added. The bis-diazo solution and a saturated solution of soda were simultaneously added to the above solution with stirring. It is necessary that at this point the reaction mixture has only a weakly alkaline reaction toward brilliant yellow paper. Crushed ice was added to the reaction vessel, and as it melted, fresh ice was added. The amount of $Na_2CO_3 \cdot 10H_2O$ required was approximately 700 g. The solution was allowed to stand for several hours or overnight.

The resulting precipitate was filtered and discarded, and the filtrate was acidified with concentrated HCl until a small amount of a dark brown precipitate of by-product phenols began to form (pH of 4.5-6.0). This precipitate was filtered and discarded, and the filtrate was acidified with concentrated HCl to complete precipitation of the product (pH 1.5-2.0).

The resulting light yellow precipitate of 3,3'-dinitrobiphenyl-4,4'-diarsonic acid was filtered, transferred to a 2-3 liter flask, and dissolved in 20-30 ml of a 40% solution of NaOH and 100-200 ml of water. A saturated solution of $FeCl_2$ was added and then a 40% solution of NaOH in an amount such that the medium was constantly alkaline to phenolphthalein (external indicator). Reduction was considered to be complete when the mass, which was initially brown (ferric hydroxide), turned black (mixed ferric and ferrous hydroxides).

The consumption of $FeCl_2 \cdot 4H_2O$ was about 250 g, while the consumption of the 40% NaOH solution was about 600 ml.

The solution was filtered into a flask containing 100-200 ml of concentrated HCl.

The precipitate was carefully pressed and washed 3-4 times with small portions of a hot 1-2% solution of NaOH. The filtrate was made alkaline with NaOH to complete precipitation of the product (pH 1.5-3). The light brown precipitate was filtered, pressed, and washed with 5-10 ml of water. It was dried in air.

The yield of 3,3'-diaminobiphenyl-4,4'-diarsonic acid was 27 g.

Found %: N 6.32%, As 33.8. $C_{12}H_{14}O_6N_2As_2$. Calculated %: N 6.48, As 34.7.

Arsenazo II.

Arsenazo II was prepared by coupling bis-diazotized 3,3'-diaminobiphenyl-4,4'-diarsonic acid with chromotropic acid.

Method of synthesis. 8.0 g (0.0185 mole) of 3,3'-diaminobiphenyl-4,4'-diarsonic acid was dissolved in 60 ml of water, 30 ml of concentrated HCl was added, the solution was cooled, and a solution of 3.0 g of $NaNO_2$ in 10 ml of water was then added.

A mixture of 15.0 (0.041 mole) of chromotropic acid(calculated as 100%) and 90 g of $Na_2CO_3 \cdot 10H_2O$ was dissolved in 50-80 ml of water. The mixture was cooled, and the bis-diazo solution was added to it with stirring. The reaction mixture was stirred for an hour, and then heated to 60-80°, filtered from chance impurities, and neutralized, and 40-70 ml of concentrated HCl was then added. The dark red, almost black precipitate was filtered, pressed, and washed with 5-10 ml of water. It was recrystallized twice from water, the product being precipitated by the addition of concentrated HCl. It was washed with 5-10 ml of water and dried in air.

The yield of arsenazo II was 19 g.

Toron II.

Toron II was prepared by coupling bisdiazotized 3,3'-diaminobiphenyl-4,4'-diarsonic acid with R salt.

Method of synthesis. 18.5 g (0.0428 mole) of 3,3'-diaminobiphenyl-4,4'-diarsonic acid was dissolved in 250-300 ml of water, 60 ml of concentrated HCl was added, the solution was cooled, and a solution of 7.1 g of $NaNO_2$ in 20-30 ml of water was added.

A mixture of 33 g of R salt (0.094 mole) (calculated as 100%) and 140 g of $Na_2CO_3 \cdot 10H_2O$ was dissolved in 250 ml of water. The mixture was cooled, and the bis-diazo solution was added to it with stirring. The mixture was stirred for an hour; it was then heated to 50-60°, filtered from chance impurities, neutralized, and diluted with 100-200 ml of concentrated HCl.

The dark orange product was filtered, pressed, again dissolved in 200-300 ml of water, and dry NaCl was then added to the complete precipitation of the slightly soluble tetrasodium salt of toron II. It was dried in air.

The yield of toron II was about 44 g.

Phenazo.

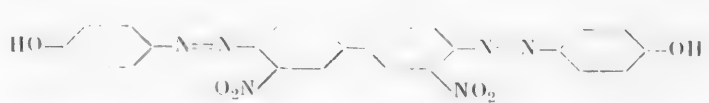

Phenazo was prepared by coupling bis-diazotized 3,3'-dinitrobenzidine with phenol.

Method of synthesis. 5.0 g (0.018 mole) of 3,3'-dinitrobenzidine, dissolved in 10 ml of concentrated H_2SO_4, was bis-diazotized with a solution of nitrosylsulfuric acid (3.0 g of $NaNO_2$ in 17 ml of concentrated H_2SO_4) by the method described above.

The bis-diazo solution was poured onto 0.5-1 kg of ice. A mixture of 5 g (0.053 mole) of phenol and 200 g of $Na_2CO_3 \cdot 10H_2O$ was dissolved in 300-400 ml of water. The mixture was cooled, and the bis-diazo solution was added to it with stirring. The mixture was stirred for an hour at room temperature. 40-60 ml of a 40% solution of NaOH was added to dissolve the precipitated phenazo, and stirring was continued for an additional 15-20 minutes. The product was precipitated by adding concentrated HCl to an acid reaction toward congo. The brown precipitate was filtered and washed with a small amount of acidified water. It was dried at a temperature not above 70°. The yield of phenazo was about 8 g.

LITERATURE CITED

[1] V. I. Kuznetsov, Zhur. Anal. Khim. 14, 8 (1958).*

[2] V. I. Kuznetsov, L. M. Budanova and L. A. Nenasheva, Zavodskaya Lab., 24, 1053 (1958).**

[3] K. L. Cheng, Anal. Chem. 28, 1738 (1956).

[4] J. Strakosch, Ber. 5, 236 (1872).

[5] H. R. Hirst and J. B. Cohen, J. Chem. Soc. 831 (1895).

[6] R. J. Fevre and E. E. Turner, J. Chem. Soc. 245 (1928).

[7] C. C. Barker and F. D. Casson, J. Chem. Soc. 4181 (1953).

[8] H. H. Hodgson and J. Walker, J. Chem. Soc. 1620 (1933).

Received May 21, 1958

* See C. B. Translation.

** Original Russian pagination. See C. B. Translation.

DIRECT SYNTHESIS OF METHYLCHLOROSILANES IN A FLUIDIZED BED

K. A. Andrianov, S. A. Golubtsov, I. V. Trofimova and N. P. Lobusevich

The information available in the literature on the synthesis of methylchlorosilanes from methyl chloride and silicon in the presence of a catalyst (copper) relates chiefly to the composition of the contact material and the effect of the method of preparation of the material on its catalytic activity [1].

In work on the synthesis of ethylchlorosilanes [2, 3], we have shown that the composition of the contact material is only one of two basic factors determining the characteristics of the direct synthesis process. A second, very important factor is the method by which contact between the reagents is accomplished, i.e., the effect of the type of apparatus on the synthesis process. In particular, it was shown that an effective method for carrying out the direct synthesis of ethylchlorosilanes [3] and of phenyltrichlorosilane [4] is in a "pseudoliquid" or fluidized bed with agitation of the powdered silicon-copper alloy by the stream of ethyl chloride (or chlorobenzene mixed with hydrogen chloride).

In the present work, which was carried out in 1954-1955, we confirmed that the principle of the fluidized bed may be effectively applied to the direct synthesis of methylchlorosilanes. Our experiments showed that the process proceeds quite well at elevated pressures (4-5 atm); the effective contact between the reagents guarantees high productivity (yield of methylchlorosilane mixture per hour, calculated on the basis of 1 kg of alloy) when standard copper-silicon alloy (20% copper) is used as the contact mass. Owing to the high heat of reaction, the question of the sufficiently rapid removal of heat from the reaction zone under these conditions becomes serious, and this, in turn, means that the apparatus must be properly constructed, particularly with respect to the cooling equipment. In an investigation of a number of cooling arrangements, it was found that the introduction of a coil, through which coolant is passed, directly into the reaction zone provides satisfactory results. It was possible to obtain satisfactory temperature control in an apparatus of this type; in such an apparatus, the yield amounted to 140-190 g of the mixture of methylchlorosilanes per hour per kg of alloy charged, and the methyldichlorosilane content of the mixture of chlorides varied from 42 to 47%.

EXPERIMENTAL

Figure 1 shows a schematic diagram of the apparatus used for the preparation of methylchlorosilanes in a fluidized bed. Methyl chloride from cylinder 1, which was contained in water bath 2, passed through throttling valve 3 into vaporizer-surge tank 4, which was heated by hot water, and then passed through a rotameter 5 into reactor 6. The reaction products passed through filter 7, for removal of entrained dust, and were then condensed in the water-cooled trap 8. The uncondensed products passed through throttling valve 9 into traps 10, which were cooled with a mixture of dry ice and acetone; here the methylchlorosilanes and unreacted methyl chloride entrained by the gas stream were collected. The effluent gases were vented to the atmosphere.

Experimental procedure. 250 g of powdered standard copper-silicon alloy (20% copper) was charged to the reactor, the electric heater was switched on, and, at a temperature of 100°, nitrogen flow to the reactor was started. Drying of the alloy in a stream of nitrogen was continued for a period of 1-2 hours, after which the nitrogen pressure in the system was increased to 4-5 atm, and feeding of the methyl chloride to the reactor at a rate of 300-380 g/ hour was begun. The reaction was continued at a temperature of 350-370° for a period of 6-8 hours, after which the methyl chloride flow was stopped, the apparatus was cooled to room temperature in a stream of nitrogen, and the methylchlorosilanes collected in traps 8 and 10 were fractionated.

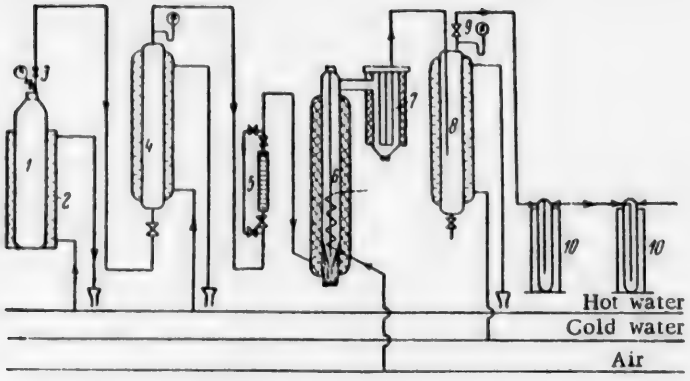

Fig. 1. Schematic diagram of the apparatus for the preparation of methylchlorosilanes in a fluidized bed.

TABLE 1

Rectification of the Methylchlorosilane Mixture

Content (in wt. %) in the fractions																	Content of dimethyldichlorosilane (%) in chlorides' mixture	
To 39°	39–42°		42–55°		55–58°		58–64.5°		64.5–67°		67–69°		69–71°		kettle residue (in %)	loss-(in %)		
fraction	fraction	chlorine	fraction	chlorine	fraction	chlorine	fraction	chlorine	fraction	chlorine	fraction	chlorine	fraction	chlorine			rectification	distillation
0.6	1.7	—	1.2	—	—	—	2.3	61.0	29.1	70.8	9.3	65.8	39	55.2	8.1	8.7	42.3	37.7
0.6	6.1	62.5	4.9	—	0.7	54.8	2.9	62.3	31.3	70.3	6.0	65.3	27.2	55.4	10.4	9.9	30.8	27.8
—	1.9	—	1.6	—	—	—	4.1	59.4	26.6	70.9	9.1	60.4	34.2	55.0	13.8	8.7	40.2	35.2
—	4.2	61.8	3.8	—	3.0	59.4	4.0	60.1	25.3	69.9	10.3	65.0	37.3	55.6	5.9	6.7	41.2	36.7

Determination of the composition of the reaction products was carried out by rectification of the condensate in a column having an efficiency of 55 theoretical plates (1300 mm in height, 12 mm in diameter, and packed with No. 0.075 2 × 2 mm cylinders formed from copper screen). The results of four experiments in which the product composition was determined by rectification are presented in Table 1; these results show that the condensate contained the usual products of the direct synthesis of methylchlorosilanes [1] – methyldichlorosilane (2-6%), trimethylchlorosilane and silicon tetrachloride (a total of 3-5%), methyltrichlorosilane (25-35%), dimethyldichlorosilane (35-40%), and a high-boiling kettle residue (5-10%). The dimethyldichlorosilane was assumed to consist of the fraction boiling at 69-71°, which contained 55.2-55.4% chlorine, and also part of the fraction boiling at 67-69° (the composition of the fraction was calculated from the data on chlorine content).

In order to obtain a preliminary approximate determination of the dimethyldichlorosilane content, we distilled the mixture of methylchlorosilanes from a flask fitted with a dephlegmator; the calculation was carried out on the basis of the yield of the fraction boiling at 64-72°and its chlorine content. Results of such determinations are compared with values obtained from rectification data in Table 1. These data indicate that it is possible to obtain an approximate value for the dimethyldichlorosilane content of the mixture by distillation from a flask fitted with a dephlegmator (the accelerated method gives results which are too low by not more than 5%).

The results of a series of experiments on the preparation of methylchlorosilanes in a fluidized bed operation in apparatus of different constructions are presented in Table 2.

An apparatus without any special cooling means was used in Experiments Nos. 1-3; the process proved to be completely uncontrollable, and in the case in which the methyl chloride was diluted with a stream of nitrogen (Experiments Nos. 2 and 3), the productivity decreased sharply. Similar results were obtained in Experiments Nos. 4-6 in which cooling was through the reactor wall.

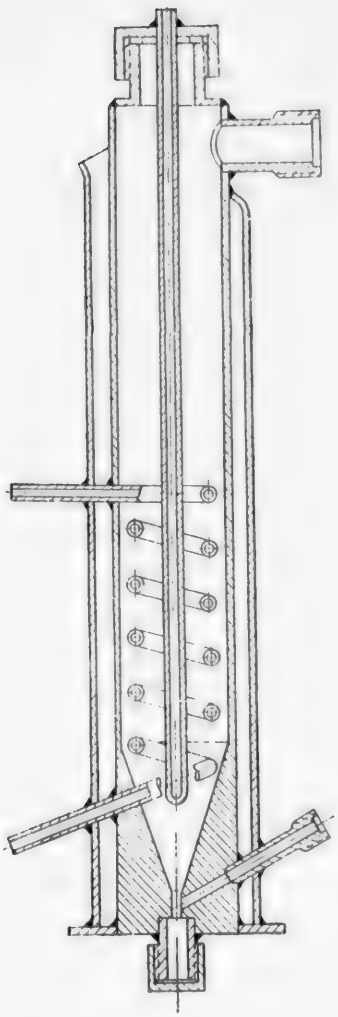

Fig. 2. Reactor for the synthesis of methylchlorosilanes in a fluidized bed.

TABLE 2

Synthesis of Methylchlorosilanes in a Fluidized Bed

Expt. No.	Time (in hours)	Temp. (°C)	Methylchlorosilane mixture yield, g		Dimethyldichlorosilane cont.% in chlorides mixture
			total for the expt.	per hr. per kg of alloy	
1	6	360—880	2380	1585	—
2*	6	330—370	74	49	35.0
3*	6	330—370	63	42	37.0
4	6	360—550	1008	720	9.5
5*	6	330—370	90	60	31.2
6*	6	330—370	93	62	39.2
7	6	360—500	1260	840	4.1
8	6	350—400	786	525	15.9
9*	6	350—400	910	610	14.4
10*	6	350—400	480	320	13.9
11	8	330—380	382	191	42.7
12	7	350—360	351	136	40.0
13	6	330—360	248	165	44.7
14	8	330—360	370	138	46.1
15	8	330—360	358	137	47.0
16	8	330—360	320	160	45.0

* Cooling by dilution of the methyl chloride with nitrogen.

In Experiments Nos. 7-10, cooling was obtained by means of a Field tube introduced into the reactor. It was not possible to obtain close temperature control or satisfactory results, probably owing to insufficient cooling surface.

In Experiments Nos. 11-16, an apparatus was used in which water or air was fed to a coil located inside the reaction zone (Figure 2). This construction provided quite satisfactory and readily reproducible results, since it was possible to control the temperature closely and to remove the heat of reaction.

SUMMARY

A method for the direct synthesis of methylchlorosilanes from methyl chloride and silicon in the presence of copper using a fluidized-bed process is proposed. A laboratory apparatus was developed for this synthesis; using this apparatus, reproducible results and fairly high yields were obtained (140-190 g of methylchlorosilane mixture per hour per kg of alloy with a dimethyldichlorosilane content of 42-47%).

LITERATURE CITED

[1] K. A. Andrianov. Organosilicon Compounds (in Russian). Goskhimizdat [State Chemical Press] (1956); U.S. Pat. 2466412 (1942); 2427605 (1947); 2447873 (1948); 2466429 (1949); 2380997 (1945).

[2] K. A. Andrianov, S. A. Golubtsov, I. V. Trofimova, A. S. Denisova and R. A. Turetskaya, Doklady Akad. Nauk SSSR, 108, 3, 465 (1956).

[3] K. A. Andrianov, S. A. Golubtsov, L. V. Trofimova,and A. S. Denisova, Zhur. Priklad. Khim., 30, 1179 (1957).*

[4] K. A. Andrianov, S. A. Golubtsov, N. N. Tishina,and L. V. Trofimova, Zhur. Priklad. Khim., 32, 201 (1959).*

Received May 15, 1958

* Original Russian pagination. See C. B. Translation.

BRIEF COMMUNICATIONS

DIFFUSION OF WATER VAPOR AND THE FLOW OF AIR IN POROUS GLASS

D. P. Dobychin

The kinetics of adsorption and catalytic phenomena depend to a great extent on the porous structure of the adsorbents and catalysts. Therefore, it becomes necessary to measure the values of the effective diffusion coefficients of gases and vapors in such porous bodies as a function of the pore structure of the bodies.

Study of the dependence of the structure of porous glass on the thermal prehistory of the original sodium borosilicate glass has permitted the development of methods for controlling the structure of porous glass and, in particular, the preparation of porous glass with wide pores having radii of the order of hundreds of thousands of angstroms [1, 2]. During a study of these porous glasses, we found it possible to relate the gas permeability and the effective diffusion coefficients of water vapor diffusing through the glass to data on the pore structure of the glass.

The value of the pore radius in these wide-pore glasses was determined by the method of Deryagin [3] from the rate of flow of air through the samples studied under Knudsen conditions. The rate of air flow through a porous plate was measured by determining the pressure increase (or decrease) in a closed, calibrated volume. During the tests, the plates were held between rubber washers in a holder having a double seal (Figure 1); the double seal prevented possible flow of air through the sides of the disk which protruded from under the edge of the rubber packing ring. The rate of air flow under a pressure drop from atmospheric to several millimeters of mercury was used to calculate the gas permeability coefficient (K_g $\frac{cm^3 \cdot mm}{cm^2 \cdot min \cdot atm}$), and the specific surface, related to unit volume (S_s m^2/cm^3), was calculated from the results of measurements of the rate of air flow at a pressure drop of from 50 to 200 mm Hg. The pore radius was calculated from the well-know relationship $r = \frac{2 \cdot \vartheta}{S_s}$, where ϑ is the volumetric porosity.

Naturally, we were unable to determine pore radii from our measurements of the adsorption of water vapor on wide-pore glasses, nor could we reliably determine the over-all pore volume; these adsorption measurements were carried out with a quartz spring balance. Therefore, the total porosity of the wide-pore glasses was determined from the values of the true and apparent densities, which were determined by the usual method.

We found it possible to determine the value of the effective diffusion coefficient for water vapor in porous glass from data obtained in tests of the water permeability of the porous glass disks under static conditions. The disks themselves served as the cover of a holder containing the adsorbent, and the holders were placed in a desiccator which contained a solution of sulfuric acid of the proper concentration to maintain a relative humidity (φ) of 35%.

By weighing the holders, the rate of adsorption of water vapor by the adsorbent and, consequently, the rate of diffusion of water vapor through the disk were measured. The porosity, thickness, and pore radii of the disks were measured before they were fixed in the holders.

As is well known [4, 5], the total resistance of a stagewise process is equal to the sum of the resistances of the stages (if the courses of the separate stages can be described by first order kinetic equations). In our case, taking into account the diffusion of the water vapor in air, diffusion in the porous disk, and adsorption by the adsorbent, and using the usual method for a uniformly accessible surface, we obtained the equation

$$\frac{1}{K_{ov}} = \frac{1}{D \cdot f(s, L)} + \frac{1}{D^*} \cdot \frac{h}{s} + \frac{1}{K_a \cdot \varphi(\sigma, l)}, \quad (1)$$

where $\frac{1}{K_{ov.}}$ is the over-all resistance of the process, K_{ov} is the over-all rate constant of the process, $\frac{1}{D \cdot f(s, L)}$ is the resistance for the stage in which the water vapor diffuses in air, D is the diffusion coefficient for water vapor in air, f (s, L) is the general form of the function relating the magnitude of the diffusion flow to the geometry of the apparatus (distance to the level of the acid, cross-section of the disk, etc.), $\frac{1}{D^*} \cdot \frac{h}{s}$ is the resistance of the stage in which water vapor diffuses through the porous disk, D^* is the effective diffusion coefficient of water vapor in the porous glass [6], h and s are the thickness and cross-section of the disk, respectively, $\frac{1}{K_a \cdot \varphi(\sigma, l)}$ is the the resistance of the stage in which water vapor is adsorbed by the adsorbent, K_a is the rate constant for the adsorbent, and $\varphi(\sigma, l)$ is the general form of the function relating the rate of adsorption of water vapor by the adsorbent to the geometry of its location (cross-section of the adsorbent layer, its height, the packing density, etc.).

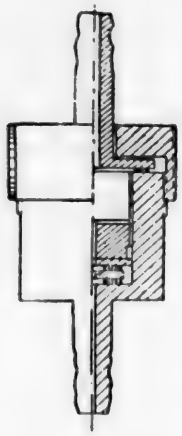

Fig. 1. Sketch of the double-seal holder for measuring the rate of flow of air through porous disks.

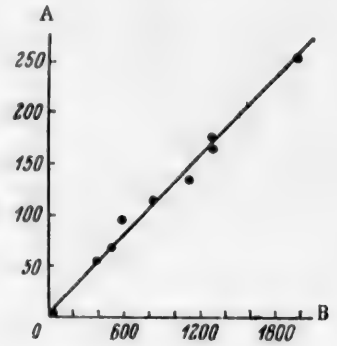

Fig. 2. Dependence of K_g/δ on pore radius. A) Gas permeability per unit pore volume, Kg/δ, B) pore radius, r (in A).

TABLE

Expt. No.	Volumetric porosity δ (cm / cc)	Gas permeability constant, K_g, $\left(\frac{cm^3 \cdot mm}{cm^2 \cdot min \cdot atm}\right)$	Pore radius (in A) gas flow method	Eff. diff. coeff. for water vapor D^*, (sq. cm./sec.)
1	0.386	26.6	495	--
2	0.552	98.5	1300	--
3	0.641	86.1	1110	—
4	0.820	210	2000	—
5	0.432	24	380	0.021
6	0.429	40.8	575	0.023
7	0.514	59.4	820	0.042
8	0.391	64.9	1300	0.044
9	0.284 **	0.15—0.3	30—40 *	0.0083

* Average of a series of adsorption determinations (Kelvin radius).

** Obtained from the value of the specific pore volume, $\nu_s = 0.18$ cm^3/g, which was determined by an adsorption method assuming the true value of the density of the porous glass to be equal to the density of the non-porous glass, $d = 2.18$ g/cm^3.

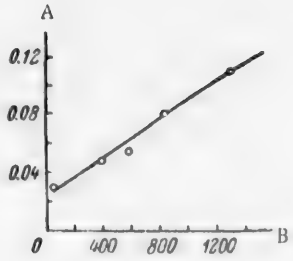

Fig. 3. Dependence of D^0/δ on pore radius. A) Effective diffusion coefficient per unit pore volume, D^0/δ, B) pore radius, r (in A).

The expression for the over-all time of the process, which is equal to the sum of the characteristic times of its stages [7], has a similar form:

$$\tau_{obs} = \tau_D + \tau_\delta + \tau_A \qquad (2)$$

where τ_{obs} is the experimentally observed adsorption time for a given amount of water vapor, τ_D, τ_δ, and τ_A are the characteristic times for the three stages of the process mentioned above.

Experimenting with different adsorbents, we carried out experiments both with holders closed by porous disks and with open holders (without porous disks). In this case, Equation (2) has the form:

$$\tau'_{obs} = \tau_D + \tau_A \qquad (3)$$

From Equations (2) and (3), we obtain an expression for the characteristic time of diffusion of water vapor through the porous plate undergoing testing:

$$\tau_\delta = \tau_{obs} - \tau'_{obs} \qquad (4)$$

The characteristic time of a stage is the time required for the total flow to pass through it if the total concentration drop (the entire motive force) occurred across that stage. Therefore, by calculating τ_δ from the experimentally determined values of τ_{obs} and τ'_{obs}, it is possible to determine the value of the effective diffusion coefficient for water vapor diffusing through the given disk:

$$D^* = \frac{1}{\tau_\delta} \cdot \frac{m}{c_{H_2O}} \cdot \frac{h}{s} \ (cm^2/sec) \qquad (5)$$

where, m is the amount of water vapor the absorption of which by adsorbents in holders with and without porous glass disks occurred in times τ_{obs} and τ'_{obs}, respectively, c_{H_2O} is the concentration of water vapor in air of 35% relative humidity φ (in g/cm^3), and h and s are the height and cross-section of the disk, respectively. The value of m was taken as 0.1 g, as found from the approximately linear (initial) portion of the kinetic adsorption curves for water vapor by the adsorbent in the holder and also as determined, with rather good accuracy, by weighing on an analytical balance.

Experimental data from two series of experiments are presented in the table.

The gas permeability referred to unit pore volume ($\frac{K_g}{\sigma}$), was proportional to the pore radius (Figure 2). The effective diffusion coefficient referred to unit pore volume, ($\frac{D^0}{\sigma}$), was a linear function of the pore radius (Figure 3). Theoretically, a direct proportionality would be expected [8]. The portion of the ordinate to the intercept of the straight line, Figure 3, probably represents the component of the over-all flow which proceeds by surface diffusion along the walls of the communicating pores [9].

The values obtained for the diffusion coefficients, D^0, for fine-pore glass (0.008 sq. cm./second) and for wide-pore glass (0.03 sq. cm./second) are in reasonable agreement with the values of the diffusion coefficient for water vapor in air, $D^0_{air} = 0.282$ sq cm /second.

LITERATURE CITED

[1] D. P. Dobychin and N. N. Kiseleva, Doklady Akad. Nauk SSSR, 113, 372 (1957).*

[2] D. P. Dobychin and N. N. Kiseleva, Zhur. Fiz. Khim., 32, 27 (1958).*

[3] B. V. Deryagin, Trudy Inst. Fiz. Khim. Akad. Nauk SSSR, 1, 150 (1950).

* Original Russian pagination. See C. B. Translation.

[4] O. E. Vlasov, Supplement to: Introduction to Heat Transfer (in Russian), F. Grebera (1933).

[5] C. M. Tu, H. Davis and H. C. Hottel, Ind. Eng. Ch. 26, 749 (1934).

[6] Ya. B. Zel'dovich, Zhur, Fiz. Khim. 13, 163 (1939).

[7] D. A. Frank-Kamenetskii, Zhur. Fiz. Khim. 13, 756 (1939).

[8] B. V. Deryagin, Doklady Akad. Nauk SSSR, 53, 627 (1946).

[9] W. M. Jones, Trans. Faraday Soc. 47, 381 (1951).

Received June 11, 1958

ACTIVATED CARBON FROM SULFITE-CELLULOSE LIQUORS

B. N. Dashkevich and M. N. Karpinskii

In the production of cellulose by the sulfite process, about 50% of the wood goes into solution in the liquor, of which there are large amounts and which contains, toward the end of the digestion process, from 8 to 10% organic material.

The spent sulfite liquor is presently used for the production of ethyl alcohol, vanillin, edible yeast, tanning extracts, concentrates used in the foundry and construction industries, and for other purposes, and owing to these various uses, the liquors are subjected to more or less complex processing [1].

The decision of the XXI Congress of the KPSS [Communist Party of the Soviet Union] and the 230% increase in cellulose production planned for the near future confronts chemical technology with the problem of seeking additional means for the utilization of the enormous amounts of liquors which will be produced by industry.

The production of activated carbon could serve as one means of using sulfite-cellulose liquors. Only a very small amount of investigation has been devoted to this problem. Müller [2] has recommended a method for the production of decolorizing charcoal which consists of partial precipitation of the calcium in the form of difficultly soluble compounds and subsequent filtration, evaporation of the filtrate, carbonization of the dry residue, and washing. Kielland [3] has proposed a method for the production of carbon by evaporation of the liquor, heating the dry residue to 160-250°, washing with acids, alkalies, or water, and then carbonizing. Berl [4] proposed a complex 10-step process for the production of highly active carbon useful for the adsorption of vapors; the process included the use of high temperatures (up to 1200°) and elevated pressures.

Assuming that the production of even very active carbons from sulfite-cellulose liquors would be practical only if the process is simple and cheap, we decided to proceed by simple evaporation of the liquor and carbonization of the dry residue with subsequent removal of the ash and activation of the carbon by solvents or gaseous materials.

EXPERIMENTAL

Evaporation of the liquors was carried out in thermostatted evaporators at temperatures of 80, 100, 150, and 200°. Under all of these temperature conditions, a dry, brown residue with a porous structure was obtained in an amount of about 10% of the liquor charge with variations of from 0.5 to 1% on either side. The dry residues were carbonized at a temperature of 350-400°, and the product was washed with 2 N hydrochloric acid and water to a neutral reaction to remove the ash. At low carbonization temperatures (up to 400°), in addition to carbon and oxides of carbon, a large amount of tarry organic products are formed, which are partially sorbed by the carbon [5]. The carbon may be treated with solvents or gaseous substances to remove the tar and increase the active surface.

We tested solvent extraction by treating the carbons obtained with benzene or gasoline hydrocarbons in a Soxhlet apparatus for 4-5 hours.

Of the possible forms of gas activation, we considered treatment with atmospheric oxygen at a temperature of 600-900° to be undesirable owing to the large and nonuniform loss of carbon in the form of oxides. It was decided to use activation by carbon dioxide or water vapor, which, in reacting with the substances adsorbed on the

TABLE 1

Results of Tests of Sulfite Carbon

Dye	Vol. of solution (in ml)	Amount of ABC or sulfite carbon (in g)	Amount of dye adsorbed by the carbon (in g/ml)		Activity of the sulfite carbon (in %)
			ABC	sulfite carbon	
Pure direct blue	45	1.0	$177 \cdot 10^{-8}$	$72 \cdot 10^{-8}$	41
Methyl green		1.0	$196 \cdot 10^{-8}$	$182 \cdot 10^{-8}$	93
Basic violet		1.0	$198 \cdot 10^{-8}$	$173 \cdot 10^{-8}$	87
Acid scarlet		0.5	$166 \cdot 10^{-8}$	$56 \cdot 10^{-8}$	34

TABLE 2

Results of Activity Tests on the Carbon

Dye	Activity of treated sulfite carbon (in %)		
	washed with benzene	washed with gasoline	carbon dioxide-activated
Pure direct blue	47	55	89
Basic violet	77	90	132
Acid scarlet	29	49	72

surface and filling the pores of the carbon, partially interact with the carbon (but by endothermic and, therefore, uniformly occurring reactions forming carbon monoxide) increasing the porosity and yielding a product with a high specific surface [6].

In our activation experiments, the carbon dioxide was passed from a gas holder through a Tishchenko flask filled with calcium chloride and then into a quartz tube charged with the sulfite carbon and heated by an electric tube furnace. Temperature control was accomplished by means of a thermocouple located in the carbon charge. Activation was carried out at a temperature of 870°. The carbon dioxide was fed at a rate of 1.0-1.2 liters/ hour which corresponded to 1 liter of gas per g of carbon charged. Activated carbon was obtained in an amount of 50-55% of the weight of the carbon charged.

The loss of carbon occurred uniformly throughout the mass, and the amount (45-50%) was within the normal limits for activation by carbon dioxide (40-50%).

Steam activation was carried out in a quartz tube filled with the carbon and heated externally by an electric furnace; 0.6 g of water per 1.0 g of carbon charged was added over a period of 3 hours from a dropping funnel. The temperature was maintained at 850°, since a higher activation temperature leads to the formation of graphite in the outer layers of carbon and to a decrease in activity of the carbon. Yields of 45-50% of activated carbon were obtained.

Although the strength of the resulting carbon granules was not high, a fact which was evident without any mechanical testing and which limited use of the carbon to a decolorizing agent, it was decided to test these carbons both for adsorption of dissolved substances and for absorption of vapors and gases.

The decolorizing properties of these carbons were tested by adsorption of dyes from aqueous solutions having a concentration of $2 \cdot 10^{-6}$ g/ ml. Equal weights of the carbons of uniform grain size were placed in a conical flask, and equal volumes of the dye solutions were added to the flasks. At the conclusion of a specified time, which was equal for a given series of tests but which varied between series from 15 minutes to 3 hours depending

on the rate of adsorption, the carbon was filtered, and the filtrates were examined by comparison with a standard in a Duboscq colorimeter. The residual concentration of the solution and the amount of dye adsorbed per ml of solution were calculated from the colorimeter readings. The activities of the sulfite carbons were expressed as per cent of the activity of Soyuzreaktivsbyta* activated birch carbon (ABC).

Table 1 presents the results of the tests of sulfite carbon prepared by calcination with subsequent removal of the ash and without additional activation.

As may be seen from Table 1, the activity of the sulfite carbon was lower than the activity of the ABC in all experiments.

The weight of carbon used for adsorption of the acid scarlet was decreased to 0.5 g, since decolorization of the solution of this dye was too rapid when 1 g of ABC was used, and this made the determination difficult.

Results of the tests of the activity of sulfite carbon treated with benzene, gasoline hydrocarbons, and carbon dioxide are presented in Table 2.

In all experiments reported in this Table, the weight of carbon was 0.5 g, the volume of dye solution was 50 ml, and the concentration of dye was $2 \cdot 10^{-6}$ g/ ml.

As may be seen from the data of Table 2, the least active carbon was the one washed with benzene; the carbon treated with the gasoline hydrocarbons was somewhat more active, and the activity of the carbon treated with carbon dioxide was still higher and approached and even exceeded the activity of the activated birch carbon.

The adsorption capacity of the sulfite carbon treated with steam was investigated in a separate series of experiments by an analogous method. This carbon had the following activities in terms of dye adsorption (in %): pure direct blue — 160, methyl green — 196, and acid scarlet — 159; i.e., the activity was higher than that of ABC in all the the experiments.

In view of the low granule strength of these carbons, only exploratory experiments were carried out on the static sorption capacity of the carbon dioxide-activated sulfite carbon for chlorine and benzyl bromide vapors and on the dynamic sorption capacity for chlorine.

Determination of the static sorption capacity was carried out by passing chlorine from a gas holder through a tube filled with the carbon until the carbon attained constant weight. The sulfite carbons had the following activities, based on the activity of ABC as 100%: without additional activation — 87, carbon dioxide-activated — 341.

Determination of the static sorption capacity of the carbons for benzyl bromide vapor was carried out by holding the carbon in an atmosphere of saturated benzyl bromide vapor at room temperature for 48 hours. The activity of the sulfite carbon activated with carbon dioxide was 280% of that of birch carbon.

The exploratory experiments on dynamic activity were carried out by passing chlorine at a uniform rate through tubes of equal diameter and length and filled with ABC or sulfite carbon activated with carbon dioxide.

Break-through was indicated by means of starch-iodide paper. Determination of the times of the protective action of carbon layers of equal length with other conditions also being equal gave an activity index for carbon dioxide-treated sulfite carbon 2.2 times higher than that of activated birch carbon (220%).

SUMMARY

1. Carbons obtained from sulfite-cellulose liquors by evaporation and carbonization of the dry residue at a temperature of 300-400° with subsequent removal of ash (but without additional treatment) had activities lower than that of activated birch carbon, and the granule strength was low.

2. Activation of the sulfite carbons by washing with benzene or gasoline hydrocarbons did not yield encouraging results.

3. Activation of the sulfite carbons with steam increased their activity for the adsorption of dissolved substances to 160-195% based on the activity of activated birch carbon (ABC).

* Transliteration of Russian — Publisher's note.

4. Activation of sulfite carbons with carbon dioxide increased their activity to 280 and 340% for static adsorption of vapors and gases and to 220% for dynamic sorption capacity as compared to activated birch carbon (ABC).

5. Activated sulfite carbons are suitable for use as decolorizing agents, and can be used for the purification of gases under steady state industrial conditions not permitting attrition of the carbon granules.

LITERATURE CITED

[1] N. I. Nikitin The Chemistry of Wood (in Russian), (Academy of Sciences USSR Press, 1954) 489.

[2] H. Müller, Ger. Pat. 468212, June 6, 1923.

[3] J. Kielland, Norwegian Pat. 68582, November 6, 1944.

[4] E. Berl, U. S. Pat. 2441125, May 11, 1948; U. S. Pat. 2567468, November 11, 1951.

[5] P. Klasson, Z. angew. chem. XII, 25, 1205 (1909).

[6] M. M. Dubinin, Physicochemical Foundations of Sorption Engineering (in Russian). (State Chemical-Technical Press, 1932) 238.

Received July 24, 1958

INVESTIGATION OF THE CHEMICAL NATURE OF CRACKED PETROLEUM RESIDUUMS

E. I. Kazakov and V. P. Kuznetsova

Up to 30% residual stock is formed during thermal cracking of crudes and topped crudes. The chemical composition and nature of these residuums are of great significance in the development of methods for their utilization. Nevertheless, the literature on this question is limited to characterization of the physical properties of petroleum residuums, and there is only a certain amount of general information as to their composition [1-6].

With the aim of shedding some light on this question, the authors considered it desirable to describe briefly in the present article the results of an investigation of the chemical nature of petroleum residuums obtained under commercial conditions during cracking of Baitugansk and Bugul'minsk crudes. The residuum was an asphaltic product with $d_4^{20} = 1.02181$, a viscosity at 80° of $\eta_{80} = 7.9$, and a Conradson carbon of 14.1; during distillation, 93% of the product boiled above 320°. The elemental composition of the residuum was (in %): C, 85; H, 9.65; S, 3.6; O, 0.87; there was no nitrogen. The residuum was separated into its basic components: the carbenes and asphaltenes were separated with petroleum ether, and the filtrate, freed from most of the solvent by distillation on a water bath, was passed through a silica gel column (ACK, 32-60 mesh) to adsorb the resins and oil. The latter was eluted with petroleum ether, and the resins were desorbed with a series of solvents [7] of increasing polarity (carbon tetrachloride, benzene, and acetone). The paraffin wax was separated from the oil with dichloroethane at -20°, and was then reprecipitated and recrystallized from acetone.

Elemental analysis was carried out on each of the components (asphaltenes, resins, paraffin wax, and hydrocarbons), and the density and molecular weight were determined; the infrared absorption spectra were also investigated.

The hydrocarbon portion was investigated by solvent extraction and chromatography.

The hydrocarbon component was present in the greatest amount (58.5%; Table 1), followed by the asphaltenes and resins (26.1%); the solid hydrocarbons (paraffin wax) were present in appreciable amount (8.1%). The content of carbenes and carboids was relatively low (3.2%). The resins (13.3%) had the following characteristics with respect to solvents: 5.1% was extracted by carbon tetrachloride, 3.9% by benzene, and 3.85% by acetone; the molecular weights of the resins separated by the solvents increased in the indicated order from 475 to 671.

This indicates that the oil contained in a cracked residuum is not a homogeneous substance.

The asphaltenes in the cracked residuum approached thermally formed asphaltenes with respect to elemental composition. During hydrogenation under pressure, along with a certain amount of cracking, condensation and other reactions leading to increased molecular weight take place with the formation of a large amount of coke (40-50%); in addition, the resulting liquid products contain a significant amount of asphaltenes which did not undergo cracking. Resins do not yield coke under similar experimental conditions.

The solid hydrocarbons separated from the cracked residuum were high molecular weight paraffins with the empirical formula $C_{37.2}H_{75}$, which corresponds to $C_nH_{2n+0.6}$. With the aim of determining the group composition and characterizing the hydrocarbons present, the neutral oil – the major component of the cracked residuum – was investigated by chromatography over silica gel (ASM brand with an activity of 11.5-12 and a grain size of 60-150 mesh). Selection of the conditions for the resolution of the neutral oil was based on experiments with a small column. Subsequent chromatographic separation of the oil was carried out in a three-stage column

TABLE 1

Component	Content (%)	d_4^{20}	Molecular wt.	Elemental composition (%)				C/H ratio	M.p. (°C)
				C	H	S	O		
Carbens and carboids	3.2	—	—	—	—	—	—	—	—
Asphaltenes	12.8	1.1477	821	85.60	6.40	4.32	3.68	13.3	—
Resins	13.3	—	555	84.75	8.40	2.50	4.35	10.0	—
Paraffin wax	8.1	0.8776	521	85.75	14.30	—	—	6.0	60
Oil	58.5	—	—	85.70	10.50	3.04	0.76	8.1	—

TABLE 2

Characteristics of the Fractions Obtained by Chromatographic Separation of the Neutral Oil

Fraction No.	Wt. (in g)	n_d^{20}	d_4^{20}	Intercept	Mol. wt.	Iodine No.	Elemental comp. (%)				Empirical formula	General formula
							C	H	S	O (by difference)		
1	14.1	1.4623	0.8311	1.046	316	0	85.9	14.1	0	0	$C_{22.6}H_{45}$	C_nH_{2n}
2	1.4	1.4862	—	—	—	—	—	—	—	—	—	—
3	13.3	1.5219	0.9286	1.057	308	24.6	85.45	11.20	3.35	0	$C_{21.9}H_{34.5}$	$C_nH_{2n-9.2}$
4	1.2	1.5356	—	—	—	—	—	—	—	—	—	—
5	6.4	1.5785	1.0061	1.075	283	34	86.12	9.10	4.68	—	$C_{20.3}H_{25.75}$	$C_nH_{2n-14.8}$
6	4.6	1.5961	1.0364	1.077	252	25	85.70	8.50	4.70	1.10	$C_{18}H_{21}$	C_nH_{2n-15}
7	5.7	1.6165	1.0625	1.085	293	30	86.30	8.50	4.50	0.7	$C_{21}H_{24.6}$	$C_nH_{2n-17.4}$
8	2.6	1.6206	1.0683	1.086	433	18	86.32	8.50	4.33	0.85	$C_{31}H_{36.8}$	$C_nH_{2n-25.2}$

charged with 500 g of silica gel; 50 g of neutral oil was used. Petroleum ether, benzene, and acetone were used in succession as the solvent and desorbent. Fractions which, on the basis of refractive index, formolite reaction, and intercept, belonged to a specific hydrocarbon group were combined. The oil was separated into 8 fractions, the characteristics of which are presented in Table 2.

Fraction No. 1 (negative formolite reaction) was a colorless liquid which solidified at room temperature (16°) owing to precipitation of the paraffin present in it. This fraction (28.2% by weight of the oil) had an index of refraction of 1.4623, a density of 0.8311, and an intercept of 1.046; there was no sulfur present. The average empirical formula, calculated on the basis of molecular weight and elemental composition, was $C_{22.5}H_{45}$, which corresponds to the C_nH_{2n} series. The somewhat decreased hydrogen content can apparently be ascribed to the presence of a significant amount of naphthenic hydrocarbons. On the basis of these data, this fraction can be assigned to naphthenic-paraffinic hydrocarbons.

Fraction No. 2 — an intermediate fraction (2.8% of the oil) — was a yellowish liquid with an index of refraction of 1.4862.

Fraction No. 3 (26.6% by weight of the oil) had an index of refraction of 1.5219, a density of 0.9286, and an intercept of 1.057, which correspond to aromatic hydrocarbons having only one aromatic ring in the molecule. The empirical formula was $C_{21.9}H_{34.5}$, which corresponds to the series $C_nH_{2n-9.2}$; the fraction contained 3.35% sulfur. The iodine number was 24.6. From a comparison of the experimental data with the literature values, it may be assumed that the fraction contained monocyclic aromatic hydrocarbons, probably with an unsaturated bond in the side chains.

Fractions Nos. 5 and 6, which comprised 21.4% of the oil, had indices of refraction of 1.5785 and 1.5961, respectively. The intercepts, 1.075 and 1.077, indicated the presence in these fractions of aromatic hydrocarbons containing two aromatic rings in the molecule. The empirical formulas of these fractions are included in the series C_nH_{2n-15}.

Fractions Nos. 7 and 8 comprised 18.4% of the oil; their indices of refraction, 1.6165 and 1.6206, densities, 1.0625 and 1.0683, and intercepts, 1.085 and 1.086, indicate that the fractions contain polycyclic hydrocarbons. The empirical formulas $C_{21}H_{24} - 0.37$ and $C_{31}H_{36.8} - 0.5$ correspond to C_nH_{2n-18} and $C_nH_{2n-25.2}$.

The major part of the sulfur compounds was concentrated in the fractions containing bicyclic and polycyclic aromatic hydrocarbons. Significant amounts of sulfur and oxygen also characterized the asphaltenes and resins, which suggests a genetic connection between these components. It should be noted that, judging from the low iodine numbers, the oil contained few unsaturates.

Thus, on the basis of the results of the chromatographic analysis, the composition of the neutral oil is as follows: paraffinic-naphthenic hydrocarbons, 30%; aromatic hydrocarbons 68%, including 27% monocyclic, 22.5% bicyclic, and 18.5% polycyclic aromatics. The loss during analysis was 2%.

The presence and the nature of the above components of the cracked residuum were confirmed by the results of our subsequent investigation of this material by infrared spectroscopy using an IKS-11 apparatus. First of all, it should be remarked that in none of the spectra was there observed an absorption band at 6.02 μ, which corresponds to double bond valence vibrations. This indicates that unsaturated hydrocarbons were absent or present in insignificant amounts in the cracked residuum investigated.

The solid hydrocarbons and Fraction No. 1 of the neutral oil gave only absorption bands corresponding to valence vibrations of CH_2, CH_3, and $-(CH_2)_n-$, and no bands characteristic of other groups were found in the spectra. The neutral oil fraction containing monocyclic aromatic hydrocarbons gave absorption bands corresponding to aromatic C–C, and the spectrum also had a region characteristic of hetero atoms. The spectra of the remaining groups of substances separated from the cracked residuum had, in addition to these bands, absorption bands in the long-wavelength region, which corresponded to valence vibrations of polycondensed aromatics.

SUMMARY

Petroleum residuum obtained by thermally cracking Baitygansk and Bugul'minsk crudes under industrial conditions are high-molecular-weight products consisting of a complex mixture of different chemical components: carbenes, carboids, asphaltenes, resins, paraffinic and naphthenic hydrocarbons, substituted monocyclic, bicyclic, and polycyclic compounds. The predominant component consists of hydrocarbons (~67%), of which the major part is aromatic.

LITERATURE CITED

[1] L. G. Gurvich. Scientific Principles of Petroleum Processing (in Russian). GONTI [State United Publishing House of Science and Technology] (1940).

[2] S. S. Nametkin. The Chemistry of Petroleum (in Russian). GONTI (1939).

[3] N. I. Chernozhukov. Petroleum Technology, III (in Russian). Gostoptekhizdat [State Scientific and Technical Publishing House of the Petroleum and Mineral-Fuel Industry] (1953).

[4] N. A. Vasil'ev. Transactions of the Grozny Petroleum Scientific Research Institute. ONTI [United Scientific and Technical Publishing Houses] (1935).

[5] A. F. Dobryanskii. Petroleum Geochemistry (in Russian). Gostoptekhizdat (1948).

[6] S. N. Obryadchikov. Petroleum Technology, II (in Russian). Gostoptekhizdat (1952).

[7] S. R. Sergienko, B. É. Davydov, I. O. Delone and M. P. Teterina, Trudy Inst. Nefti Akad. Nauk SSSR, 4, (1954); 6 (1935).

Received August 23, 1958

DEHYDRATION OF n-AMYL ALCOHOL ON ALUMINUM OXIDE

I. S. Lishanskii, A. A. Korotkov, G. A. Andreeva and A. G. Zak

Institute of High-Molecular Compounds, Academy of Sciences USSR

Dehydration of aliphatic alcohols with more than three carbon atoms on active aluminum oxide leads to the formation of a mixture of isomeric olefins which differ in the position of the double bond and in the structure of the chain. There are 5 possible pentene isomers and these boil within the temperature limits 20 – 38° at atmospheric pressure. Due to the comparatively low yield and the difficulties of isolating the product from such a mixture, dehydration has not found application as a method of preparing 1-pentene. The latter is usually obtained by organomagnesium synthesis (from allyl bromide and ethylmagnesium bromide) or from n-amyl alcohol by pyrolysis of its acetate [1]. In the latter case the 1-pentene yield does not exceed 30% (calculated on alcohol).

As we needed to prepare considerable amounts of 1-pentene under laboratory conditions, we attempted to find conditions for dehydrating n-amyl alcohol leading to the least isomerization.

EXPERIMENTAL

n-Amyl alcohol (n_D^{20} 1.4108, d_4^{20} 0.816, b.p. 135 – 137°; according to literature data: b.p. 138°, n_D^{20} 1.4101, d_4^{20} 0.817) was dehydrated at 400 ± 5° in a quartz tube, filled with active aluminum oxide (granule diameter 5 mm, length 6 – 8 mm, height of catalyst bed 30 cm, volume of catalyst bed 90 ml) and placed in a vertical tubular electric furnace. The alcohol was introduced into the upper part of the tube from a constant-level bottle and the emergent products were condensed and then distilled. In the first distillation on a Widmer column, 50 cm in height, the fraction boiling at 20 – 40° was collected. A second distillation was carried out on a column 120 cm in height with a packing of nichrome spirals (wire diameter 0.2 mm, spirals, 3 mm); the reflux number was 50 and the take-off rate 1 drop in 5 – 6 seconds. The 1-pentene fraction was collected over the temperature range 29.8 – 30.4° at a pressure of 750 – 760 mm Hg. The refractive index was determined for each experiment. A sample taken from a mixture of the products of all the experiments was examined by chromatographic analysis which showed that it did not contain traces of isomeric pentenes*.

DISCUSSION OF RESULTS

In the first series of experiments we used a catalyst on which isopropyl alcohol had been dehydrated for a long period at 360°. The catalyst was regenerated with air at 450° for 2 hours. In the second series of experiments we used fresh catalyst which was also regenerated with air for 2 hours at 450°.

The results of the experiments are given in the table which shows that the dehydrating activity of the catalyst, determined from the over-all yield of hydrocarbons, was practically unchanged during the whole series of experiments and was the same for the two catalyst samples used. At the same time the 1-pentene yield changed and passed through a slight maximum.

* The chromatographic analysis was carried out in the analytical laboratory of the Leningrad Scientific Research Institute by M. I. Dement'eva, to whom we are grateful.

Results of Experiments on the Dehydration of n-Amyl Alcohol. Temperature 400 ± 5°, Space Velocity (on liquid) 1 vol/ vol of cat · hr

Alcohol passed (in g)	Condensate collected				I distillation, 20-40°			II distillation				
	total (g)	water (g)	hydrocarbons		taken (g)	yield of amylenes		taken (g)	yield of α-amylene		n_D^{20} of α-amylene frac.	Yield of α-amylene (wt. % on original alcohol)
			in g	in wt. %		in g	in wt. %		in g	in wt. %		
I series of experiments												
137.2	132.9	27.1	105.8	77.0	105.8	98.5	93.0	98.5	26.4	26.8	1.3729	19.2
165.5	164.1	35.1	129.0	78.0	129.0	124.0	96.2	124.0	49.0	39.5	1.3724	29.8
141.0	138.0	29.0	109.0	77.5	109.0	104.5	95.8	104.5	39.2	37.5	1.3725	27.8
143.6	142.5	30.0	112.5	77.5	112.5	108.0	96.0	108.0	40.5	37.5	1.3722	28.2
166.1	162.7	35.2	127.5	76.7	127.5	120.4	94.5	120.4	54.1	45.1	1.3722	32.6
130.3	128.9	27.1	101.8	77.5	101.8	97.4	95.6	97.4	46.2	47.6	1.3727	34.6
148.2	145.6	30.6	115.0	77.8	115.0	110.7	96.3	110.7	54.0	48.8	1.3726	36.4
111.8	109.3	23.8	85.5	72.5	85.5	82.2	96.4	82.2	46.3	56.5	1.3724	39.2
128.4	126.2	30.4	95.8	74.5	95.8	91.0	94.5	91.0	22.0	24.2	1.3725	17.1
148.8	140.0	30.2	110.2	75.7	110.2	106.0	96.2	106.0	16.0	15.1	1.3723	10.8
136.0	135.2	28.2	107.0	79.2	107.0	98.3	91.8	98.3	10.1	10.3	1.3720	7.5
II series of experiments												
140.6	130.5	26.1	104.4	74.4	104.4	95.4	91.5	95.4	29.8	31.3	1.3724	21.2
154.5	148.0	26.3	121.7	78.6	121.7	105.0	86.4	105.0	40.0	38.1	1.3729	25.9
144.6	133.7	23.3	110.4	76.4	110.4	99.7	90.2	99.7	50.3	50.5	1.3722	34.8
144.2	140.6	28.8	111.8	77.5	111.8	100.0	89.5	100.0	47.9	47.9	1.3721	33.2
138.1	130.2	26.1	104.1	75.5	104.1	96.0	92.0	96.0	47.7	49.8	1.3722	34.6
131.9	128.0	26.0	102.0	77.3	102.0	95.7	93.7	95.7	36.9	38.6	1.3724	28.0
155.0	151.9	32.7	119.2	76.9	119.2	108.4	91.0	108.4	37.8	35.0	1.3722	24.4

The figure gives a graphical representation of the relation between the 1-pentene yield and log ΣV, where ΣV is the total amount of alcohol passed through the catalyst. As the graph shows, the specificity of the catalyst fell sharply after a definite operating time, expressed as the amount of alcohol dehydrated.

It is impossible to draw an unequivocal conclusion from available literature data on the reasons for the formation of mixtures of isomeric olefins in the dehydration of alcohols on active aluminum oxide. Thus, Oblad et al. [2], who studied the isomerization of 1-pentene and 2-pentene on various types of active aluminum oxide, both neutral and acid-treated, found that mixtures of both n-pentenes and isopentenes were formed in all cases. The authors proposed a mechanism for the isomerization of normal olefins on aluminum oxide involving the intermediate formation of a carbonium ion.

Musaev and Zizin [3] found that in the dehydration of n-butyl alcohol over aluminum oxide the 1-butene content of the product fell and the 2-butene increased with a rise in temperature. In the case of secondary butyl alcohol no such change in the composition of the butene mixture with a change in temperature was observed. In the opinion of the authors this meant that the butenes obtained by dehydration did not isomerize further and the change in composition in the case of n-butanol had another explanation.

The results we obtained agree with the conclusions of Musaev and Zizin. Actually, the change in composition of the pentene mixtures formed at constant temperature and space velocity cannot be explained by Oblad's mechanism, according to which the temperature conditions are decisive with respect to the nature of the olefin isomerization. There is also a short reference [4] in the literature on "stereoselectivity" observed in the catalytic dehydration of 1-butanol, 2-butanol, 2-pentanol and 3-pentanol. However, no experimental data were given.

It has to be assumed that the actual act of dehydration of n-amyl alcohol leads to the formation of a mixture of 1-pentene and 2-pentene, which at the given temperatures and catalyst contact time undergo a certain degree of isomerization of the carbon skeleton. Under constant experimental conditions this secondary process cannot lead to the change in specificity of the catalyst that we observed. We can only conclude that the relative numbers of active centers of different stereospecificity determine the composition of the initial mixture of 1-

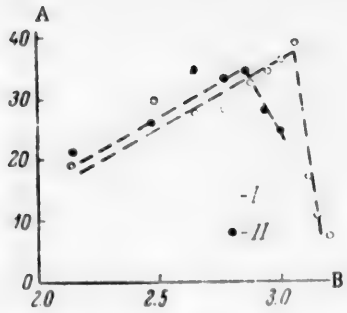

Relation between 1-pentene yield and the total amount of alcohol passed over the catalyst (ΣV). A) 1-Pentene yield (in %), B) value of log ΣV. I and II refer to the experiment series.

pentene and 2-pentene. The nature of the change in this composition we observed gives grounds for assuming that the formation of active centers also occurs during use of the catalyst and at first there is predominant formation of one type of active center on which dehydration occurs without migration of the double bond. Subsequently this type of center is either suppressed or converted into another type, promoting migration of the double bond.

SUMMARY

1. On investigating the dehydration of n-amyl alcohol on active aluminum oxide at 400° we observed that the 1-pentene content of the mixture of isomeric pentenes formed changes in relation to the amount of alcohol passed through the catalyst and passes through a maximum.

2. This phenomenon may be explained by assuming that on active aluminum oxide there exist active centers of different stereospecificity which are formed during operation of the catalyst and then partially changed or suppressed.

LITERATURE CITED

[1] N. I. Shuikin and V. A. Tulupov, Zhur. Obshchei Khim. 27, 6, 1449 (1957).*

[2] Oblad et al., Ind. Eng. Ch. 39, 1462 (1947).

[3] M. R. Musaev and V. G. Zizin, Zhur. Priklad. Khim. 29, 5, 803 (1956).*

[4] H. Pines and W. Haag, J. Org. Chem. 23, 2, 328 (1958).

Received January 29, 1959

* Original Russian pagination. See C. B. Translation.

INTERACTION OF ADIPIC AND SEBACIC ACIDS WITH UREA AND ACETYLUREA

M. S. Dudkin

In 1946 Cherbuliez and Landolt described a new method of preparing acid amides by heating saturated monobasic organic acids with urea [1]. Later, amides of various monobasic unsaturated aromatic acids were synthesized both by heating these acids with urea [2] and also with acetylurea [3]. The preparation of mono- and diamides of dibasic acids by such a method and the interaction of these acids with urea and acetylurea have not been investigated sufficiently though it is known that heating malonic acid with urea gives products of unknown structure while succinic and phthalic acids form amides [4].

The purpose of our work was to study the interaction of adipic and sebacic acids with urea and acetylurea on heating.

Interaction of Adipic Acid with Urea

A mixture of 14.6 g of adipic acid, twice recrystallized from ethyl alcohol (m.p. of acid 152°), and 18 g of urea, recrystallized from water (m.p. of urea 133°) was carefully mixed in a mortar and heated in a round-bottomed flask on an oil bath for 2 hours at 160 or 230°.

The mixture of substances melted forming a homogeneous solution. Further heating was accompanied by the evolution of gases. The cooled product was purified by two recrystallizations from water, dried and analyzed.

The nitrogen content was determined by the Kjeldahl method and the carboxyl groups by titration with potassium hydroxide solution in the presence of phenolphthalein. The number of amide groups was determined by the method of Zil'berman and Skorikova [5], who developed it for application to the analysis of adipic acid amides.

Heating at 160° gave a product with the following characteristics: the yield (after recrystallization from water) was 22.8% and the m.p. 224 – 225° (according to the chemists handbook [6], 220° and according to [7], 226°).

Found %: N 19.34, 19.46; amide groups 22.90 and 22.46; the acid number was zero.

$C_6H_{12}O_2N_2$ (adipic diamide). Calculated %: N 19.43; amide groups 22.92%.

Heating at 230° gave a product with the following characteristics: yield (after recrystallization from water) 32%.

Found %: N 19.60, 19.62; amide groups 21.95 and 22.26; the acid number was zero.

Interaction of Sebacic Acid with Urea

A mixture of 10 g of sebacic acid, twice recrystallized from ethyl alcohol (m.p. of acid 134°), and 9 g of urea was mixed, heated, and purified as described above.

Heating at 160° gave a product with the following characteristics: yield (after recrystallization from water) 32% and m.p. 172 – 173° ([7] 170°).

Found %: N 7.26, 7.11; amide groups 8.50 and 8.22; acid number 274.4 and 273.5.

$C_{10}H_{19}O_3N$ (sebacic monoamide). Calculated %: N 6.95, amide groups 7.95 and acid number 278.7.

Heating at 230° gave a product with the following characteristics: yield (after recrystallization from alcohol) 34.5% and m.p. 182-183°.

Found %: N 17.35, 17.47; the acid number was zero.

$C_{11}H_{21}O_3N_3$ (sebacic amidourcide). Calculated %: N 17.2.

Interaction of Adipic Acid with Acetylurea

Adipic acid and acetylurea, prepared by Higershoff's method (melting point 218°), in various molar ratios were carefully ground in a mortar and heated in a round-bottomed flask at 230° for two hours. After recrystallization from alcohol, the product was dried and analyzed.

At a molar ratio of acid to urea of 1 : 1, the product obtained had the following characteristics: yield (after recrystallization from alcohol) 26% and m.p. 205 – 206° (according to [7], 210°).

Found %: N 9.96, 10.06; amide groups 10.8 and 11.1; acid number 223.0 and 222.0.

$C_6H_{11}O_3N$ (adipic acid monoamide). Calculated %: N 9.64, amide groups 11.04 and acid number 385.9.

At a molar ratio of sebacic acid to urea of 1 : 2, the product obtained had the following characteristics: yield (after recrystallization from alcohol) 34% and m.p. 223°.

Found %: N 19.12, 19.25; amide groups 22.45 and 22.67, acid number zero.

Interaction of Sebacic Acid with Acetylurea

Sebacic acid and urea were reacted in various molar ratios as described above.

At a molar ratio of acid to urea of 1 : 1, the product obtained had the following characteristics: yield (after recrystallization from alcohol) 28% and m.p. 172°.

Found %: N 7.32, 7.35; amide groups 8.23 and 8.06; acid number 278.4 and 278.0.

At a molar ratio of acid to acetylurea of 1 : 2 the product had the following characteristics: yield (after recrystallization from alcohol) 39% and m.p. 208° (according to [7] 208 – 210°).

Found %: N 13.49, 13.56; amide groups 15.2 and 15.6; acid number zero.

$C_{10}H_{22}O_2N_2$ (sebacic diamide). Calculated %: N 13.99, amide groups 16.00.

Thus, depending on temperature and the molar ratio of the reagents, it is possible to obtain different amides by the interaction of adipic and sebacic acids with urea. The formation of cyclic compounds of the amide type is improbable under these conditions due to their instability.

That just amides are formed is demonstrated by the data obtained on the amide groups present in the molecules, the values of the melting points obtained, and data on the nitrogen content.

Heating adipic acid with excess urea both at 160° and 230° formed adipic diamide.

Heating sebacic acid with excess urea at 160° formed the monoamide and at 230°, the amidoureide of this acid.

When adipic and sebacic acids were heated at 230° with acetylurea (at a molar ratio of reagents of 1 : 1) the monoamides of these acids were formed and when the reagent ratio was 1 : 2, the diamides of the acids were formed.

Under the conditions examined, the yields of adipic and sebacic amides were low and varied from 22.8 to 39%. This may be explained by the fact that when urea and also acetylurea are heated at high temperatures side processes probably occur, for example, the formation of biuret and partial sublimation of the starting materials. In addition, part of the amides synthesized was probably lost during the two recrystallizations.

SUMMARY

1. It was shown that heating adipic and sebacic acids with urea under various conditions formed amides.

2. Depending on the ratios of the amounts of reagents, heating adipic and sebacic acids with acetylurea formed mono- or diamides.

LITERATURE CITED

[1] Cherbuliez and Landolt, Helv. chim. Acta 29, 1438 (1946).

[2] A. Rahman and M. Forooq, Current Sci. 21, 338 (1952).

[3] E. T. Roe, H. Scanlan and D. Swern, J. Am. Chem. Soc. 6, 2215 (1949).

[4] W. Pike, Ber. 6, 1104 (1873); A. Piutti, Ann. 214, 17 (1882); F. Dunlap, Am. Chem. J. 18, 332 (1896).

[5] E. Zil'berman and Z. Skorikiva, Zavodskaya Lab. 7, 808 (1954).

[6] Chemists Handbook, II [in Russian], 476 (1951).

[7] Dictionary of Organic Compounds [in Russian], 1, 31 (1949).

Received July 8, 1958

CATALYTIC HYDROGENATION OF QUINOLINE

A. N. Kost, L. D. Pertsov, L. G. Yudin and S. F. Kalinkin

1-Acyl-1,2,3,4-tetrahydroquinolines have an insecticide action [1] and are effective agents against blood-sucking insects [2, 3] and mites [4, 5]. These compounds may be synthesized by hydrogenation of quinoline to 1,2,3,4-tetrahydroquinoline with subsequent acylation. In the case of 1-formyltetrahydroquinoline these reactions may be combined and when quinoline is heated with formic acid, reduction (due to formic acid) and formylation occur simultaneously [1, 6].

When quinoline is reduced with sodium in alcohol [7], tin in hydrochloric acid [8], or formic acid [1, 6] only the pyridine ring is hydrogenated to form 1,2,3,4-tetrahydroquinoline, but these methods are inconvenient for the synthesis of large amounts.

In catalytic hydrogenation over nickel catalysts the pyridine ring is also reduced first but under more drastic conditions a mixture of cis- and trans-decahydroquinolines is formed [9, 10]. Thus, Yur'ev and Mironenko showed that hydrogenation to 1,2,3,4-tetrahydroquinoline proceeds rapidly over nickel on aluminum oxide (100 atm, 80 – 100°) but when the temperature was raised to 180° the main product was trans-decahydroquinoline [11]. Over especially active Raney nickel, 1,2,3,4-tetrahydroquinoline was obtained at room temperature and a pressure of 1 – 3 atm [12]. In hydrogenation over reduced nickel it was established that not only 1,2,3,4-tetrahydroquinoline was formed, but also traces of 5,6,7,8-tetrahydroquinoline. In the gas phase at 260 – 280° there occurs hydrogenation of the benzene ring and partial hydrogenolysis of a carbon-carbon bond, leading to ethyl-o-toluidine, methyl-o-toluidine, and o-toluidine and also to isomerization of the pyridine ring to form methylindole.

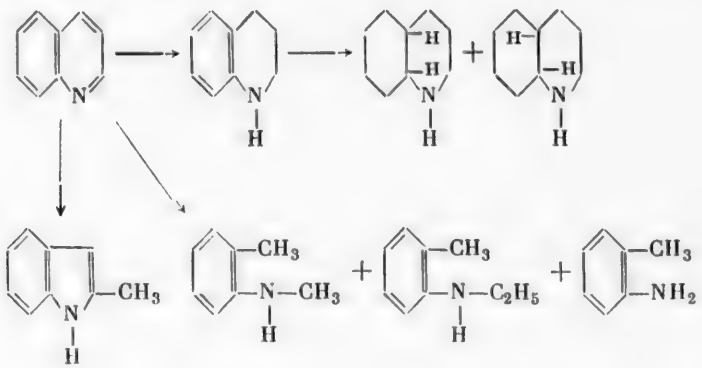

For hydrogenating quinoline we used nickel on chromic oxide, which is widely used at the present time as an industrial catalyst. The reaction was carried out in an autoclave with a stirrer and hydrogen was periodically introduced above the liquid hydrogenated.

The catalyst was found to be quite effective and hydrogenation of quinoline over it began at 90° and 80 atm. In examining the reaction products it was necessary to determine the mixture's content of original quinoline, 1,2,3,4-tetrahydroquinoline and decahydroquinoline. Naturally it might be supposed that 5,6,7,8-tetrahydroquinoline or hydrogenolysis products would be formed, but with the conditions chosen we did not detect any fractions corresponding to these subtances and according to literature data they are only formed as side products of reactions under very drastic conditions [13, 14].

For analysis of the catalyzate, a sample (100 g) was taken and vacuum distilled twice from a Favorskii flask with a pear fractionating column 50 cm high. If some decahydroquinoline was obtained by the reaction then it was readily separated by such a distillation as its boiling point (b.p. 58 – 62° at 3 mm) is 15 – 20° below that of tetrahydroquinoline (b.p. 80 – 87° at 3 mm). As regards quinoline, it could not be separated by distillation from tetrahydroquinoline, which has a similar boiling point, and therefore, in parallel, 100 g of acetic anhydride was added to another sample (100 g), the mixture boiled for 15 minutes, the excess acetic anhydride and acetic acid removed by distillation and the residue vacuum distilled. The presence of a low-boiling fraction indicated that the reaction did not proceed to completion and the mixture contained original quinoline (b.p. 98 – 100° at 9 mm). 1-Acetyl-1,2,3,4-tetrahydroquinoline distilled at 147 – 151° at 9 mm. After a series of experiments it was established that with hydrogenation for 12 hours at 140 – 145° and 80 – 100 atm the catalyzate did not contain original quinoline and consisted of a mixture of decahydroquinoline (about 40%) and tetrahydroquinoline (about 50%). When the temperature was reduced to 110 – 115° (10 – 11 hours, 80 – 100 atm) a catalyzate was obtained which contained 80 – 90% of tetrahydroquinoline and 2 – 8% of decahydroquinoline. Reduction of the reaction time to 7.5 – 8 hours led to a sharp fall in yield and the catalyzate contained 56% of tetrahydroquinoline and 36% of original quinoline. In all these experiments the catalyzate contained 4 – 8% by weight of a tarry residue which can be assumed to have formed as a result of polymerization of 1,2-dihydroquinoline, the first hydrogenation product. These very unstable compounds were recently synthesized by the action of lithium aluminum hydride on quinoline [15].

The continuous introduction of hydrogen during the whole of the process through a bubbler made it possible to reduce the tarry impurity content of the catalyzate to 1% (since, obviously, the dihydroquinoline was unable to polymerize and then was hydrogenated smoothly), to reduce the time of the process to 7 – 8 hours, and to raise the yield of tetrahydroquinoline.

EXPERIMENTAL

For the hydrogenation we used quinoline from the Khar'kov coal tar chemical plant (TU MKhP 93 – 47) and this was redistilled. It had b.p. 103 – 105° at 10 mm, n_D^{20} 1.6227, d_4^{20} 1.0996 and the picrate had m.p. 203°, which correspond to literature data [16].

Experiment No. 1. The hydrogenation was carrie out in a 3 liter autoclave with a stirrer which was charged each time with 1 kg of quinoline and 50 g of catalyst (industrial nickel on chromic oxide catalyst). The reactor was charged with hydrogen to a pressure of 50 atm and then the temperature raised to 110 – 115° over one hour after which, when the pressure fell to 75 – 80 atm further hydrogen was introduced and the pressure raised to 100 atm. For the first 4.5 hours such additions had to be made every 15 – 20 minutes and then after every 30 – 60 minutes. The experiment lasted for 10 hours. After the autoclave had been cooled and the pressure released, the contents were unloaded and the catalyst removed (on a Buchner funnel). We obtained 1012 g of catalyzate, i.e., 101% (on the weight of starting material). Distillation of the catalyzate in vacuum from a Favorskii flask gave: 80.9 g of a mixture of cis- and trans-decahydroquinolines with b.p. 58 – 62° at 3 mm (7.8% of the theoretical amount) and 890.5 g of 1,2,3,4-tetrahydroquinoline with b.p. 80 – 84° at 3 mm (i.e., 85.3% of theoretical, calculated on the starting quinoline, or 90% of the weight of catalyzate), n_D^{20} 1.5936 and d_4^{20} 1.0611, which agree with literature data [16].

The residue in the flask weighed 40.5 g (i.e., about 4% of the catalyzate weight). When the decahydroquinoline fraction was cooled to 0 – 5°, transdecahydroquinoline crystallized and this had m.p. 48° (from pentane) and b.p. 203 – 205° at 741 mm and its picrate had m.p. 158° (from benzene), which agree with literature data [11]. The cis-isomer was not isolated in a pure state.

Experiment No. 2. Into an 8 liter autoclave with a bubblerwere placed 6 kg of quinoline and 300 g of catalyst (nickel on chromic oxide). The initial hydrogen pressure was 50 atm. Over a period of 1 hour the temperature of the reaction mixture was raised to 105 – 110° and the pressure to 100 atm (with continuous input of hydrogen from a compressor). Hydrogen adsorption began at 95 – 100° and was complete (at 105 – 110° and 100 – 105 atm) after 7 – 8 hours. After the reaction mixture had been held at this temperature for two hours, the heater was switched off, the pressure reduced, the autoclave unloaded, and the catalyst removed. We obtained 6150 g of catalyzate (i.e., 102.5% on the weight of starting quinoline). Fractional distillation from a liter Favorskii flask yielded 5965 g (96.4% of theoretical) of 1,2,3,4-tetrahydroquinoline with b.p. 82 – 86° at 4 mm and n_D^{20} 1.5934. Distiallation also gave 120 g (about 2% of theoretical) of decahydroquinoline with b.p. 62 – 65° at 4 mm. 60 g (i.e., about 1% of the weight of catalyzate) of tarry residue remained in the flask.

SUMMARY

It was shown that quinoline obtained from cool tar may be catalytically hydrogenated to 1,2,3,4-tetrahydroquinoline over an industrial catalyst (nickel on chromic oxide) in up to 96% yield.

LITERATURE CITED

[1] L. G. Yudin, A. N. Kost, E. Kh. Zolotarev and A. N. Mirza, Vestnik MGU, Ser. Khim. 2, 169 (1958).

[2] B. Travis, F. Morton, H. Jones and J. Robinson, J. Econ. Entomol., 42, 686 (1949).

[3] E. Kh. Zolotarev, A. N. Kost, M. L. Fedder, L. G. Yudin and I. A. Yurgenson, Nauchn. Doklady Vysshei Shkoly, 1, 44 (1958).

[4] H. Gouck and J. Gilbert, J. Econ. Entomol. 48, 499 (1955).

[5] E. Kh. Zolotarev, T. V. Kalakutskaya, A. N. Kost and L. G. Yudin, Author's Certificate No. 111935 from January 1, 1958.

[6] A. N. Kost and L. G. Yudin, Zhur. Obshchei Khim. 25, 1947 (1955).*

[7] E. Bamberger and S. Willamson, Ber. 27, 1465 (1894).

[8] L. Hoffmann and W. Koenigs, Ber. 16, 728 (1883).

[9] V. I. Ipat'ev, Zhur. Russ. Fiz. Khim. Obshchestvo 40, 493 (1908).

[10] A. Skita and W. Meyer, Ber. 45, 3589 (1912).

[11] Yu. K. Yur'ev and G. I. Mironenko, Uch. Zap. MGU 6, 277 (1936).

[12] H. Adkins and H. Billica, J. Am. Chem., Soc. 70, 695 (1948).

[13] S. Tsushima and S. Sudzuki, J. Chem. Soc. Japan, 64, 1295 (1943); Ch. A. 41, 3801 (1947).

[14] M. Padoa and A. Carughi, Atti Linc. [5], 15, II, 113 (1906); Zbl. I, 1011 (1906).

[15] V. Michovich and M. Mikhailovich, Lithium Aluminum Hydride and Its Application in Organic Chemistry [in Russian] (Foreign Lit. Press, 1957) p. 171.

[16] I. I. Eru, E. M. Sakhnovskaya and V. A. Pychko, Zhur. Obshchei Khim. 8, 1563 (1938).

Received June 9, 1958

* Original Russian pagination. See C. B. Translation.

SOLUTION OF QUARTZ IN FELDSPAR MELTS

V. Z. Petrova, A. I. Avgustinik, P. F. Konovalov and
E. P. Konovalova

Despite numerous investigations of the role of quartz in ceramic materials, the problem of its effect on the strength of ceramics has not been solved adequately. Thus, Marzal and Matisovsky [1, 2] consider that an increase in the quartz content of porcelain leads to an increase in the size of compression "phase" strains, increasing the mechanical strength of this material. Palatzky [3] and Genin [4] demonstrated the opposite. The latest investigations of Wildemann [5] shed some light on this problem due to the use of a complex method which was not used in previous investigations. Nonetheless the results of the work of all the authors mentioned remain inadequate, making it impossible to arrive at unequivocal conclusions to this problem.

All this compelled us to study first of all the strictly glassy phase of porcelain and determine the effect of dissolved quartz on its mechanical strength and then to turn to more complex compositions approaching that of porcelain.

TABLE 1

Composition of Masses

Mass No.	Content (in %)	
	feldspar	quartz
1	90	10
2	80	20
3	70	30
4	60	40
5	50	50

The solution of quartz in feldspar has been studied by a number of authors. Nazarenko and Razumova [6] studied the shielding role of quartz; Hamano [7] studied the formation of diffusion layers around quartz grains, but these authors were not interested in the effect of the solution of quartz on the mechanical strength of porcelain and the formation of "phase" strains in the system quartz – glass phase due to the difference in the expansion coefficients of these two phases.

Samples for investigation were prepared by semidry pressing at a pressure of 1000 kg/ cm^2 and a moisture content of 7 – 8% to give discs 20 mm in diameter and 3mm thick from a mixture of potash feldspar with the composition (in %): SiO_2 66.64, $Al_2O_3 + TiO_2$ 18.53, Fe_2O_3 0.27, CaO 0.72, MgO 0.09, K_2O 9.65, Na_2O 3.22, (the firing loss was 0.72) and rock crystal, ground to pass through a sieve with 10,000 holes/ cm^2. The compositions of the masses are given in Table 1.

The samples were fired in a Silit furnace at up to 1200, 1280, and 1350° for four periods of 1, 2.5, 5 and 9 hours at these temperatures, with the temperature raised by 200° per hour.

The main investigation methods were quantitative x-ray structural analysis from ionization curves on a Hiprotsement apparatus [8, 9], determination of the microhardness on an MPT-3 apparatus, and microscopic examination by means of an MIM-8 metallographic microscope.

Quantitative x-ray determination of the undissolved quartz was carried out on powdered samples with an internal standard in the form of chemically pure calcium fluoride (Table 2).

The standard ionization curve is given in Fig. 1 and the standard calculated curve in Fig. 2. The x-ray structural analysis data were compared with data from microscopic analysis on clear and opaque polished sections by determining the quartz in 100 fields.

TABLE 2

Composition of Standards and Calibration Curve Data for X-ray Analysis

Standard No.	Composition of standards (in parts by weight)			Peak height (in mm)		Ratio of peak heights of quartz and calcium fluoride
	quartz	feldspar	CaF_2 (over 100%)	quartz	CaF_2	
1	5	95	25	3.5	24.0	0.1458
2	10	90	25	7.0	25.0	0.2800
3	15	85	25	12.0	32.0	0.375
4	20	80	25	14.5	29.0	0.500
5	25	75	25	19.0	27.0	0.703
6	30	70	25	22.3	40.8	0.546
7	35	65	25	26.0	31.0	0.838
8	40	60	25	29.0	34.0	0.852
9	45	55	25	38.5	36.0	1.069

TABLE 3

Data From X-ray and Microscopic Investigations

Given quartz content (in %)	By internal standards method			Without internal standard	From polished section (340 x)	From polished sec. in trans. light (340 x)
	peaks heights		ratio of peak heights	quartz content after firing (in %)		
	quartz	CaF_2				
10	1.5	31	0.048	1	2.8	2.7	4.5
20	1.8	25	0.072	2.5	4.0	3.9	6.1
30	3	22	0.136	5.0	4.8	4.3	6.7
40	6	27	0.222	6.3	5.8	6.2	8.5
50	7	31.5	0.225	9.0	9.0	9.2	12.1

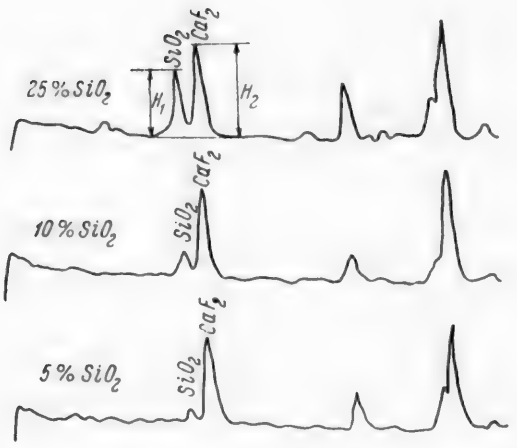

Fig. 1. X-ray structural ionization curves of standard mixtures.

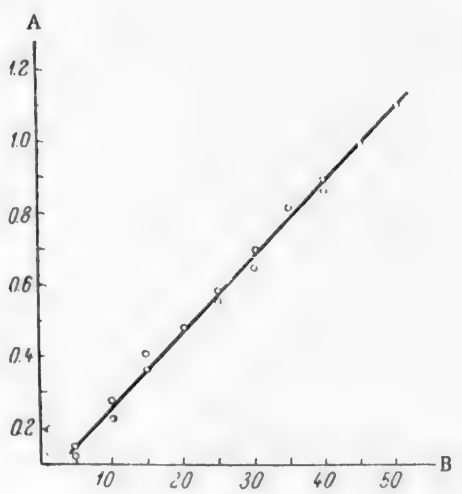

Fig. 2. Standard graph for quantitative determination of quartz in mixtures. A) Ratio of peak heights, B) quartz content (in %).

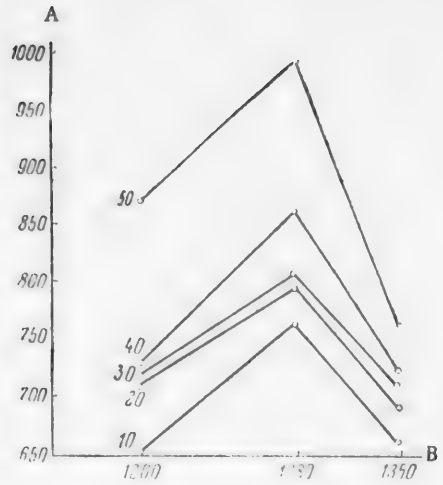

Fig. 3. Effect of firing temperature change on microhardness with a firing time of 9 hours. A) Microhardness (in kg/ cm^2), B) firing temperature (in °C). The numbers on the curves correspond to the percentage SiO_2 content.

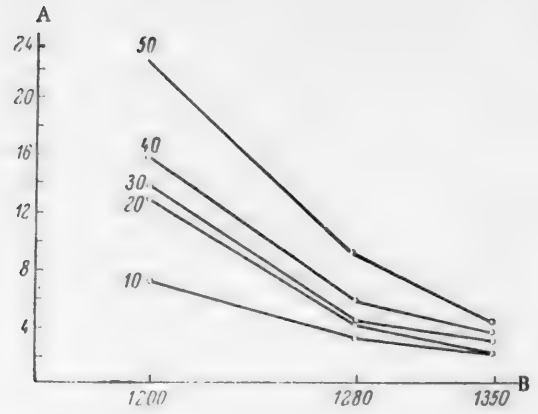

Fig. 4. Effect of firing temperature change on quartz solution with a firing time of 9 hours. A) Amount of undissolved quartz after firing (in %), B) firing temperature (in °C). The numbers on the curves correspond to the percentage SiO_2 content.

The results of the x-ray structural and microscopic analyses are given in Table 3. From the voluminous material obtained for five masses fired at 3 temperatures for various times, as an example we give data for firing at 1280° for 9 hours (Table 3).

Control investigations of other compositions fired to different temperatures both with internal standards and without them led to the conclusion that with one crystalline phase present (quartz) it is possible to determine this phase quantitatively without an internal standard which hampers the preparation of homogeneous mixtures.

As Table 3 shows, data from microscopic investigations of transparent polished sections are very high and this may be explained by a calculation error due to allowing for quartz grains in the thickness of the sample. Therefore, the most accurate results may be obtained by determining the quartz in sections polished after etching with a mixture of 9 parts of 14% H_2SiF_6 and 1 part of 30% HF for 15 – 30 minutes, depending on the glass-phase content; the higher the glass-phase content the higher was the etching time.

The nature of the change in microhardness in relation to firing temperature is given in Fig. 3 where each point is the result of 50 determinations.

The kinetic curves of quartz solution in relation to temperature for a 9 hour firing time are given in Fig. 4.

The data given above indicate that the solubility of quartz is in direct proportion to firing temperature and time.

The presence of a maximum on the microhardness curves (Fig. 3) may be explained by the most favorable conditions for the appearance of compression stresses in the glass phase surrounding the quartz grains. Strains arise (on cooling) in the grains themselves and at the boundary of the quartz grain with the glass phase.

Indirect confirmation of this hypothesis is provided by the nature of impressions on the polished section field. The greater the quartz grain on which the impression was made with the diamond pyramid, the greater was the "halo" pattern of the glass phase observed around this grain. These observations were made on 120 samples and the reproducibility of the nature of these friability "halos" made it possible to relate this phenomenon to the distribution of stresses in the quartz and at the quartz-glass phase boundary.

The existence of lower microhardnesses at lower and higher firing temperatures (Fig. 3) may be explained by the large amount of unreacted quartz at 1200° and almost complete solution of quartz at 1350°, as is shown by Fig. 4.

SUMMARY

1. Quantitative determinations of the quartz content of a feldspar melt (similar to porcelain) may be carried out by x-ray measurement without an internal standard or from a section etched with a mixture of 9 parts of 14% H_2SiF_6 and 1 part of 30% HF as the results obtained by these two methods agree.

2. A maximum was observed in the microhardness of a feldspar melt with quartz dissolved in it with firing at 1280° for 9 hours and this is explained by the fact that much quartz remains undissolved with a firing temperature of 1200°, while at 1350° the quartz is almost completely dissolved, i.e., the mechanical properties of the cooled melt containing quartz are optimal at approximately 1280°. The nature of the impressions from a diamond pyramid in determination of the microhardness indicate a distribution of strains of various signs in the glass phase at the quartz-glass phase boundary.

3. The solution of quartz in a feldspar melt is in direct proportion to firing temperature.

LITERATURE CITED

[1] G. Marzell, Ber. deut. keram. Ges. 32, 7, 203 (1955).

[2] L. Matisovsky, J. Am. Cer. Soc. 40, 9, 299 (1957).

[3] L. A. Palatzky and W. Tümmler, Silicattechnik, 2, 68 (1958).

[4] L. G. Genin, Steklo i Keramika. 4, 35 (1958).*

[5] T. Wildemann, Sprechsaal 1, 2 (1959); 2, 29 (1959).

[6] M. F. Nazarenko and V. A. Razumova, Trudy Kazakh. Akad. Nauk 1 (1958).

[7] Kenyo Hamano, Referatnyi Zhur. Khim. 45230 (1958); J. Cer. Assoc. Japan 64, 726 (1956).

[8] Moran and Kell, Silikates ind. 23, 5, 248 (1958).

[9] S. C. Sobe and R. Z. Cook, J. Am. Cer. Soc. 34, 5, 145 (1951).

Received June 3, 1959

* Original Russian pagination. See C. B. Translation.

INVESTIGATION OF THE EFFECT OF ANTIMONY ON THE NATURE OF LEAD PASSIVATION IN SULFURIC ACID SOLUTIONS

É. S. Vaisberg, E. V. Krivolapova and B. N. Kabanov

In a series of works [1 – 3] it has been shown that during the operation of a lead-acid battery, antimony accumulates on the negative electrode due to corrosion of the lead-antimony lattice of the positive electrode. The stationary potential of antimony is much more positive than that of lead in sulfuric acid and the hydrog overvoltage on antimony is extremely low. Therefore antimony deposited on the negative electrode hinders discharge and considerably increases the rate of self-discharge of the electrode, promoting its "sulfatization"*

A sharp fall in the practical capacity of the negative electrode (when it is poisoned with antimony), by virtue of all that has been said above, is usually only connected with the impossibility of sufficiently complete discharge of the electrode.

The purpose of the present investigation was to determine how the presence of antimony on the negative electrode affects its passivation on discharge. To exclude the effect of the degree of charge on the discharge time, the experiments were carried out with smooth electrodes with a freshly cleaned surface.

MEASUREMENT PROCEDURE

All the measurements were made on flat electrodes, cast from SV grade lead and 8% lead-antimony alloy. The apparent surface of the electrode was 6 cm^2. Before immersion in the solution, the electrode surface was renewed with a sharp steel chisel. The sulfuric acid solution was prepared from chemically pure sulfuric acid and distilled water, then purified for many hours by passage of a current between smooth electrodes of SV grade lead and diluted to concentrations of 2, 6.68, 9.8 and 11.37 N. The electrode potential was measured against a mercurous sulfate electrode, covered with sulfuric acid solution of the same concentration as that in which the electrode was polarized. As the first experiments showed that after removal of the external layer the electrode surface was oxidized by atmospheric oxygen at room temperature, all subsequent experiments were carried out with preliminary cathode polarization for 20 minutes at a current density of $2 \cdot 10^{-4}$ a/ cm^2 of the apparent surface. For experiments on passivation of lead and lead-antimony electrodes we used anode polarization in four different sulfuric acid concentrations (see above) at the same current density of $2 \cdot 10^{-4}$ a/cm^2 at 30°.

RESULTS OF MEASUREMENTS

The results of the measurements are shown in Fig. 1. The time (in min) is plotted along the abscissa and the voltage (in volts relative to a mercurous sulfate electrode) along the ordinate. As Fig. 1 shows, the

* The term "sulfatization" is used here to denote the phenomenon beginning most frequently of all when the battery stands for quite a long period in a discharged state and consisting of the fact that such a battery cannot be charged as lead sulfate is not converted to lead on the passage of a cathode current. As was recently shown [4], sulfatization is produced by a number of organic substances which either reduce the rate of solution of lead crystals by being adsorbed on their surface or hamper the discharge of lead ions (Pb^{++}) by being adsorbed on the lead.

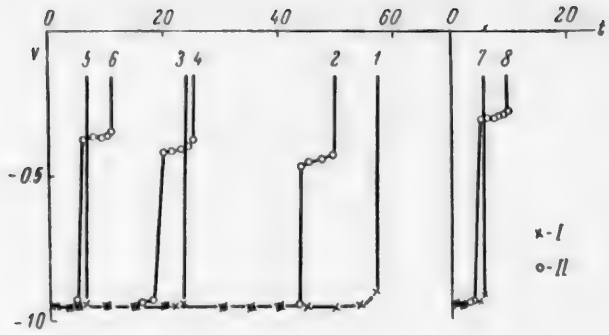

Fig. 1. Change in potential V (in v) of lead and lead-antimony electrodes at an anode polarization current of $2 \cdot 10^{-4}$ a/ cm^2 with time t (in min.) in sulfuric acid solutions of various concentrations. H_2SO_4 concentration (normality): 1, 2 – 2; 3, 4 – 6.68; 5, 6 – 9.8; 7, 8 – 11.37. Electrodes: I) lead, II) lead-antimony.

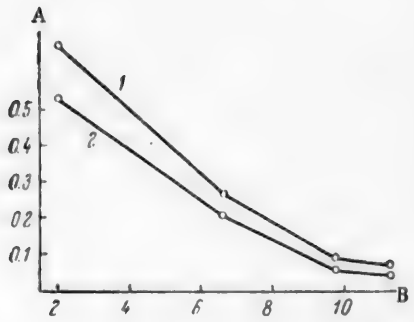

Fig. 2. Relation between the thickness of the passivating $PbSO_4$ layer and the sulfuric acid concentration for lead and lead-antimony electrodes. A) Amount of electricity (in coul / cm^2), B) H_2SO_4 concentration (normality). Electrodes: 1) lead, 2) lead-antimony.

presence of antimony in the electrode accelerated passivation of the latter. In addition, with anode polarization of lead-antimony electrodes the time-potential curves showed a plateau at a potential close to the equilibrium value for the electrode reaction $Sb + H_2O = SbO^+ + 2H^+ + 3e$. The length of this plateau remained almost constant with a change in sulfuric acid concentration (from 2 N to 11.37 N), while the plateau corresponding to the oxidation of lead to lead sulfate decreased by a factor of approximately 10.

DISCUSSION OF RESULTS

At the beginning of our experiments the anode current density was $2 \cdot 10^{-4}$ a/ cm^2, i.e., in the region of current densities ($10^{-5} - 10^{-3}$ a/ cm^2) where the overvoltage of the process $Pb \rightarrow PbSO_4$ is determined by the supersaturation of the sulfuric acid solution with lead sulfate [5]. It is known [6] that passivation of lead due to covering of its surface by a layer of crystals of insoluble and nonconducting $PbSO_4$ under anode polarization leads to a sharp displacement of potential to the positive side at the moment when a small part of the original true surface of the electrode remains free. The true current density (at a constant polarization current strength) at this moment reaches the region of current densities (above 10^{-3} a/cm^2) where the lead ionization overvoltage assumes a considerable value [5].

An increase in the sulfuric acid concentration (under otherwise equal conditions of anode polarization) leads to a decrease in the amount of lead sulfate passivating the electrode due to a decrease in the diffusion coefficient and the solubility of this salt [7]. Figure 2, which was obtained from data given in Fig. 1, shows the nature of the relation we obtained between the thickness of the lead sulfate layer on the passivated electrode and the sulfuric acid concentration. Curve 1 gives the thickness of the $PbSO_4$ layer for lead electrodes and curve 2, that for lead-antimony electrodes. The layer thickness was determined from the amount of electricity passing through the electrode up to the sharp change in potential in a positive direction (in the case of the antimony electrode, up to the first sharp change in potential in a positive direction). Fig. 2 shows that the curve for lead-antimony electrodes lies below that for lead electrodes so that the amount of $PbSO_4$ formed on a lead-antimony electrode is less than that formed on a lead electrode (at the same H_2SO_4 concentration) always by the same proportion, which is on the average 27%, regardless of the sulfuric acid concentration. This may be explained by the fact that part of the surface of the lead-antimony electrode is occupied by antimony.

The melting point diagram of the lead-antimony system shows that antimony hardly forms any compounds with lead. When an 8% (with respect to antimony) alloy is cooled, coarse crystals of lead are first deposited. When, as a result of this, the antimony content reaches 13% the melt crystallizes, forming fine crystals of antimony and lead. Calculation shows that in an 8% antimony electrode, antimony crystals occupy about 15% of the surface. Since antimony in sulfuric acid is oxidized at a potential which is several tenths of a volt more positive (~0.5 v) than for anode oxidation of metallic lead to lead sulfate and occupies a considerable part of the true surface of the electrode, passivation of a lead-antimony electrode begins correspondingly earlier than for a lead electrode. For the same reason, the true current density from the very beginning of anode polarization will be higher on an 8% antimony electrode by a factor of ~1.2 and as lead crystals lying on the surface are consumed, it will increase, and thus must also accelerate passivation of the electrode*. Up to the beginning of passivation, the working lead surface on lead and lead-antimony electrodes has such a size relative to the initial one that the true current density is increased by 1 – 2 orders. As a result, the electrode is passivated and the potential of the lead electrode is displaced in a positive direction before the oxidation of lead sulfate to lead dioxide begins and the potential of the lead-antimony electrode is displaced before the oxidation of antimony begins. The oxidation products of antimony [$Sb_2(SO_4)_3$ and $(SbO)_2SO_4$] are quite readily soluble in sulfuric acid and therefore the amount of electricity consumed in oxidation of antimony must correspond to the amount of antimony crystals lying on the surface.

At first glance it would seem natural to assume that parallel with the oxidation of antimony at these potentials (lying 0.5 – 0.55 v above equilibrium for the $Pb/PbSO_4$ system), i.e., with a high overvoltage, the lead crystals liberated must be oxidized to lead sulfate. However, the results of our experiments showed that the amount of electricity consumed in the oxidation of lead at potentials corresponding to the second plateau on the potential-time curve is only an insignificant fraction of that consumed in the oxidation of antimony. This is seen from the fact that the length of the plateau, corresponding to the antimony oxidation potentials (Fig. 1), changes only insignificantly with an increase in the sulfuric acid concentration from 2 to 11.37 N. In addition, if, at the end of the plateau corresponding to the oxidation potentials of antimony, the anodically polarized electrode is immediately polarized cathodically (with preliminary washing with sulfuric acid solution) in a cell with an acidified normal solution of Na_2SO_4, then the potential-time curve shows only one plateau, corresponding to the process $PbSO_4 \rightarrow Pb$. The size of this plateau is equal to the size of the first plateau, corresponding to the process $Pb \rightarrow PbSO_4$, which occurred during anode polarization of the same lead-antimony electrode.

Apparently, at such positive potentials (0.5 v) there is adsorption passivation of lead crystals liberated by solution of antimony crystals, i.e., passivation requires an amount of electricity less than 10^{-3} coul./cm^2.

It is reported in the literature [8] that even a slight increase of 40 mv (potentiostatic method) in the potential at which lead is oxidized to lead sulfate leads to a sharp fall in the amount of lead sulfate formed (the amount of it formed at a potential 40 mv more positive is 28% of the amount of $PbSO_4$ formed at the usual low potential for oxidation of lead to lead sulfate). These data agree well with the results of our measurements.

SUMMARY

It was shown that antimony is capable of passivating a lead electrode. From this it follows that the fall in the practical capacity of the negative electrode of a lead-acid battery due to its poisoning by antimony is not only connected with the fall in degree of charging of the negative electrode.

LITERATURE CITED

[1] Crennell and Milligan, Trans. Faraday Soc. 27, 103 (1931).

[2] Crennell and Milligan, World Pow. XVII, 264 (1932).

[3] Vinal, Craig and Snyder, Bur. Standards I. Res. 10, 795 (1933).

* Calculation by the empirically derived equation of Peikert, which was recently shown [7] to reflect the properties of a passivated lead electrode, showed that with an increase in current density by a factor of 1.2 the practical capacity of the electrode falls by 15%. In the calculation by Peikert's equation: τI^n = const., where τ is the discharge time, I is the current density, and n is a constant, we used the value n = 1.2 as this was found experimentally for a lead electrode in 8 N sulfuric acid [7].

[4] B. N. Kabanov and G. I. Popova, Zhur. Priklad. Khim. 32, 1 (1959).*

[5] B. N. Kabanov, Doklay Akad. Nauk. SSSR, 31, 338 (1941).

[6] B. N. Kabanov, D. I. Leikis and E. I. Krepakova, Doklady Akad. Nauk SSSR, 98, 988 (1954).

[7] B. N. Kabanov, Doklady Akad. Nauk SSSR, 31, 582 (1941).

[8] Fleischmann and Thirsk, Trans. Faraday Soc., 51, 1, 71 (1955).

Received July 31, 1958

* Original Russian pagination. See C. B. Translation.

DETERMINATION OF THE TRUE SPECIFIC GRAVITY OF CELLULOSE

V. I. Sharkov and V. P. Levanova

The specific gravity of cellulose samples is usually determined by flotation in inert organic liquids which do not cause the cellulose to swell and whose densities are close to that of cellulose.

Hermans' modification of this method [1], in which the liquid medium is carbon tetrachloride, is usually used. According to his description, determination of the specific gravity consists of drying cellulose balls, 2 – 3 mm in diameter and weighing 0.5 – 1.0 mg, in a stream of dry air, which is then displaced with carbon tetrachloride vapor. At the end of this operation the vessel with the cellulose balls is cooled and sufficient carbon tetrachloride condensed in it for flotation. All these operations are carried out in a specially constructed apparatus. When the carbon tetrachloride has been condensed, the ampoule with it and the cellulose is sealed and inserted into a water thermostat, the temperature in which is slowly raised or lowered at a given rate. The temperature at which the cellulose balls are in a suspended state, i.e., neither sinking nor floating, corresponds to a definite specific gravity of the carbon tetrachloride, and consequently of the cellulose balls. Hermans' method gives results which agree well, but requires a long time (8 – 10 hours) and is complicated to carry out.

TABLE 1

Specific Gravity of Liquids at Various Temperatures

Liquid	Temp. (in °C)	Specific gravity of liquid
Carbon tetrachloride	20	1.594
	30	1.575
	40	1.555
	50	1.535
	60	1.516
	70	1.496
Bromobenzene	10	1.509
	20	1.495
	30	1.482
	40	1.468
	50	1.454
	60	1.441
	70	1.427
	80	1.414

To simplify this method we replaced the drying of the cellulose samples in a current of dry air and displacement of the latter by carbon tetrachloride vapor by a preliminary drying in an ordinary drying cupboard at 105° to an absolutely dry state, then moistened the pieces with a small amount of absolute alcohol and washed out the latter with carbon tetrachloride. These operations ensured rapid displacement of air and thorough permeation of the cellulose samples with carbon tetrachloride.

For determining the specific gravity, balls 1 – 2 mm in diameter were prepared from fibrous cellulose samples and lumps ~0.5 mm in diameter were obtained from powdered cellulose by pressing the material on a glass plate with a spatula. Cellulose lumps or balls (5 – 6 pieces) were placed on a No. 2 glass filter and dried at 105° for 3 hours in a drying cupboard. When the glass filter with the balls had been dried in a desiccator, it was placed in a Bunsen flask and its contents washed with absolute ethanol which was then displaced by dry carbon tetrachloride in such a way that air did not come in contact with the cellulose lumps. The carbon tetrachloride was periodically replaced by a fresh portion. After 30 minutes washing, the contents of the filter with the cellulose lumps were transferred to a dry tube, which was filled with carbon tetrachloride, sealed, and then placed in a water thermostat, fitted with a stirrer and thermometer with scale divisions of 0.1°.

To determine the specific gravity, the water in the thermostat was heated to a temperature at which all the balls sank and was kept at this temperature for 30 minutes. The temperature was then lowered 0.5 – 1.0° at a time and kept at each temperature for 20 minutes. At the same time we counted the number of balls that floated, sank, or were suspended at each temperature.

TABLE 2

Results of Measuring the Specific Gravities of Various Cellulose Preparations

Characteristics of cellulose sample	Value of specific gravity	
	by Hermans' method	by our simplified method
Cotton cellulose (absorbent cotton)	1.545	1.545
Cotton hydrocellulose	1.562	1.562
Viscose silk 1	1.508	1.507
Viscose silk 1 after partial dioxanolysis	1.507	1.507
Viscose silk 1 after partial ethanolysis	1.537	1.537

The temperature at which the greatest number of balls were in a suspended state was taken as the flotation temperature. The specific gravity of the cellulose was found from this temperature by means of Table 1. On examining cellulose preparations with a specific gravity below 1.500, we replaced the carbon tetrachloride by bromobenzene. Data on its density at similar temperatures are also given in Table 1.

The values found for the specific gravities of cellulose were corrected to 20° by the formula

$$d_{20^\circ} = d_t + k\,(t^\circ - 20),$$

where d_t is the specific gravity found at the flotation temperature and k is the expansion coefficient of cellulose, which equals $8 \cdot 10^{-5}$.

The specific gravity may also be determined by the above method by raising the temperature.

The results we obtained by determining the specific gravity by this method were compared with results obtained by Hermans' method.

The value of the specific gravity of each cellulose sample was determined 2 – 3 times. The discrepancies between parallel experiments did not exceed ± 0.001.

Table 2 gives the results of measuring the specific gravities of various cellulose preparations.

The data in Table 2 show that the two methods give practically identical results. Samples of viscose silk, which Hermans' considered had to be first freed from air under vacuum, showed identical results.

The method we propose for determining the specific gravity of cellulose is quite simple to accomplish and requires not more than 1.5 – 2.0 hours which is considerably shorter than the time required for a determination by Hermans' method.

SUMMARY

A simplified variation of the flotation method is proposed for determining the true specific gravity of various cellulose preparations.

LITERATURE CITED

[1] P. H. Hermans, J. J. Hermans, and D. Vermaas, J. Pol. Sci. 1, 3, 162 (1946).

Received March 17, 1959

PARAMAGENTIC RESONANCE IN COALS

V. I. Losev and É. A. Bylyna

In recent years communications have appeared in the literature on the existence of paramagnetic resonance in such carbon-containing substances as graphite [1, 2], activated wood charcoal and carbonized organic substances [3 – 5], coals, and petroleums [6 – 11].

The effective d-factor for all these substances was found to be equal to 2.004 ± 0.002. It was observed [11] that the intensity of the effect in all cases increased by a factor of approximately 3 with cooling to liquid-air temperatures and similarly for the free radical (which was used as a standard).

In the present work we measured the paramagnetic resonance in a number of coals from the Donets Basin relative to their degree of metamorphism (table) and also examined Estonian peat, but paramagnetic resonance was not detected in it.

As a calibration material we used diphenylpicrylhydrazyl (DPH):

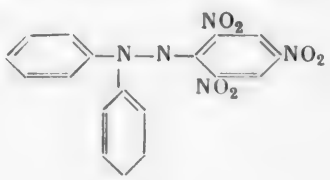

with a d-factor of 2.003 ± 0.001 at a frequency of 9450 Mc, which agrees well with data of other authors [12]. The measurements on the coals were carried out at the same frequency and at 22° on an apparatus with a sensitivity of $5 \cdot 10^{15}$ atoms. The samples were stored in bottles with tightly fitting ground stoppers, rapidly ground in an agate mortar before a determination, and placed in a molybdenum glass tube and the measurements made. All the samples, apart from the peat, showed a readily measureable effect.

The effective d-factor of the absorption lines in all cases was determined by nuclear resonance at a frequency of 9450 Mc. It was found to be equal to 2.003 ± 0.001.

Grade of coal	Donbass deposit	C content (in %)	Control "free radicals"
Long-flame (L)	Dobropol'e	76.36	$1 \cdot 10^{17}$
Gas (G)	Dobropol'e	82.29	$3 \cdot 10^{17}$
Soft steam (SS)	Nikitovka	85.32	$4.0 \cdot 10^{17}$
Coke (C)	Avdakovo	87.48	$4.7 \cdot 10^{17}$
Steam-clinkering (SC)	(Chumakovo)	88.52	$5.3 \cdot 10^{17}$
Poor (P)	(Chumakovo)	89.43	$7.2 \cdot 10^{17}$
Anthracite	(Chumakovo)	90.53	$1.0 \cdot 10^{18}$

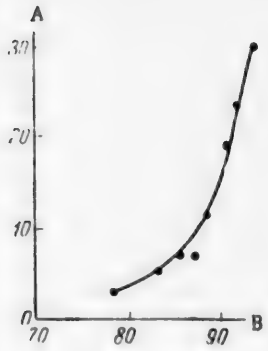

Fig. 1. Paramagnetic resonance of coal. A) Amount of adsorbed radicals (30 units ≈ $2.5 \cdot 10^{19}$ free radicals/ g), B) C concentration (in %).

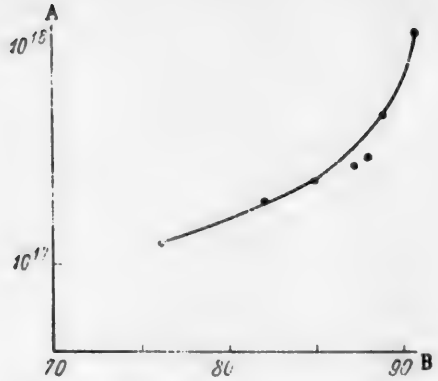

Fig. 2. Paramagnetic resonance of coal according to the data of Ingram et al. [4 – 6]. A) Number of adsorbed radicals (free radicals/ g), B) C concentration (in %).

The approximate "free radical" concentration was determined by comparing the absorption lines with those of a standard sample containing 1% of DPH. There is no doubt that relative to the standard sample these concentrations were approximate for each coal, but the relative accuracy of these concentrations lay within the limits of 10%.

Figure 1 gives a curve of the "free radical" concentration against the degree of metamorphism of the coals, which agrees well with the data obtained by Ingram et al. (Fig. 2).

The authors of the present article agree with Ingrams's opinion that the "free radical" concentration is a function of the degree of metamorphism. Moreover, since a number of investigators both in the Soviet Union and abroad [13 – 19] have now arrived at the conclusion that the structure of molecular compounds of carbonaceous substances is a condensed aromatic nucleus with side chains attached to it, the so-called "fringe", and that the degree of condensation of the nuclei increases with metamorphism, while the number of side chains decreases; in the opinion of the authors of the present article, this function is a function of the degree of condensation of the aromatic rings.

LITERATURE CITED

[1] L. G. Gastle, Phys. Rev. 92, 1063 (1953).

[2] L. G. Gastle, Phys. Rev. 95, 846 (1954).

[3] G. R. Hennig, B. Smaller, and E. L. Yasaitis, Phys. Rev. 95, 1088 (1954).

[4] D. J. E. Ingram and L. E. Bennett, Phil. Mag. 45, 545 (1954).

[5] D. J. E. Ingram and J. G. Tapley, Phil. Mag. 42, 1221 (1954).

[6] D. J. E. Ingram, J. G. Tapley, R. Jackson, R. L. Bond, and A. R. Murnaghan, Nature 174, 797 (1954).

[7] A. Etienne and I. Uebersfeld, J. Chem. phys. 51, 328 (1954).

[8] I. Uebersfeld, A. Etienne, and L. Combrisson, Nature 174, 614 (1954).

[9] L. E. Bennett, D. J. E. Ingram, and J. G. Tapley, Rept. Bristol. Conf., "Defects in solid state" (1955).

[10] G. R. Hennig, B. Smaller, and E. L. Yasaitis, Phys. Rev. 95, 1088 (1954).

[11] N. S. Garif'yanov and B. L. Kozyrev, Zhur. Eksp. Teor. Fiz. 30, 2 (1956).*

[12] T. L. Chu, E. Pake, D. E. Paul, J. Townsend, and S. L. Weissman, Phys. Rev. 57, 504 (1953).

* See English Translation.

[13] K. U. Howard, Chemistry of Solid Fuel [Russian translation] (Foreign Lit. Press, 1951) p. 1.

[14] V. I. Zabavin, Izvest. Akad. Nauk SSSR, Otdel. Tekh. Nauk 5, 27 (1941).

[15] S. G. Aronov, Zhur. Priklad. Khim. 25, 9, 927 (1952).*

[16] I. G. C. Dryden, Fuel 32, 199 (1953).

[17] D. W. van Krevelen, Brenn. Chem. 35, 289 (1954).

[18] W. K. Ruston, Fuel 26, 74 (1947).

[19] V. I. Kasatochkin, Izvest. Akad. Nauk SSSR, Otdel. Tekh. Nauk 9, 195 (1952); Doklady Akad. Nauk SSSR* 86, 759 (1952); Izvest. Akad. Nauk SSSR, Otdel. Tekh. Nauk 10 (1953).

Received December 8, 1958

*Original Russian pagination. See C. B. Translation.

1-(4'-SULFOPHENYL)-3-METHYL-5-PYRAZOLONE FROM ACETOACETAMIDE

P. A. Levin

Phenylhydrazine and its derivatives very readily interact with acetoacetamide to form as final products 1-phenyl-3-methyl-5-pyrazolone and its derivatives [1 – 5]. The reaction between 4-sulfophenylhydrazine and acetoacetamide proceeds readily in an aqueous medium according to the scheme:

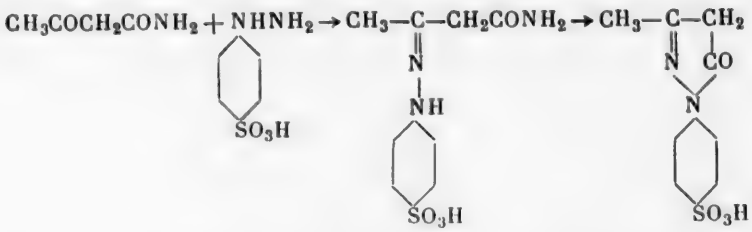

The 1-(4'-sulfophenyl)-3-methyl-5-pyrazolone obtained finds application in the synthesis of pyrazolone dyes and in analytical chemistry.

Strong mineral acids catalyze ring formation. This process can also occur under the action of the sulfonyl group of acetoacetamide sulfophenylhydrazone. To have homogeneous synthesis conditions, the solution of acetoacetamide (obtained from diketene) was reacted with a sufficient excess of ammonia to convert the sulfophenylhydrazine to the ammonium salt. Hydrochloric or sulfuric acid was then added to the solution and the process was completed by precipitation of the pyrazolone (in high yield when hydrochloric acid was used). Synthesis in a glass vessel and a wooden tub gave good yields (close to quantitative) and a high-quality product. Other method of preparing sulfophenylmethylpyrazolone were less efficient [6 – 9].

The product of reaction between phenylhydrazinesulfonic acid and acetoacetamide solution in the absence of free ammonia was not the sulfophenylhydrazone of acetoacetamide, as was first assumed, but the ammonium salt of sulfophenylmethylpyrazolone.

EXPERIMENTAL

Interaction between sulfophenylhydrazine and acetoacetamide in the absence of free ammonia. To 4 g of sulfophenylhydrazine in 25 ml of water was added a neutralized solution of acetoacetamide, prepared by dissolving 2 ml of diketene in 20% ammonia. After being stirred for 1 hour, the orange solution formed was filtered and evaporated to dryness on a water bath. The light orange, crystalline reaction product formed was very readily soluble in water (salted out with a mixture of sodium hydroxide and sodium chloride), readily soluble in methyl and ethyl alcohols and less so in benzyl alcohol; it was insoluble in ether, benzene, acetone, pyridine, chlorobenzene and isoamyl alcohol. The substance could not be recrystallized from mixtures of ligroin and alcohol, water and acetone, alcohol and ether, benzene and methyl alcohol, and alcohol and pyridine. After 2 reprecipitations with benzene from alcohol solution, the product was obtained in a purified state as a pink crystalline powder with a conversion point of 262°. According to the physical and chemical properties, the substance obtained was the ammonium salt of sulfophenylmethylpyrazolone. When a hot solution of the salt in a mixture of alcohol and

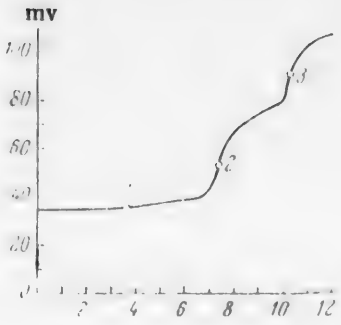

Potentiometric titration curve of 25 ml of 0.012 N phenylmethylpyrazolonesulfonic acid with 0.101 N NaOH. 1) Free sulfonic acid (pH 1.4), 2) Na salt of sulfonic acid (pH 3.7), 3) enolate of Na salt of sulfonic acid (pH 9).

acetone (1 : 2) was cooled, a flocculent, yellow, crystalline substance with a conversion point of 172° was precipitated and this was probably a reaction product of sulfophenylmethylpyrazolone and acetone.

Synthesis in the presence of excess ammonia. A solution of acetoacetamide, prepared from 0.0275 mole of diketene and containing 100% excess of ammonia, was added to a 10% suspension of 0.025 mole of sulfophenylhydrazine. The condensation was carried out by stirring for 50 minutes. A further 1.5 ml of ammonia had to be added for the sulfophenylhydrazine to dissolve completely. The reaction mixture was acidified with 3 times the amount of 25% sulfuric acid required to produce an acid reaction to Methyl Violet (green color), heated to 50 – 60° and stirred for a further 40 minutes, and then cooled to 5 – 10°.

The sulfophenylmethylpyrazolone formed an almost colorless crystalline precipitate. The yield was 5.45 g (80.3%, calculated on sulfophenylhydrazine). In addition to pyrazolone (0.122 g), the filtrate contained 0.47 g of unreacted sulfophenylhydrazine. The total yield of pyrazolone was 82.3%.

An analogous synthesis with 0.05 mole of sulfophenylhydrazine and with hydrochloric acid used for acidification, even when the condensation time was 20 minutes, gave a sulfophenylmethylpyrazolone yield of 13.5 g and a total yield (allowing for the pyrazolone in the filtrate) of 99.9%.

Preparation of Sulfophenylmethylpyrazolone Under Production Conditions

Preparation of acetoacetamide. The amide was prepared in a 0.5 liter flask with a stirrer (300 rpm) from 130 ml (1.145 mole) of 16% ammonia cooled to 7°, and 37.6 ml of diketene (0.44 mole, 90% diketene content), added at a rate of 2 – 3 ml per minute. The reaction continued for 30 minutes after the addition of all the diketene. The end of the reaction was indicated by the disappearance of oily drops and the smell of diketene. The acetoacetamide solution was a clear, colorless liquid with d_4^{23} 1.046.

Condensation of acetoacetamide with sulfophenylhydrazine. The apparatus for the condensation and cyclization was a wooden tube of 1.5 liter capacity with an anchor-shaped stirrer (200 – 250 rpm) and an electrical heating element in a stainless steel tube and a spiral lead condenser. The amide solution was added with stirring to a suspension of 85.4 g (0.94 mole, 88% pure) of phenylhydrazinesulfonic acid in 675 ml of water. The sulfophenylhydrazine reacted completely after 25 minutes. The temperature at the beginning of the reaction was 10° and at the end, 16 – 17°.

Cyclization. Concentrated hydrochloric acid was added at 3 – 4 ml per minute to the solution of acetoacetamide sulfophenylhydrazone. The separation of sulfophenylmethylpyrazolone began after the addition of 50 ml of acid (weakly acid reaction to congo). A stable foam was formed. A permanent acid reaction (to congo and then to Methyl Violet – green color) was reached after the addition of 97 ml of acid with each portion of the last 25 ml of acid added after the acid reaction to congo from the previous portion had disappeared.

The heater was used to raise the temperature of the mixture rapidly to 45° and stirring was continued for 40 minutes at this temperature. The casing of the heating apparatus darkened. The mixture, cooled to 8°, was filtered through a cotton filter and washed with 250 ml of water (cooled). The well-pressed paste contained 44% of moisture. The dry product was a white, friable crystalline powder. The yield was 104.1 g. The bulk weight was 0.485 g/ cc and the specific volume 2.06 cc/ g. The anhydrous pyrazolone content of the product was 89.6% (sulfophenylmethylpyrazolone crystallizes with 1 molecule of H_2O) and the soda-insoluble residue was 0.22%. The product was analyzed by nitrosation in a solution with a free hydrochloric acid content of 10 – 15%.

The filtrate and wash waters contained 6.0% of ammonium chloride, 0.7% of sulfophenylmethylpyrazolone, about 0.5% of ammonium acetate and traces of acetoacetamide.

The total yield of sulfophenylmethylpyrazolone was 99.7% of which 91.4% was in the form of a dry product. The portion contained in the filtrate could be isolated and the ammonia also readily regenerated from the filtrate.

For example, evaporation of 50 ml of the filtrate and treatment of the dry residue with water yielded 0.172 g of pure pyrazolone. Sulfophenylmethylpyrazolone could also be isolated from the filtrate in the form of the dye "Light-stable Acid Yellow" by the addition of 0.1 g of soda and 0.1 g of diazotized aniline to 50 ml of ice-cooled filtrate. After 2 hours standing and subsequent boiling, the mixture yielded 0.165 g of dye. It was possible to obtain 0.198 g of dye by salting out. On titration with alkali, sulfophenylmethylpyrazolone behaved (figure) as a dibasic acid (sulfonic acid group and enol group), which was completely dissociated (as a sulfonic acid) in 0.01-0.02 N solutions.

SUMMARY

1. 1-(4'-sulfophenyl)-3-methyl-5-pyrazolone may be obtained from acetoacetamide (from diketene) in a yield close to quantitative (99.7%, 91.4% in the precipitate) and as a high-grade product both in normal laboratory and in wooden (production) apparatus.

2. It is also possible to isolate about half of the pyrazolone contained in the filtrate in the pure form or as a dye.

LITERATURE CITED

[1] L. Claisem and K. Meyer, Ber 35, 583 (1902).

[2] P. A. Levin, Zhur. Obshchei Khim. 26, 2274 (1956).*

[3] P. A. Levin, Med. Prom. SSSR.

[4] U. S. Pat. 2637732 (1953).

[5] Swiss Pat. 300334 (1954).

[6] P. A. Levin, Zhur. Obshchei Khim. 27, 2864 (1957).*

[7] P. A. Levin, Zhur. Obshchei Khim. 27, 1374 (1957).*

[8] Mollenhoff, Ber. 25, 1941 (1892).

[9] I. S. Ioffe and Z. Ya. Khavin, Zhur. Obshchei Khim. 17, 522 (1947).

Received October 27, 1958

* Original Russian pagination. See C. B. Translation.

CONVERSION OF ETHERATES (OXONIUM COMPOUNDS OF SULFURIC ACID WITH β-CHLORO ETHERS) INTO A CRYSTALLINE STATE

A. K. Seleznev

Organic Chemistry Laboratory of the Groznyy Petroleum Institute

Ethers form oxonium complexes with many substances, for example of halogens, hydrogen halides, salts, and acids. Sulfuric acid has a strong affinity for ethers and due to this, these compounds are almost completely extracted by sulfuric acid from various solutions, for example, in organic halogen compounds. The first problems on the complex compounds of diethyl ether with sulfuric acid were investigated by McIntosh and Archibald [1]. Pound [2] made a careful study of a mixture of sulfuric acid and diethyl ether. Favorskii [3] obtained compounds of sulfuric acid with dioxane. Chelintsev and Kozlov [4] investigated the heats of formation and molecular weight of compounds of sulfuric acid with ethers and their conversion into a crystalline state at very low temperatures.

The existence of sulfuric acid–ether complexes was also confirmed by Usanovich, Sabinina, and Zavarikhina [5] by investigating the electroconductivity and viscosity of these systems. The high electroconductivity of sulfuric acid in ether was reported even earlier by Plotnikov [6]. Aschan and Schwalbe [7] used these compounds for the preparation of mainly terpene alcohols from the corresponding terpenes with a double bond and found that they gave an effect which could not be obtained with sulfuric acid without the ether. They obtained sulfates from the alcohols menthol, borneol, and others by means of diethyloxonium sulfate. All the alcohols formed sulfates from oxonium sulfate much more readily than by the direct action of sulfuric acid. In work on the synthesis of β-chloro ethers from cracking olefins [8 – 12] sulfuric acid is frequently used to extract the chloro ethers from a mixture with dichlorides, and also a mixture with dichlorides and alcohols which are difficulty soluble in water. With β-chloro ethers sulfuric acid forms oxonium compounds of the type $Cl-CH_2-CH_2\diagdown\!\!\diagup O \cdot H_2SO_4$ (C_5H_{11}). Alcohols form sulfates from an oxonium sulfate much more readily than by the direct action of sulfuric acid:

$$Cl-CH_2-CH_2\diagdown\!\!\diagup O\!<\!\begin{matrix}H\\OSO_3H\end{matrix} + C_5H_{11}OH \rightarrow C_5H_{11}OSO_3H + H_2O + Cl-CH_2-CH_2\diagdown\!\!\diagup O.$$
(C_5H_{11})

The ester $C_5H_{11}OSO_3H$ is isolated as the salt on neutralization.

The purpose of the present work was to convert sulfuric acid compounds of β-chloro ethers into a crystalline state by cooling with liquid air. At the beginning of our investigations we repeated the experiments of Chelintsev and Kozlov [4] on the conversion of etherates into a crystalline state. McIntosh and Archibald cooled the compound $(C_2H_5)_2O \cdot H_2SO_4$ to 70 to -80° with a cooling mixture of solid CO_2 and ether and found that at these temperatures the etherate only thickened and changed to a gummy mass which showed no signs of crystallizing. Chelintsev and Kozlov [4] were the first to convert the etherates $H_2SO_4 \cdot (C_2H_5)_2O$, $H_2SO_4 \cdot 2(C_2H_5)_2O$, $H_2SO_4 \cdot (C_5H_{11})_2O$ and $H_2SO_4 \cdot 2(C_5H_{11})_2O$ into a crystalline state by cooling with liquid air.

TABLE 1

Results of Experiments to Determine the Melting Points of Etherates

Etherates	Melting point according to the data of Chelintsev and Kozlov [4], measured with a toluene thermometer (in °C)	Melting point according to data of the present work, measured with a thermocouple (in °C)
$H_2SO_4 \cdot (C_2H_5)_2O$	—66— —64	—124
$H_2SO_4 \cdot 2(C_2H_5)_2O$	—88	—137
$H_2SO_4 \cdot (C_5H_{11})_2O$	—67— —68	—107
$H_2SO_4 \cdot 2(C_5H_{11})_2O$ . . .	—74	—124

TABLE 2

Results of Experiments to Determine the Melting Points of Etherates

Etherates	Melting point measured with a thermocouple (in °C)
$H_2SO_4 \cdot O\langle^{CH_2—CH_2—Cl}_{C_3H_7\ (n)}$	—116
$H_2SO_4 \cdot 2O\langle^{CH_2—CH_2—Cl}_{C_3H_7\ (n)}$	—117.3
$H_2SO_4 \cdot O\langle^{CH_2—CH_2Cl}_{C_4H_9\ (n)}$	—106.6
$H_2SO_4 \cdot 2O\langle^{CH_2—CH_2Cl}_{C_4H_9\ (n)}$	—120
$H_2SO_4 \cdot O\langle^{CH_2—CH_2C}_{C_4H_9\ (i)}$	—115.3
$H_2SO_4 \cdot 2O\langle^{CH_2—CH_2Cl}_{C_4H_9\ (i)}$	—120
$H_2SO_4 \cdot O\langle^{CH_2—CH_2Cl}_{C_5H_{11}\ (i)}$	—112.4
$H_2SO_4 \cdot 2O\langle^{CH_2—CH_2Cl}_{C_5H_{11}\ (i)}$	—114.6
$H_2SO_4 \cdot O\langle^{CH_2—CH_2Cl}_{C_6H_{13}\ (n)}$	—106.4
$H_2SO_4 \cdot 2O\langle^{CH_2—CH_2Cl}_{C_6H_{13}\ (n)}$	—112.4

EXPERIMENTAL

Before studying the crystallization conditions of etherates (compounds of sulfuric acid with β-chloro ethers) and determining their melting points, we carried out experiments with the etherates studied by Chelintsev and Kozlov [4]. For this purpose we prepared diethyl (b.p. 35°, d_4^{20} 0.7136, n_D^{20} 1.3525) and diisoamyl (b.p. 172.5 to 173°, d_4^{20} 0.7768, n_D^{20} 1.4078) ethers in a pure state. Absolute sulfuric acid was prepared [13] (m.p. 10.4°). The etherates were prepared by mixing sulfuric acid and the ethers in accurately weighed amounts with strong cooling. A tube (0.4 cm in diameter) with the etherate and a thermocouple in a glass pocket was placed in a wider tube, immersed in an unsilvered Dewar vessel with liquid air. Through the walls of the Dewar vessel we could readily observe what occurred in the tube and determine the crystallization point of the etherate. The melting point of the etherate could be observed in another empty and unsilvered Dewar vessel to which the tube with the etherate was transferred. Under these conditions the temperature rose slowly. A copper/constantan thermocouple was used to determine the crystallization and melting points. A PP-1 potentiometer was used to record the temperature given by the thermocouple. The accuracy of temperature measurement by the thermocouple was checked with pure substances. For this purpose we used: diethyl ether (n_D^{20} 1.3525, m.p. -116.3°), isopentane (2-methylbutane, n_D^{20} 1.3535, m.p. -160°) and liquid oxygen (b.p. -182°).

For a more accurate determination of crystallization and melting points of the etherate, the latter (one drop) was introduced into an even narrower tube with a thermocouple. It was curious that the etherate crystallized instantaneously as flakes with an audible crackle. The results of the experiments are given in Table 1.

The melting points of the etherates (Table 1) according to our determinations were found to be considerably lower than according to the data of Chelintsev and Kozlov.

The next experiments on the crystallization conditions of etherates and the determination of their melting points were carried out with β-chloro ethers; the latter were obtained in a pure state [11, 12]. The conditions for preparing the etherates and the experimental procedure were described above. The experimental results are given in Table 2.

LITERATURE CITED

[1] McIntosh and Archibald, Trans,* 85, 919 (1904).

[2] Pound, J. Chem. Soc. 99, 1, 698 (1911).

[3] A. E. Favorskii, Zhur. Russ. Khim. Obshchestvo 38, 774 (1906).

[4] V. V. Chelintsev and N. A. Kozlov, Zhur. Russ. Khim. Obshchestvo 46, 708 (1914).

[5] M. Usanovich, L. Sabinina, and R. Zavarikhina, Zhur. Obshchei Khim. 3, 87 (1933).

[6] V. A. Plotnikov, Investigation of the Electrochemistry of Nonaqueous Solutions [In Russian] (Kiev, 1908) p. 8.

[7] O. Aschan and A. Schwalbe, Finska Kem. Medd. 40, 133; 41, 98 (1932).

[8] A. K. Seleznev, Zhur. Priklad. Khim. 27, 3 (1954).**

[9] A. K. Seleznev, Zhur. Priklad. Khim. 29, 1 (1956).**

[10] A. K. Seleznev, Zhur. Priklad. Khim. 29, 3 (1956).**

[11] A. K. Seleznev, Zhur. Priklad. Khim. 31, 4 (1958).**

[12] A. K. Seleznev, Zhur. Priklad. Khim. 31, 12 (1958).

[13] M. Usanovich, Zhur. Obshchei Khim. 2, 215 (1934).

Received December 25, 1958

* As in original – Publisher's note.

** See C. B. Translation.

COHYDROLYSIS OF DIMETHYLDICHLOROSILANE WITH (1-CYANO-1-METHYLETHOXY)-METHYLDICHLOROSILANE

I. K. Stavitskii and S. N. Borisov

All-Union Synthetic Rubber Scientific Research Institute

In recent years there has been an increase in interest in siloxane polymers containing polar groups in the organic radicals at the silicon atom, in connection with the possibility of using such polysiloxanes to prepare materials with valuable technical properties (high heat and oil and gasoline resistance, improved adhesion, etc.).

It is reported in the literature [1, 2] that the group $N\equiv C-\overset{CH_3}{\underset{CH_3}{C}}-O-$ in (1-cyano-1-methylethoxy) organochlorosilanes has a high resistance to hydrolysis but this opinion has been disputed [3]. It was also shown that cohydrolysis of dimethyldichlorosilane with (1-cyano-1-methylethoxy)phenyldichlorosilane in a ratio of 99 : 1 leads to an oily product (M = 540), polycondensation of which with sulfuric acid gives a rubber-like polymer. However, the latter was strongly cross-linked (solubility in benzene 30%) and the rubber based on it, obtained by the procedure used for the polysiloxane rubber SKT, did not have good working properties (tensile strength 21 kg/ cm^2 and relative elongation 160%). However, the structurization of the polymer was not the result of cleavage of the 1-cyano-1-methylethoxy groups as the nitrogen content of the polymer was found to be 0.3% as compared with 0.2% by calculation.

The lack of study of the hydrolysis resistance of the $NCC(CH_3)_2O$ group compelled us to undertake a further investigation in this direction.

EXPERIMENTAL

For the work, we used rectified dimethyldichlorosilane (DDS) with a hydrolyzable chlorine content of 54.88% (calculated, 54.94% Cl) and (1-cyano-1-methylethoxy)methyldichlorosilane* (CMDS, b.p. 75 – 76° at 24 mm; n_D^{20} 1.4230; found%: Cl 35.57, N 7.85; calculated%: Cl 35.79, N 7.07**).

At a rate of 20 drops per minute 15 g of CMDS was introduced from a dropping funnel into a flask containing 15 g of water and 12.6 g of ethyl alcohol (the final HCl content of the aqueous alcohol layer was 17.4%). We obtained 8 g of a solid insoluble product with 1.19% N (calc. for $\left[CH_3\left(NCC-\overset{CH_3}{\underset{CH_3}{C}}-O\right)SiO\right]_n$ 9.78% N).

* Synthesized by V. M. Vdovin in the laboratory of Corresponding Member of the Academy of Sciences USSR A. D. Petrov (Inst. Org. Chem. Acad. Sci. USSR) by the reaction of acetone cyanhydrin with methyltrichlorosilane in the presence of pyridine.

** The average results from several determinations are given. The nitrogen was determined by R. I. Ryvkina.

A mixture of 245.2 g of DDS and 19.8 g of CMDS (molar ratio of reagents 95 : 5) was introduced at a rate of 1.25 mole per hour into a mixture of 265 g of water and 222.6 g of rectified alcohol with vigorous stirring (the final HCl content of the aqueous alcohol layer, allowing for the chemically bound water, was 24.4%). The dry, neutral, oily hydrolyzate (132.2 g, 85.2% of theoretical) had n_D^{20} 1.4000, d_4^{20} 0.9721, M = 404 and contained 0.32% of OH groups. The low content of hydroxyl groups indicated that the polycondensation product from the cohydrolysis had a cyclic structure.

Found, % : N 0.45.

Calculated, % : N 0.9.

Polycondensation of the hydrolyzate with sulfuric acid by the method developed for cyclic polydimethylsiloxanes finally led (after neutralization and drying) to a porous, inelastic polymer which was only 32.8% soluble in benzene. The nitrogen content of the polycondensation product found was 0.14% as compared with 0.45% in the original siloxane oil. These data indicate that the polymer had a cross-linked structure.

The results obtained lead to the conclusion that under the comparatively drastic hydrolysis and polycondensation conditions used to obtain polydimethylsiloxane rubber [4], in the acid medium there is partial cleavage of the 1-cyano-1-methylethoxy groupsat the RO—Si bond since cleavage of the CN group should not lead to structurization of the polymer.

For further elucidation a cohydrolysis was carried out in a practically neutral medium.

A mixture of 245.2 g of DDS and 19.8 g of CMDS, and an alkali solution (5.1 N NaOH, 17.1%) were simultaneously added over a period of two hours with vigorous stirring to a flask with 180 ml of water so that the reaction mixture, which contained a mixed indicator (phenolphthalein–bromothymol blue), remained a bluish-green color. The dry, neutral hydrolyzate had n_D^{20} 1.4050, d_4^{20} 0.9840, η = 168 centipoises, M = 1089 and the OH group content was 0.14% (112.0 g, 71.2%). The nitrogen content of the polymer was found to be 0.64% as compared with 0.9% by calculation, indicating partial cleavage of 1-cyano-1-methylethoxy groups under the given hydrolysis conditions.

SUMMARY

In the cohydrolysis of (1-cyano-1-methylethoxy)methyldichlorosilane with dimethyldichlorosilane in acid and neutral media the 1-cyano-1-methylethoxy groups were not sufficiently stable to hydrolysis.

LITERATURE CITED

[1] K. C. Frisch, and M. Wolf, J. Org. Chem. 19, 657 (1953).

[2] A. D. Petrov, V. F. Mironov and V. M. Vdovin, Izvest. Akad. Nauk SSSR, Otdel. Khim. Nauk* 1123 (1955); V. M. Vdovin, Author's Abstract of Candidate's Dissertation [In Russian], Institute of Organic Chemistry, Acad. Sci. USSR (Moscow 1957).

[3] W. Hahn, Makrom. Chem. 11, 64 (1953).

[4] I. K. Stavitskii, Khim. Nauka i Prom. 3, 331 (1957); I. K. Stavitskii et al., Trudy Konf. po Khim. i Prakt. Prim. Kremneorg. Soed., TsBTI, Leningrad 2, 57 (1958).

Received December 8, 1958

*Original Russian pagination. See C. B. Translation.

PREPARATION OF PURE LINALYL CHLORIDE

G. V. Pigulevskii, V. G. Kostenko, and L. F. Andreeva

The investigations of Troyan, Bakina, and Pigulevskii [1, 2] showed that the action of PCl_3 on linalool in the absence of solvent yielded linalyl chloride The structure of the latter was demonstrated by oxidation with ozone and the Raman spectrum. Linalyl chloride was characterized as the nitrosate with m.p. 109°. However, it was not certain that the linalyl chloride was homogeneous. The Raman spectrum could only show the presence of primary - secondary and secondary-tertiary double bonds. We therefore under took a new investigation to obtain more homogeneous linalyl chloride.

We obtained linalyl chloride under conditions which were modified somewhat in comparison with those used previously. However, it contained from 57 – 64% of geranyl chloride. For removing the latter we decided to make use of the fact that lithium aluminum hydride readily reduces primary chlorides, but hardly reacts with tertiary chlorides [3 – 7]. We studied the conditions for reducing geranyl chloride and found that it was completely converted into dihydromyrcene even at room temperature. Linalyl chloride was not reduced under these conditions,. The mixture of linalyl chloride and dihydromyrcene was readily separated by fractional distillation. The linalyl chloride we isolated was the most homogeneous (see table).

Hydrogenation of linalyl chloride and dihydromyrcene demonstrated the presence of two double bonds. These results showed that the double bonds were not reduced during reduction of the chlorides with lithium aluminum hydride and that the chloride contained no cyclic chlorides.

Linalyl chloride differs from geranyl chloride in a lower specific gravity, a lower refractive index, and in having rotatory power.

The Raman spectra and infrared absorption spectra obtained agreed with the structure of linalyl chloride. The Raman spectrum had two lines of equal intensity ($\Delta\nu$ 1640 cm^{-1} and 1673 cm^{-1}), characteristic of the double bonds of linalyl chloride.* The infrared spectrum (Fig. 1) contained absorption bands with maxima in the region of 835 cm^{-1} and 922 cm^{-1} with the second band, corresponding to the deformation oscillation (CH) in the $-CH=CH_2$ group, considerably more intense than the first, characteristic of the (CH) oscillation in the $CR_1R_2=CHR_3$ group. In the infrared spectrum of the mixture obtained from the reaction of linalool with PCl_3 (Fig. 2), the ratio of the intensities of these bands was different and this is explained by the presence of geranyl chloride in the mixture.

EXPERIMENTAL

Synthesis of linalyl chloride. Linalool was isolated from coriander oil. Its constants were: b.p. 71° (5 mm), d_4^{20} 0.8653, n_D^{20} 1.4626, $[\alpha]_D$ + 14.0.

A sample of 63 g of linalool was placed in a three-necked flask fitted with a mechanical stirrer with a mercury seal, a reflux condenser, and a dropping funnel. Then 18.9 ml of PCl_3 was slowly added dropwise to the linalool. The temperature of the reaction mixture was kept within the limits of -13 to -10°. The reaction continued for 3 hours. To the product obtained was added 19 ml of previously cooled methyl alcohol. The upper layer was separated from the solid precipitate of phosphorous acid, diluted with ether, and washed with water, sodium carbonate solution and again with water until neutral. The ether solution was dried with Na_2SO_4,

* The same lines with the same intensity are present in the linalool spectrum [6].

Characteristics of Linalyl Chloride

Author	Boiling point (in °C)	$[\alpha]_D$	D_4^{20}	n_D^{20}
Pigulevskii and Troyan [1]	93—95 (8 mm)	—1.70°	0.9435	1.4816
Pigulevskii and Bakina [2]	79—80 (6 mm)	—4.7°	0.9368	1.4777 (16°)
In our experiments	89—90 (12 mm)	—8.4°	0.9243	1.4745

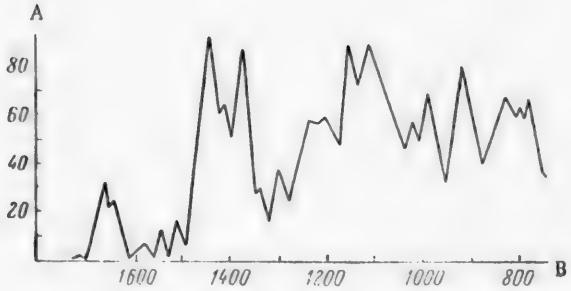

Fig. 1. Infrared spectrum of linalyl chloride. A) Degree of absorption (in %), B) wave number (in cm^{-1}).

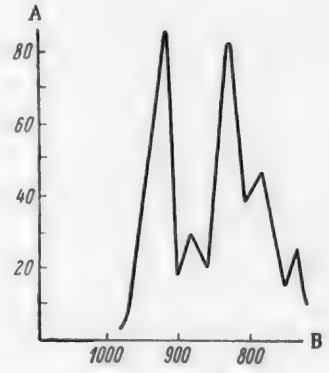

Fig. 2. Infrared spectrum of mixture obtained by the reaction of linalool with PCl_3. A) Degree of absorption (in %), B) wave number (in cm^{-1}).

and the ether removed under reduced pressure in a stream of nitrogen. The residue was vacuum distilled twice to yield a fraction (30 g) with b.p. 83 — 86° (8 mm), $[\alpha]_D^{20}$ -5.10° n_D^{20} 1.4750. The primary chloride content [6] was 64.3 and 62.9%.

Reduction of mixture of chlorides with lithium aluminum hydride. The reaction was performed in a three-necked flask fitted with a mechanical stirrer with a mercury seal, a reflux condenser, and a dropping funnel, in a nitrogen atmosphere.

Over a period of an hour 260 ml of an ether solution of lithium aluminum hydride (4.57 g) was slowly added to 30 g of chlorides, dissolved in 1 liter of absolute ether. The reaction mixture was left for 2 hours at room temperature with continuous stirring. Then 600 ml of moist ether and 1 liter of water were added to the mixture successively (slowly at first and then more rapidly when the evolution of gas ceased). The ether solution was washed with a weak solution of sodium hydroxide and water. In its turn, the precipitate of basic aluminum salts was treated with alkali solution. The aqueous solution obtained was extracted with ether. The combined ether extracts were then dried and the ether removed. The residue was vacuum distilled three times in a stream of nitrogen. As a result, two fractions were collected. The first fraction (5 g) was dihydromyrcene. Its constants were: b.p. 43 — 45° (12 mm), d_4^{20} 0.8125, n_D^{20} 1.4542, α_D — 0.18°. The second fraction was linalyl chloride. Its constants were: b.p. 89 — 90°)12 mm), α_D^{20} — 8.4°, d_4^{20} 0.9243, n_D^{20} 1.4745, MR_D 52.49.

Analysis of linalyl chloride.

Found %: Cl 20.21, 20.27; C 70.36, 70.34; H 10.26, 10.37.
$C_{10}H_{17}Cl$. Calculated %: Cl 20.58, C 69.56, H 9.86.
Primary chloride content: 3.84%, 3.18%.

Hydrogenation of linalyl chloride.

Sample 1.2130 g, Pt 0.225 g. C_2H_5OH 10 ml.
334 ml of H_2 (0°, 760 mm) was absorbed. Calculated: 330 ml H_2.

Hydrogenation of dihydromyrcene.

Sample 0.8333 g, Pt 0.192 g, C_2H_5OH 10 ml.
291 ml of H_2 (0°, 760 mm) was absorbed. Calculated:291 ml H_2.

Raman spectrum of linalyl chloride. The spectrum was plotted by means of a three-prism ISP-51 spectograph. Slit 0.04 mm. Exposure 7 hours.

$\Delta\nu$: 637(8), 1255(3), 1331(1), 1381(3), 1432(8), 1456(7), 1638(10), 1671(10), 2852(3), 2916(2), 2973(2).

Reduction of geranyl chloride with lithium aluminum hydride. Geranyl chloride was reduced under conditions similar to those for the reduction of linalyl chloride.

To 4.5 g of geranyl chloride, dissolved in 200 ml of ether, was added 39 ml of an ether solution containing 0.685 g of lithium aluminum hydride. The reaction continued for 3 hours. Vacuum distillation yielded 3.9 g of dihydromyrcene with the following constants: b.p. 44 – 46° (12 mm), d_4^{20} 0.8060, n_D^{20} 1.4538, $\alpha_D^{20} = 0$.

Primary chloride content [6]: 0.96%, 1.20%.

SUMMARY

The mixture of chlorides obtained as a result of the reaction of PCl_3 with linalool contained 40% of linalyl chloride and 60% of geranyl chloride.

A method was developed for the preparation of linalyl chloride, based on treatment of the chloride mixture with lithium aluminum hydride. Geranyl chloride was completely reduced to dihydromyrcene at room temperature. Linalyl chloride did not react under these conditions and could be isolated in a pure form.

LITERATURE CITED

[1] G. V. Pigulevskii and G. B. Troyan, Doklady Akad. Nauk SSSR 72, 519 (1950); I. I. Vanin and A. A. Chernoyarova, Zhur. Obshchei Khim. 7, 885 (1937).

[2] G. V. Pigulevskii and L. A. Bakina, Zhur. Obshchei Khim. 27, 816 (1957).*

[3] J. L. Everett and G. Kon, J. Chem. Soc. 3131 (1950).

[4] J. E. Johnson, R. H. Blizzard, and H. Carhart, J. Am. Chem. Soc. 70, 3664 (1948).

[5] G. Laber, Lieb. Ann. 588, 79 (1954).

[6] G. V. Pigulevskii and A. T. Ryskal'chuk, Vegetable Raw Materials [In Russian] Moscow-Leningrad, 5, 166 (1950).

[7] K. V. Leéts, A. I. Pilyavskaya, and M. I. Korovkina, Zhur. Obshchei Khim. 27, 2969 (1957).*

Received December 20, 1958

* Original Russian pagination. See C. B. Translation.

BOOK REVIEW

Yu. S. Musabekov. Synthetic Chemistry at a New Stage.
Yaroslavl' Book Press, 1958. 15,000 copies.

In addition to the resolution on the basic problem of accelerating the expansion of the chemical industry and, in particular, the production of synthetic materials to satisfy the needs of the population and the requirements of the national economy, the May Plenary session of the Central Committee of the Communist Party of the Soviet Union appealed to us to disseminate chemical knowledge among the population. This dissemination is the purpose of the brochure reviewed, which appeared at the beginning of 1959* in the series "The Reserves of Our Seven Year Plan." Its main subject is the fulfillment of this plan and the prospects of the development of synthetic chemistry in the near future.

The book has 6 sections (not counting the introduction). Section I, "Expansion of Synthetic Chemistry," gives a short historical review of the development of organic chemistry in general and the synthesis of high-molecular compounds (polymers) in particular. This shows the role of Russian and foreign chemists (Butlerov, Berthelot, and Kekule) who began synthetic trends in organic chemistry.

Considerable attention is paid to that very interesting class of highly complex and promising substances, high-molecular compounds, methods of synthesizing them and specific concepts of polymerization, polycondensation, etc.

The author is correct in noting: "Synthetic chemistry now makes it possible to produce substances and materials with previously set properties" (p. 20). This is one of the main problems of contemporary science.

A characteristic of the development of natural sciences in the 20th century is the obliteration of the boundaries between the different fields and the origination and rapid growth of the so-called composite sciences such as geochemistry, biochemistry, biophysics, mechanochemistry, etc. The study of high molecular compounds is one of these important branches of contemporary natural science. As Academician Nesmeyanov noted, this is rather a new stage in the development of science and not just in chemical sciences.

Section II, "Rubbers," deals with the importance of raw and processed rubber in modern life, the history of the discovery of natural rubber, the classical experiments of Butlerov on the synthesis of alcohol and the polymerization of unsaturated hydrocarbons, and the first synthesis of methyl rubber by Butlerov's student, Kondakov. There is a description of the work of S. V. Lebedev on the preparation of the first synthetic rubber on an industrial scale and the start of the first synthetic rubber factory in the worl in Yaroslavl' (in June 1932).

The author describes quite cursorily present work in Yaroslavl' on increasing the strength of rubber by reinforcing it with synthetic resins, on the development of accelerators, plasticizers,and fillers and on the radical improvement of the vulcanization process and the synthesis of butyl rubber. The author hardly considers the different types of raw and processed rubber, neither gives nor compares their characteristics and presents no illustrative, either tabular or graphical material. This is one of the omissions of the work.

In Section III, "Chemical Fibers," the factual material is presented in the same way as in the previous section. Beginning with a review of the early history and then developing the concept, the author approached the problem in the light of the resolution of the May plenary session on artifcial and synthetic fibers. After explaining the concept of "chemical fibers" and ways of preparing them, the author uses a series of examples to illustrate the various known types of fibers (viscose, polyamide fibers, polyester fibers, khlorin, etc.) and also gives their foreign names. Here the factual material is concluded with a description of the future development of the Yaroslavl' Sovnarkhoz (Council of National Economy) in the production and application of chemical fibers.

* Subscribed for publication December 8, 1958.

In Section IV, "Plastics and Resins," the author emphasizes the great growth in plastic plant capacity in the seven year plan, as envisaged by the May Plenary session, as compared with other synthetic materials. Having given a basically accurate definition of plastics on page 55, Musabekov is not satisified with this and on the next page he then identified the above clear idea with the indistinct and dubious "state of a polymeric material."

Strictly speaking, Yu. S. Musabekov makes another methodical omission in not giving here (or anywhere in the book) a classification of plastics with respect to the heating of their basic binder, i.e., division into thermosetting and thermoplastic materials. At the same time, later on he uses unexplained ideas, for example, the term "thermoplastics" (p. 69 and 70). In discussing fluoroplastics, it should be noted that together with the rare combination of different unique properties of teflon, which is indisputably a positive factor, the material is extremely difficult to work. There is a one-sided description of polyethylene on which almost nothing factual is stated apart from the fact that its is an extremely good electrical insulator and a promising cheap material.

The chapter mentions the use of synthetic resins and plastics in the production of ionites, foam plastics and in the varnish and paint industry and the production of adhesives. However, nothing is said in the book on such new trends in the chemistry of high-molecular compounds as the preparation of polymers from heteroorganic compounds and complex polymers. Neither is there mention of polymers with a stereoregular structure (the work of the Italian chemists Natta et al.).

Section V, "Nutritional Substances and Their Substitutes," gives a review of the main achievements of chemical science in the processing and synthesis of nutritional substances: carbohydrates, vitamins, fats and proteins. The problem of freeing the natural fats used in industry (mainly for soap manufacture) for feeding purposes is of great economic importance. The author considers this problem. Material is also given in this section on the application of synthetic detergents and new data on the structure and synthesis of the most complex high-molecular compounds, namely proteins (the work of Zelinskii and Bresler).

Having mentioned to a greater or lesser extent the work of the Yaroslavl' economic region in almost each section, the author even devotes a special section (VI) to this problem, entitling it "Development of the Chemical Industry in the Yaroslavl' Economic Region." A short account is given here of the role of the Yaroslavl' region in developing the chemical industry and chemical science in Russia from the middle ages up to the present time. Special mention is made of the work of Yaroslavl' chemists (Sokolov, Konovalov, and Morozov) and the part which D. I. Mendeleev played in developing the chemical industry of the Yaroslavl' region.

Detailed factual data are given by the author on research work in chemistry and chemical technology carried out by a number of foundations and research institutes in Yaroslavl', and also the state and prospects of development of the rubber, chemical, and petroleum processing industries of the Yaroslavl' Sovnarkhoz as a foundation for the production of synthetic materials.

To the shortcomings of the work reviewed we should add certain inaccuracies and vagueness encountered in the text. Thus, for example, it is incomprehensible why the author considers melamine and urea (typical organic compounds) as intermediate between mineral and organic substances (p. 74).

The statement on p. 67 that the synthesis of polyethylene became an industrial reaction only after Ziegler's discovery of the polymerization of ethylene at normal pressure is incorrect. "High pressure polyethylene" was produced by us and abroad for a number of years. The formula for acrylonitrile given on p. 34 should be corrected as it shows insufficient bonds in the CN group. The reaction scheme for the polymerization of butadiene on p. 18 lacks the coefficient - in the left-hand part (as is also the case for ethylene on p. 59). The formula of caprone (p. 46) should have an imino group instead of an amino group. Then there is some doubt on the term "organochemical industry" used by the author (p. 58) and the statement that high-molecular compounds have " the flexibility of gases" (p. 8). The history of the discovery of polyethylene is not given completely accurately* (p. 67).

* ". . . . In 1933 – 1936 the British investigators Fawcett and Gibson and their co-workers were able to obtain solid, high-molecular polymers of ethylene for the first time. . . At approximately the same time polyethylene was obtained by the Soviet scientist A. I. Dintses" (A. V. Topchiev and B. A. Krentsel'. Polyolefins—New Synthetic Materials (Izd. AN SSSR, 1958) p. 4.

Despite these slight shortcomings, the publication of the work reviewed should be approved. It helps those who wish to become acquainted in general terms with the state and problems of contemporary organic synthesis, especially in the promising field of high-molecular compounds. It also gives the reader a clear impression of the important role of the Yaroslavl' economic region as one of the main reserves of our seven year plan.

I. G. Filatov

ERRATA

Volume 32, Number 4, April, 1959

Equation (6), page 782, was omitted from the published journal. It should read as follows:

$$E = \frac{4.575 \cdot T_1 \cdot T_2}{T_2 - T_1} \cdot \lg \frac{K_2}{K_1} = 13\,700 \text{ cal/mole}. \qquad (6)$$

SIGNIFICANCE OF ABBREVIATIONS MOST FREQUENTLY ENCOUNTERED IN SOVIET PERIODICALS

FIAN	Phys. Inst. Acad. Sci. USSR.
GDI	Water Power Inst.
GITI	State Sci.-Tech. Press
GITTL	State Tech. and Theor. Lit. Press
GONTI	State United Sci.-Tech. Press
Gosenergoizdat	State Power Press
Goskhimizdat	State Chem. Press
GOST	All-Union State Standard
GTTI	State Tech. and Theor. Lit. Press
IL	Foreign Lit. Press
ISN (Izd. Sov. Nauk)	Soviet Science Press
Izd. AN SSSR	Acad. Sci. USSR Press
Izd. MGU	Moscow State Univ. Press
LEIIZhT	Leningrad Power Inst. of Railroad Engineering
LET	Leningrad Elec. Engr. School
LETI	Leningrad Electrotechnical Inst.
LETIIZhT	Leningrad Electrical Engineering Research Inst. of Railroad Engr.
Mashgiz	State Sci.-Tech. Press for Machine Construction Lit.
MEP	Ministry of Electrical Industry
MES	Ministry of Electrical Power Plants
MESEP	Ministry of Electrical Power Plants and the Electrical Industry
MGU	Moscow State Univ.
MKhTI	Moscow Inst. Chem. Tech.
MOPI	Moscow Regional Pedagogical Inst.
MSP	Ministry of Industrial Construction
NII ZVUKSZAPIOI	Scientific Research Inst. of Sound Recording
NIKFI	Sci. Inst. of Modern Motion Picture Photography
ONTI	United Sci.-Tech. Press
OTI	Division of Technical Information
OTN	Div. Tech. Sci.
Stroiizdat	Construction Press
TOE	Association of Power Engineers
TsKTI	Central Research Inst. for Boilers and Turbines
TsNIEL	Central Scientific Research Elec. Engr. Lab.
TsNIEL-MES	Central Scientific Research Elec. Engr. Lab.—Ministry of Electric Power Plants
TsVTI	Central Office of Economic Information
UF	Ural Branch
VIESKh	All-Union Inst. of Rural Elec. Power Stations
VNIIM	All-Union Scientific Research Inst. of Meteorology
VNIIZhDT	All-Union Scientific Research Inst. of Railroad Engineering
VTI	All-Union Thermotech. Inst.
VZEI	All-Union Power Correspondence Inst.

Note: Abbreviations not on this list and not explained in the translation have been transliterated, no further information about their significance being available to us. — Publisher.

more collected reports on...

Soviet Pharmaceutical Research

". . .a storehouse of factual references"

SOVIET research in PHARMACEUTICAL CHEMISTRY | 1956

THIS VALUABLE COLLECTION of translations not only gives researchers a more intimate insight into the thinking, methodology, and trends of the Soviet medicinal and pharmaceutical chemists, but it also reports significant contemporary advances in pharmaceutical research.

These 109 selected papers from the 1956 issues of Journal of Applied Chemistry, Bulletin of the Academy of Sciences–Division of Chemical Sciences, Journal of Analytical Chemistry, Colloid Journal, and Journal of General Chemistry will be a valuable addition to all medical and pharmaceutical libraries and should be accessible to all researchers in the field. Sections may be purchased separately as follows:

I Pharmaceutical Chemistry:
Ion Exchange
Miscellaneous
(22 papers) $12.00

II Medicinal Chemistry:
Anti-infective compounds
Steroids and related compounds
Heterocyclic compounds
Miscellaneous
(70 papers) 45.00

III Pharmacognosy:
Alkaloids
Miscellaneous
(17 papers) 10.00

THE COMPLETE COLLECTION $60.00

"At a time when the Western World eyes the achievements of science in the U.S.S.R. with a mixture of admiration and apprehension, it is gratifying to be able to read the English translation of hundreds of Russian articles in the fields of Pharmaceutical Chemistry (Vol. 1), Pharmacognosy (Vol. 2), and Medicinal Chemistry (Vol. 3)... In the application of quantitative physical measurements to problems of pharmacy, the careful recording of data and their evaluation can be termed excellent. American pharmaceutical investigators will have much to learn from these researches (Vol. 1)... Libraries of departments of medicine, chemistry, and pharmacy in universities and the pharmaceutical industry will find it essential to acquire the books, and for some specialists the pertinent volumes may become a storehouse of factual references."–*Alfred Burger in Journal of Chemical Education*

SOVIET PHARMACEUTICAL RESEARCH (1949-55)

I Pharmaceutical Chemistry:
Solubility
Stability
Ion Exchange
Emulsions
Suspensions
Gels
Miscellaneous
(74 papers) ..... $ 95.00

II Pharmacognosy:
Alkaloids
Oils
Glycosides
Miscellaneous
(87 papers) 90.00

III Medicinal Chemistry:
Structure-Activity Relationships
General
(91 papers) 100.00

THE COMPLETE COLLECTION $200.00

NOTE: Individual papers from each collection are available at $7.50 each. Tables of contents sent upon request.

CONSULTANTS BUREAU 227 West 17th Street · New York 11, N. Y.

RESEARCH BY SOVIET EXPERTS

Translated by Western Scientists

INSTABILITY CONSTANTS OF COMPLEX COMPOUNDS

by K. B. Yatsimirskii and V. P. Vasil'ev

Instability constants quantitatively characterize the equilibrium in solutions of complex compounds and, in this connection, are very widely used by chemists in different fields (analytical chemistry, electrochemistry, technology of nonferrous and rare metals, etc.) for appropriate calculations.

The instability constants of 1381 complex compounds are given. The authors have prefaced the summary of instability constants with an introductory section which examines methods of calculating instability constants from experimental data, the effect of external conditions (temperature and ionic strength) on the stability of complexes and the main factors determining the stability of complex compounds in aqueous solutions.

Cloth 200 pages $6.75

SOVIET RESEARCH ON COMPLEXES AND CO-ORDINATION CHEMISTRY

This collection consists of 372 articles by Russian scientists in the general area of the chemistry of complexes. These reports have been complied from the Consultants Bureau translations of the following Soviet journals:

Journal of General Chemistry
Journal of Analytical Chemistry
Bulletin of the Academy of Sciences
Division of Chemical Sciences
Proceedings of the Academy of Sciences
Journal of Applied Chemistry
Soviet Journal of Atomic Energy

The articles have been grouped into five volumes, each of which may be purchased separately.

I. Inorganic Complexes—103 articles $65.00
II. Metal-Organic Complexes—86 articles $45.00
III. Thermodynamic and Kinetic Studies—57 articles .. $37.50
IV. Complexes in Analytical Chemistry—57 articles .. $37.50
V. Condensed Inorganic Systems; Miscellaneous —38 articles .. —31 articles .. $45.00

Complete collection .. $200.000

Tables of contents on request

Payment in sterling may be made to Barclays Bank in London, England

CONSULTANTS BUREAU

227 West 17th Street · New York 11, N. Y.